PhD THESIS - TESIS DOCTORAL

MODALIDAD DE COMPENDIO DE ARTÍCULOS

ATMOSPHERIC MERCURY: LONG-TERM (LATE PLEISTOCENE - HOLOCENE) VARIATIONS IN MERCURY ACCUMULATION RECONSTRUCTED USING ENVIRONMENTAL ARCHIVES

Marta Pérez Rodríguez

PROGRAMA DE DOUTORAMENTO DE MEDIO AMBIENTE E RECURSOS NATURAIS

FACULTADE DE BIOLOXÍA

SANTIAGO DE COMPOSTELA

2017

USC
UNIVERSIDADE
DE SANTIAGO
DE COMPOSTELA

Don Antonio Martínez Cortizas, Catedrático de Universidade do Departamento de Edafoloxía e Química Agrícola da Facultade de Bioloxía da Universidade de Santiago de Compostela,

DECLARA

que ésta tese de doutoramento, titulada "Long-term (Late Pleistocene – Holocene) variations in mercury accumulation reconstructed using environmental archives", foi realizada por Dona Marta Pérez Rodríguez baixo a miña supervisión e é idónea para ser presentada como Tese por compendio de Artigos. A doutoranda participou de xeito activo na investigación reflexeda nos artigos e a súa contribución foi decisiva para levar a cabo os traballos. Todos os coautores participantes nos artigos, tanto doutores como non doutores, están en coñecemento e aceptaron a inclusión das publicacións nesta Tese de Doutoramento. Ningún dos traballos foi ou será presentado por ningún dos coautores noutra tese de Doutoramento.

Santiago de Compostela, a 10 de Maio de 2017

Don Antonio Martínez Cortizas

USC
UNIVERSIDADE
DE SANTIAGO
DE COMPOSTELA

Abstract

The principal aim of this PhD research is to gain further insights into the variations in atmospheric Hg deposition over long timescales (late Pleistocene and Holocene) in the northern and southern hemispheres, by the use of environmental archives (peat and lake sediments). For this purpose, five archives from different areas of the world and with records that operate at different time scales were studied: Rano Aroi (Easter Island, Chile), Pinheiros (Estado de Minas Gerais, Brazil), Lago Hambre (South Patagonia, Chile), Limnopolar Lake (South Shetland Islands, Antarctica) and Sandhavn (South Greenland). These records have been studied previously by geochemical, paleoclimatic and palynological means, enabling the multi-proxy approach that is needed for the assessment of a subject with the complexity of Hg cycling. This work pays special attention to understanding the processes involved in Hg deposition and accumulation, the interactions between these processes and the spatial and temporal variability in their relative importance. Furthermore, the research included a methodological assessment that aimed to select a suit of relatively cost- and time-efficient methodologies, which is necessary for multi-core/multi-site studies. Eight factors were identified as the main drivers of Hg concentration - through deposition-uptake and also through accumulation - in the peat and lake sediments studied: anthropogenic pollution, volcanic activity, organic matter decomposition, catchment processes, (lake) primary productivity, atmospheric Hg depletion events, vegetation type and direct and indirect climatic effects. Essentially, lake sediments and peatlands are environmental archives that can be used as records of atmospherically deposited Hg, thus providing a "picture" of the Hg cycle. However, the use of such archives as Hg atmospheric records is conditioned by factors that operate in different geographical and temporal scales. Thus, the Hg determined in the samples does not directly reflect atmospheric deposition, but results of changing combination different factors.

Keywords: mercury cycle, peatlands, lake sediments, paleoenvironment, atmospheric deposition

USC
UNIVERSIDADE
DE SANTIAGO
DE COMPOSTELA

Resumen

El principal objetivo de esta tesis doctoral es obtener información sobre las variaciones de la deposición atmosférica de mercurio a escalas largas de tiempo (Pleistoceno tardío y Holoceno) en los hemisferios Norte y Sur, usando archivos ambientales (turberas y sedimentos lacustres). Con este propósito, se estudiaron cinco archivos de diferentes partes del mundo y de diferentes escalas de tiempo: Rano Aroi (Isla de Pascua, Chile), Pinheiros (Estado de Minas Gerais, Brasil), Lago Hambre (Sur de la Patagonia, Chile), Lago Limnopolar (Islas Shetland del Sur, Antártida) y Sandhavn (Sur de Groenlandia). Estos registros han sido objeto de estudio en diferentes ámbitos como geoquímica, paleoclimatología, evolución de turberas y palinología, lo que ha permitido el enfoque multi-indicador necesario para la evaluación de un problema con la complejidad del ciclo del Hg. Se presta especial atención a entender cómo los procesos relacionados con la deposición y acumulación de Hg en los archivos ambientales, interaccionan y cambian su peso relativo en el tiempo y el espacio. Se incluye un aspecto metodológico para la aplicación de técnicas más baratas y de más rápidas para ayudar en estudios más amplios. Se identificaron ocho factores como los principales impulsores de la concentración de Hg – a través de la deposición-absorción y la acumulación- en los registros estudiados: contaminación, actividad volcánica, descomposición de materia orgánica, procesos de captación, productividad primaria, eventos de agotamiento atmosférico, el tipo de vegetación y los efectos climáticos. Los sedimentos lacustres y las turberas son archivos ambientales que pueden utilizarse como registros de Hg depositado atmosféricamente, ya que proporcionan una "imagen" del ciclo de Hg pasado. Pero este uso está condicionado por factores que operan en diferentes escalas geográficas y temporales. Por lo tanto, el Hg determinado en las muestras no refleja directamente la deposición atmosférica, es el resultado de la combinación de diferentes factores.

Palabras clave: ciclo del mercurio, turberas, sedimentos lacustres, paleoambiente, deposición atmosférica.

USC
UNIVERSIDADE
DE SANTIAGO
DE COMPOSTELA

Resumo

O principal obxectivo desta tese doctoral é obter información sobre as variacións da deposición atmosférica de mercurio a escalas longas de tempo (Pleistoceno tardío e Holoceno) nos hemisferios Norte e Sur, usando arquivos ambientais (turberas e sedimentos lacustres). Con este propósito, estudáronse cinco arquivos de diferentes partes do mundo e de diferentes escalas de tempo: Rano Aroi (Illa de Pascua, Chile), Pinheiros (Estado de Minas Gerais, Brasil), Lago Hambre (Sur da Patagonia, Chile), Lago Limnopolar (Illas Shetland do Sur, Antártida) e Sandhavn (Sur de Groenlandia). Estes registros foron obxecto de estudo en diferentes ámbitos como xeoquímica, paleoclimatología, evolución de turberas e palinología, o que permitiu o enfoque multi-indicador necesario para a avaliación dun problema coa complejidad do ciclo do Hg. Préstase especial atención a entender como os procesos relacionados coa deposición e acumulación de Hg nos arquivos ambientais, interaccionan e cambian o seu peso relativo no tempo e o espazo. Inclúese un aspecto metodológico para a aplicación de técnicas máis baratas e de máis rápidas para axudar en estudos máis amplos. Identificáronse oito factores como os principais impulsores da concentración de Hg - a través da deposición-absorción e a acumulación- nos registros estudados: contaminación, actividade volcánica, descomposición de materia orgánica, procesos de captación, productividad primaria, eventos de agotamiento atmosférico, o tipo de vegetación e os efectos climáticos. Os sedimentos lacustres e as turberas son arquivos ambientais que poden utilizarse como registros de Hg depositado atmosféricamente, e proporcionan unha "imaxe" do ciclo do Hg pasado. Pero este uso está condicionado por factores que operan en diferentes escalas xeográficas e temporais. Polo tanto, o Hg determinado nas mostras non reflicte directamente a deposición atmosférica, si non que é o resultado da combinación de diferentes factores.

Palabras chave: ciclo do mercurio, turberas, sedimentos lacustres, paleoambiente, deposición atmosférica.

USC
UNIVERSIDADE
DE SANTIAGO
DE COMPOSTELA

This PhD thesis is based on the following papers:

Marta Pérez-Rodríguez, Ingrid Horák-Terra, Luis Rodriguez-Lado, Jesús R. Aboal, Antonio Martínez Cortizas (2015). Long-Term (~57 ka) Controls on Mercury Accumulation in the Southern Hemisphere Reconstructed Using a Peat Record from Pinheiro Mire (Minas Gerais, Brazil). *Environmental Science and Technology*, 49, 1356-1364. **JCR IF (2015): 5.393, D1 in Engineering, Environmental and Environmental Sciences**

Marta Pérez-Rodríguez, Ingrid Horák-Terra, Luis Rodriguez-Lado, Antonio Martínez Cortizas (2016). Modelling mercury in minerogenic peat combining FTIR-ATR spectroscopy and partial least squares (PLS). *Spectrochimica Acta Part A: Molecular and Biomolecular Spectroscopy*, 168, 65-72. **JCR IF (2015): 2.653, Q2 in Spectroscopy**

Marta Pérez-Rodríguez, Benjamin-Silas Gilfedder, Yvonne-Marie Hermanns, Harald Biester (2016). Solar Output Controls Periodicity in Lake Productivity and Wetness at the Southernmost South America. *Scientific Reports*, 6:37521. **JCR IF (2015): 5.228 , D2 in Multidisciplinary Sciences**

In preparation:

Marta Pérez-Rodríguez, Olga Margalef, J. Pablo Corella, Sergi Pla-Rabes, Santiago Giralt, Antonio Martínez Cortizas. ~71 kyr of mercury deposition in the Southern Hemisphere recorded by Rano Aroi mire, Easter Island (Chile).

Harald Biester, **Marta Pérez-Rodríguez**, Benjamin-Silas Gilfedder, Antonio Martínez Cortizas, Yvonne-Marie Hermanns. Total solar insolation and algae productivity increase mercury accumulation in a prostine Southern Hemispheric lake.

Marta Pérez-Rodríguez, Harald Biester, Jesús R. Aboal, Manuel Toro, Antonio Martínez Cortizas. The role of ice-cover, climate and volcanism on extreme mercury enrichment in enrichment in Limnopolar Lake (Antarctica) sediments during the last 1600 years.

Marta Pérez-Rodríguez, Noemí Silva-Sánchez, Malin E. Kylander, Richard Bindler, Tim M. Mighall, J. Edward Schofield, Kevin J. Edwards, Antonio Martínez Cortizas. Industrial-era lead mercury contamination in southern Greenland implicates US sources.

USC
UNIVERSIDADE
DE SANTIAGO
DE COMPOSTELA

Index

1. Summary

Mercury (Hg) is a naturally occurring element that is found throughout the world. Due to the toxicity of its methylated forms (MeHg) to wildlife and human health, Hg is considered a metal of major environmental concern. According to numerous health and governmental organizations, billions of people are currently at risk of high exposure to poisoning by Hg due to a diet rich in fish (high content of MeHg) or by exposure to Hg emitted from artisanal and small-scale gold mining, mainly in low- and middle-income countries.

Several industrial processes such as fuel combustion, cement production, metal smelting, large-scale gold mining with non-Hg methods as well as commercial Hg mining, has been emitted thousands of tons of Hg directly to the atmosphere since 1850. In addition to human related processes, several natural processes emit Hg to the environment, such as volcanic activity (geothermal vents, volcanoes) and emissions from natural enriched soils. Other types of Hg cycling mechanisms such as forest fires or oceanic emissions are considered mixed natural-anthropogenic sources.

Primary sources transfer Hg from slow-cycling lithospheric reservoirs to the fast cycling atmospheric, oceanic and the terrestrial environments, thereby increasing the global pool of Hg in surface reservoirs. After deposition, Hg can be reemitted from the surface reservoirs to the atmosphere, therefore constituting a secondary

source. Recycling from surface reservoirs results in an effective lifetime of 1.6 years before transfer to soil and deep ocean pools. Due to its volatility as Hg0 and the redox transformations of Hg in the environment, deposition and release are influenced by multiple environmental factors including seasonality, vegetation cover, temperature, light, moisture, atmospheric turbulence and the presence of reactants.

Several factors control Hg dynamics in different environments such as ice dynamics, ocean surface temperature, soil carbon content, riverine discharge, type of precipitation [rain vs. snow], and methylation rates. In addition, human activity has played a key role in increasing Hg abundance in the environment. A combination of natural and anthropogenic factors ensures that the biogeochemical cycle of Hg is particularly susceptible to global change. Thus, the use of environmental archives is essential to Hg research, as they provide a unique link between current and past Hg dynamics in the environment. Environmental or natural archives are those physical (natural) structures that due to their formation process and evolution can store proxies of environmental change. Such archives, such as peatlands, ice cores and lake sediments, have had an essential role in the reconstruction of atmospheric deposition of Hg on a local, regional, and global scale.

Peatlands and lake sediments have a wide geographic distribution (peatlands cover more than 4 million km^2 worldwide) and have proved to provide accurate Hg deposition records. Pollution is considered one of the main drivers behind Hg concentration in records worldwide that cover the last centuries or last millennia – mainly by the effect of Industrial or the Pre-Industrial activities, respectively. However, contributions from natural sources have also been recorded.

Large differences in the estimated background Hg fluxes exist between different records, hampering our understanding of the emission sources, the atmospheric processes involved and the rates of exchange between terrestrial, oceanic and atmospheric pools. These differences in fluxes could be due to a variety factors that could affect Hg accumulation in lake sediments and peatlands, complicating their use as archives of atmospheric deposition. In lakes, these factors include the size and land-use of the watershed, Hg mobility in sediments, diagenesis, primary productivity and algal scavenging. In peatlands, on the other hand, the spatial variability in peat surface, vegetation type and decomposition rate are still

poorly understood which limits the use of Hg records from peat archives for the reconstruction of atmospheric deposition of Hg.

In spite of several advances that have been made during the last decade to examine the underlying processes that occur in archives of Hg deposition, the number of reliable records is still very limited. Furthermore, most of the studies are from the Northern Hemisphere (mainly Europe and North America) and spanning the Holocene (last 11,000 years). However, the few available long-term studies showed that non-anthropogenic factors such as changes in climatic conditions or decomposition rate, can have strong influence in records of Hg accumulation. This implies that also in Holocene records an effort needs to be made to disentangle the anthropogenic and natural controls on Hg concentration.

The principal aim of this PhD research is to gain further insights into the variations in atmospheric Hg deposition over long timescales (late Pleistocene and Holocene) in the northern and southern hemispheres, by the use of environmental archives (peat and lake sediments). For this purpose, five archives from different areas of the world and with records that operate at different time scales were studied: **Rano Aroi** (Easter Island, Chile), **Pinheiros** (Estado de Minas Gerais, Brazil), **Lago Hambre** (South Patagonia, Chile), **Limnopolar Lake** (South Shetland Islands, Antarctica) and **Sandhavn** (South Greenland). These records have been studied previously by geochemical, paleoclimatic and palynological means, enabling the multi-proxy approach that is needed for the assessment of a subject with the complexity of Hg cycling. This work pays special attention to understanding the processes involved in Hg deposition and accumulation, the interactions between these processes and the spatial and temporal variability in their relative importance. Furthermore, the research included a methodological assessment that aimed to select a suit of relatively cost- and time-efficient methodologies, which is necessary for multi-core/multi-site studies.

There is a wide variety of concentrations and rates of Hg accumulation in the studied records. The enrichment values in some cases reached values of up to 800 times the minimum value, suggest the combination of different factors (natural and due to human activity) that have interacted and possibly changed over time.

Eight factors were identified as the main drivers of Hg concentration in the peat and lake sediments studied here: **anthropogenic pollution, volcanic activity, organic matter decomposition, catchment processes, (lake) primary**

productivity, atmospheric Hg depletion events, vegetation type and direct and indirect climatic effects. These factors controlled Hg concentrations in the studied records through deposition-uptake and also through accumulation.

As previously mentioned, **pollution** has been considered one of the main drivers controlling Hg concentrations in records that cover the last centuries or millennia – mainly showing the effect of industrial or pre-industrial activities, respectively. Previous studies from areas in proximity of the ones that are the subject of this thesis have pointed towards the importance of anthropogenic Hg enrichment, however only the Greenland peat record (Sandhavn, spanning the last ~700 cal. yr) provided a clear signal of Hg pollution. Several reasons may explain the lack of evidence of recent atmospheric pollution in most of the studied cores, such as the relatively low resolution for the last centuries in the Pleistocene records (Rano Aroi and Pinheiros) or the overlapping effect of other processes driving Hg concentrations (Limnopolar Lake and Lago Hambre).

At Sandhavn, the results demonstrated that the Hg accumulation rate has steadily increased since the beginning of the 19th century, with maximum values of 9.3 $\mu g\ m^{-2}\ yr^{-1}$ recorded ~1940, which is in agreement with previous records from Greenland. The accumulation rates are generally low in comparison with other records from Europe and North America probably because i) Sandhavn is located at a long distance from the major sources of pollution or ii) mid-latitudinal records have been affected more strongly by Hg enrichment due to the more intense peat mineralization.

The detailed chronology of metal pollution provided by the detrending of the Pb isotopic ratio record (extracting the effect of geogenical mixing), indicated that widespread pollution started AD ~1740-1780, which is in agreement with previous studies using Pb that found that modern metal pollution in Greenland had begun prior to the 19th century; maximum pollution signatures occurred AD ~1960-1970. The isotopic composition of the Sandhavn peat record since the 19th century and the timing of Pb enrichment clearly points to the dominance of pollution sources from the USA. There is no direct evidence for the origin of Hg, but according to the Pb isotope results we would expect the main source of Hg contamination also to be North America. However, Hg has a complex behavior in the environment. Its relatively long residence time in the atmosphere (>1 year) favors long-range transport and homogenization at a hemispheric scale, making it

more difficult to determine its precise origin.

The **volcanic emissions** produce a natural mobilization of Hg from geogenic reservoirs. However, there are regional differences in average Hg emissions. Unlike ice cores, peat and lake sediments are usually collected from lower altitudes, which often implies that enrichments in Hg due to volcanic eruptions are superposed on stronger variability in Hg influx by other processes that the relatively "clean" high altitude ice records.

The Deception Island volcano significantly influenced the geochemistry of the Limnopolar Lake that is located at a distance of 30 km, mainly by increasing the volcanic vs. catchment inorganic fluxes during several episodes of the last 1600 yr. The chronology of volcanic eruptions of Deception Island and excursions of Hg concentration in Limnopolar Lake (Hg accumulation rates between 300 to 4900 m^{-2} yr^{-1} against a background ~9 µg m^{-2} yr^{-1}) and recent tephra records are similar. Nevertheless, Hg concentration and volcanic activity seem to be decoupled from AD ~1800 onwards, which is not in fase of high volcanic activity in Deception Island. Therefore, the nearby volcano appears to be the main source of Hg in Limnopolar Lake, but other mechanisms have been involved.

The effect of volcanic eruptions on the Hg concentrations in the Rano Aroi peatland (Easter Island) is less evident. In fact, there is no evidence, in the form of tephra layers, of recent volcanic activity in the peat cores. On a volcanic island, outgassing by active fumaroles, which does not produce tephra, could act as the primary Hg source and may be related to some of the very high peaks in Hg concentration detected (> 1000 ng g^{-1}). Either way, other processes such as deposition liked to rainfall events probably have a stronger control on Hg dynamics at Rano Aroi.

It has been argued that **organic matter decomposition** has a strong influence on Hg accumulation in peatlands, which may impose limitations to the use of peat bogs as reliable Hg atmospheric records. Nevertheless, the available literature is almost exclusively based on studies of Holocene peat deposits. Using the C/N ratio as an indicator of the degree of peat decomposition, the longer-term peat records presented here (Rano Aroi and Pinheiros) have a limited effect of peat decomposition on Hg concentrations. In these records, the main decay processes had completed by ca. 10-11 cal kyr BP in Pinheiros and 5 cal kyr BP in Rano Aroi. Only in Pinheiros the decay of organic matter in the youngest sections has affected

Hg content. In Rano Aroi, only the clear increase in Hg concentration at ~40 cal kyr BP may have responded to an extreme oxidation event driven by a drought period. The results indicated a two-fold increase in Hg concentrations.

Both direct aerial deposition of Hg on the lake surface and remobilization of atmospheric inputs through **fluxes from the catchment** are to be considered in Hg reconstruction in lacustrine environments. A huge amount of pollutants have been deposited and stored in the catchment surface soils of many lake sites, mainly due to the industrial emissions during the last centuries. Thus, processes such as watershed erosion and other catchment processes may have a strong influence on Hg concentration in lake sediments or peatlands receiving water inputs from sources other than precipitation (usually as runoff from upslope area) such as Pinheiros and Rano Aroi. In both records, catchment erosion has influenced Hg concentration but in an opposite way. In Pinheiros the mineral matter erosion from the quartzitic catchment produced a dilution effect: on the organic matter to which Hg is bound and by inputs of low Hg-containing mineral matter. In Rano Aroi, the catchment erosion mobilized atmospherically deposited Hg and associated and retained to organometallic complexes (mostly with Fe) from the volcanic soils. Thus, superficial runoff driven by precipitation may transport Hg to the mire and amplify the effect of wet deposition during rainfall events.

Similarly to Rano Aroi, in Limnopolar Lake the atmospherically deposited Hg (probably from Deception Island volcano) is accumulated in the catchment. But instead of stabilization of Hg through the formation of organometallic complexes, at Rano Aroi part of the gaseous Hg is deposited and stabilized on the ice-snow pack that covers the lake and its catchments during most of the year or during prolonged cold periods with permanent ice cover. Here, peaks in Hg concentrations are related to release of such accumulated Hg after thawing.

Previous research in Lago Hambre has suggested that Hg scavenging in the water column and accumulation in the sediments are mainly controlled by fluxes from the catchment soils. However, the multirpoxy approach (with spectroscopic and geochemical data) enabled the identification of unequivocal proxies of primary productivity, which showed a strong dependency on total solar irradiance (TSI). For the last 4.5 cal kyr BP the strong variations in Hg accumulation corresponded to changes in TSI and associated changes in **aquatic productivity**. The accumulation of Hg was highest during drier periods when insolation and lake productivity were

high and erosion fluxes from the catchment were low, indicating that sediment Hg accumulation (and potential Hg methylation) in this highly productive lake was controlled by insolation and the related algae productivity.

Atmospheric mercury depletion events (**AMDEs**) result from the oxidation of gaseous elemental Hg to highly reactive forms and subsequently rapid elimination of the oxidized Hg species through precipitation. In Limnopolar Lake, the combination of Hg emission by volcanic activity and amplification of the signal by the freezing and thawing of the lake and the basin, could explain the recorded changes in Hg content. But, AMDEs could also help to explain the extraordinary high levels of Hg found in some samples from the sediment. With the exception of a significant correlation between the Br/C molar ratio (used as a proxy of AMDEs) and high Hg accumulation peaks, there are no other data that support the link between Hg maxima and AMDEs. However, the proximity of the coast (< 2 km) and the cold periods during which most of the Hg peaks occurred are favourable conditions for the generation of AMDEs.

Differences in **vegetation type** can affect the net deposition and sequestration of Hg in peatlands, however no systematic sampling was carried out on the vegetation that could potentially affect the accumulation of Hg in peatlands and lake sediments. Vegetation samples were only collected in the Easter Island field sampling campaign and Hg results show a wide range of Hg concentrations reaching 11,117 ng g-1, on an unidentified rush (Juncus) sample. It has been hypothesized that an increase in the abundance of rush, coupled to more humid conditions by ~20 cal kyr BP, is related to detected peaks in Hg. However, there is no evidence for the presence of rush in the mire catchment at present and the available pollen and macroremains data do not support this hypothesis.

Climate has undoubtedly been the main driver of Hg accumulation in the records presented in this PhD thesis, with the exception of Sandhavn.In all the other records climate played a major role, both directly and indirectly. The broad influence of climate on the records presented here could be due to two main reasons, i) the remote location of the sampling sites limit the direct effect of anthropogenic activities and/or ii) the long time-span of some of the records implies that different periods of very distinct climatic conditions are recorded (e.g. the transition between dry and wet climates during the Late Pleistocene at Tropical and Subtropical latitudes such as in Rano Aroi and Pinheiros).

The peat records of Pinheiros and Rano Aroi provided an exceptional opportunity to examine how two main **climatic** periods –Late Pleistocene and Holocene– affected the Hg cycle at tropical and subtropical latitudes. The results of these long-term records (Rano Aroi and Pinheiros) suggest, as it is generally accepted by extensive monitoring, that wet deposition (i.e. the wash out of Hg by rainfall) is the main source of Hg to peatlands. This is in contrast with recent short-term studies with Hg isotopes that indicate that gaseous and particulate Hg (i.e. dry deposition) are the main species deposited into peatlands. The long temporal perspective provided by the Pleistocene records might highlight the dominance of the longer-term wet deposition processes. Additionally, at the timing of the Heinrich event 1 (17 cal kyr BP) characterized by dry and very cold conditions, the Pinheiros peatland recorded an extraordinary high Hg concentration. A similar effect was found in the Rano Aroi record at the end of the Last Glacial Maximum (at 20 cal kyr BP) when humid conditions prevailed in Eastern Island. Both, colder and humid conditions would have favored Hg accumulation since Hg deposition is controlled by temperature and humidity variations. The increased in peat oxidation between ~40 and 42 cal kyr BP that led to an increase in Hg concentrations was also driving by climate conditions, more specifically long-term drought.

In Lago Hambre, changes in primary productivity in the lake during the last ~4.5 kyr cal BP, and thereby indirectly also changes in Hg content in the sediments, were related to TSI, Total solar irradiance is obviously a parameter that is transferred to the Lago Hambre palaeoenvironmental record through climatic factors.

The freezing and thawing of lake ice regulated the accumulation of Hg in Limnopolar Lake and in its catchment. Freeze-thawing processes are also directly controlled by climate. The ice-snow layer over the lake and the catchment may have acted as a Hg sink during 9 - 10 months per year. Periods of sustained general cold climatic conditions may have extended the effect of this Hg trap at least from years to decades. This is consistent with the high Hg concentrations and accumulation rates corresponding to phases of minima in insolation (colder periods) as the Wolf, Spörer, Maunder and Dalton minima.

Regarding the **methodological aspects**, it appeared that spectroscopic analysis in combination with multivariate analysis, in particular Partial Least Squares statistics can be efficiently and reliably used to predict Hg concentrations in

minerogenic peat, at least within the same core. This approach can be used to reduce the costs of multi- core approaches facilitating the study of spatial variability within and between mires.

Essentially, lake sediments and peatlands are environmental archives that can be used as records of atmospherically deposited Hg, thus providing a “picture” of the Hg cycle. However, the use of such archives as Hg atmospheric records is conditioned by factors that operate in different geographical and temporal scales. Thus, the Hg determined in the samples does not directly reflect atmospheric deposition, but results of a changing combination of the eight different factors described in this thesis.

USC
UNIVERSIDADE
DE SANTIAGO
DE COMPOSTELA

1. Resumen

El mercurio (Hg) es un elemento natural de distribución global. Debido a la toxicidad de sus formas metiladas, tanto para la vida salvaje como para la salud humana, el Hg se considera un metal de preocupación ambiental. De acuerdo a numerosas organizaciones gubernamentales y para la salud, miles de millones de personas están bajo un alto riesgo de exposición al envenenamiento por Hg, principalmente por dietas ricas en pescado (con un alto contenido de metil mercurio) o a la exposición al Hg emitido por la minería artesanal o a pequeña escala de oro en países en vías de desarrollo.

Diferentes procesos industriales como la combustión de gasolina, la producción de cemento, la fundición de metales o la minería de oro a gran escala, así como la propia minería de Hg, han emitido directamente a la atmósfera miles de toneladas de Hg desde 1850. Además de las emisiones de Hg causadas por la actividad humana, existen numerosos procesos naturales que emiten mercurio al medio ambiente como la actividad volcánica (volcanes y fuentes hidrotermales) o las emisiones de suelos naturalmente enriquecidos. Otros procesos reemisionan el Hg en el medio ambiente, como los incendios forestales y las emisiones oceánicas. Estos son consideradas fuentes mixtas i.e. naturales y de origen antrópico.

Las fuentes primarias son aquellas que transfieren el Hg desde los depósitos de la litosfera a la atmósfera y después a la tierra y los océanos, es decir, incrementando la

reserva global de mercurio en reservorios superficiales. Después de la deposición, el Hg puede ser re-emitido desde los reservorios superficiales a la atmósfera, constituyendo lo que se conoce como fuente secundaria. El reciclado del Hg desde los reservorios superficiales, le da una vida útil (efectiva) de 1,6 años, antes de ser transferidos a depósitos de larga duración como el suelo y el océano profundo. Debido su volatilidad como Hg^0 (mercurio elemental) y las transformaciones redox del Hg en el medio ambiente, su deposición y evasión están influenciadas por múltiples factores incluyendo, la estacionalidad, la vegetación, la temperatura, la luz, la humedad, los cambios atmosféricos o la presencia de reactantes.

Diferentes factores controlan la dinámica del Hg en diferentes ambientes como la dinámica de la cobertura de hielo, la temperatura del océano, el contenido de carbono en los suelos, las descargas de los ríos y el tipo de precipitación (lluvia vs. nieve), así como las tasas de metilación. Además, la actividad humana ha jugado un papel clave en el incremento de la abundancia del Hg en el medio ambiente. La combinación de factores naturales y de origen antrópico, hacen que el ciclo biogeoquímico del Hg sea particularmente susceptible al cambio global. Así el uso de archivos ambientales en la investigación del ciclo del Hg es esencial, ya que nos proporcionan la única conexión entre la dinámica del Hg en el medio ambiente presente y pasado. Los archivos ambientales o naturales son aquellas estructuras físicas (naturales) que debido a su proceso de formación y evolución pueden almacenar información ambiental. Así, las turberas, los testigos de hielo y sedimentos lacustres han tenido un papel esencial en la reconstrucción de la deposición atmosférica del Hg a escala local, regional y global.

Las turberas y los sedimentos lacustres tienen una amplia distribución geográfica (las turberas cubren más de 4 millones de km^2 en todo el mundo) y además han probado ser unos registros precisos de la deposición de Hg. La contaminación se considera uno de los principales controles de las concentraciones de Hg en los registros de todo el mundo que cubren los últimos siglos o milenios, debido principalmente al efecto de las actividades Industriales o Pre-Industriales (respectivamente). Sin embargo, las contribuciones desde fuentes naturales también han sido registradas.

Existen grandes diferencias en las estimaciones de los niveles de Hg de fondo entre diferentes registros, lo que dificulta entender las fuentes de emisión y los procesos atmosféricos involucrados, así como las tasas de intercambio entre las

reservas terrestres, oceánicas y atmosféricas. Estas diferencias en los niveles de fondo pueden ser debidas a al efecto de una gran cantidad de factores que pueden modificar las acumulación de Hg en turberas y sedimentos lacustres. Todo ello complica su uso como archivos de la deposición atmosférica de Hg. En sedimentos lacustres, entre otros factores, se incluyen el tamaño y el uso de la cuenca hidrográfica, la movilidad del Hg en los sedimentos, la diagénesis, la productividad primaria en el lago y la retirada de Hg por acción de las algas. Por otra parte, en turberas la variabilidad espacial dentro de la turbera, el tipo de vegetación, la descomposición de la materia orgánica son algunos de los cuestiones que necesitan resolverse para un uso adecuado de los testigos de turba como registros de la deposición atmosférica de Hg.

A pesar de que en las últimas décadas se han hecho numerosos avances para entender los procesos subyacentes que ocurren en los archivos ambientales y que afectan a la acumulación de Hg, la variabilidad de registros utilizados es todavía muy limitada. Así, la mayoría de estudios se han llevado a cabo en Hemisferio Norte – principalmente Europa y América del Norte – y cubren el perdiodo Holoceno (últimos 11.000 años). Los pocos estudios disponibles que recogen periodos más largos han mostrados que otros factores diferentes a la actividad humana pueden jugar un papel fundamental en el control de las concentraciones de Hg. Esto lleva a la necesidad de considerar qué procesos actúan controlando la acumulación de Hg en los archivos en periodos más largos de tiempo así como incrementar el esfuerzo para desentrañar los controles naturales de la concentración de Hg en los registros Holocenos.

El principal objetivo de esta tesis doctoral es obtener información sobre las variaciones de la deposición atmosférica de mercurio a escalas largas de tiempo (Pleistoceno tardío y Holoceno) en los hemisferios Norte y Sur, usando archivos ambientales (turberas y sedimentos lacustres). Con este propósito, se estudiaron cinco archivos de diferentes partes del mundo y de diferentes escalas de tiempo: **Rano Aroi** (Isla de Pascua, Chile), **Pinheiros** (Estado de Minas Gerais, Brasil), **Lago Hambre** (Sur de la Patagonia, Chile), **Lago Limnopolar** (Islas Shetland del Sur, Antártida) y **Sandhavn** (Sur de Groenlandia). Estos registros han sido objeto de estudio en diferentes ámbitos como geoquímica, paleoclimatología, evolución de turberas y palinología, lo que ha permitido el enfoque multi-indicador necesario para la evaluación de un problema de la complejidad del ciclo del Hg. Dentro de este objetivo general, se presta especial atención a entender cómo los procesos

relacionados con la deposición y acumulación de Hg en los archivos ambientales, interaccionan y cambian su peso relativo en el tiempo y el espacio. Además, esta investigación incluye un aspecto metodológico para la aplicación de técnicas más baratas y más rápidas para ayudar en estudios multi-testigo / multi-localización.

Existe una amplia variedad de concentraciones y de tasas de acumulación de Hg en los registros estudiados. Los valores de enriquecimiento dentro de los propios testigos, que alcanzó en algunos casos valores de hasta 800 veces el valor mínimo, sugiere la combinación de diferentes factores (naturales y debidos a la actividad humana) que han interactuado y posiblemente cambiado a lo largo del tiempo.

Ocho son los principales factores identificados como responsables de la acumulación de Hg: **la contaminación, la actividad volcánica, la descomposición de la materia orgánica, los procesos relativos a la cuenca, la productividad primaria, los eventos de depleción de Hg, el tipo de vegetación y los efectos directos e indirectos debidos al clima**. Estos factores han controlado las concentraciones de Hg tanto a través de la deposición y captación del Hg como modificando la acumulación en los registros.

Tal y como se mencionó anteriormente, la **contaminación** ha sido considerado uno de los principales factores responsables de las variaciones en la accumulación del Hg en registros ambientales de todo el mundo que cubren los últimos siglos o milenios, mostrando el efecto de las actividades Industriales o Pre-Industriales (respectivamente). Estudios llevados a cabo en áreas próximas a los registros estudiados en esta tesis, hacían referencia a la presencia de Hg de contaminación. Sin embargo, solo el registro de turba de Groenlandia (Sandhavn, que cubre los últimos ~700 años) muestra una señal clara de Hg proveniente de contaminación. Varias razones pueden explicar la falta de evidencias de contaminación reciente en la mayoría de los registros estudiados, como la baja resolución en los últimos siglos en los registros Pleistocenos (Rano Aroi y Pinheiros) o que otros procesos que controlen la acumulación de Hg hayan impedido distinguir la señal de contaminación.

En cuanto a Sandhavn los resultados demuestran que la acumulación de Hg ha ido incrementándose de forma continua desde principios del s. XIX, alcanzando valores máximos alrededor de AD 1940 (~9.3 μg m^{-2} yr^{-1}). Los valores de acumulación son similares a los determinados en otros registros de Groenlandia, pero menores en comparación con registros de Europa y Norte América debido

probablemente a que i) Sandhavn está más lejos de las fuentes de contaminación localizadas en Norte América y Europa o ii) que los registros de latitudes medias o templadas se han visto más afectadas a un enriquecimiento de Hg debido a procesos cortos e intensos de descomposición de la materia orgánica de la turbera.

La cronología detallada de la contaminación metálica proporcionada por la desviación de relación isotópica del plomo (Pb) (extrayendo el efecto de la señal geogénica), indicó que la contaminación generalizada comenzó ~AD 1740-1780, en concordancia con otros trabajos, en los que usando Pb, se establece que la contaminación reciente en Groenlandia es anterior al s. XIX. Los valores de contaminación por plomo más elevados, se encontraron alrededor de AD 1960-1970. La composición isotópica del registro de Sandhavn a partir del s. XIX, junto con la cronología de enriquecimiento en Pb y el ratio de exceso de $^{206}Pb/^{207}Pb$ (que fue de 1.222, que refleja el Pb generado por contaminación), señala claramente el predominio de las fuentes de contaminación de los EEUU. No hay evidencias directas del origen del Hg de contaminación, pero con los resultados del Pb es de esperar que la principal fuente de contaminación por Hg sea también Norte América. Sin embargo, el Hg tiene un comportamiento complejo en el medio ambiente y su tiempo de residencia relativamente largo (> 1 año) favorece el transporte a larga distancia y la homogeneización a escala hemisférica, dificultando la determinación de su origen de una forma precisa.

Las **emisiones volcánicas** producen una movilización natural del Hg desde las reservas geogénica aunque existen diferencias a nivel regional en cuanto a la media de las emisiones. A diferencia de los testigos de hielo, en turberas y sedimentos de lagos que son normalmente muestreados a bajas altitudes, el enriquecimiento en Hg por erupciones volcánicas es escaso y normalmente refleja una influencia regional.

El volcán de Isla Decepción ha influido significativamente la geoquímica del Lago Limnopolar, que está situado a 30 km, incrementando los flujos de material volcánico frente al material de la cuenca así como el registro de Hg en los sedimentos durante los últimos 1.600 años. La cronología de las erupciones volcánicas de la Isla Decepción, los picos de Hg en el Lago Limnopolar (tasas de acumulación de Hg entre 300 y 4.900 $\mu g\ m^{-2}\ yr^{-1}$ frente a los niveles de fondo de ~9 $\mu g\ m^{-2}\ yr^{-1}$) y el registro de material piroclástico del lago son muy similares. Aunque estp no ocurre en la fase más reciente de actividad volcánica (desde AD ~1800

hasta el presente) dónde hay un desacoplamiento. El volcán fue, posiblemente, la principal fuente de Hg en el lago, pero debe haber otros mecanismos implicados que controlan la acumulación en el sedimento.

El efecto de las erupciones volcánicas en las concentraciones de Hg acumulado en la turbera de Rano Aroi (Isla de Pascua) es menos evidente. De hecho, no existen evidencias en forma de material piroclástico de erupciones volcánicas recientes en los dos testigos de turba estudiados. Sin embargo, en una isla volcánica, como Isla de Pascua, no se puede descartar la posibilidad de que la emisión de Hg a través de fumarolas pueda ser una fuente primaria, y pueda estar relacionado con los picos de mayor concentración (> 1.000 ng g^{-1}). Aunque por otra parte, otros procesos como la deposición ligada a las precipitaciones tengan un mayor control sobre la dinámica del Hg en Rano Aroi.

Se ha argumentado que la **descomposición de la materia orgánica** puede controlar la acumulación de Hg en las turberas, lo que impone limitaciones en el uso de las mismas como registros precisos de la deposición atmosférica de Hg. Sin embargo la mayoría de los estudios están basados exclusivamente en turberas Holocenas. Usando la relación C/N (carbono / nitrógeno) como un indicador del grado de descomposición, los registros más antiguos incluidos en esta tesis (Rano Aroi y Pinheiros) han mostrado un efecto muy limitado de la descomposición en las concentraciones de mercurio. En estos registros la principal descomposición de la materia orgánica (antes de su estabilización) se alcanza entre los primeros 10.000 u 11.000 cal BP en Pinheiros y a los 5.000 cal BP en Rano Aroi. Solo en Pinheiros la degradación de la materia orgánica de las sección más jóvenes ha afectado al contenido de Hg. En Rano Aroi, sólo el claro aumento en la concentración de Hg a ~40.000 cal BP puede haber respondido a un evento de oxidación extrema impulsado por un período de sequía. Los resultados indicaron por este proceso un aumento de dos veces en las concentraciones de Hg.

En las estimaciones de los valores de Hg en los sedimentos de un lago se debe de considerar tanto las aportaciones aéreas directas de Hg en la superficie del lago como las que provienen de la re-movilización de las aportaciones atmosféricas sobre la **cuenca hidrográfica** y que llegan a través de flujos superficiales. Se estima que hay una gran cantidad de contaminantes (incluyendo Hg) depositados y almacenados en los suelos de las cuencas, debido principalmente a las emisiones industriales de los últimos siglos. De esta forma, la erosión y otros procesos

relacionados con las cuencas pueden tener un papel relevante en el contenido de Hg de los sedimentos lacustres o de aquellas turberas que reciben el agua desde fuentes distintas de la precipitación (por lo general escorrentía superficial) tal y como sucede en Rano Aroi y Pinheiros. En ambos registros la erosión de la cuenca ha modificado el contenido de mercurio pero de manera opuesta. En Pinheiros la erosión del material mineral de la cuenca de cuarzo produjo un efecto de dilución (principalmente entre los ~57.000 y los 40.000 cal BP) i) sobre la materia orgánica a la cual el mercurio está unido ii) y por las entrada en la turbera de material mineral de bajo contenido en Hg. Por otra parte en Rano Aroi, la erosión de la cuenca produjo la movilización del Hg depositado desde la atmósfera y asociado y retenido por los complejos organometálicos abundantes en los suelos volcánicos. De esta forma la erosión superficial impulsada por las precipitaciones pueden transportar el Hg desde la cuenca a la turbera y amplificar así el efecto de la deposición húmeda durante los periodos de lluvias. Al igual que en Rano Aroi, en el Lago Limnopolar el Hg de origen atmosférico (principalmente de las emisiones del volcán de Isla Decepción) se acumula en la cuenca. En este caso, en lugar de quedar ligado a los compuestos organometálicos, el Hg gaseoso se deposita y estabiliza en la capa de hielo y nieve que cubre tanto el lago como la cuenca la mayor parte del año o durante periodos más largos bajo condiciones de frío intenso. Así, los incrementos de las concentraciones de Hg están relacionadas con la liberación durante el periodo de deshielo del Hg acumulado previamente en el hielo.

Investigaciones previas en el Lago Hambre sugirieron que la deposición de Hg mediado por algas y la acumulación en los sedimentos eran controlados principalmente por los flujos de materia orgánica y Hg desde los suelos de la cuenca. Sin embargo, el enfoque multi-señal (con datos espectroscópicos y geoquímicos) permitió identificar señales inequívocas de la **productividad primaria**, que mostró una fuerte dependencia de la irradiancia solar total (total solar irradiance o TSI – siglas en inglés –). Para los últimos 4.500 cal BP las fuertes variaciones en la acumulación de Hg correspondieron a los cambios en la TSI y la productividad acuática. La acumulación de Hg fue mayor durante los periodos más secos, cuando la insolación y la productividad del lago fueron altas y los flujos de erosión de la cuenca fueron bajos, indicando que la acumulación de Hg del sedimento (y potencialmente la metilación de Hg) en este lago de alta productividad primaria fue controlada por insolación y la productividad de algas.

Los **eventos de agotamiento de mercurio atmósfera** (atmospheric mercury depletion events o **AMDEs** – siglas en inglés –) resultan de la oxidación en la atmósfera de Hg gaseoso elemental a formas altamente reactivas y, posteriormente, la eliminación rápida de las especies de Hg oxidadas a través de la precipitación. En el caso de Limnopolar la combinación emisiones volcánicas y amplificación de la señal por los procesos de la cuenca pueden explicar por si mismos los altos contenidos de Hg encontrados. Pero, los AMDEs ayudarían a reforzar los extraordinarios valores encontrados en algunas muestras de los sedimentos. Con la excepción de una correlación significativa entre la relación Br/C (usada como indicados de los eventos de agotamiento de Hg en este registro) y los valores más elevados de Hg, no hay otros datos que apoyen la relación entre el Hg y los eventos de agotamiento. Sin embargo la proximidad a la costa (< 2km) y las condiciones frías en las que se produjeron los mayores picos de Hg indican un ambiente muy favorable para que se produzcan los AMDEs.

Diferencias en el **tipo de vegetación** puede afectar a la deposición neta y retención del Hg en las turberas. Sin embargo en los registros incluidos en esta tesis doctoral no se llevó a cabo un muestreo sistemático de la vegetación que potencialmente podría haber afectado a acumulación de Hg en las turberas y sedimentos lacustres. Únicamente se recogieron muestras de vegetación en la campaña de muestreo de Isla de Pascua. Las determinaciones de Hg mostraron un rango muy amplio de concentraciones en estas muestras de vegetación, desde 342 ng g^{-1} a 11.117 ng g^{-1} correspondiendo este último valor a una muestra de un junco no identificado. Se especula con la posibilidad de que un incremento de la abundancia de los juncos, unido a condiciones más húmedas puedan ayudar a explicar el incremento de Hg alrededor del 20.000 cal BP y en general las mayores concentraciones de Hg en los periodos húmedos. Sin embargo no hay certeza de la presencia de juncos en la turbera y los datos disponibles de polen y macrorestos no ayudan a apoyar esta especulación.

El **clima** ha sido indudablemente el principal impulsor de la acumulación de Hg en los registros presentados en esta tesis doctoral. Con la excepción de Sandhavn, en los otros registros el clima ha desempeñado un papel principal, tanto directa como indirectamente. La amplia influencia del clima en los registros aquí presentados podría deberse a dos razones principales: i) la ubicación remota de los sitios de muestreo limita el efecto directo de las actividades de origen antrópico y / o ii) el largo período de tiempo cubierto por algunos de los registros

que incluyeron condiciones climáticas contrastadas (por ejemplo, la transición entre los climas secos y húmedos durante el Pléistoceno Tardío en las latitudes tropicales y subtropicales, como en Rano Aroi y Pinheiros).

Los registros de turba de Pinheiros y Rano Aroi proporcionaron una oportunidad excepcional para examinar cómo dos periodos climáticos principales -el Pleistoceno Lateral y el Holoceno- afectaron al ciclo del Hg en las latitudes tropicales y subtropicales. Los resultados de estos registros a largo plazo (Rano Aroi y Pinheiros) sugieren, como es generalmente aceptado por el monitoreo extensivo, que la deposición húmeda (es decir, el lavado de Hg por la lluvia) es la principal fuente de Hg a las turberas. Esto contrasta con estudios recientes dónde utilizando isótopos de Hg en registros a corto plazo se indica que el Hg gaseoso y particulado (es decir, deposición en seco) son las especies principales depositadas en las turberas. La larga perspectiva temporal proporcionada por los registros del Pleistoceno podría poner de relieve la dominancia de los procesos de deposición húmeda a largo plazo. Además, durante el evento Heinrich 1 (17.000 cal BP) caracterizado por condiciones secas y muy frías, la turbera de Pinheiros registró una concentración extraordinariamente alta de Hg. Un efecto similar se encontró en el registro de Rano Aroi al final del último máximo glacial (a 20.000 cal BP) cuando las condiciones húmedas prevalecieron en la Isla de Pascua. Ambos, condiciones más frías y húmedas habrían favorecido la acumulación de Hg ya que la deposición de Hg está controlada por variaciones de temperatura y humedad. El aumento de la oxidación de la turba entre ~ 40.000 y 42.000 cal BP que condujo a un aumento en las concentraciones de Hg también fue impulsado por las condiciones climáticas, más específicamente por un periodo largo de sequía.

En el Lago Hambre, los cambios en la productividad primaria en el lago durante los últimos ~ 4.500 cal BP, e indirectamente también los cambios en el contenido de Hg en los sedimentos, se relacionaron con TSI, la irradiancia solar total; que es, obviamente, un parámetro climáticos.

La congelación y descongelación del hielo del lago reguló la acumulación de Hg en el Lago Limnopolar y en su cuenca. Los procesos de congelación-descongelación también son controlados directamente por el clima. La capa de hielo-nieve sobre el lago y la cuenca pudo haber actuado como sumidero de Hg durante 9-10 meses al año. Durante los períodos de condiciones climáticas frías largas se puedo haber extendido el efecto de trampa de Hg de años a décadas. Esto

es consistente con las altas concentraciones de Hg (y las tasas de acumulación) correspondientes a las fases de mínimos en insolación (períodos más fríos) como los mínimos de Wolf, Spörer, Maunder y Dalton.

En cuanto a los **aspectos metodológicos**, parece que el análisis espectroscópico en combinación con el análisis multivariado, en particular PLS, puede utilizarse de manera eficiente y fiable para predecir las concentraciones de Hg en la turba minerogénica, al menos dentro del mismo testigo. Este enfoque puede utilizarse para reducir los costos de los enfoques multi-testigo que facilitando el estudio de la variabilidad espacial dentro y entre los turberas.

Esencialmente, los sedimentos de los lagos y las turberas son archivos ambientales que pueden utilizarse como registros de Hg depositado atmosféricamente, proporcionando así una "imagen" del ciclo de Hg. Sin embargo, el uso de estos archivos como registros atmosféricos Hg está condicionado por factores que operan en diferentes escalas geográficas y temporales. Por tanto, el Hg determinado en las muestras no refleja directamente la deposición atmosférica, si no que es el resultado de una combinación cambiante de los ocho factores diferentes descritos en esta tesis.

2. Introduction

2.1. Mercury as a global pollutant

Mercury (Hg) is a naturally occurring element and is found throughout the world. Its volatility at ambient temperature and an unpredictable behaviour in the environment, make Hg fate on the environment "one of the most insidiously interesting and scientifically challenging biogeochemical cycles at the Earth's surface" (Fitzgerald and Lamborg, 2003). Furthermore, because of the toxicity of its methylated forms, both to wildlife and human health, Hg is considered as a metal of environmental concern (WHO, 1989).

The attention to health effects derived from Hg pollution began with a well-known poisoning accident in the 1950s, when Chisso Corporation's chemical residues were released into the nearby Minamata Bay, Japan. The wastewater discharge produced an increased amount of organic and extremely toxic Hg forms in the bay (methylmercury, MeHg), consequently boosting their contents in local marine organisms (mainly fish and shellfish) and entering in the food chain. This resulted in devastating health effects to local population who consumed fish as main food source (Kurland et al., 1960). Prenatal or postnatal exposure to MeHg produces neurological impacts in adults and children, including sensory disturbance, difficulty in coordinating movements, and tremors, among others symptoms (this syndrome is known as Minamata disease, (Harada, 1995). With increasing awareness of environmental stewardship, an incidence of acute Hg

poisoning from industrial pollution like Minamata's has become rare. However, the scale of chronic exposure to a lower dose of Hg as a result of global pollution or occupational hazard has grown (Ha et al., 2017).

According to the Food and Agriculture Organization (FAO) and the World Health Organization (WHO), billions of people are at risk of high exposure to poisoning by Hg due to their diet rich in fish (high content of MeHg) (World Health Organization, 2011) or by exposure of Hg emitted by artisanal and small-scale gold mining, mainly in low- and middle-income countries (Veiga et al., 2006). Recent research estimated that 112000 tons of Hg have been emitted directly to the atmosphere since 1850 from by-product sources (fuel combustion, cement production, metal smelting, large-scale gold mining with non-Hg methods) and 720000 tons of Hg were mined during the same period for commercial use (Streets et al., 2011). Commercial Hg use includes: Hg-containing products (e.g., batteries) and manufacturing processes that involve Hg (e.g., vinyl chloride monomer production). Other studies include an additional 540000 tons of Hg from other commercial Hg uses and non-atmospheric discharges from chlor-alkali plants and mining (Horowitz et al., 2014). The effects of artisanal and small-scale gold mining are also remarkable. For example, it has been calculated that this activity has released about 2000 to 3000 tons of Hg to Brazilian Amazon environment since 1980's (Malm, 1998).

In last decades, these concerns have drawn the attention of the political agenda. Following the international actions, the European Union (EU) adopted in 2005 the "Community Strategy Concerning Mercury" (COM, 2005). The Strategy aimed to reduce Hg levels both in relation to human exposure and the environment, addressing most aspects of the Hg life cycle. It identified twenty priority actions to be undertaken, both within the EU and internationally. The degree of implementation of these actions was reviewed in 2010, and it was declared that the implementation of the Mercury Strategy was in an advanced stage (COM, 2005). However the text highlighted the necessity of further international actions for the coming years. Giving the global aspect of the Hg problem, internal EU legislation alone cannot guarantee effective protection of the population.

In 2013 the EU signed the Minamata Convention on Mercury, spearheaded by the United Nations Environment Programme with the aim "to protect the human health and the environment from anthropogenic emissions and releases

of mercury and mercury compounds" (UNEP, 2013). The European Commission adopted on February 2, 2016 a ratification package that will allow the EU to ratify the Convention once the legislative process is concluded. On December 1, 2016 Minamata Convention has 128 signatures and 35 ratifications (Minamata Convention on Mercury web).

The Article 19 section (e) of the Minamata Convention, concerning to Research, development and monitoring, highlights the necessity of cooperating to develop and improve the *Information on the environmental cycle, transport (including long-range transport and deposition), transformation and fate of mercury and mercury compounds in a range of ecosystems, taking appropriate account of the distinction between anthropogenic and natural emissions and releases of mercury and of remobilization of mercury from historic deposition* (UNEP, 2013). It therefore stresses the need to investigate current sources of Hg and their impact on the environment and health; as well as studying the mercury cycle, in the present and the past.

2.2. Global biogeochemical mercury cycling

2.2.1. Chemical species of mercury

The chemical symbol for mercury, Hg, is derived from the Latin name hydrargyrum, which means silver water. The name refers to the appearance of elemental mercury (Hg^0) which is readily recognized as a silvery liquid at room temperature and has a high vapour pressure (Brown et al., 2008) for a heavy metal. In the natural environment, it can exist in the gaseous or liquid state. Gaseous elemental mercury (GEM) is the dominant form in the atmosphere. Most natural waters are nearly saturated, or even supersaturated with respect to the atmospheric Hg^0 (Morel et al., 1998; Fitzgerald et al., 2007).

However, other species of Hg occur naturally in the environment. Elemental Hg can be oxidized into divalent mercury (Hg II), in the atmosphere, and washed out by rainfall (Hall, 1995). Mercury divalent compounds, both organic and inorganic, exist in gaseous, dissolved and solid states, being Hg (II) much more prevalent in waters than in the atmosphere (Swartzendruber and Jaffe, 2012). Although it is not a chemical Hg species, particulate-bound mercury, or Hg (p), refers to Hg that is extracted from particles, either airborne or waterborne. It has been shown that the observed Hg (p) concentration depends on the size of particles that are collected

by the technique, for example most airborne measurements include only particles < 2.5 μm (aerodynamic diameter) (Swartzendruber and Jaffe, 2012). Finally, monomethylmercury and dimethylmercury (MMHg or Me-Hg and DMHg) are organic forms of Hg. They are organometallic compounds formed by of one/two methyl groups (CH_3)/(CH_3-)$_2$ bonded to a Hg ion. Hg (II) can be readily methylated in aquatic systems. Mercury methylation appears to be predominately biotic, although some abiotic production is likely in natural waters (Benoit et al., 2002). Both methyl compounds are significantly toxic and Me-Hg can accumulate up the aquatic food chain and lead to high concentrations in predatory fish (National Research Council, 2000).

2.2.2. Sources and reservoirs of mercury: mercury cycle

The traditional classification of Hg sources as natural, mixed or anthropogenic, is useful to stress the emission mechanisms to the environment. Volcanoes, geothermal vents and emission by natural enriched soils are considered purely natural emissions, while land emissions, forest fires and ocean emissions are considered as mixed sources because a significant fraction of their Hg burden was previously deposited including some anthropogenic Hg (Selin et al., 2008). Anthropogenic Hg can be sourced from a wide array of activities. For the year 2000 the largest sources, in order of importance, were: coal combustion, gold production, nonferrous metal smelting, cement production, waste incineration and caustic soda manufacturing (Pacyna et al., 2006). Other additional sources account for the emissions in relation to various uses of Hg as battery making or production of electrical lighting, wiring devices and electrical switches (Pacyna et al., 2006).

However, research in the last decades has demonstrated that the Hg fluxes within and between different reservoirs (air, soils, oceans, ice, atmosphere) are also relevant for defining its global biogeochemical cycle (e.g. Mason and Sheu, 2002; Sunderland and Mason, 2007; Selin et al., 2008; Holmes et al., 2010; Smith-Downey et al., 2010; Driscoll et al., 2013) (Figure 1). This led to the adoption of a different classification of Hg sources as primary and secondary sources, having into account not only the initial emission, but also the subsequent transferences to other compartments and the processes involved.

Primary sources transfer Hg from long-lived lithospheric reservoirs to the atmosphere and then to land and oceans, i.e. increasing the global pool of Hg in

surface reservoirs (Driscoll et al., 2013). They would include naturally originated Hg (e.g. from weathering of Hg-rich materials and volcanic emissions). Degassing carries out the natural mobilization of Hg from the geogenic reservoirs through volcanic emissions, and are estimated around 500 Mg Hg yr^{-1} (Selin et al., 2008), ranging between 80 and 600 Mg yr^{-1} (see references in Driscoll et al., 2013). Studies on Mt. Etna emissions (Sicily, Italy) determined that only 1% (by mass) is in of particulate form, and Hg^0 is the main species (Bagnato et al., 2007). However, primary sources are nearly always augmented by human activities (mining, fuel combustion, waste incineration) (Mason et al., 1994; Mason and Sheu, 2002).

Most Hg in the atmosphere is in the form of Hg^0 emitted from primary sources, although there is also Hg (II) and Hg(p) that are released by fuel combustion (Selin et al., 2008). The Hg life time in the atmosphere is ~0.5 years (Selin et al., 2008), allowing a long transport from the sources to remote locations such as the Arctic and Antarctica (Lindqvist and Rodhe, 1985; Mason et al., 1994; Ebinghaus et al., 2002; Sigler et al., 2003; Ariya et al., 2004; Lindberg et al., 2007; Durnford et al., 2010; Dastoor et al., 2015; Steffen et al., 2015).

After deposition, Hg can be reemitted from the surface reservoirs to the atmosphere, therefore constituting a secondary source. Mercury from secondary sources is then spread among and within ecosystems (Driscoll et al., 2013). Recycling from surface reservoirs results in an effective lifetime of 1.6 years against transfer to long-lived reservoirs in the soil and deep ocean (Selin et al., 2008).

Due to its volatility as Hg^0 and the redox transformations of Hg in environment, deposition and evasion are influenced by multiple environmental factors including seasonality, vegetative cover and its life cycle, temperature, light, moisture, atmospheric turbulence and the presence of reactants that change with the surfaces e.g. soil, water or snow (Zhu et al., 2016).

In land surfaces, on which ~60% of the Hg is deposited (Mason and Sheu, 2002), meteorological parameters (e.g., solar radiation, soil/air temperature, atmospheric turbulence), soil substrate characteristics (e.g., Hg content, soil moisture, organic matter, porosity and microbial activity), and ambient air characteristics (e.g., Hg^0 and O_3 concentration) can influence the air–surface exchange of Hg^0 (Zhu et al., (2016) and references there in). It is remarkable the role of solar radiation in controlling Hg emissions from soil substrates, enhancing Hg (II) reduction to Hg^0

and facilitating its evasion (Gustin et al., 2002). By this mechanism –facilitated reduction from the Hg pool of the soil- for example, agriculture operations resulting that disturb the soil surface, as tilling, may be important sources of Hg to the atmospheric (Bash and Miller, 2007).

Similarly, vegetation plays an important role as Hg pool. Isotopes measurements have shown that freshly deposited Hg – more reactive with respect to volatilization and methylation than the native Hg- that is not immediately volatilized, is associated preferentially with vegetation (Hintelmann et al., 2002). Biomass burning releases around 600 Mg yr^{-1} (annual average for the period 1997 – 2006), which is equivalent to 8% of the total Hg emission (Friedli et al., 2009). Other processes affecting land, as for example runoff, are sometimes neglected in global Hg models (Selin et al., 2008) although it was estimated as 40 Mg yr^{-1} for pre-industrial times (Mason et al., 1994).

The deep-ocean sedimentation is the ultimate sink of Hg (Selin, 2009; Mason et al., 2012). Atmospheric deposition is the dominant source of Hg to most remote water bodies (Mason et al., 1994; Selin et al., 2008) and similar to freshwater and land systems; Hg (II) can be deposited by dry and wet deposition and Hg0 as dry deposition (Selin, 2009). The contributions from other sources to open ocean regions are much smaller on a global scale (Mason et al., 2012). Inputs from rivers could be equivalent to 25 to 41% of atmospheric deposition in Surface Atlantic, North Pacific and the Mediterranean Sea, but unimportant in the North Atlantic or the rest of the Pacific (Sunderland and Mason, 2007). On the other hand, hydrothermal vents are estimated to contribute to less than 20% of atmospheric inputs (Lamborg et al., 2006; Mason et al., 2012).

In surface waters, processes controlling the concentration of dissolved gaseous Hg directly regulate air-water Hg^0 flux (Zhu et al., 2016). More than ~70% of the Hg deposited in the ocean is re-emitted to the atmosphere as Hg^0 but also some as $(CH_3)_2Hg$ (Mason and Sheu, 2002; Soerensen et al., 2010; Corbitt et al., 2011). Evasion as Hg^0 and Hg removal from the surface ocean by particle scavenging reduce the pool of potentially bioavailable Hg(II) that may be methylated (i.e. toxic forms) and bioaccumulated into marine organism (Mason et al., 2012).

Polar regions are areas in which Hg retention is of particular interest due to the high concentrations found in the biota – mainly in the Arctic (Muir et al., 1992; Atwell et al., 1998; Douglas et al., 2012; Kirk et al., 2012) and to a lesser extent

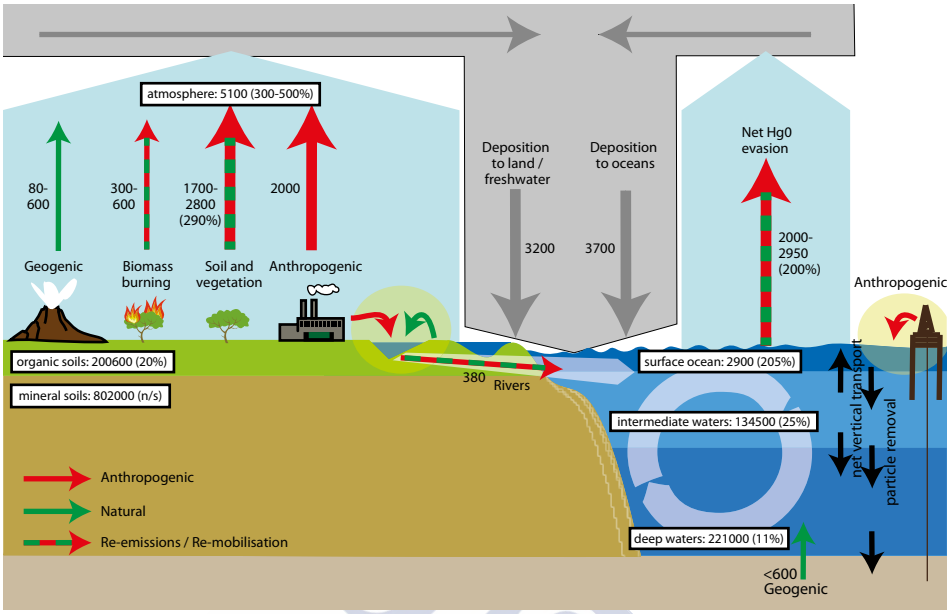

Figure 1. The global mercury cycle from AMAP (2013), adapted from Mason et al., 2012

in Antarctica (Bargagli et al., 1998; Bargagli, 2008; Carravieri et al., 2013) - and because of the predicted increase (~25%) in atmospheric Hg deposition in the Arctic by 2020 (AMAP, 2011). Since the observation of episodes of unexpected low Hg^0 air concentrations – known as Atmospheric Mercury Depletion Events (AMDEs) (Schroeder et al., 1998)-, first in the Arctic air during springtime and later in Antarctica (Ebinghaus et al., 2002), there has been an increasing interest to characterize and study their impact in the global Hg cycle (e.g. Holmes et al., 2010). Halogens (mainly atomic bromine and bromine oxide) are thought to play essential roles in AMDEs (e.g. Ariya et al., 2002, 2004; Calvert and Lindberg, 2003; Simpson et al., 2007; Faïn et al., 2008), in the proposed mechanisms (i.e. photo-chemical activation under daylight and marine evasions under darkness (Faïn et al., 2008; Nerentorp Mastromonaco et al., 2016)). Although it is known that this process also occurs at temperate and low latitudes (Obrist et al., 2011), in the Arctic it is estimated that AMDEs alone are responsible for the deposition of up to 100 tons of Hg per year north of the polar circle (Ariya et al., 2004; Durnford and Dastoor, 2011) constituting a significant part of the region's annual Hg deposition (i.e. Ariya et al., 2004). Between 20 – 50 % of the freshly deposited, highly reactive (Lalonde et al., 2002) Hg during AMDEs is returned from the snow cover to the atmosphere within 24 hours (see references values in Durnford et al.,

2012). Sublimation and snow melting could also release Hg that was retained by processes such as burial through snow accumulation or ice layer formation (Douglas et al., 2008). Furthermore, recent research in East Antarctica proposes a net microbial methylation, probably carried out by microaerophilic bacteria such as Nitrospina, within the sea ice together with methylmercury photodegradation, and microbial Hg(II) and Hg^0 volatilization (Gionfriddo et al., 2016).This would imply annual (Antarctic) sea ice as one plausible source of MeHg in the (Southern Ocean) marine ecosystem (Gionfriddo et al., 2016).

2.2.3. Global biogeochemical mercury cycle: anthropogenic and climate change. Uncertainties.

It is not likely that the previously described Hg cycle has been invariable over time. Factors as ice-content-extent, ocean surface temperature, soil carbon content, riverine discharge, type of precipitation – rain vs. snow -, and methylation rates (between others), control Hg dynamics in different environments, and all of them are closely affected by climate (e.g. Selin, 2009; Rydberg et al., 2010a; Denkenberger et al., 2012; Stern et al., 2012; McKinney et al., 2015). In addition to this, human activity has played a key role increasing the emission of Hg to the environment (see Section 2.1 Mercury as a global pollutant). Both, climatic and anthropogenic factors make that the biogeochemical cycle of Hg particularly susceptible to global change (Stern et al., 2012).

Regarding human activity, several works have estimated the Hg fluxes at present-day and before preindustrial activities, establishing two differentiated Hg cycles: the current and the preindustrial global Hg cycle (e.g. Mason et al., 1994; Mason and Sheu, 2002; Selin et al., 2008). In their global model, Selin et al., (2008) estimated an extra input of 3400 tons of Hg per year by anthropogenic activities, increasing in 3550 tons of Hg the atmosphere (versus the 2050 tons in pre-industrial times) and rising the deposition on the soil and on the ocean (Selin et al., 2008). Thus, the higher Hg input to the superficial oceans waters may affect the methylmercury accumulated in ocean fish, which derives from in situ production (Mason et al., 2012).

According to the model (Selin et al., 2008), enrichment factors (i.e. present-day versus preindustrial times) vary geographically around the world. Mercury enrichment factor is > 2 everywhere, indicating the global extent of Hg pollution. In Central Africa it is > 4, due to the effect of artisanal mining, and it exceeds

5-fold in Eastern Europe and 10-fold in East Asia (Selin et al., 2008). Even more, Hg0 fluxes – from the surface reservoirs to atmosphere - are statistically higher in East Asia than those observed in other world regions (Zhu et al., 2016); but if this is because Hg in this area currently accounts for almost 40% of the total primary global anthropogenic emissions, (mainly from coal combustion data from 2010, (Pirrone et al., 2010; AMAP/UNEP, 2013), or is due to changes in the secondary remissions (Zhu et al., 2016) is still unknown. So, despite the available data, factors influencing the dynamics of Hg sources and reservoirs are still not clear, bringing uncertainties about the processes driving Hg environmental distribution.

Regarding climate factors, there are also large uncertainties about the Hg cycle. In general, a weaker global circulation and elevated temperatures will affect atmospheric oxidation rates and patterns of deposition globally (Krabbenhoft and Sunderland, 2013). In land areas where ecosystems primary productivity is stimulated by precipitation and CO_2, Hg retention by soils will likely increase (Hararuk et al., 2013) although changes in wildfires dynamics (high frequency, scale and intensity) may result in higher emissions from soils (Amos et al., 2013). Recent reviews for the Arctic (e.g. Macdonald et al., 2005; Stern et al., 2012; McKinney et al., 2015) - whose conclusions might be comparable to other areas - showed that warmer conditions could drive Hg cycle both increasing and decreasing their risk in the environment. Higher Hg emissions are expected from melting glaciers, permafrost, and wetlands driven by C losses (e.g. Rydberg et al., 2010a; Stern et al., 2012), and several processes may theoretically increase net Hg methylation in Arctic ecosystems as warmer, longer ice free seasons are more frequent, or by enhancing inputs of soil nutrients (between other) (Schuster et al., 2011; Stern et al., 2012). On the other hand, processes that may also be enhanced under warming temperatures may produce a decrease in Hg availability, as elevating photo-demethylation rates or the increase in particles loading into aquatic systems due to the ice-permafrost melting, through increased scavenging and burial of Hg (Stern et al., 2012). The effects of a changing Hg cycle in food webs are also considered complex and uncertain (Stern et al., 2012; McKinney et al., 2015).

In a global perspective, there is agreement that although the main factors controlling Hg fluxes have been identified and the links between environmental Hg cycling and major global change drivers (warming, hydrology, and emission controls) are moderately understood, this is not enough (Krabbenhoft and

Sunderland, 2013; Zhu et al., 2016), and more research is needed because *it remains challenging to forecast a future environment driven by multiple synergistic and antagonistic drivers operating simultaneously* (Krabbenhoft and Sunderland, 2013).

2.3. State of the Art

In this context of global change, the use of environmental archives in Hg research is essential, as they provide a unique link between current and past Hg loadings to the environment (Biester et al., 2007). Environmental or natural archives are those physical (natural) structures that due to their process of formation and evolution can store environmental information; they constitute the abiotic memory function of ecosystems (Martínez Cortizas, 2000).

According to the International Atomic Energy Agency (IAEA, web), the main characteristics of an ideal archive are: i) high temporal resolution; ii) responsive to small changes in one or a few environmental variables; iii) be a closed system to retain information; iv) record a continuous time series of variation; v) be global in distribution; and vi) be accurately and precisely datable. Although none meet all of the ideal criteria, the most frequently used natural archives are: peatlands, lake sediments, marine sediments, corals, ice-snow, tree rings and speleothems. Despite the huge potential of natural archives to help to understand the human footprint on the environment, the *experience has shown that these archives must be examined with an understanding of the processes* because they can modify the story told by the records (Blais et al., 2015).

Peatlands, lake sediments and glacial snow/ice have been extensively employed in reconstructing past Hg deposition histories worldwide, since they are widely believed to accurately preserve the deposition history through time, either as a direct record or modulated by an indirect signal (Goodsite et al., 2013). However, the evaluation of the characteristics and problems associated with the use of natural archives to reconstruct past Hg fluxes (e.g. Shotyk, 1996; Benoit et al., 1998; Biester et al., 2007; Goodsite et al., 2013; Cooke and Bindler, 2015; Hansson et al., 2015), indicates that there are advantages and disadvantages and that the biogeochemical information provided by each type of archive is supplementary and complementary. For example, (Biester et al., 2007) found a disagreement between lake sediments and peatlands in the estimation of Hg atmospheric depositions rates corresponding to the last decades; while the former

show an increase of 3-5 times the background, peat studies suggests increases of up to 30 to 500-fold. This inconsistency was attributed to an overestimation of Hg accumulation due to an underestimation of peat ages and a poorly understood Hg behaviour during peat diagenesis (Biester et al., 2007). Another example of complementarity of the information provided by the archives is provided by an evaluation of four types of archives (lake sediments, glacial ice, marine sediments and peat records) to reproduce recent trends in atmospheric Hg deposited in the Arctic (Goodsite et al., 2013). While glacial ice on Greenland Summit seems to be an accurate record of gaseous Hg0 deposition, corroborated with aerosol data for the last decades, data from lake sediments and peatlands from northern Canada and southern Greenland (respectively) showed many discrepancies (Goodsite et al., 2013). They showed a poor agreement with estimations from ice records and direct measurements, probably due to climate-driven changes in Hg transfer rates from air to catchments, waters and subsequently into sediments, and post-depositional diagenesis in peatlands (Goodsite et al., 2013). Thus, the insufficient knowledge of the processes that affect the reconstruction of Hg deposition fluxes seems problematic for understanding the global Hg cycle as well as the perturbations by anthropogenic activity.

2.3.1. Ice and snow

During centuries and millennia, ice and snow accumulate in cold regions at high latitudes as well as in mountain areas of mid and tropical latitudes. Mercury deposited from the atmosphere is retained in snow and ice layers that accumulate and compact through time. The potential of polar ice sheets as palaeoenvironmental archives has been widely recognize, mainly because the extensive use of ice cores to reconstruct climate change (Petit et al., 1981, 1999) and past atmosphere composition (e.g. Schwander et al., 1988; Etheridge et al., 1996). Studies performed in Summit Station, Greenland, demonstrated that despite post-depositional processes (as photoreduction) may modify atmospheric Hg daily concentrations, the deeper firn air should provide a record of past atmospheric Hg0 changes (Faïn et al., 2008, 2009; Zheng, 2015).

Early studies on remote Arctic areas using ice cores (Weiss et al., 1971, 1975; Dickson, 1972; Appelquist et al., 1978) found excessively high Hg concentrations, up to 900 pg g^{-1} (vs. <0.05 – 2.0 pg g^{-1} in the last studies), whose temporal and spatial changes were not consistently explained by sample contamination and

were attributed to human impact (Boutron et al., 1998). Modern studies in the North American Arctic, using ultra clean procedures, have shown Hg increases during the Colonial Period (~1603–1850) and North American "Gold Rush" (1850–1900) (Schuster et al., 2002; Beal et al., 2015). However, these increases represent minor fractions in relation to the maxima occurred during the 20th, which reached the zenith between the 1970s and 1980s, followed by a general decrease likely due to reduced emissions (Schuster et al., 2002; Faïn et al., 2009; Beal et al., 2015). A study based on an ice core from Himalaya-Tibet suggests a similar Hg depositional history, rising at the onset of the Industrial Revolution followed by a dramatic increase after World War II, but differs for recent decades as it does not show a declining trend since the mid- to late-1900s, as there was no reduction in Hg emissions in Asia (Kang et al., 2016).

Despite the human influence in Hg emissions, ice-records have effectively captured natural emissions as volcanic activity. For example, Schuster et al., (2002) found three major volcanic events (Tambora, Krakatau, and Mount St. Helens) that contributed to 6% of the total Hg accumulated in ice cores from Wyoming (North America). Long records collected in Antarctica (from tens of thousands to hundreds of thousands of years) showed increases in Hg deposition during the Last Glacial Maxima (~18 000 years) (Vandal et al., 1993) and all the coldest climate stages during the last 670 000 years (Jitaru et al., 2009). Although these increases were initially associated with increased marine productivity – as a main source of pre-industrial Hg - (Vandal et al., 1993), a increased in oxidation of Hg^0 by sea-salt-derived halogens in the cold atmosphere seems the most probable explanation (Jitaru et al., 2009).

Notwithstanding the quality of the information provided by ice cores as records of global signals, they present several disadvantages as archives. Their limited geographical distribution and the remote location of sites susceptible to sampling restrict the sampling areas and increase logistic costs. Thus, with the exception of Greenland, North American Arctic and Antarctica, the data available for other areas of the world is scarce and dispersed, e.g. Western China (Zhang et al., 2012), Himalaya (Kang et al., 2016). Another main problem is obtaining an accurate absolute ice-core chronology (Gabrielli and Vallelonga, 2015) necessary for reconstruction.

2.3.2. Lake sediments

Lake sediments are composed of a mixture of organic and inorganic material generated within the own lake and by fluxes from the catchment and the atmosphere. The continuous deposition builds a sequence in which Hg is effectively retained (Rydberg et al., 2008). Unlike ice cores, lakes are widely distributed throughout the world and their sediments have been used in many locations as archives of Hg historical deposition; between other, **North America** (Thomas, 1972; Johnson et al., 1986; Rada et al., 1989; Swain et al., 1992; Swain, 1997; Kamman and Engstrom, 2002; Engstrom et al., 2007; Outridge et al., 2007; Mast et al., 2010; Rossmann, 2010; Drevnick et al., 2016; Wiklund et al., 2017), **Greenland** (Bindler et al., 2001a; Lindeberg et al., 2006), **Scandinavia** (Bindler et al., 2001b; Lindeberg et al., 2007; Rydberg et al., 2008), **Svalbard** (Drevnick et al., 2012), **United Kingdom** (Aston et al., 1973; Yang and Rose, 2003; Yang et al., 2016), **Pyrenees** (Corella et al., 2017), **Patagonia** (Guevara et al., 2005; Ribeiro Guevara et al., 2010; Hermanns and Biester, 2013a, 2013b; Hermanns et al., 2013; Rizzo et al., 2014; Daga et al., 2016), **Brazil** (Lacerda et al., 1999), **Andes** (Cooke et al., 2009a, 2009b, 2011),**Tibet** (Yang et al., 2010a; Kang et al., 2016) or **Uganda** (Yang et al., 2010b). Despite this wide geographic distribution, most investigations were done in Northern United States and Canada.

The increased in Hg concentration due to the effect of human activity has been recorded by lake sediments. Pre-Colonial mining and smelting activities, that generated a substantial Hg pollution, have been recorded in lake sediments from the Andes area (Cooke et al., 2009b, 2011), where mining produced a peak in Hg as early as ~500 BC and AD ~1450 during Chavín and Inca states (Cooke et al., 2009b), whereas smelting activities resulted in Hg 20-fold higher than background concentrations (at AD ~1200) (Cooke et al., 2011). Pre-industrial (AD ~1550) Hg pollution derived from mining activities was also recorded in lakes of the Pyrenees by (Corella et al., 2017), with enrichments of up to ~2. Nevertheless, a recent study indicates that atmospheric Hg emissions from early mining were modest at a global scale as compared to more recent industrial-era emissions (Engstrom et al., 2014).

The increase in Hg emissions due to modern industrial activity has been clearly recorded in sediments from several lakes around the world (e.g. Aston et al., 1973; Rada et al., 1989; Bindler et al., 2001b; Mast et al., 2010; Yang et al., 2010a,

2016), as well as recent decreases in North America and Europe (e.g. Bindler et al., 2001b; Mast et al., 2010). Additionally, lake sediments have also recorded Hg deposited after long-range transport, in particular in lakes from remote areas; e.g. cores collected in northern Canada showed increasing Hg inputs from 1500's and more rapidly after AD 1750 and 1900 (respectively) due to the effect of regional-global emissions in an area with no local industrial sources of Hg (Lockhart et al., 1995). Data from lake sediments from remote regions of Tibet show the current increasing trend in pollution in Asia with a start around the AD 1970s and 1980s due to the Asian Industrial revolution (Yang et al., 2010a).

Contributions form natural sources have also been recorded. Mercury emissions from volcanic activity and forest fires have been registered in mountain lakes from the Northern Patagonian Andes, a region highly susceptible to volcanic activity because it is part of the Southern Volcanic Zone – it includes at least 60 historically and potentially active volcanoes (Ribeiro Guevara et al., 2010; Daga et al., 2016).

Despite all of this, several investigations have also identified processes that may alter the concentration of Hg in lake sediments, complicating their use as archives of atmospheric deposition.

The **size and land uses of the watershed** have been proved to have a relevant influence on Hg concentrations in the sediments (e.g. Fitzgerald et al., 2005; Engstrom et al., 2007; Drevnick et al., 2016). A recent extensive study (165 dated sediments cores from 138 lakes across western North America) on Hg accumulation rates showed that, for lakes not directly affected by point sources (smelter or mining activity), two groups were clearly discernible: i) lakes with little or not watershed perturbation and ii) lakes with watersheds with an extensive agricultural or urban cover (Drevnick et al., 2016). The disturbance of the watershed, by reducing Hg retention by soils and enhanced Hg deposition in urban areas, may be the main cause of this separation (Drevnick et al., 2016). Inputs by erosion and watershed runoff could be equal or higher than the direct atmospheric deposition, also in relatively small catchments (Fitzgerald et al., 2005).

The effect of Hg **mobility in sediments and diagenesis** have been considered as likely processes since the fist works (e.g. Aston et al., 1973; Matty and Long, 1995). Lockhart and co-authors (Lockhart et al., 2000) tested Hg mobility using lake records from Canada with an independently known history of Hg inputs, finding a good agreement. Some studies also addressed in detail the role of organic

matter and its digenesis – chemical and physical changes that occur within the sediment after deposition (Sanei and Goodarzi, 2006; Rydberg et al., 2008). In spite of the important role of soluble organic matter in Hg concentrations and the 20-25% of carbon loss after the first 10-15 years, not obvious loss of Hg was found over time (Rydberg et al., 2008).

Finally, and not far from the role of the organic matter, within lake **primary productivity** has been shown to have a significant effect on Hg accumulation, mainly through faster rates of algal - scavenging and sedimentation (Outridge et al., 2007; Stern et al., 2009). These investigations suggest that these processes, which are climatically driven, could imply an overestimation of atmospheric Hg contributions to High Arctic lakes, since the increased productivity may enhance the accumulation of Hg in sediments without significant variations in atmospheric fluxes.

2.3.3. Peatlands

Peatlands are wetlands formed by the accumulation of peat and have current peat-forming vegetation. Peat – dead and decaying plant material - accumulates because the net production of organic matter exceeds its decomposition. On their surface, atmospherically deposited elements, such as Hg, can be trapped. The continuous growth of the peat deposit allows the record formation. Similar to lakes, peatlands are world wide distributed: they cover over 400 million ha in about 180 countries (Parish et al., 2008). Thus, peatlands have been abundantly used as Hg deposition records; in **North America** (Norton et al., 1997; Benoit et al., 1998; Givelet et al., 2003; Roos-Barraclough et al., 2006; Outridge and Sanei, 2010; Outridge et al., 2011), **Greenland** (Shotyk et al., 2003), **Scandinavia** (Pheiffer-Madsen, 1981; Shotyk et al., 2003; Bindler et al., 2004; Steinnes and Sjøbakk, 2005; Rydberg et al., 2010a), **Faroe Islands** (Shotyk et al., 2005), **United Kingdom** (Coggins et al., 2006; Farmer et al., 2009), **Germany** (Biester et al., 2012), **Switzerland** (Roos-Barraclough et al., 2002), **Belgium** (Allan et al., 2013), **Czech Republic** (Zuna et al., 2012), **France** (Enrico et al., 2016), **Spain** (Martínez Cortizas et al., 1999, 2012; Corella et al., 2017), **China** (Tang et al., 2012; Li et al., 2016), **Patagonia** (Biester et al., 2002, 2003; Franzen et al., 2004) and **New Zealand** and **Nova Scotia** (Lamborg et al., 2002).

Several investigations performed on peat cores were able to show the effect of industrial pollution, although the sources were not always clearly identified. For

example, the study of three peat cores from western Ireland showed maximum Hg accumulation occurring between AD 1950 and 1970, and concentrations were significantly lower than those found in other European peat records (Coggins et al., 2006). The authors related the chronology of Hg pollution with the influence of North American sources, due to long-range transport, and the lower concentrations with the prevailing westerly winds bringing clean, marine air to the sector. Another multisite study, using cores from different areas in Scotland, recorded Hg maxima at different times possibly reflecting local/regional influences until AD 1970s (Farmer et al., 2009). Similarly, regional anthropogenic Hg sources during and after the Industrial Revolution – coal burning and smelter Hg emissions – may have been responsible for the extremely high accumulation rates in peatland records from Eastern Belgium, which exceeded the pre-Industrial values by a factor of 63 (Allan et al., 2013), much higher than 4.2 fold found in Northern Spain (Martínez Cortizas et al., 2012) and 4 in Sweden (Bindler et al., 2004).

Peat records also recorded other modifications in atmospheric Hg deposition. For example, an 8000 years reconstruction in Canadian peatlands showed the effect of biomass burning for agricultural activities by Native North Americans (Givelet et al., 2003). The increase in rainfall had a positive effect by increasing the deposition of Hg emitted to the atmosphere by different sources, as metal smelting from ancient China cultures (Tang et al., 2012) and volcanic emissions (Roos-Barraclough et al., 2002).

An exceptional use of Hg records was the one developed by Martínez Cortizas and co-authors (Martínez Cortizas et al., 1999). Using a 4000 years record from Northwest of Spain they demonstrated that changes in temperature may have influenced Hg deposition and Hg thermal stability in peat. Cold climates seem to have promoted an increase in Hg accumulation as well as the preservation of Hg with low thermal stability. Conversely, lower accumulation and larger proportions of Hg with moderate to high thermal stability characterized warm climates. The findings have not only implications for the Hg cycle, but also Hg thermal lability was proposed as a paleotemperature proxy (Martínez Cortizas et al., 1999).

However, there are still issues to be solved regarding the use of peat cores to reconstruct Hg atmospheric deposition. Some of them have been previously identified and revised (e.g. Benoit et al., 1998; Biester et al., 2007).

One of the main issues concerns the **spatial variability** in the Hg accumulation

within the same peatland. The studies (e.g. Bindler et al., 2004; Martínez Cortizas et al., 2012) show that within bog variability is high, and data for a single core reconstruction do not necessarily provides a representative estimation of atmospheric fluxes (although chronologies were quite similar). Bindler et al. (Bindler et al., 2004) suggest that, for a reliable reconstruction of Hg fluxes, it is the necessary to incorporate data from multiple sites or at least multiple cores. As the work done by Allan et al., (2013) shows, this approach can provide excellent results. However, the cost and logistics are sometimes an insurmountable problem.

Related to the within bog variability it is the effect of **vegetation type** in Hg sequestration. Rydberg et al., (2010b) analysed for Hg living plants in a mire from northern Sweden with two different types of vegetation. They found differences in peat and living mosses depending on whether the area was pine-covered or had no tree vegetation and significant differences in Hg concentrations for two Sphagnum species.

The effect of **decomposition of the peat organic matter** and its role on the release of Hg, is another issue that has been considered in several investigations. In peat sections dated to pre-anthropogenic times Hg enrichments were found to coincide with comparatively low C/N ratios, which indicate higher peat decomposition (Biester et al., 2003). The increase in peat humification promoted by dry conditions at the surface of the peatland, may lead to a 2-3 fold increase in Hg concentrations independent of the changes in atmospheric deposition (Martínez Cortizas et al., 2007). Because of this, (Biester et al., 2003) suggested that all peat properties affected by humification processes should be normalized to the same degree of humification using a "Mass Loss Compensation Factors". On the contrary (Zaccone et al., 2009) did not found a major effect of the degree of decomposition in Hg concentrations, concluding that atmospheric deposition was the main driver of Hg fluxes during the last decades.

Other processes that could modify the suitability of peatlands as archives of Hg deposition were discussed by Biester et al., (2007). As previously mentioned, one of the focus of their critical review was to understand the differences in Hg deposition rates between lakes and peat cores (3-5 times vs. 30-500 times above the natural background, respectively). The authors suggest that peat decomposition may result in lower background Hg accumulation. At the same time, the downward migration and accumulation of ^{210}Pb at the limit of the water table could produce

and underestimation of peat ages and Hg accumulation rates as well.

3. Justification and Objectives

The previous sections have put in value the relevance of Hg for human health and the complexity of its global cycle in the environment. Similarly, the most commonly investigated environmental archives (ice-cores, lake sediments and peat records) have been proof to be useful to understand the Hg cycle in the past and in at present, and may also help to model future scenarios. However, following the recommendation of Blais et al., (2015), it is necessary to examine the underlying processes that occur in the archives to understand what is going on and unravel the true story.

In relation to this topic, several advances have been made in the last decade but on a limited sample of records; i.e. most of the studies are from Northern Hemisphere records – Mainly Europe and North America - and are based on Holocene (last 11,000 years) records. The few longer term studies, as those of (e.g. Vandal et al., 1993; Roos-Barraclough et al., 2002; Hermanns and Biester, 2013a), showed that other factors than human activity could have a main role in controlling Hg accumulation. This leads to the need to consider whether some of the processes that control the accumulation of Hg in the archives, such as the effect of decomposition, climate and human activity, occur at long time scales. Finally, with advances in the use of environmental proxies and the incorporation of new techniques, it is necessary to look for tools that allow a better understanding of the studied system as well as facilitate multi core or broader studies.

The main objective of this PhD thesis is to gain insights into the variations in atmospheric Hg deposition over long time scales (late Pleistocene and Holocene) in the Northern and Southern hemispheres, through the use of environmental archives (peat and lake sediments). Within this general objective, this work pays special attention to understanding how the processes that control and modify the deposition and accumulation of Hg in the environmental archives i) change their relative weight over time ii) in different environments and iii) the relationships between them. Figure 2 describes the research line followed in this thesis through a backward glance, from the Hg determined in the samples and the multiproxy approach to the processes – and the interaction between them – on a given time scale and location. A minor methodological aspect addressed is the application of cheaper, and low time consuming, techniques to aid in multi-core/multi-site studies and what kind of information can be obtained from them.

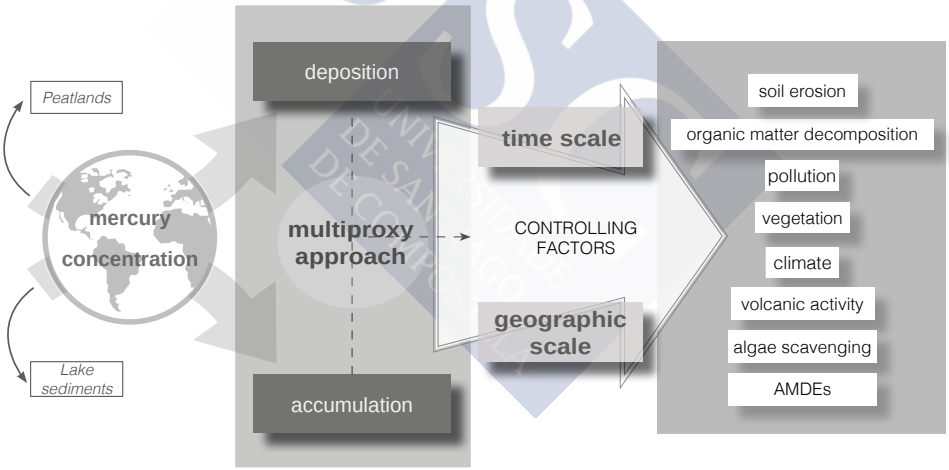

Figure 2. Research line followed in this Doctoral Thesis

4. Material and methods

4.1. Study sites

To achieve the objectives, five archives from different areas of the word and different time scales were studied. Figure 3 shows the location and the type (lake sediments or peat) of the archives studied whereas Table 1 summarizes the main characteristics. All the records used in this PhD thesis have been subject to previous studies on different topics as geochemistry, paleoclimate, peatland development and palynology, providing detailed background information and allowing a multi proxy study. See more information in the corresponding chapters and institutional acknowledgments section for groups implicated in the research.

Two of the cores have sections with ages dating back to the late Pleistocene, and both were collected in tropical or subtropical peatlands from remote areas. **Rano Aroi** (ARO) is a mire located in an ancient Pleistocene volcano crater in Easter Island (at 511 m a.s.l.). The two Rano Aroi cores studied here (ARO 08 02 and ARO 06 01, 4 and 13.9 m deep respectively) cover different temporal range (38.7 kyr BP-present day and 71.0-8.5 kyr BP, respectively) and were retrieved in different parts of the peatland, although less than 50 meters apart. Climatic conditions have been shown to be the main driver in the development of the peatland during the last ~71 kyr BP, as was also responsible for the increase in soil erosion from the small basin over the peatland during high precipitation

phases (Margalef et al., 2013, 2014). **Pinheiros** (PI) is a minerogenic, valley mire located in Serra do Espinhaço Meridional, state of Minas Gerais, Brazil. Although minerogenic, the location of the mire on the mountain summit (higher elevations at 1300 – 1320 m a.s.l.) and the rather small catchment area (~1.4 km^2) makes it quite sensitive to variations in rainfall. Previous studies in the area also show that the climate played a main role in the development of the mire and in their geochemical properties (Horák-Terra et al., 2014). The studied core was sampled in 2010 to a depth of 3.24 m and covers the last ~57.0 kyr BP.

Table 1. Summary of the characteristics of the environmental archives used in this work.

Records	Type of archive		Age section		Hemisphere		manuscript nº
	Peatland	Lake sediments	Holocene	Late Pleistocene	North	South	
Rano Aroi	x	-	x	x	-	x	I
Pinheiros	x	-	-	x	-	x	II, III
Lago Hambre	-	x	x	-	-	x	IV, V
Limnopolar Lake	-	x	x	-	-	x	VI
Sandhavn	x	-	x	-	x	-	VII

Two lake sediments from the South Hemisphere provided us an exceptional opportunity to complement the information obtained with the peat studies. **Lago Hambre** (LH) is a small (0. 013 km^2) and deep lake located near the Strait of Magellan in southern Patagonia (Chile). A long sediment core was recovered from the deepest part of the lake in 2008 using a 5 m long piston corer and a 41 cm long gravity core was also taken, to recover the unconsolidated recent deposits (Hermanns and Biester, 2013a). Although the deeper sections of the lake sediments have late Pleistocene sections (reaching 17.0 cal kyr BP; Hermanns and Biester, 2013a), in the two papers presented here only the Holocene sections – last ~12.0 and 4.5 cal kyr BP (respectively) were use. Previous studies indicated that the input of inorganic and organic matter from the catchment soils were driven by climate and played a main role in the geochemistry of the lake, including the

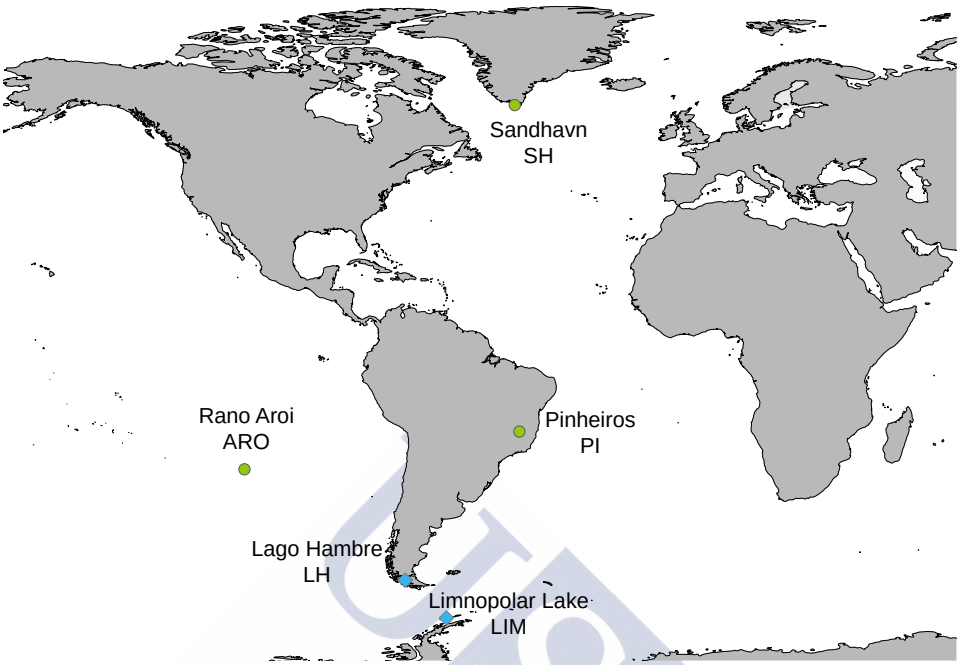

Figure 3. Map showing the location of the study sites. Circles: Peatlands; Diamonds: Lake Sediments

processes controlling Hg accumulation (Hermanns and Biester, 2013a; Hermanns et al., 2013). In addition, the sediments of the lake recorded four previously known volcanic eruptions of Reclus, Mt Burney and Hudson volcanoes.

Limnopolar Lake (LIM) is a small lake (0.022 km^2) located in Byers Peninsula, the westernmost part of Livingston Island (South Shetland Islands, Antarctica). The lake has a small catchment area of 0.58 km^2 and is ice covered except for 2–3 months during the summer. The results of previous studies on the same core (LIM-03, 57 cm deep) indicate that volcanic activity, most probably of the nearby Deception Island volcano, has played a major role in the chemical and mineralogical composition of the lake's sediments during the last ~1600 years recorded in the retrieved core (Martínez Cortizas et al., 2014).

A short core (40 cm) was collected in 2008 from a small peatland nearby the Norse farmstead of **Sandhavn** (SH), located on the coast of Greenland approximately 50 km northwest of Cape Farewell (the most southerly point on the island). In a small rock depression isolated from the groundwater table, the

peat has been continuously accreting since AD ~1250. The area of the peatland – under the influence bimodal wind direction – and the age of the record, make it a reasonable archive of Hg atmospheric depositions both from North American and European sources. Previous studies demonstrated that in addition to the effect of cooler climates on peat growth and carbon accumulation during the Little Ice Age (LIA), human activity played a significant role in peat geochemistry during the late Norse period (13th–14th centuries AD) and during the 20th century (Silva-Sánchez et al., 2015). Palynological data and the chronology of lead enrichments suggested North America as a probable source of pollution for the area (Silva-Sánchez et al., 2015).

4.2. Analytical methods

As previously stated, the samples included in this thesis have been used in several other research studies. Thus, the analytical techniques used to determine the various geochemical parameters, pollen data, and age-depth models are described in detail in previous works. In the papers included in this PhD thesis only a brief description of techniques, as well as sampling campaigns and sample preparation is included. On the other hand, a detailed description of the techniques used to obtain unpublished data is provided.

4.2.1.Mercury determination

Was carried out with a well-established analytical technique using a DMA-80 (Milestone) that is based on thermal decomposition, Hg amalgamation and atomic absorption detection. After the instrument was switched on and the measurement conditions were reached, the measurement set was started with procedural blanks samples and reference materials. For the measurements, 20 mg of dried-ground and homogenize sample plus 200 µl of ultrapure water were introduce in the nickel sample holders of the auto-sampler. All samples weights were loaded into the instrument for a precise calculation of the concentrations. The settings used were as following: drying (300ºC) 60 seconds, decomposition (850ºC) 180 seconds, purge 60 seconds, amalgamation 12 seconds, record 30 seconds.

The material and methods section of each chapter includes information on the laboratories where the analyses were performed as well as the quality indicators of the analyses.

4.2.2. Infrared spectroscopy (IR)

A total of 110 dry and ground peat samples were measured for the spectroscopy study in Pinheiros (Manuscript III). Attenuated total reflectance FTIR-ATR was performed using a Gladi-ATR (Pike Technologies) spectrometer at the IR-RAMAN facility of the RIAIDT (University of Santiago de Compostela), scanning in the 4000– 400 cm^{-1} region with a spectral resolution of 4 cm^{-1}.

In Lago Hambre (Manuscript IV) a total of 650 samples were analysed in dedicated facilities at the Universität Bayreuth. FTIR spectra of freeze-dried and ground samples of lake sediment were obtained using a Vector 22 FTIR spectrometer (BrukerOptik, Ettlingen, Germany) in absorption mode, with subsequent baseline subtraction on KBr pellets (200 mg dried KBr and 2 mg sample). Measurements were recorded from 4,500 to 300 cm^{-1} using a resolution of 2 cm^{-1}. Thirty-two scans were taken per sample and averaged to obtain the final spectra.

In both studies (Manuscript III and IV) in order to improve the comparison between samples, each FTIR spectrum was re-scaled to relative absorbance i.e. dividing the absorbance value of each point of the spectrum by the summed values of the analysed spectral region.

4.2.3. Lead isotopic analyses

Peat samples were ashed at 450°C overnight to remove any organic matter. The remaining residue was digested using an acid mixture of HNO3 and HF contained within closed digestion vessels in a MARS-Xpress microwave system (CEM, Mattheus, USA). A ratio of 0.16 ml HF: 50 mg ash was determined to be the correct mixture required to digest the samples (Kylander et al., 2004). After digestion, the samples were dried and Pb was isolated by ion exchange chromatography (Weiss et al., 2004).

Isotopic measurements were determined using an IsoProbe Multi Collector-Inductively Coupled Plasma-Mass Spectrometer (MC-ICP-MS) (Thermo, Manchester, UK) at the Naturhistorika Riksmuseet, Sweden. The instrument was equipped with a CETAC desolvator and a T1H concentric nebuliser for introducing the sample. Seven independently adjustable Faraday cups in static mode were used for isotope ratio measurements. Averaged acid blank intensities were subtracted

from raw intensities to correct for Faraday cup offset and instrumental and solvent blanks. Corrections for Hg interference on ^{204}Pb were typically ≤0.1%. Instrumental mass bias was corrected by spiking samples with NIST-SRM 977 Tl to Pb/Tl ratio of 2:1 and using optimised Tl ratios and the exponential law (see Weiss et al. [2004] for details).

4.3. Statistical calculations

Because the objectives and type of data available for each study were different, the applied statistics were not always the same. In each study case, data transformations (e.g. Z-scores, logarithmic transformations) and statistics used to interpret the dataset (e.g. Principal Component Analysis, Principal Component Regression, Partial Least Squares, phi coeficiente) are described and justified. All data analyses and the statistics were done using (R CoreTeam, 2014).

5. General Discussion

Each manuscript presented in this PhD thesis is considered a case of study and therefore has its own background, justification and discussion. The general discussion section aims to integrate the ideas and compare the hypothesis presented and discussed in the papers and manuscripts. For this purpose, the general discussion section is organized into nine sub-sections: the first one includes the variations in the concentrations and accumulation rates of the records and each of the remaining sub-sections dealing with one of the main processes that were found to influence Hg accumulation in peat and lake sediments. As such, the study cases, which form the essential body of this thesis, should be considered as the scientific basis and the reference for the general discussion. The Manuscript III falls a bit apart from this rationale, as it is an additional methodological subsection relative to the application of cheaper techniques (FTIR) to aid in Hg modelling and the set up of multicore studies and what kind of information can be obtained.

5.1. Mercury concentrations and accumulation rates

The records analysed in this PhD thesis show a wide range of variation in the Hg content. Table 2 summarizes the results including the ages when the maxima and minima were detected. To control for the deviation caused by the extremely high values, in addition to average and standard deviation values, median and median absolute deviation are reported.

Table 2. Summary of Hg concentrations and accumulation rates of the records studied here. The records are listed by the codes. (p) peatland and (l) lake sediments. Superscripts 1 and 2 indicate the core ARO 06 01 and 08 02 respectivelly.

Records		Concentrations (ng g^{-1})				Accumulation rates (µg m^{-2} yr^{-1})			
		Max	Min	Avg/ Median	Sd/ MAD	Max	Min	Avg/ Median	Sd/ MAD
ARO (p)	Value[1]	1023	35	154/ 133	135/ 62	-	-	-	-
	Age (kyr cal BP)	*~20.6*	*~43.0*			-	-		
~71 kyr	Value[2]	1088	37			-	-		
	Age (kyr cal BP)	*~4.7*	*~18.0*			-	-		
PI (p)	Value	370	11	164/ 167	66/ 50	-	-	-	-
~57 kyr	*Age (kyr cal BP)*	*~17.4*	*~26.7*			-	-		
LH (l)	Value	362	10	186/ 185	42/ 33	127	10	30/ 29	10/ 6
~4.5 kyr	*Age (kyr cal BP)*	*~3.6*	*~4.2*			*~4.4*	*~4.2*		
LIM (l)	Value	11286	14	365/ 34	1415/ 583	4901	2	159/ 9	656/ 267
~1600 yr	*Age (AD)*	*~1878*	*~1617*			*~1878*	*~460*		
SH (l)	Value	297	47	134/ 110	82/ 70	9	0.6	3/ 2	2/ 2
~700 yr	*Age (AD)*	*~1962*	*~1429*			*~1941*	*~1482*		

Relative to the concentrations, Rano Aroi and Limnopolar Lake records have maxima values higher than 1000 ng g^{-1}, exceeding 11000 ng g^{-1} in Limnopolar Lake. The other records have maxima values between 300 to 370 ng g^{-1}. In relation to the minima, lakes Lago Hambre, Limnopolar and Pinheiros have values ~10 ng g^{-1}. Rano Aroi and Sandhavn peatlands have minima 4 fold lower than the lake records. There are few differences between mean and median values for each record, with the exception of Limnopolar whose mean is 10 times greater than its median, which is not surprising considering that the record has several peaks

of very high concentrations (Manuscript VI). Despite the reduced accumulation rates data availability, the results also show that Limnopolar has the highest Hg accumulation rate, while Sandhavn has the minimum.

Maxima Hg concentrations found in Limnopolar and Rano Aroi are comparatively high with respect to other records worldwide, even in sections affected by anthropogenic emissions. For example, for the Industrial Period maxima of ~800 ng g^{-1} were reported for the Czech Republic (Zuna et al., 2012), >400 ng g^{-1} for Scotland (Yang et al., 2001; Farmer et al., 2009), ~600 ng g^{-1} in Northeast China (Tang et al., 2012), ~ 130 ng g^{-1} for Canada (Outridge et al., 2011). However according to the age of the samples (20.6 and 4.7 cal kyr BP in Rano Aroi) anthropogenic industrial activity should be discarded.

The comparison of maxima and minima within the records show also a wide range of enrichment (Table 3). Limnopolar has a range of variation in Hg content of 800 and 2000 fold (concentration and accumulation rate, respectively), 36 – 13 in Lago Hambre and 6 - 16 fold in Sandhavn. Using the value of the median, instead of the minimum, the ratios become more equal (~ 2-3) for the lowest peak concentrations (Pinherios, Lago Hambre and Sandhavn), while remaining extremely high in Rano Aroi and Limnopolar). In order to explain these high levels of Hg enrichment within the same record, it is necessary to evaluate a likely combination of factors (natural and anthropogenic) that might have interacted and possibly changed over time.

Table 3. Ratios of mercury enrichment values (concentrations and accumulation rates) from the records studied here.The records are listed by the codes. (p) peatland and (l) lake sediments.

Records	**Concentrations**		**Accumulation rates**	
	Max/min	Max/median	Max/min	Max/median
ARO (p)	31	8		
PI (p)	34	2		
LH (l)	36	2	13	4
LIM (l)	806	332	2451	551
SH (p)	6	3	16	5

5.2. Pollution

Human activity (i.e. pollution) has been considered one of the main drivers controlling Hg concentrations in records worldwide distributed that cover the last centuries or millennia – mainly showing the effect of Industrial or the Pre-Industrial activities, respectively. The human processes, which released Hg in both periods, are usually different. While in the Pre-industrial time mining and smelting were the main human activities causing pollution (e.g. Martínez Cortizas et al., 1999; Cooke et al., 2009a, 2011; Corella et al., 2017), from AD 1850 several sources have been emitting Hg to the atmosphere as a byproduct (fuel combustion, cement production, metal smelting, large-scale gold mining), as well as commercial products (e.g. batteries) and manufacturing processes that involve Hg directly (e.g. vinyl chloride monomer production) (Streets et al., 2011).

Investigations performed in areas near to the ones studied in this PhD attest for the presence of Hg pollution (see e.g. (Sun et al., 2006) for Antarctica, (Hermanns and Biester, 2013b) South Patagonia, (Lacerda et al., 1999) and Brazil; or human activities potentially causing of Hg pollution signal, as fires in Easter Island (Rull et al., 2015) or in South Patagonia (Morello et al., 2012). However only the Greenland record (Sandhavn) provided a clear signal of the effect of Hg pollution. Several reasons may explain the lack of evidence of recent atmospheric pollution in some of the studied cores. In the case of the Pleistocene records (Rano Aroi and Pinheiros), the time resolution of each peat section we have analysed is of a few hundred years and the pollution may has been averaged out, due to the sampling strategy or by low sampling resolution in Rano Aroi. For Limnopolar and Lago Hambre it is likely that other processes driving the Hg accumulation may overlap with the pollution signal. In Lago Hambre, we cannot rule out that the modern sections of the core (which reach AD 1850) do not cover the pollution period, stated as beginning at AD ~1900 in other studies in the area (Biester et al., 2002; Hermanns and Biester, 2013b).

At Sandhavn, a previous multiproxy study already showed evidence for Pb enrichment beginning by AD ~1845 and, based on the timing of the events and other proxy data (long-distance pollen and crytotephras), it was suggested that the source area was most probably northeastern North America (Silva-Sánchez et al., 2015). The Hg accumulation rates (<1.0 - 10 μg m^{-2} yr^{-1}, minimum and maximum) determined are in agreement with other Greenland records (Bindler et

al., 2001a) but generally low in comparison with other records from Europe and North America (e.g. (Benoit et al., 1994; Bindler, 2003; Farmer et al., 2009). These observations may be explained in two ways: i) Sandhavn is located far from any major sources of pollution in North America and Europe or/and ii) by a lower peat decomposition (see the discussion section about organic matter decomposition).

The chronology provided by Hg accumulation rates is similar to other studies in the area, although there may be slight mismatches. On one hand, the maximum value of Hg pollution agrees with previous data obtained on snow and ice from Summit Station at North Greenland (at ~1400 km) (Boutron et al., 1998; Faïn et al., 2009) and its chronology is close to the AD 1950 also found in a nearby peat record (~150 km northwest) (Shotyk et al., 2003). On the other, lake sediments records of lakes from Kangerlussuaq Fjord (~850 km northwest) point to an onset of Hg pollution at least by the late 19th century but possibly as early as the 17th century (Bindler et al., 2001a) (between ~50 years before to ~60 years later that in Sandhavn). The records also show a disagreement in the maxima of Hg pollution. The mismatch in the chronology of Sandhavn and the lakes from Kangerlussuaq Fjord is probably due to the meteorology of the ice margin (i.e. depletion events) that could drive Hg enrichment (Bindler et al., 2001a). This, together with the agreement with summit data suggests that our chronology of Hg pollution is more reliable.

To get a better perspective of metal pollution in South Greenland, Hg chronology was compared with data from another long-range atmospheric metal pollutant (Pb) from the same record (Silva-Sánchez et al., 2015). The results show the same significant increase by the end of the AD ~1800s but also some differences as: i) the start of pollution (AD ~1845 for Pb and just before ~1800 for Hg) and ii) their peak values (at AD ~1980 and ~1940, respectively). The isotopic Pb residuals (i.e. the detrending between the trajectory of the unpolluted trend and the observed (polluted) values from the past two centuries, Manuscript VII) suggest an earlier beginning of pollution, between AD ~1740 – 1780, in agreement with other studies using Pb that found that modern metal pollution in Greenland begun prior to the 19th century (Massa et al., 2015). Simultaneous with Hg and Pb concentrations trend, isotopic Pb residuals indicate an increased in pollution from the beginning of AD ~1800. Finally, the highest Pb pollution signal indicated by the isotopes dates to the AD 1940s and 1970s, and agrees with data obtained from analyses of the Summit ice cores (Rosman et al., 1994; Faïn et al., 2009).

The fall in gasoline Pb consumption in the USA since AD 1970, declining ~80% by the early AD 1980s (Nichols, 1997), probably contributed to the pronounced increase in isotopic residual values from AD ~1979. Additionally, when more than two sources of Pb pollution are involved, the calculation of trends and residuals proposed by us seems to be a helpful and precise approach to determine changes in the chronology of the Pb isotopic signature.

We do not have direct evidence for the origin of Hg, but according to the Pb isotope results we would expect the main source for Hg contamination to be also northern North America. However, Hg has a complex behavior in the environment. Its relatively long residence time in the atmosphere (1 year) favors long-range transport and homogenization at a hemispheric scale, making more difficult to determine its precise origin. The combined analyses of Pb and Hg may provide the means to assist further in the identification of such pollution sources in northern latitudes and to obtain a better perspective of metal pollution.

5.3. Volcanic activity

Volcanic emissions produce a natural mobilization of Hg from geogenic reservoirs and are estimated around 500 Mg Hg yr^{-1} (Selin et al., 2008). However, there are regional differences in Hg average emissions. Mercury fluxes in South and Central America are up to 12 times higher than those in Africa for the period 1980 – 2000 (Nriagu and Becker, 2003); and fluxes from Mt Etna (Italy) could be equivalent to 5% of the estimated annual industrial atmospheric Hg released in the Mediterranean area (data from the period 2004-2006; Bagnato et al., 2007). Thus, at a regional scale, it has been shown that the volcanogenic Hg contribution is not trivial (Nriagu and Becker, 2003; Bagnato et al., 2007) and must be taken into account as a significant source.

Nonetheless, evidence of Hg associated to volcanic eruptions in environmental records is not as common as expected. Ice cores from high elevations have proved to be the most reliable for this purpose. An ice core collected from the Upper Fremont Glacier (Wyoming, US), and representing the last 270-years (Schuster et al., 2002), provided a record of global (Tambora (at 1815) and Krakatu (at 1883); (Delmas et al., 1992; Cole-Dai et al., 2000)) and regional (Mount St. Helens (at 1980); (Nafth, 1993)) volcanic Hg emissions. But even in this case, and despite the proximity of Mount St. Helens (600 km) and the magnitude of the eruptions, volcanic events only contributed 6% of the total Hg vs. 52% of

anthropogenic inputs (Schuster et al., 2002). In peat and lake sediments, usually from lower altitudes, enrichments in Hg due to volcanic eruptions are even scarcer and generally show a regional influence area, as observed in lakes located in the proximity of Southern Volcanic Zone, in Northern Patagonian (Guevara et al., 2010).

Previous studies demonstrated the influenced of regional volcanism in two of the records studied in this PhD, Limnopolar Lake and Lago Hambre, but their effect on Hg concentrations were completely different. Lago Hambre record has several tephra layers corresponding to the eruptions of Reclus, Mt Burney and Hudson but no Hg signal was apparently linked to them (see (Hermanns and Biester, 2013a)). Only a Hg peak below the Mt Burney tephra could have been taken as an indication of a regional (Mt Burney ~300 km NE) volcanic event; but the lack of correlation of this peak in the Hg record of a peat core, sampled not far from the lake, excludes the volcanic activity as its cause (Hermanns and Biester, 2013a). The authors suggested that mechanisms linked to the fluxes of organic matter from the catchment to the lake may have been the main process controlling Hg accumulation (Hermanns and Biester, 2013a; Hermanns et al., 2013). The re-evaluation of Lago Hambre Hg data (Manuscript V), based on the climatic and environmental reconstruction of the area (Manuscript IV), enabled to refine the previous hypotheses but also definitely confirmed the absence of a direct effect of volcanism on the accumulation of Hg (see Manuscript IV and V).

Several tephra layers found in Limnopolar sediments attest for the effect of volcanic activity - probably of Deception Island volcano (30 km to the SE) – during the last ~1600 years (Toro et al., 2013). Volcanic eruptions have influenced the geochemistry of the lake by increasing the volcanic vs. catchment inorganic fluxes (Martínez Cortizas et al., 2014). Unlike Lago Hambre, volcanic eruptions have had an effect on the Hg record of Limnopolar Lake (Manuscript VI). Three of the identified tephra layers from Deception Island Volcano match reasonably well with five of the nine large peaks in Hg content (Hg accumulation rates between 300 to 4900 $\mu g\ m^{-2}\ yr^{-1}$), specifically with tephras L4 (AD ~1300), L3 (AD ~1450 – 1470) and L1 (AD ~1840 – 1860). On the other hand, there was no Hg peak corresponding to tephra layer L2 (AD ~1570 – 1650) and there are no tephra layers associated to some Hg peaks (AD ~549, ~884, ~1715 and ~1758). Additionally, the chronology of volcanic eruptions of Deception Island (see references in Bartolini et al., 2014) and that of Limnopolar's Hg main peaks and recent tephra records

is quite similar; although not for the most recent phase of high volcanic activity in Deception Island (from AD. ~1800 to the present), which does not correspond with the same number of Hg peaks (Figure 4 in Manuscript VI). A second order of Hg peaks (Hg accumulation rates higher than 15 μg m^{-2} yr^{-1}) has no relation with tephra layers neither with volcanic eruptions in Deception Island (Bartolini et al., 2014). Thus, it seems evident that although volcanic activity played a role in the extremely high levels of Hg found in Limnopolar sediment samples, probably as a main Hg source, other mechanisms may have also be involved (see Manuscript VI).

Finally, and somewhat more speculatively, is the effect of volcanic eruptions in the Hg accumulated at Rano Aroi peatland since, unlike Limnopolar and Lago Hambre, there is no evidence of recent volcanic activity in the peat cores (i.e. tephra layers). However, on an island containing more than 70 volcano craters (Baker et al., 1974; González-Ferrán et al., 2004), the possible degassing by active fumaroles that could act as primary Hg sources can not be ruled out; despite other processes are suggested to control the Hg deposition (see catchment effect and climate effect). Similarly, although we have no data to support it, the Hg peak at ~4.7 cal kyr BP (ARO 08 02) and/or at ~8.5 cal kyr BP (ARO 06 01) match reasonably well with the previously mentioned South Patagonia volcanic eruptions at ~4.2 cal kyr BP and ~7.7 cal kyr BP identified as Mt Burney (52ºS 72ºW) and Hudson (45ºS 72ºW), respectively (McCulloch and Davies, 2001; Stern, 2008) (see further discussion in Manuscript I relative the 0.5 kyr of mismatch between Hg peak and tephra layer). If this was true, i) both volcanoes would have been operating as large scale Hg sources given that a rise in Hg was found in Rano Aroi (Easter Island, ~4000 km) but not in peat and lake sediment records (South Patagonian (Biester et al., 2003; Hermanns and Biester, 2013a) and Manuscript VI) closer to the volcanoes (<300 km); ii) or other mechanisms would have been involved in enhancing Hg accumulation.

5.4. Organic Matter Decomposition

Changes in superficial wetness or in the water table level played a critical role in the cycling of elements coupled to organic matter dynamics, as Hg. It has been suggested that factors associated to peat organic matter evolution and mass loss should control Hg accumulation in peatlands (Biester et al., 2003, 2006, 2007; Martínez Cortizas et al., 2007), which may impose some limitations to the use of

bogs as reliable atmospheric Hg archives (Biester et al., 2007). Using the C/N ratio as indicator of degree of peat decomposition, it was found that Hg concentrations are higher in more decomposed peat due to the mass losses during decay (Biester et al., 2003) and could reach a 2-3 times increases at short term periods independent from atmospheric fluxes (Martínez Cortizas et al., 2007). On the contrary, other studies using absorbance measurements of alkaline peat extracts as an index of humification found higher Hg concentrations in poorly decomposed peat, which allowed to identify the atmospheric pollution input (e.g. Givelet et al., 2003; Shotyk et al., 2005; Bao et al., 2016). In the same line, studies on Hg retention by humic acids fractions indicate that the highest Hg concentrations occur in low humified peat and are associated to atmospheric pollution –supporting the use of bogs as archives of atmospheric Hg deposition (Zaccone et al., 2009). However, a recent comparison of different methods to determine the degree of peat decomposition concluded that the alkaline extract mainly reflects the formation of humic acids through humification and, to a lower extent, mass loss associated to mineralization (Biester et al., 2014), questioning some of the results mentioned above.

The previous observations are almost exclusively based on Holocene peats, since only one of the cores from the mentioned studies covers part of the Late-Pleistocene, reaching 14 kyr (Biester et al., 2003). This could be a limitation to study a process (i.e. organic matter decomposition) that depends on time but also on climate changes. Additionally most of the previous studies are base on one decomposition proxy despite it has been suggested that more than one should be included to obtain a more representative assessment of long-term peatland evolution (Hansson et al., 2013). For this purpose multirpoxy approach of Rano Aroi (Easter Island) and Pinheiros (Brazil), which extend back to ~71 and ~57 kyrs respectively, are unique to address the long-term effect of organic matter decomposition and of major climate changes on Hg accumulation (Manuscript I and II). At high latitudes, organic matter degradation can be limited and small climatic variations could induce strong changes. Sandhavn has a detailed chronology of changes in decomposition during cold periods (mainly LIA, see pollution discussion) (Silva-Sánchez et al., 2015), providing an opportunity to get insights into the effect of short-term decomposition. On the other hand, Limnopolar Lake has a very limited input of organic matter, which may be an advantage to observe the effects of its changes in Hg accumulation. Detailed information about decomposition and proxies used are found in the manuscripts (I, II and VII) and previous studies (Margalef et al., 2013, 2014; Horák-Terra et

al., 2014; Silva-Sánchez et al., 2015).

As a result of long-term processes, the degree of peat decomposition/mass loss, indicated by C/N ratios, show a rapid increased with depth in the upper 50 cm and 390 cm in Pinheiros and Rano Aroi (respectively) and almost stable values below (Supporting Information, Figure S4, Manuscript II and Figure 3, Manuscript I). This may indicate that the main decay of organic matter by decomposition - before its stabilization - was reached at 10-11 cal kyr BP in Pinheiros and 5 cal kyr BP in Rano Aroi. Changes in C/N ratio in older sections should respond to other factors than long-term changes in peat organic matter. In Pinheiros, the dominant sapric (i.e. highly decomposed) nature of the studied peat core is also indicated by the general low signal of the polysaccharide components (1030–1080 cm^{-1}; FTIR data, Manuscript III), which is somewhat unusual for spectroscopic fingerprints of peat, but agrees with the Pleistocene age of most samples (only the 50 cm from 240 cm correspond to Holocene peat). However, the large abundance of quartz (main absorbance at 1084 cm^{-1}) masked the O-H stretching from the polysaccharides signal, so no other FTIR based humification indices could be used to compare with the C/N ratio.

Due to the stable values of long-term decomposition in the Pleistocene sections of both cores (Pinheiros and Rano Aroi), mass loss associated with organic matter peat decomposition can be ruled out as a major factor of Hg accumulation. In the case of Pinheiros, this was also confirmed by the information obtained through prediction models - base on geochemical (PCR-model) and FTIR data (PLS-model). In these models, the regression coefficients, which are a measure of the relative weight of each factor involved in Hg content for the whole record, indicate that peat decomposition is the least important one (Figure 4 for Manuscript II and Figure 4 Manuscript III). Taking into account the chronology, the role of peat decomposition on Hg concentrations is limited to the Holocene section and almost negligible in peats with ages older than 10-11 cal kyr BP (Manuscript II).

There is no correlation between the decline in organic matter decomposition and Hg concentration in peat sections younger than 5 cal kyr BP in Rano Aroi (Figure 5, Manuscript I). Mercury concentrations remain low and, as previously mention, the high peak at 4.7 cal kyr BP is probably related to volcanic activity. The cause of two small increases at 1.2 cal kyr BP and at the superficial sample is unknown, but the effect of peat decomposition is unlikely. Only the clear

increase in Hg concentration at ~40 cal kyr BP may have responded to increased decomposition in Rano Aroi. An extreme oxidation event, as a consequence of a dry phase occurred between ~40-42 cal kyr BP (Margalef et al., 2013), resulted in a 2 fold increase in Hg concentrations (compared to the lower values of the peat core).

The rates of peat accumulation, and the decomposition of organic matter at Sandhavn, were limited in the period ~AD 1400-1800 (Silva-Sánchez et al., 2015) – encompassing much of the Little Ice Age (LIA) – at least when compared with peatlands from mid-latitudes. Although this might have affected Hg accumulation, there is no apparent change and values remained low (peat background values). The increase in Hg accumulation rate just before AD 1800's is in agreement with other records from Greenland (see Manuscript VII) and associated with to atmospheric pollution. The comparison of these findings with those from mid-latitudes records that have been more affected by enrichments in Hg, driven by intense peat mineralization at short term phases (i.e. Martínez Cortizas et al., 2007), supports the suitability of cold high latitude environments as sensitive Hg peat archives, with reduced post-depositional processes as peat organic matter decomposition.

There is not much information about organic mater and its role on Hg accumulation in Limnopolar Lake. The lake is ultraoligotrophic and the lake bottom is covered by a patchy carpet of the moss Drepanocladus longifolius (Mitt.) Broth ex Paris (Toro et al., 2013), which constitutes the main organic matter source. Thermo-desorption analysis showed variable temperature ranges of Hg release (Figure 3, Manuscript VI), which indicates differences in Hg binding strength. Similar Hg release characteristic have been observed in other sediments (Biester et al., 2000) where the peak at low temperatures (200ºC in Limnopolar) is thought to be due to relatively weakly bound Hg-OM (here mainly mosses), while with increasing degradation of the organic matter and decrease of the redox potential it appears to be bound to organo-sulfides or occurs as metacinnabar (HgS). The observation that sulphide-bound Hg appears only in the deeper/older sediments indicates that organic matter turnover is extremely slow in this lake due to the low temperatures.

5.5. The effect of the processes occurring in the catchment area

Both direct aerial deposition of Hg on the lake surface and remobilization of atmospheric inputs through fluxes from the catchment are to be, necessarily, considered in Hg estimations (Schroeder and Munthe, 1998). A huge amount of pollutants have been deposited and stored in the catchment surface soils of many lake sites, mainly due to the industrial emissions during the last centuries/ decades. Thus, processes as watershed erosion appear to be the main vectors of terrigenous Hg fluxes toward the lake water column (Ouellet et al., 2009) and processes related with catchment land uses (e.g., agricultural, residential) have been proved to influence Hg concentrations in lake sediments (e.g., Drevnick et al., 2016). Nowadays, the release of pollutants stored in the soils has become one of the dominant sources for lakes and, in many cases, lake sediments do not show a decline or the decline is not as large as expected according to reductions in emission (e.g., Yang and Smyntek, 2014; Yang, 2015; Drevnick et al., 2016).

Similarly to lakes, Hg concentrations in peatlands receiving water inputs from sources other than precipitation, usually as runoff from upslope areas through drainage from surrounding mineral soils, could be affected by catchment soil erosion. Four out of five Hg records studied in this PhD investigation (Rano Aroi, Pinheiros, Lago Hambre and Limnopolar), have been influenced by some kind of effect related to catchment soil erosion.

Pinheiros mire is located on a quartzitic valley in Serra do Espinaço Meridional (Figure 1 and S1 in Manuscript II). Despite it is situated at the mountain summit the upper part of the small catchment area had a profound influence on the dynamics of the mire. Previous research on morphological, physical, chemical and elemental properties of five mountain mires of the area found that erosion of the catchment soils has played a main role on the genesis and evolution of the peatlands (Horák-Terra et al., 2014). The authors found that fluxes of mineral mater (dominated by quartz and indicated by increases in Si) from the catchment resulted in a dilution of the organic matter content (Horák-Terra et al., 2014). The second component (Cp2) of the PCA performed by us using only data from Pinheiros, showed the same relation between elements (silicon vs. organic matter), pointing to the same process. The regression analysis suggests that catchment erosion had the largest (negative) effect on Hg content (Manuscript II). This is because quartzite is the dominant lithological material in the catchment, and it has negligible Hg contents.

Thus, mineral matter fluxes from the catchment produced a double dilution effect: on organic matter to which Hg is bound and by inputs of low Hg-containing mineral matter.

However, from the methodological point of view these results have another implication for the interpretation of Hg accumulation rates and other estimations obtained using peat bulk density (a property that in this case is controlled by the input of quartz) (see Table 1, Factor loadings, Manuscript II). Mercury accumulation rates are calculated using peat bulk density, and thus, they depend upon both local fluxes of mineral matter and degree of peat decomposition/mass loss. Increased fluxes of mineral matter from the catchment (which provide almost no Hg to the peat) increase the bulk density and consequently the estimated mass accumulation rates. The dilution effect on Hg concentrations due to the addition of allochthonous mineral matter with low Hg content does not compensate for the apparent increase in Hg accumulation rates due to the higher bulk density. This leads to a situation where, for example, the maximum Hg concentration in Pinheiros within the core (370 ng g^{-1} at 74 cm) has an estimated accumulation rate of 9.9 μg m^{-2} yr^{-1}, which is similar to that of sample at 218 cm (9.6 μg m^{-2} yr^{-1}) with a concentration 4.7-fold lower (79 ng g^{-1}) but a bulk density 4.5-fold higher. Thus, the analysis of the processes affecting Hg contents on Pinheiros core was done on the concentrations and not on the accumulation rates.

Rano Aroi is located in an ancient Pleistocene volcano crater and the crater slopes form its small catchment area (0.15 km2). From previous investigations, it is known that during high rainfall events there was an increase in soil erosion and enhanced fluxes of mineral matter from the small basin into the peatland (Margalef et al., 2013, 2014).

Although a low release of Hg can occur from the catchment materials due to weathering (see discussion in Manuscript I), metal-hummus complexes found in (andic) volcanic soils (García-Rodeja et al., 2004), could bound Hg deposited from the atmospheric pool (Nóvoa-Muñoz et al., 2008; Peña-Rodríguez et al., 2012). Thus, mobilization of Hg due to soil erosion could have also taken place in Rano Aroi as Hg-humus complexes that were transported to the mire by superficial runoff (Manuscript I). Increases in Fe content during high rainfall periods (Margalef et al., 2013, 2014) and a higher Hg content during the former supports the effect of this mechanism. The comparison of Hg concentration with

the long-term background fluxes of inorganic particulate material and the delivery of large amounts of terrigenous particles (PC1 and PC2 respectively) shows agreement only during the shorter wet events and not for the long-term trends (see Figure 4, Manuscript I). This indicates that inorganic matter fluxes (themselves) did not affect the concentration of Hg, but could have amplified the effect of wet deposition during rainfall events (see climate discussion).

Limnopolar has a catchment area of 0.58 km^2 and despite it has a main inlet, surface runoff significantly contributes to the lake volume during snowmelt and the period of thawing of the active soil layer. Similarly to Rano Aroi, the atmospherically deposited Hg is accumulated in the catchment. Instead of bind to metal humus complexes, part of the gaseous Hg is deposited and stabilized on the ice-snow pack (Durnford and Dastoor, 2011) that covers the lake and its catchments during most part of the year and even longer (i.e. years) in phases of intense cold periods. Mercury accumulated during ice-covered phases (both in the lake and in the catchment) will be transferred to the lake or lost through the outlets in the thaw period. Similar to rainfall events that controlled soil erosion in Rano Aroi and the increase in Hg concentration in the peatland, the climatic conditions drove the freezing and thawing lake dynamics, regulating the accumulation of Hg in Limnopolar Lake and its catchment.

5.6. The role of primary productivity

Previous research in Lago Hambre has suggested that Hg scavenging in the water column and accumulation in the sediments are mainly controlled by fluxes from the catchment soils (Hermanns et al., 2013). The evaluation of the geochemical data by PCA showed a covariation between Hg and other soil-derived elements (such as Cu and Y) that was interpreted as an underlying common transport mechanism. Using the entire record (17.3 cal kyr), Hg accumulation was also mainly related with terrestrial OM fluxes and DOM leaching from the catchment soils (Hermanns and Biester, 2013a). The authors based this conclusion not only in the similar depth records of Hg and other organic-bound elements (e.g. Cu and Y), but in the covariation of the former with short-term variations in C content, which are only evident in some parts of the record (Hermanns and Biester, 2013a). Although a significant correlation between changes in aquatic productivity (indicated by variations in N/C ratios an the hydrogen index) and Hg concentrations was found for some sections of the last 4.5 cal kyr BP, it was not considered to reflect a direct

causal relationship (Hermanns et al., 2013).

Later research performed in Lago Hambre, developed for this PhD thesis, based on new and previous data, allowed a re-evaluation of the processes and mechanisms involved in Hg accumulation in the lake sediment. The multirpoxy approach (with spectroscopic and geochemical data) enabled not only to obtain an environmental and climatic reconstruction of the last 12.5 cal kyr BP but also to identify unequivocal proxies of primary productivity of the lake (Manuscript IV)

The application of principal component analysis (PCA) to the FTIR data allowed a sensitive detection of in-lake productivity signals, which showed a strong dependency on total solar irradiance (TSI, based on ^{10}Be, Steinhilber et al., 2009) changes throughout the Holocene; which was also found in high latitude lakes (Hu et al., 2003). One of the specific spectra extracted from FTIR-PCA data, for samples of the past 5.5 cal krys BP, was related to algaenan (a structural component of the cell wall of freshwater green algae) and corroborated by the significant positive correlation (r= 0.74, n=226) with the hydrogen index (HI, a proxy of organic matter source, which typically shows high values for autochthonous organic matter) (Meyers and Lallier-Vergès, 1999). FTIR-PCA components obtained for sediments accumulated between 12.5 cal kyr BP and 5.5 cal kyr BP showed an absorbance spectrum typical of biogenic silica, indicating a predominance of diatoms as primary producers during this period.

For the last 4.5 cal kyr BP the strong variations in Hg accumulation corresponded to changes in TSI and aquatic productivity. The accumulation of Hg was highest during drier periods when insolation and lake productivity was high and erosion fluxes from the catchment were low (Manuscript V). This indicates that sediment Hg accumulation (and potential Hg methylation, see discussion in the Manuscript V) in this highly productive lake was controlled by insolation and the related algae productivity, and to a lesser extent by Hg fluxes supplied by erosion from the catchment soils - as it was previously suggested (Hermanns and Biester, 2013a; Hermanns et al., 2013). Mercury concentrations in algae sampled in the lake were found to be higher than the average of the sediments (187 vs. 50 ng g^{-1}), which suggests that other mechanisms occurring in the water column must explain this large difference. Several factors, as the effects of terrestrial dissolved organic matter or the presence of suboxic/anaerobic microzones in sinking particles, have been proposed as stimulating factors to active methylation in the water column

(Schartup et al., 2015; Gascón Díez et al., 2016). These conditions are found in Lago Hambre, so it is likely that the high Hg uptake by algae is due to water-column methylation in anaerobic micro-niches in settling particles, especially at times of high productivity and eutrophication (Manuscript V).

This new approach supports some of the previous results - such as the use of HI as an indicator of primary productivity in the lake – but establishes a more complete background to discuss and re-evaluate the hypotheses previously raised about Hg accumulation.

The mechanisms described above do not appear to have been relevant in Limnopolar Lake. The main reason is that Limnopolar is an ultraoligotrophic lake, so the primary productivity is low and the Hg uptake by algae may be quite low or inexistent. Hg-thermo-desorption analyses point to a key role of the organic matter at different stages of degradation. Most of the organic matter of the sediments seems to derive from the patchy carpet of the moss Drepanocladus longifolius that lives at the surface of the sediments (almost fresh remains of the moss were found in several layers of the cores) and not from microorganisms living in the water column.

5.7. Atmospheric Mercury Depletion Events (AMDEs)

These events result from the oxidation of gaseous elemental Hg into highly reactive forms in the atmosphere caused by reactive halogens (such as bromine), and the oxidized Hg species are then rapidly removed causing a depletion of atmospheric Hg concentrations (Schroeder et al., 1998; Steffen et al., 2008). AMDEs were initially observed in polar environments, first in the Arctic (Schroeder et al., 1998) and later in Antarctica (Ebinghaus et al., 2002) but are known to also occur at temperate and low latitudes (Obrist et al., 2011). Despite this, they have been seldom detected in mid-latitude environments (e.g. Peleg et al., 2007; Brunke et al., 2009).

Because their location at high latitudes, Sandhavn and Limnopolar are the more likely study sites to find the effect of Hg depletion events. Research done in Kangerlussuaq (west Greenland) lakes proposed that depletion events may have led to a gradient of Hg concentrations in the sediments, higher in lakes located close to the ice margin and lower in those close to the coast (Bindler et al., 2001a). Sandhavn is located at the coast, relatively far from the ice-sheet. The good match

of the chronology of Hg accumulation rates with other Hg pollution records in the area, as well as the similar chronology of lead isotopic composition from the same core (see the discussion relative to pollution), suggest that AMDEs exerted none, or little, control on Hg content.

In Limnopolar, the combination of the processes described (emission of Hg by volcanic activity and amplification of the signal by the freezing and thawing of the lake and the basin) could explain the Hg content in the record; but, if depletion events have occurred, they would help to support the extraordinary high levels of Hg found in some Limnopolar sediment samples.

The Br/C molar ratio was used as a proxy of AMDEs in the Limnopolar Hg record (Manuscript VI). Bromine concentration in lichen samples has been shown to be a good indicator of AMDEs (Carignan and Sonke, 2010), but in soils and sediments it is also known to occur mostly as organo-bromine compounds (e.g. Asplund and Grimvall, 1991; Biester et al., 2004) resulting from biotic and abiotic halogenation of organic matter (e.g. Keppler et al., 2000; Leri et al., 2014). The ratio shows a significant correlation with high Hg accumulation peaks (see more information in Manuscript VI) suggesting a possible causal link between Hg maxima and AMDEs.

The proximity of the coast (< 2 km) and the cold periods in which most of the Hg peaks are concentrated are favourable conditions for the generation of Hg depletion events due to i) unlimited availability of bromine and ii) conditions enhancing the formation of ice crystals, a key factor in springtime Hg depletion events, as a dominant source of sea salt aerosols and bromine compounds (Rankin et al., 2002; Douglas et al., 2005). All these considerations do not demonstrate the role of AMDEs on the Hg peaks recorded in Limnopolar core (Figure 4 and Figure 5, Manuscript VI), but point to a complementary process that may account for the large Hg accumulation.

5.8. Vegetation

Differences in vegetation type can affect the net deposition and sequestration of Hg in peatlands (Rydberg et al., 2010b). However, this was not one of the principal research objectives of this PhD investigation. The main reason is that no systematic sampling was carried out on the vegetation that could potentially affect the accumulation of Hg in peatlands and lake sediments. Some vegetation

samples were only collected in Easter Island field sampling campaign; and even there, the samples are from the whole island an not exclusively from the peatland area. In any case, the results show a wide range of Hg concentrations, from 341 ng g^{-1} to 11175 ng g^{-1} (rhizome of Scirpus californicus and an unidentified rush sample, respectively). According to the data presented in Table 1 of the Rano Aroi study, it is undoubtedly the rush sample the one deserving more interest. It has been speculated that an increase in the abundance of rush, coupled to more humid conditions by ~20 cal kyr BP, might help to explain the observed increase in Hg (Figure 6, Manuscript I) and, also, the generally higher Hg concentrations in humid periods. However, we have no certainty of the presence of rush in the mire catchment at present and the available pollen and macroremains data (Margalef et al., 2013, 2014; Margalef, 2014) do not allow to support this speculation.

It could be possible to discern whether long-term changes in vegetation type have played a role on Hg concentrations using δ13C data in Pinheiros and Rano Aroi. The changes in $\delta^{13}C$ values found in both records (between −19‰ to −24.1‰ in Pinheiros and −15 ‰ to −26 ‰ in Rano Aroi; maximum and minimum respectively) have been related with shifts in the predominant C_3-C_4 metabolic pathways of photosynthesis in vegetation (see Manuscript II and I). The general trend indicates a transition from the dominance of C_4 plants (higher ratios: -19 and -15‰) in the older sections of both records (~57 and 71 kyr BP, Pinheiros and Rano Aroi respectively) to the dominance of C_3 plants (lower ratios: -24 and -26‰) since ~26 cal kyr BP (Pinheiros) and ~47 cal kyr BP (Rano Aroi). However, this approximation is not unequivocal to determine the role of vegetation in Hg accumulation. As explained in the corresponding chapters and in the Climate discussion section below, changes in vegetation C_3 and C_4 can not be disentangled from changes in climate and, in this case, with humidity conditions. So to be able to separate both processes other proxies would be necessary. FTIR data fails to provide new information on vegetation remains in Pinheiros, probably due to the highly decomposed peat. Even more, the spectroscopy-based PLS model has to be complement with $\delta^{13}C$ data to reliably reproduce the changes in the factors controlling Hg content over time, which point to a complex carbon isotopic signal.

5.9. Climate, the effect of precipitation, temperature and insolation.

Climate has undoubtedly been the main driver of Hg accumulation in the records presented in this PhD thesis. With the exception of Sandhavn, where it seems

that climate had not effect, in the other records it has played a main role, both directly and indirectly. The broad influence of climate on the records presented here could be due to two main reasons i) the remote location of the sampling sites limit the direct effect of anthropogenic activities and/or ii) the long period of time covered by some of the records which include contrasted climatic conditions (e.g. the transition between dry to wet climates during the Late Pleistocene, see Manuscripts I and II).

As mentioned above, the effect of clime in Hg records could be either direct or indirect. Here, a climate direct effect refers to the modification of the deposition or accumulation of Hg directly by the action of a climate element such as precipitation or temperature. In contrast, the indirect climate mediation refers to the effect that some climatic factors had on the deposition or accumulation of Hg but mediated by other processes such as organic matter degradation or soil erosion. The effect of climate on this factor could be produced continuously or sporadically.

The peat records of Pinheiros and Rano Aroi provided an exceptional opportunity to observe how two main climatic periods – accounting from the Late Pleistocene to the present– affected the Hg cycle at tropical and subtropical latitudes. As previously mention, the $\delta^{13}C$ variations more likely reflect the transition from arid (rich in C_4 plant remains) to humid periods (rich in C_3 plan remains).

In Pinheiros, arid conditions dominated from ~57 to ~26 cal kyr BP, after that a wet-humid period began an extended until the last ~3 cal kyr BP, when conditions became drier again. Pollen data supports this interpretation of $\delta^{13}C$ variations (Supporting Information, Figure S6, Manuscript II). Due to the evolution of the peatland, the role of climate on peat Hg concentrations changed along these phases. During the dryer phase (~57 to ~26 kry cal BP), high rainfall events resulted in high inputs of inorganic matter due to erosion of the catchment soils, diluting the content of organic matter and Hg concentrations in peat. According to the PCR model (Manuscript II), Hg associated to wet deposition is low during all the dry period when the soil erosion effect has the strongest weight (Manuscript II). With the development of the mire, the impact of catchment erosion decreased and enhanced accumulation of organic matter led to higher and more stable Hg concentrations. The shift in climate conditions by ~26 cal kyr BP led to a higher weight of wet deposition on Hg concentrations in peat.

In this record, an extraordinary high Hg concentration (3 standard deviations

higher than the expected value by the model) was found at the timing of Heinrich event 1 (H1), which was characterized by dry and very cold conditions (Lowell et al., 1995; Sagnotti et al., 2001). No clear reason was found for this peak, although the effect of multiple factors is the most likely explanation (Manuscript II).

In Rano Aroi (Margalef et al., 2013, 2014), the drier-colder climatic conditions extended from ~71 to ~55 krys BP, when a transition started ending at ~43 cal kyr BP. After ~43 cal kyr BP the predominance of C_3 vegetation indicates a more humid climate (Margalef et al., 2013, 2014). Similarly to Pinheiros, the drier phase was punctuated by negative excursions in $\delta^{13}C$ that were interpreted as short wetter events, but the effect on Hg concentrations is completely different. Increases in Hg concentration seem to match – at least partially – with the wet events, suggesting enhanced Hg-wet deposition over the peatland and the catchment (see discussion section in Manuscript I). Additionally, during these events there was an increase in catchment soil erosion, driven by precipitation. In contrast to Pinheiros, in Rano Aroi the increased input of mineral fluxes from the catchment soils resulted in increases of Hg concentrations in peat, most probably due to inputs of metal (Hg)-humus complexes, which are typically abundant in volcanic soils (see the effect of the catchment).

Between ~40 - 42 cal kyr BP a long-term drought resulted in increased peat oxidation that led to an increase in Hg concentrations (see the effect of organic matter decomposition). With the exception of the abrupt rainfall events, under prevalent humid conditions (from ~42 cal kyr BP to the present) there was not a general increase in Hg wet-deposition since the background values continued to be low. The ~20 cal krys BP Hg maximum corresponds to a cold phase occurred at the end of the Last Glacial Maximum, when humid conditions in Eastern Island prevailed (Margalef et al., 2014). Both, colder and humid conditions would have favored Hg accumulation in Rano Aroi since Hg deposition is controlled by temperature and humidity variations (Martínez Cortizas et al., 1999; Corella et al., 2017).

The results of these long-term records (Rano Aroi and Pinheiros) suggest, as it is generally accepted by extensive monitoring (Gay et al., 2013), that wet deposition (i.e. the wash out of Hg by rainfall) is the main source of Hg to peatlands. In contrast to our results, recent short term studies (Enrico et al., 2016) performed in the French Pyrenees have found that gaseous and particulate Hg (i.e. dry deposition)

are the main species deposited into peatlands. This apparent inconsistency most probably arises from the different time scales of the studies. The long temporal perspective provided by the Pleistocene records might highlight the dominance of the longer-term wet deposition processes.

In Lago Hambre, total solar irradiance directly controlled primary productivity in the lake and indirectly the Hg content in the sediments. During the last ~4.5 cal kyr BP higher TSI corresponded to higher green algae production and Hg uptake by them, probably accompanied by increased methylation (Manuscript V). Additionally, periods of high TSI (and productivity) largely corresponded to periods of low mineral matter fluxes from the catchment (Figure 2, Manuscript IV), indicating relatively dry conditions due to weaker westerly winds at Lago Hambre. Our results confirm that there were not important inputs of Hg from the catchment during periods of high productivity and higher uptake by algae (Manuscript V).

The freezing and thawing lake dynamics regulated the accumulation of Hg in Limnopolar Lake and its catchment, a process also directly controlled by climate. Annually, Limnopolar Lake is ice covered except for 2–3 months during the summer. The ice break-up in the lake has been observed to start in December near the lake outlets or inlets, however ice blocks or thin ice layers could persist until February (Toro et al., 2007) (see pictures in Figure 9.3 in Camacho et al., 2014). The ice-snow layer over the lake and the catchment may have acted as a Hg sink during 9 - 10 months per year. Periods of sustained general cold climatic conditions may have extended the effect of this Hg trap from years to decades. This is consistent with high Hg concentrations and accumulation rates corresponding to phases of minima in insolation (colder periods). The comparison of the TSI record (Steinhilber et al., 2009) (Figure 4, Manuscript VI), with Hg accumulation shows that six of eight Hg peaks (>270 μg m^{-2} yr^{-1}) coincided with periods of low irradiance. Peaks at AD ~1300, ~1450 and ~1715, ~1820 correspond with the Wolf, Spörer, Maunder and Dalton minima; and peaks at AD ~550 and ~1750 coincided with relative low insolation. Even more, without considering the samples with extremely high accumulation (only those with <270 μg m^{-2} yr^{-1}), the record also shows increases of Hg accumulation during periods of low irradiance (Figure 5, Manuscript VI). As indicated above, under such cold conditions it is likely that the lake and its basin remained snow/ice-covered for long periods of time, enhancing Hg accumulation in the snowpack. During thawing, the more material stored in

the ice the more transferred to the lake and its sediments. Finally, the lake snow/ice-cover also promotes reducing conditions in the sediment and the longer the period is the more intense the reducing conditions will be. This may have also had an effect on the heterotrophic degradation of the organic matter in the lake, which should interact with Hg (Manuscript VI).

6. Conclusions

Lake sediments and peatlands are environmental archives that can be used as records of atmospherically deposited Hg and thus providing a "picture" of the Hg cycle. However, this use - as Hg atmospheric records - is conditioned by factors which operate in a geographic and time scale. Thus, the Hg determined in the samples does not directly reflect the atmospheric deposition, but result of the factors effects. The sources and processes that affect Hg deposition and accumulation in the records varied depending on the **location and the period of time studied**. Additionally their final effect on the concentration of Hg might change along the evolution of the record or due to the interaction with other factors.

Due to the long-residence time in the atmosphere, Hg sources could have a **local, regional of global effects** and in some cases is not simple determined the **geographic scale** of the main source. Sandhavn provided a good example of this issue. It is located in geographic position susceptible of North America and European Hg pollution sources, and the chronology of Hg alone does not allow determine which one is the main source are, despite the timing of Industrial trends in both areas are well-known and quite different. According to the lead isotopic results it would be expected the main source of Hg contamination to be also from US, but it does not prove it and hemispheric mixing and long-range transport might be driving.

In other cases, the effect of a **local process** may overlap regional or global Hg signals, such as the volcanic activity of Deception Island as a local Hg source over Limnopolar Lake sediments. The dynamics of freezing and thawing in the lake and its catchment show a high sensitivity by changes in insolation, probably because of its extreme polar location. Both facts limits information on long-term Hg transport to remote polar areas but constitutes a valuable model of local or regional environments.

Similarly, the control that the aquatic productivity exerted on Hg accumulation in sediments on Lago Hambre, restricts its use as a reliable record of atmospheric Hg deposition but nevertheless it helps to understand the role of productive and eutrophic lakes in the Hg cycle.

Specific characteristics of the records could modify also the effect of **regional processes**. While rainfall events dominate the Hg wet deposition in Rano Aroi record and amplified its effect through the erosion of the volcanic soils from the catchment; in Pinheiros they produce a strong dilution of Hg concentrations due the input of mineral matter from quartzitic catchment.

The **time scale** covered by a record also determines the factors that may affect it, and therefore the information that it provides as an archive of atmospheric Hg deposition. In records covering **long periods of time**, such as Pinheiros and Rano Aroi (Late Pleistocene and Holocene) there is a wide range of processes that could be observed and that could modify Hg record. There is also a strong interaction between the processes and the system itself. Thus, in Pinheiros the results of rainfall precipitations under dry conditions, low peatland developed and scarce catchment vegetation is an increased the input of inorganic matter from the catchment producing the mentioned dilution effect on Hg concentrations. With a greater development of peatland and more vegetation covering the basin (during a prolonged humid period), the effect of the precipitations produces an increase of the concentration of Hg, linked to the wet deposition.

The relative weight of the factors on Hg concentration also changes with the time scale. **Long-term records** studied here (Rano Aroi and Pinheiros) suggest that wet deposition (i.e. the wash out of Hg by rainfall) is the main source of Hg to peatlands, in contrast to recent short-term studies that indicate that gaseous and particulate Hg (i.e. dry deposition) are the main species deposited into peatlands. This apparent inconsistency most probably arises from the different time scales

of the studies. The long temporal perspective provided by the Pleistocene records might highlight the dominance of the longer-term wet deposition processes. Similarly, processes as organic matter decomposition that main driver of Hg content in Holocene reconstructions, seems to have a low overall weight at Pleistocene scale. Notwithstanding strong oxidative events caused by droughts periods may increase Hg concentrations up to 2 times.

By the other hand, processes as AMDEs that has been shown a mainly role driving Hg atmospheric concentrations in annual or monthly records, its role a long term scales using records that account hundreds or thousands years is difficult to show and demonstrate.

Essentially, peat and lake sediments are potential records of atmospheric Hg deposition. **The recording of these depositions is highly conditioned by the local, regional, and global characteristics of archives, sources, and control factors.** This is due to the dynamic behaviour of Hg in the atmosphere and in the environment.

From the **methodological** point of view, the multiproxy approach has been shown a useful tool to obtain a complete interpretation of the systems and separates the different sources and factors that affect the Hg content in the record and thus, be able to obtain an accurate reconstruction of Hg atmospheric deposition. In cases of pollution sources it seems recommended the comparison of Hg record with other metals, which would help to establish the possible scale of pollution sources (local, regional or global). Lead Isotopic studies prove to be an invaluable support to determined the most probable dominant Hg source.

Multivariate statistics (PCA, PCR and PLS) proved to be a very useful tool to complement multirpoxy approach. Specifically, the principal components analysis followed by principal components regression enabled us to determine the evolution of the weight of the latent processes governing the accumulation of Hg through time in Pinheiros record. This novelty approximation seems more suitable for long records and with a regular age-depth model.

Spectroscopic data in combination with multivariate analysis, specifically PLS statistics can efficiently be use to predict Hg concentrations in minerogenic peat, at least within the same core. Although the model could be very precise in the prediction of Hg concentration, it might not reproduce the changes with

time/depth of the relative weights of the driving processes. Supplementing models with extra data (like $\delta^{13}C$ ratios in our case) may be required to use the model for the interpretation of the underlying processes. Although more research is needed on different types of peatlands, this methodology (MIR-spectroscopy combined with PLS) may enable to reduce the cost of multi- core approaches to study the spatial variability within mire or between mires (of a similar type and area) in Hg accumulation, and probably also other peat properties.

7. References

Allan M., Le Roux G., Sonke J.E., Piotrowska N., Streel M., and Fagel N., 2013. Reconstructing historical atmospheric mercury deposition in Western Europe using: Misten peat bog cores, Belgium. Science of The Total Environment 442, 290–301

AMAP A., 2011. Assessment 2011: mercury in the Arctic (Oslao, Norway)

AMAP/UNEP, 2013. Technical Background Report for the Global Mercury Assessment (Oslo, Norway)

Amos H.M., Jacob D.J., Streets D.G., and Sunderland E.M., 2013. Legacy impacts of all-time anthropogenic emissions on the global mercury cycle. Global Biogeochemical Cycles 27, 410–421

Appelquist H., Ottar Jensen K., Sevel T., and Hammer C., 1978. Mercury in the Greenland ice sheet. Nature 273, 657–659

Ariya P.A., Khalizov A., and Gidas A., 2002. Reactions of Gaseous Mercury with Atomic and Molecular Halogens: Kinetics, Product Studies, and Atmospheric Implications. The Journal of Physical Chemistry A 106, 7310–7320

Ariya P.A., Dastoor A.P., Amyot M., Schroeder W.H., Barrie L., Anlauf K., Raofie F., Ryzhkov A., Davignon D., Lalonde J., et al., 2004. The Arctic: A sink for mercury. Tellus, Series B: Chemical and Physical Meteorology 56, 397–403

Asplund G. and Grimvall A., 1991. Organohalogens in nature. Environmental Science and Technology 25, 1346–1350

Aston S.R., Bruty D., Chester R., and Padgham R.C., 1973. Mercury in lake sediments: a possible indicator of Technological Growth. Nature 241, 450–451

Atwell L., Hobson K.A., and Welch H.E., 1998. Biomagnification and bioaccumulation of mercury in an arctic marine food web: insights from stable nitrogen isotope analysis. Canadian Journal of Fisheries and Aquatic Sciences 55, 1114–1121

Bagnato E., Aiuppa A., Parello F., Calabrese S., D'Alessandro W., Mather T.A., McGonigle

A.J.S., Pyle D.M., and Wängberg I., 2007. Degassing of gaseous (elemental and reactive) and particulate mercury from Mount Etna volcano (Southern Italy). Atmospheric Environment 41, 7377–7388

Baker P.E., Buckley F., and Holland J.G., 1974. Petrology and geochemistry of Easter Island. Contributions to Mineralogy and Petrology 44, 85–100

Bao K., Shen J., Wang G., Sapkota A., and McLaughlin N., 2016. Estimates of recent Hg pollution in Northeast China using peat profiles from Great Hinggan Mountains. Environmental Earth Sciences 75

Bargagli R., 2008. Environmental contamination in Antarctic ecosystems. Science of the Total Environment 400, 212–226

Bargagli R., Monaci F., Sanchez-Hernandez J.C., and Cateni D., 1998. Biomagnification of mercury in an Antarctic marine coastal food web. Marine Ecology Progress Series 169, 65–76

Bartolini S., Geyer A., Martí J., Pedrazzi D., and Aguirre-Díaz G., 2014. Volcanic hazard on Deception Island (South Shetland Islands, Antarctica). Journal of Volcanology and Geothermal Research 285, 150–168

Bash J.O. and Miller D.R., 2007. A note on elevated total gaseous mercury concentrations downwind from an agriculture field during tilling. Science of the Total Environment 388, 379–388

Beal S., Osterberg E.C., Zdanowicz C., and Fisher D., 2015. An ice core perspective on mercury pollution during the past 600 years. Environmental Science and Technology 49, 7641–7647

Benoit J.M., Fitzgerald W.F., and Damman A.W.H., 1994. Historical atmospheric mercury deposition in the mid-continental US as recorded in an ombrotrophic peat bog. Mercury Pollution: Integration and Synthesis 187–202

Benoit J.M., Fitzgerald W.F., and Damman A.W.H., 1998. The biogeochemistry of an ombrotrophic bog: Evaluation of use as an archive of atmospheric mercury deposition. Environmental Research 78, 118–133

Benoit J.M., Gilmour C.C., Heyes A., Mason R.P., and Miller C.L., 2002. Geochemical and Biological Controls over Methylmercury Production and Degradation in Aquatic Ecosystems. In Biogeochemistry of Environmentally Important Trace Elements, (American Chemical Society), pp. 19–262

Biester H., Gosar M., and Covelli S., 2000. Mercury Speciation in Sediments Affected by Dumped Mining Residues in the Drainage Area of the Idrija Mercury Mine, Slovenia. Environmental Science and Technology 34, 3330–3336

Biester H., Kilian R., Franzen C., Woda C., Mangini A., and Schöler H.F., 2002. Elevated mercury accumulation in a peat bog of the Magellanic Moorlands, Chile (53°S) - An anthropogenic signal from the Southern Hemisphere. Earth and Planetary Science Letters 201, 609–620

Biester H., Martinez-Cortizas A., Birkenstock S., and Kilian R., 2003. Effect of Peat Decomposition and Mass Loss on Historic Mercury Records in Peat Bogs from Patagonia. Environmental Science and Technology 37, 32–39

Biester H., Keppler F., Putschew A., Martinez-Cortizas A., and Petri M., 2004. Halogen Retention, Organohalogens, and the Role of Organic Matter Decomposition on Halogen Enrichment in Two Chilean Peat Bogs. Environmental Science and Technology 38, 1984–1991

Biester H., Bindler R., and Martínez Cortizas A., 2006. Mercury in mires. In Peatlands: Evolution and Records of Environmental and Climatic Changes, I. Martini, A. Martínez Cortizas, and W. Chesworth, eds. (Elsevier B.V), pp. 465–478

Biester H., Bindler R., Martinez-Cortizas A., and Engstrom D.R., 2007. Modeling the Past Atmospheric Deposition of Mercury Using Natural Archives. Environmental Science and Technology 41, 4851–4860

Biester H., Hermanns Y.-M., and Martinez Cortizas A., 2012. The influence of organic matter decay on the distribution of major and trace elements in ombrotrophic mires – a case study from the Harz Mountains. Geochimica et Cosmochimica Acta 84, 126–136

Biester H., Knorr K.-H., Schellekens J., Basler A., and Hermanns Y.-M., 2014. Comparison of different methods to determine the degree of peat decomposition in peat bogs. Biogeosciences 11, 2691–2707

Bindler R., 2003. Estimating the natural background atmospheric deposition rate of mercury utilizing ombrotrophic bogs in Southern Sweden. Environmental Science and Technology 37, 40–46

Bindler R., Renberg I., Appleby P.G., Anderson N.J., and Rose N.L., 2001a. Mercury Accumulation Rates and Spatial Patterns in Lake Sediments from West Greenland: A Coast to Ice Margin Transect. Environmental Science and Technology 35, 1736–1741

Bindler R., Olofsson C., Renberg I., and Frech W., 2001b. Temporal trends in mercury accumulation in lake sediments in Sweden. Water, Air, and Soil Pollution 1, 343–355

Bindler R., Klarqvist M., Klaminder J., and Förster J., 2004. Does within-bog spatial variability of mercury and lead constrain reconstructions of absolute deposition rates from single peat records? The example of Store Mosse, Sweden. Global Biogeochemical Cycles 18, 1–12

Blais J.M., Rosen M.R., and Smol J.P., 2015. Using natural archives to track sources and long-term trends of pollution: an introduction. In Environmental Contaminants. Using Natural Archives to Track Sources and Long-Term Trends of Pollution, J.M. Blais, M.R. Rosen, and J.P. Smol, eds. (Springer), pp. 1–3

Boutron C.F., Vandal G.M., Fitzgerald W.F., and Ferrari P., 1998. A forty year record of mercury in central Greenland snow in snow deposited Greenland reported from previous studies of Greenland snow by major Combined probably plagued by major contamination problems during estimated contributions from natural Hg sources. Goephysical Research Letters 25, 3315–3318

Brown A.S., Brown R.J.C., Corns W.T., and Stockwell P.B., 2008. Establishing SI traceability for measurements of mercury vapour. The Analyst 133, 946–953

Brunke E.-G., Labuschagne C., Ebinghaus R., Kock H.H., and Slemr F., 2009. Total gaseous mercury depletion events observed at Cape Point during 2007andndash;2008. Atmospheric Chemistry and Physics Discussions 9, 20979–21009

Calvert J.G. and Lindberg S.E., 2003. A modeling study of the mechanism of the halogen-ozone-mercury homogeneous reactions in the troposphere during the polar spring. Atmospheric Environment 37, 4467–4481

Camacho A., Villaescusa J.A., Rochera C., and Jørgensen S.E., 2014. Chapter 9 - Modeling the Response of the Planktonic Microbial Community to Warming Effects

in Maritime Antarctic Lakes: Ecological Implications. In Ecological Modelling and Engineering of Lakes and Wetlands, N.-B.C. and F.-L.X.B.T.-D. in E.M. Sven Erik Jørgensen, ed. (Elsevier), pp. 231–250

Carignan J. and Sonke J., 2010. The effect of atmospheric mercury depletion events on the net deposition flux around Hudson Bay, Canada. Atmospheric Environment 44, 4372–4379

Carravieri A., Bustamante P., Churlaud C., and Cherel Y., 2013. Penguins as bioindicators of mercury contamination in the Southern Ocean: Birds from the Kerguelen Islands as a case study. Science of the Total Environment 454–455, 141–148

Coggins A.M., Jennings S.G., and Ebinghaus R., 2006. Accumulation rates of the heavy metals lead, mercury and cadmium in ombrotrophic peatlands in the west of Ireland. Atmospheric Environment 40, 260–278

Cole-Dai J., Mosley-Thompson E., Wight S.P., and Thompson L.G., 2000. A 4100-year record of explosive volcanism from an East Antarctica ice core. Journal of Geophysical Research 105, 24431–24441

COM, 2005. Communication from the Commision to the Council and the European Parliament - Community Strategy Concerning Mercury

Cooke C.A. and Bindler R., 2015. Lake Sediment Records of Preindustrial Metal Pollution. In Environmental Contaminants. Using Natural Archives to Track Sources and Long-Term Trends of Pollution, J.M. Blais, M.R. Rosen, and J.P. Smol, eds. (Spinger), pp. 101–119

Cooke C.A., Balcom P.H., Biester H., and Wolfe A.P., 2009a. Over three millennia of mercury pollution in the Peruvian Andes. Proceedings of the National Academy of Sciences of the United States of America 106, 8830–8834

Cooke C.A., Balcom P.H., Kerfoot C., Abbott M.B., and Wolfe A.P., 2011. Pre-colombian mercury pollution associated with the smelting of argentiferous ores in the bolivian andes. Ambio 40, 18–25

Cooke C. A., Balcom P.H., Biester H., and Wolfe A. P., 2009b. Over three millennia of mercury pollution in the Peruvian Andes. Proceedings of the National Academy of Sciences 106, 8830–8834

Corbitt E.S., Jacob D.J., Holmes C.D., Streets D.G., and Sunderland E.M., 2011. Global source-receptor relationships for mercury deposition under present-day and 2050 emissions scenarios. Environmental Science and Technology 45, 10477–10484

Corella J.P., Valero-Garcés B.L., Wang F., Martínez-Cortizas A., Cuevas C.A., and Saiz-Lopez A., 2017. 700 years reconstruction of mercury and lead atmospheric deposition in the Pyrenees (NE Spain). Atmospheric Environment

Daga R., Ribeiro Guevara S., Pavlin M., Rizzo A., Lojen S., Vreca P., Horvat M., and Arribére M., 2016. Historical records of mercury in southern latitudes over 1600 years: Lake Futalaufquen, Northern Patagonia. Science of the Total Environment 553, 541–550

Dastoor A., Ryzhkov A., Durnford D., Lehnherr I., Steffen A., and Morrison H., 2015. Atmospheric mercury in the Canadian Arctic. Part II: Insight from modeling. Science of The Total Environment 509–510, 16–27

Delmas R.J., Kirchber S., Palais J.M., and Petit J.-R., 1992. 1000 years of explosive volcanism recorded at the South Pole. Tellus B 44, 335–350

Denkenberger J.S., Driscoll C.T., Branfireun B.A., Eckley C.S., Cohen M., and Selvendiran P., 2012. A synthesis of rates and controls on elemental mercury evasion in the Great Lakes Basin. Environmental Pollution 161, 291–298

Dickson E.M., 1972. Mercury and Lead in the Greenland Ice Sheet: A Reexamination of the Data. Science 177, 536–538.

Douglas T.A., Sturm M., Simpson W.R., Brooks S., Lindberg S.E., and Perovich D.K., 2005. Elevated mercury measured in snow and frost flowers near Arctic sea ice leads. Geophysical Research Letters 32, 1–4

Douglas T.A., Sturm M., Simpson W.R., Blum J.D., Keeler G.J., Perovich D.K., Biswas A., Johnson K., and Alvarez-aviles L., 2008. Influence of Snow and Ice Crystal Formation and Accumulation on Mercury Deposition to the Arctic. Environmental Science and Technology 42, 1542–1551

Douglas T.A., Loseto L.L., MacDonald R.W., Outridge P., Dommergue A., Poulain A., Amyot M., Barkay T., Berg T., Chetelat J., et al., 2012. The fate of mercury in Arctic terrestrial and aquatic ecosystems, a review. Environmental Chemistry 9, 321–355

Drevnick P.E., Yang H., Lamborg C.H., and Rose N.L., 2012. Net atmospheric mercury deposition to Svalbard: Estimates from lacustrine sediments. Atmospheric Environment 59, 509–513

Drevnick P.E., Cooke C.A., Barraza D., Blais J.M., Coale K.H., Cumming B.F., Curtis C.J., Das B., Donahue W.F., and Eagles-Smith C.A., 2016. Spatiotemporal patterns of mercury accumulation in lake sediments of western North America. Science of The Total Environment 568, 1157–1170

Driscoll C.T., Mason R.P., Chan H.M., Jacob D.J., and Pirrone N., 2013. Mercury as a global pollutant: Sources, pathways, and effects. Environmental Science and Technology 47, 4967–4983

Durnford D. and Dastoor A., 2011. The behavior of mercury in the cryosphere : A review of what we know from observations. 116

Durnford D., Dastoor A., Figueras-Nieto D., and Ryjkov A., 2010. Long range transport of mercury to the Arctic and across Canada. Atmospheric Chemistry and Physics 10, 6063–6086

Durnford D.A., Dastoor A.P., Steen A.O., Berg T., Ryzhkov A., Figueras-Nieto D., Hole L.R., Pfaffhuber K.A., and Hung H., 2012. How relevant is the deposition of mercury onto snowpacks?-Part 1: A statistical study on the impact of environmental factors. Atmospheric Chemistry and Physics 12, 9221–9249

Ebinghaus R., Kock H.H., Temme C., Einax J.W., Löwe A.G., Richter A., Burrows J.P., and Schroeder W.H., 2002. Antarctic springtime depletion of atmospheric mercury. Environmental Science and Technology 36, 1238–1244

Engstrom D.R., Balogh S.J., and Swain E.B., 2007. History of mercury inputs to Minnesota lakes : Influences of watershed disturbance and localized atmospheric deposition. Limnology and Oceanography 52, 2467–2483

Engstrom D.R., Fitzgerald W.F., Cooke C.A., Lamborg C.H., Drevnick P.E., Swain E.B., Balogh S.J., and Balcom P.H., 2014. Atmospheric Hg emissions from preindustrial gold and silver extraction in the Americas: A reevaluation from lake-sediment archives. Environmental Science and Technology 48, 6533–6543

Enrico M., Roux G. Le, Marusczak N., Heimbürger L.-E., Claustres A., Fu X., Sun R.,

and Sonke J.E., 2016. Atmospheric Mercury Transfer to Peat Bogs Dominated by Gaseous Elemental Mercury Dry Deposition. Environmental Science and Technology acs.est.5b06058

Etheridge D.M., Steele L.P., Langenfelds R.L., Francey R.J., Barnola J.M., and Morgan V.I., 1996. Natural and anthropogenic changes in atmospheric Co2 over the last 1000 years from ais in Antarctic ice and firm. Journal Of Geophysical Research-Atmospheres 101, 4115–4128

Faïn X., Ferrari C.P., Dommergue A., Albert M., Battle M., Arnaud L., Barnola J.-M., Cairns W., Barbante C., and Boutron C., 2008. Mercury in the snow and firn at Summit Station, Central Greenland, and implications for the study of past atmospheric mercury levels. Atmospheric Chemistry and Physics Discussions 7, 18221–18268

Faïn X., Ferrari C.P., Dommergue A., Albert M.R., Battle M., Severinghaus J., Arnaud L., Barnola J.-M., Cairns W., Barbante C., et al., 2009. Polar firn air reveals large-scale impact of anthropogenic mercury emissions during the 1970s. Proceedings of the National Academy of Sciences of the United States of America 106, 16114–16119

Farmer J.G., Anderson P., Cloy J.M., Graham M.C., MacKenzie A.B., and Cook G.T., 2009. Historical accumulation rates of mercury in four Scottish ombrotrophic peat bogs over the past 2000 years. Science of the Total Environment 407, 5578–5588

Fitzgerald W.F. and Lamborg C.H., 2003. Geochemistry of Mercury in the Environment. In Treatise on Geochemistry: Second Edition, B. Sherwood Lollar, ed. (Elsevier), pp. 107–148

Fitzgerald W.F., Engstrom D.R., Lamborg C.H., Tseng C.M., Balcom P.H., and Hammerschmidt C.R., 2005. Modern and historic atmospheric mercury fluxes in northern Alaska: Global sources and arctic depletion. Environmental Science and Technology 39, 557–568

Fitzgerald W.F., Lamborg C.H., and Hammerschmidt C.R., 2007. Marine biogeochemical cycling of mercury. Chemical Reviews 107, 641–662

Franzen C., Kilian R., and Biester H., 2004. Natural mercury enrichment in a minerogenic fen--evaluation of sources and processes. Journal of Environmental Monitoring : JEM 6, 466–472

Friedli H.R., Arellano A.F., Cinnirella S., and Pirrone N., 2009. Initial estimates of mercury emissions to the atmosphere from global biomass burning. Environmental Science and Technology 43, 3507–3513

Gabrielli P. and Vallelonga P., 2015. Contaminant records in ice cores. In Environmental Contaminants. Using Natural Archives to Track Sources and Long-Term Trends of Pollution, J.M. Blais, M.R. Rosen, and J.P. Smol, eds. (Springer), pp. 393–430

García-Rodeja E., Nóvoa J.C., Pontevedra X., Martínez-Cortizas A., and Buurman P., 2004. Aluminium fractionation of European volcanic soils by selective dissolution techniques. Soils of Volcanic Regions in Europe 56, 325–351

Gascón Díez E., Loizeau J.L., Cosio C., Bouchet S., Adatte T., Amouroux D., and Bravo A.G., 2016. Role of Settling Particles on Mercury Methylation in the Oxic Water Column of Freshwater Systems. Environmental Science and Technology 50, 11672–11679

Gay D.A., Schmeltz D., Prestbo E., Olson M., Sharac T., and Tordon R., 2013. The Atmospheric Mercury Network: Measurement and initial examination of an ongoing atmospheric mercury record across North America. Atmospheric Chemistry and Physics 13, 11339–11349

Gionfriddo C.M., Tate M.T., Wick R.R., Schultz M.B., Zemla A., Thelen M.P., Schofield R., Krabbenhoft D.P., Holt K.E., and Moreau J.W., 2016. Microbial mercury methylation in Antarctic sea ice. Nature Microbiology 1, 16127

Givelet N., Roos-Barraclough F., and Shotyk W., 2003. Predominant anthropogenic sources and rates of atmospheric mercury accumulation in southern Ontario recorded by peat cores from three bogs: comparison with natural "background" values (past 8000 years). Journal of Environmental Monitoring : JEM 5, 935–949

González-Ferrán O., Mazzuoli R., and Lahsen A., 2004. Geología del complejo volcánico Isla de Pascua-Rapa Nui, Chile. V Región-Valparaiso.

Goodsite M.E., Outridge P.M., Christensen J.H., Dastoor A., Muir D., Travnikov O., and Wilson S., 2013. How well do environmental archives of atmospheric mercury deposition in the Arctic reproduce rates and trends depicted by atmospheric models and measurements? Science of the Total Environment 452–453, 196–207

Guevara R., Rizzo A., Sánchez R., and Arribére M., 2005. Heavy metal inputs in Northern Patagonia lakes from short sediment core analysis. Journal of Radioanalytical and Nuclear Chemistry 265, 481–493

Guevara S.R., Meili M., Rizzo A., Daga R., and Arribére M., 2010. Sediment records of highly variable mercury inputs to mountain lakes in Patagonia during the past millennium. Atmosphere 10, 3443–3453

Gustin M.S., Biester H., and Kim C.S., 2002. Investigation of the light-enhanced emission of mercury from naturally enriched substrates. Atmospheric Environment 36, 3241–3254

Ha E., Basu N., Bose-O 'reilly S., Dórea J.G., Mcsorley E., Sakamoto M., and Chan H.M., 2017. Current progress on understanding the impact of mercury on human health. Environmental Research 152, 419–433

Hall B., 1995. The gas phase oxidation of elemental mercury by ozone. In Mercury as a Global Pollutant, (Springer), pp. 301–315

Hansson S. V, Rydberg J., Kylander M., Gallagher K., Bindler R., Gallagher K., and Bindler R., 2013. Evaluating paleoproxies for peat decomposition and their relationship to peat geochemistry. Holocene 23, 1666–1671

Hansson S. V, Bindler R., and De Vleeschouwer F., 2015. Using Peat Records as Natural Archives of Past Atmospheric Metal Deposition. In Environmental Contaminants. Using Natural Archives to Track Sources and Long-Term Trends of Pollution, pp. 323–354

Harada M., 1995. Minamata disease: methylmercury poisoning in Japan caused by environmental pollution. Critical Reviews in Toxicology 25, 1–24

Hararuk O., Obrist D., and Luo Y., 2013. Modelling the sensitivity of soil mercury storage to climate-induced changes in soil carbon pools. Biogeosciences 10, 2393–2407

Hermanns Y.-M. and Biester H., 2013a. A 17,300-year record of mercury accumulation in a pristine lake in southern Chile. Journal of Paleolimnology 49, 547–561

Hermanns Y. and Biester H., 2013b. Anthropogenic mercury signals in lake sediments

from southernmost Patagonia, Chile. Science of the Total Environment 445–446, 126–135

Hermanns Y.M., Cortizas A.M., Arz H., Stein R., and Biester H., 2013. Untangling the influence of in-lake productivity and terrestrial organic matter flux on 4,250 years of mercury accumulation in Lake Hambre, Southern Chile. Journal of Paleolimnology 49, 563–573

Hintelmann H., Harris R., Heyes A., Hurley J.P., Kelly C.A., Krabbenhoft D.P., Lindberg S., Rudd J.W.M., Scott K.J., and St. Louis V.L., 2002. Reactivity and mobility of new and old mercury deposition in a boreal forest ecosystem during the first year of the METAALICUS study. Environmental Science and Technology 36, 5034–5040

Holmes C.D., Jacob D.J., Corbitt E.S., Mao J., Yang X., Talbot R., and Slemr F., 2010. Global atmospheric model for mercury including oxidation by bromine atoms. Atmospheric Chemistry and Physics 10, 12037–12057

Horák-Terra I., Martínez Cortizas A., De Camargo P.B., Silva A.C., and Vidal-Torrado P., 2014. Characterization of properties and main processes related to the genesis and evolution of tropical mountain mires from Serra do Espinhaço Meridional, Minas Gerais, Brazil. Geoderma 232–234, 183–197

Horowitz H.M., Jacob D.J., Amos H.M., Streets D.G., and Sunderland E.M., 2014. Historical mercury releases from commercial products: Global environmental implications. Environmental Science and Technology 48, 10242–10250

Hu F.S., Kaufman D., Yoneji S., Nelson D., Shemesh A., Huang Y., Tian J., Bond G., Clegg B., and Brown T., 2003. Cyclic variation and solar forcing of Holocene climate in the Alaskan subarctic. Science (New York, N.Y.) 301, 1890–1893

IAEA, 2015. International Atomic Energy Agency

Jitaru P., Gabrielli P., Marteel A., Plane J.M.C., Planchon F.A.M., Gauchard P.-A., Ferrari C.P., Boutron C.F., Adams F.C., Hong S., et al., 2009. Atmospheric depletion of mercury over Antarctica during glacial periods. Nature Geoscience 2, 505–508

Johnson M., Culp L.R., and George S.E., 1986. Temporal and Spatia Trends in Meta Loadings to Sediments of the Turkey Lakes, Ontario. Canadian Journal of Fisheries and Aquatic Sciences 43, 754–762

Kamman N.C. and Engstrom D.R., 2002. Historical and present fluxes of mercury to Vermont and New Hampshire lakes inferred from 210 Pb dated sediment cores. Atmospheric Environment 36, 1599–1609

Kang S., Huang J., Wang F., Zhang Q., Zhang Y., Li C., Wang L., Chen P., Sharma C.M., Li Q., et al., 2016. Atmospheric Mercury Depositional Chronology Reconstructed from Lake Sediments and Ice Core in the Himalayas and Tibetan Plateau. Environmental Science and Technology 50, 2859–2869

Keppler F., Eiden R., Niedan V., Pracht J., and Schöler H.F., 2000. Halocarbons produced by natural oxidation processes during degradation of organic matter. Nature 403, 298–301

Kirk J.L., Lehnherr I., Andersson M., Braune B.M., Chan L., Dastoor A.P., Durnford D., Gleason A.L., Loseto L.L., Steffen A., et al., 2012. Mercury in Arctic marine ecosystems: Sources, pathways and exposure. Environmental Research 119, 64–87

Krabbenhoft D.P. and Sunderland E.M., 2013. Global Change and Mercury. Science 341, 1457–1458

Kurland T., Faro S.N., and Siedler H., 1960. Minamata disease. The outbreak of a neurologic disorder in Minamata, Japan, and its relationship to the ingestion of seafood contaminated by mercuric compounds. World Neurology 1, 370–395

Kylander M.E., Weiss D.J., Jeffries T., and Coles B.J., 2004. Sample preparation procedures for accurate and precise isotope analysis of Pb in peat by multiple collector (MC)-ICP-MS. Journal of Analytical Atomic Spectrometry 19, 1275–1277

Lacerda L.D., Ribeiro M.G., Cordeiro R.C., Sifeddine A., and Turcq B., 1999. Atmospheric mercury deposition over Brazil during the past 30,000 years. Ciência E Cultura Journal of the Brazilian Association for the Advancement of Science 51, 363–371

Lalonde J.D., Poulain A.J., and Amyot M., 2002. The role of mercury redox reactions in snow on snow-to-air mercury transfer. Environmental Science and Technology 36, 174–178

Lamborg C.H., Fitzgerald W.F., Damman A.W.H., Benoit J.M., Balcom P.H., and Engstrom D.R., 2002. Modern and historic atmospheric mercury fluxes in both hemispheres: Global and regional mercury cycling implications. Global Biogeochemical Cycles 16, 1104

Lamborg C.H., Von Damm K.L., Fitzgerald W.F., Hammerschmidt C.R., and Zierenberg R., 2006. Mercury and monomethylmercury in fluids from Sea Cliff submarine hydrothermal field, Gorda Ridge. Geophysical Research Letters 33, 18–21

Leri A.C., Mayer L.M., Thornton K.R., and Ravel B., 2014. Bromination of marine particulate organic matter through oxidative mechanisms. Geochimica et Cosmochimica Acta 142, 53–63

Li Y., Ma C., Zhu C., Huang R., and Zheng C., 2016. Historical anthropogenic contributions to mercury accumulation recorded by a peat core from Dajiuhu montane mire, central China. Environmental Pollution 216, 332–339

Lindberg S., Bullock R., Ebinghaus R., Engstrom D., Feng X., Fitzgerald W., Pirrone N., Prestbo E., and Seigneur C., 2007. A synthesis of progress and uncertainties in attributing the sources of mercury in deposition. Ambio 36, 19–32

Lindeberg C., Bindler R., Renberg I., Emteryd O., Karlsson E., and Anderson N.J., 2006. Natural Fluctuations of Mercury and Lead in Greenland Lake Sediments. Environmental Science and Technology 40, 90–95

Lindeberg C., Bindler R., Bigler C., Rosén P., and Renberg I., 2007. Mercury Pollution Trends in Subarctic Lakes in the Northern Swedish Mountains. Ambio 36, 401–405

Lindqvist O. and Rodhe H., 1985. Atmospheric mercury - a review. Tellus B 37 B, 136–159

Lockhart W.L., Wilkinson P., Billeck B.N., Hunt R. V., Wagemann R., and Brunskill G.J., 1995. Current and historical inputs of mercury to high-latitude lakes in Canada and to Hudson Bay. Water, Air, and Soil Pollution 80, 603–610

Lockhart W.L., Macdonald R.W., Outridge P.M., Wilkinson P., DeLaronde J.B., and Rudd J.W.M., 2000. Tests of the fidelity of lake sediment core records of mercury deposition to known histories of mercury contamination. Science of the Total Environment, The 260, 171–180

Lowell T. V, Heusser C.J., Andersen B.G., Moreno P.I., Hauser A., Heusser L.E., Schlüchter C.H., Marchant D.R., and Denton G.H., 1995. Interhemispheric correlation of late Pleistocene glacial events. Science 269, 1541–1549

Macdonald R.W., Harner T., and Fyfe J., 2005. Recent climate change in the Arctic and its impact on contaminant pathways and interpretation of temporal trend data. Science of the Total Environment 342, 5–86

Malm O., 1998. Gold mining as a source of mercury exposure in the Brazilian Amazon. Environmental Research 77, 73–78

Margalef O., 2014. The last 70 ky of Rano Aroi (Easter Island, 27 ° S) peat record: New insights for the Central Pacific paleoclimatology. Universitat de Barcelona

Margalef O., Cañellas-Boltà N., Pla-Rabes S., Giralt S., Pueyo J.J., Joosten H., Rull V., Buchaca T., Hernández A., Valero-Garcés B.L., et al., 2013. A 70,000 year multiproxy record of climatic and environmental change from Rano Aroi peatland (Easter Island). Global and Planetary Change 108, 72–84

Margalef O., Martínez Cortizas A., Kylander M., Pla-Rabes S., Cañellas-Boltà N., Pueyo J.J., Sáez A., Valero-Garcés B.L., and Giralt S., 2014. Environmental processes in Rano Aroi (Easter Island) peat geochemistry forced by climate variability during the last 70kyr. Palaeogeography, Palaeoclimatology, Palaeoecology 414, 438–450

Martínez Cortizas A., 2000. Archivos geoquímicos para la reconstrucción de los Paleoambientes cuaternarios: Ideas y Ejemplos. In II Jornadas Do Quaternário Da APEQ, (Porto), pp. 12–15

Martínez Cortizas A., Pontevedra-Pombal X., García-Rodeja E., Nóvoa-Muñoz J.C., and Shotyk W., 1999. Mercury in a Spanish Peat Bog: Archive of Climate Change and Atmospheric Metal Deposition. Science 284, 939–942

Martínez Cortizas A., Biester H., Mighall T., and Bindler R., 2007. Climate-driven enrichment of pollutants in peatlands. Biogeosciences 4, 905–911

Martínez Cortizas A., Peiteado Varela E., Bindler R., Biester H., and Cheburkin A., 2012. Reconstructing historical Pb and Hg pollution in NW Spain using multiple cores from the Chao de Lamoso bog (Xistral Mountains). Geochimica et Cosmochimica Acta 82, 68–78

Martínez Cortizas A., Rozas Muñiz I., Taboada T., Toro M., Granados I., Giralt S., Pla-Rabés S., Cortizas A.M., Muñiz I.R., Taboada T., et al., 2014. Factors controlling the geochemical composition of Limnopolar Lake sediments (Byers Peninsula, Livingston Island, South Shetland Island, Antarctica) during the last ca. 1600 years. Solid Earth 5, 651–663

Mason R.P. and Sheu G.R., 2002. Role of the ocean in the global mercury cycle. Global Biogeochemical Cycles 16, 1093

Mason R., Fitzgerald W., and Morel F., 1994. The biogeochemical cycling of elemental mercury: Anthropogenic influences. Geochimica et Cosmochimica Acta 58, 3191–3198

Mason R.P., Choi A.L., Fitzgerald W.F., Hammerschmidt C.R., Lamborg C.H., Soerensen A.L., and Sunderland E.M., 2012. Mercury biogeochemical cycling in the ocean and policy implications. Environmental Research 119, 101–117

Massa C., Monna F., Bichet V., Gauthier É., Losno R., and Richard H., 2015. Inverse modeling of past lead atmospheric deposition in South Greenland. Atmospheric

Environment 105, 121–129

Mast M.A., Manthorne D.J., and Roth D.A., 2010. Historical deposition of mercury and selected trace elements to high-elevation National Parks in the Western US inferred from lake-sediment cores. Atmospheric Environment 44, 2577–2586

Matty J.M. and Long D.T., 1995. Early diagenesis of mercury in the Laurentian Great Lakes. Journal Great Lakes Research 21, 574–586

McCulloch R.D. and Davies S.J., 2001. Late-glacial and Holocene palaeoenvironmental change in the central Strait of Magellan, southern Patagonia. Palaeogeography, Palaeoclimatology, Palaeoecology 173, 143–173

McKinney M.A., Pedro S., Dietz R., Sonne C., Fisk A.T., Roy D., Jenssen B.M., and Letcher R.J., 2015. A review of ecological impacts of global climate change on persistent organic pollutant and mercury pathways and exposures in arctic marine ecosystems. Current Zoology 61, 617–628

Meyers P. and Lallier-Vergès E., 1999. Lacustrine records of changes in Late Quaternary continental environments and climates: an overview of sedimentary organic matter indicators. Journal of PalaeoLimnology 21, 345–372

Minamata Convention on Mercury web (UNEP)

Morel F.M.M., Kraepiel A.M.L., and Amyot M., 1998. the Chemical Cycle and Bioaccumulation of Mercury. Annual Review of Ecology and Systematics 29, 543–566

Morello F., Borrero L., Massone M., Stern C., Garcia-Herbst A., McCulloch R., Arroyo-Kalin M., Calas E., Torres J., Prieto A., et al., 2012. Hunter-gatherers, biogeographic barriers and the development of human settlement in Tierra del Fuego. Antiquity 86, 71–87

Muir D.C.G., Wagemann R., Hargrave B.T., Thomas D.J., Peakall D.B., and Norstrom R.J., 1992. Arctic marine ecosystem contamination. Science of The Total Environment 122, 75–134

Nafth D., 1993. Ice-core records of the chemical quality of atmospheric deposition and climate from mid-latitude glaciers, Wind River Range, Wyoming. Colorado Schoold of Mines, Golden, Colorado

National Research Council, 2000. Toxicological effects of methylmercury

Nerentorp Mastromonaco M., Gårdfeldt K., Jourdain B., Abrahamsson K., Granfors A., Ahnoff M., Dommergue A., Méjean G., and Jacobi H.W., 2016. Antarctic winter mercury and ozone depletion events over sea ice. Atmospheric Environment 129, 125–132

Nichols A.L., 1997. Lead in Gasoline. In Economic Analyses at EPA: Assessing Regulatory Impact, R.D. Morgenstern, ed. (Washington DC: Resources for the Future), pp. 49–86

Norton S.A., Evans G.C., and Kahl J.S., 1997. Comparison of Hg and Pb fluxes to Hummocks and Hollows of ombrotrophic Big Heath Bog and to Nearby Sargent Mt. Pond, Maine, USA. Water, Air, and Soil Pollution 100, 271–286

Nóvoa-Muñoz J.C., Pontevedra-Pombal X., Martínez-Cortizas A., and García-Rodeja Gayoso E., 2008. Mercury accumulation in upland acid forest ecosystems nearby a coal-fired power-plant in Southwest Europe (Galicia, NW Spain). Science of The Total Environment 394, 303–312

Nriagu J. and Becker C., 2003. Volcanic emissions of mercury to the atmosphere: Global

and regional inventories. Science of the Total Environment 304, 3–12

Obrist D., Tas E., Peleg M., Matveev V., Faïn X., Asaf D., and Luria M., 2011. Bromine-induced oxidation of mercury in the mid-latitude atmosphere. Nature Geoscience 4, 22–26

Ouellet J.F., Lucotte M., Teisserenc R., Paquet S., and Canuel R., 2009. Lignin biomarkers as tracers of mercury sources in lakes water column. Biogeochemistry 94, 123–140

Outridge P.M. and Sanei H., 2010. Does organic matter degradation affect the reconstruction of pre-industrial atmospheric mercury deposition rates from peat cores? — A test of the hypothesis using a permafrost peat deposit in northern Canada. International Journal of Coal Geology 83, 73–81

Outridge P.M., Sanei H., Stern G. A., Hamilton P.B., and Goodarzi F., 2007. Evidence for control of mercury accumulation rates in Canadian High Arctic Lake sediments by variations of aquatic primary productivity. Environmental Science and Technology 41, 5259–5265

Outridge P.M., Rausch N., Percival J.B., Shotyk W., and McNeely R., 2011. Comparison of mercury and zinc profiles in peat and lake sediment archives with historical changes in emissions from the Flin Flon metal smelter, Manitoba, Canada. The Science of the Total Environment 409, 548–563

Pacyna E.G., Pacyna J.M., Steenhuisen F., and Wilson S., 2006. Global anthropogenic mercury emission inventory for 2000. Atmospheric Environment 40, 4048–4063

Parish F., Sirin A., Charman D., Joosten H., Minayeva T., Silvius M., and Stringer L., 2008. Assessment on Peatlands, Biodiversity and Climate Change: Main Report (Kuala Lumpur and Wetlands International, Wageningen)

Peleg M., Matveev V., Tas E., Luria M., Valente R.J., and Obrist D., 2007. Mercury depletion events in the troposphere in mid-latitudes at the Dead Sea, Israel. Environmental Science and Technology 41, 7280–7285

Peña-Rodríguez S., Pontevedra-Pombal X., Fernández-Calviño D., Taboada T., Arias-Estévez M., Martínez-Cortizas A., Nóvoa-Muñoz J.C., and García-Rodeja E., 2012. Mercury content in volcanic soils across Europe and its relationship with soil properties. Journal of Soils and Sediments 12, 542–555

Petit J.-R., Briat M., and Royer A., 1981. Ice age aerosol content from East Antarctic ice core samples and past widn strngth. Nature 293, 391–394

Petit J.R., Jouzel J., Raynaud D., Barkov N.I., Barnola J.-M., Basile I., Bender M., Chappellaz J., Davis M., Delaygue G., et al., 1999. Climate and atmospheric history of the past 420,000 years from the Vostok ice core, Antarctica. Nature 399, 429–436

Pheiffer-Madsen P., 1981. Peat bog records of atmospheric mercury deposition. Nature 293, 127–130

Pirrone N., Cinnirella S., Feng X., Finkelman R.B., Friedli H.R., Leaner J., Mason R., Mukherjee A.B., Stracher G.B., Streets D.G., et al., 2010. Global mercury emissions to the atmosphere from anthropogenic and natural sources. Atmospheric Chemistry and Physics 10, 5951–5964

R CoreTeam, 2014. R: A Language and Environment for Statistical Computing.

Rada R.G., Wiener J.G., Winfrey M.R., and Powel D.E., 1989. Recent increases in

atmospheric deposition of mercury to North-Central Wisconsin Lakes Inferred From Sediment Analyses. Archives of Environmental Contamination and Toxicology 18, 175–181

Rankin A.M., Wolff E.W., and Martin S., 2002. Frost flowers: Implications for tropospheric chemistry and ice core interpretation. Journal of Geophysical Research Atmospheres 107

Ribeiro Guevara S., Meili M., Rizzo A., Daga R., and Arribére M., 2010. Sediment records of highly variable mercury inputs to mountain lakes in Patagonia during the past millennium. Atmospheric Chemistry and Physics 10, 3443–3453

Rizzo A., Arcagni M., Campbell L., Koron N., Pavlin M., Arribére M.A., Horvat M., and Ribeiro Guevara S., 2014. Source and trophic transfer of mercury in plankton from an ultraoligotrophic lacustrine system (Lake Nahuel Huapi, North Patagonia). Ecotoxicology 23, 1184–1194

Roos-Barraclough F., Martinez-Cortizas A., García-Rodeja E., Shotyk W., García-Rodeja E., and Shotyk W., 2002. A 14 500 year record of the accumulation of atmospheric mercury in peat: volcanic signals, anthropogenic influences and a correlation to bromine accumulation. Earth and Planetary Science Letters 202, 435–451

Roos-Barraclough F., Givelet N., Cheburkin A.K., Shotyk W., and Norton S.A., 2006. Use of Br and Se in peat to reconstruct the natural and anthropogenic fluxes of atmospheric Hg: A 10000-year record from Caribou Bog, Maine. Environmental Science and Technology 40, 3188–3194

Rosman K.J.R., Chisholm W., Boutron C.F., Candelone J.P., and Hong S., 1994. Isotopic evidence to account for changes in the concentration of lead in Greenland snow between 1960 and 1988. Geochimica et Cosmochimica Acta 58, 3265–3269

Rossmann R., 2010. Protocol to Reconstruct Historical Contaminant Loading to Large Lakes : The Lake Michigan Sediment Record of Mercury. Environmental Science and Technology 44, 935–940

Rull V., Cañellas-Boltà N., Margalef O., Sáez A., Pla-Rabes S., and Giralt S., 2015. Late Holocene vegetation dynamics and deforestation in Rano Aroi: Implications for Easter Island's ecological and cultural history. Quaternary Science Reviews 126, 219–226

Rydberg J., Gälman V., Renberg I., and Mart A., 2008. Assessing the Stability of Mercury and Methylmercury in a Varved Lake Sediment Deposit. Environmental Science and Technology 42, 4391–4396

Rydberg J., Klaminder J., Rosén P., and Bindler R., 2010a. Climate driven release of carbon and mercury from permafrost mires increases mercury loading to sub-arctic lakes. Science of The Total Environment 408, 4778–4783

Rydberg J., Karlsson J., Nyman R., Wanhatalo I., Näthe K., and Bindler R., 2010b. Importance of vegetation type for mercury sequestration in the northern Swedish mire, Rödmossamyran. Geochimica et Cosmochimica Acta 74, 7116–7126

Sagnotti L., Macrí P., Camerlenghi A., and Rebesco M., 2001. Environmental magnetism of antarctic late pleistocene sediments and interhemispheric correlation of climatic events. Earth and Planetary Science Letters 192, 65–80

Sanei H. and Goodarzi F., 2006. Relationship between organic matter and mercury in recent lake sediment : The physical – geochemical aspects. Applied Geochemistry 21, 1900–1912

Schartup A.T., Balcom P.H., Soerensen A.L., Gosnell K.J., Calder R.S.D., Mason R.P., and Sunderland E.M., 2015. Freshwater discharges drive high levels of methylmercury in Arctic marine biota. Proceedings of the National Academy of Sciences 112, 11789–11794

Schroeder W.H. and Munthe J., 1998. Atmospheric mercury—An overview. Atmospheric Environment 32, 809–822

Schroeder W.H., Anlauf K.G., Barrie L. a, Lu J.Y., and Steffen A., 1998. Arctic Springtime Depletion of Mercury. Nature 394, 331–332

Schuster P.F., Krabbenhoft D.P., Naftz D.L., Cecil L.D., Olson M.L., Dewild J.F., Susong D.D., Green J.R., and Abbott M.L., 2002. Atmospheric Mercury Deposition during the Last 270 Years: A Glacial Ice Core Record of Natural and Anthropogenic Sources. Environmental Science and Technology 36, 2303–2310

Schuster P.F., Striegl R.G., Aiken G.R., Krabbenhoft D.P., Dewild J.F., Butler K., Kamark B., and Dornblaser M., 2011. Mercury Export from the Yukon River Basin and Potential Response to a Changing Climate. Environmental Science and Technology 45, 9262–9267

Schwander J., Stauffer B., and Sigg A., 1988. Air mixing in firn and the age of the air at pore close- off. Annals of Glaciology 10, 141–145

Selin N.E., 2009. Global Biogeochemical Cycling of Mercury : A Review.

Selin N.E., Jacob D.J., Yantosca R.M., Strode S., Jaeglé L., and Sunderland E.M., 2008. Global 3-D land-ocean-atmosphere model for mercury: Present-day versus preindustrial cycles and anthropogenic enrichment factors for deposition. Global Biogeochemical Cycles 22, 1–13

Shotyk W., 1996. Peat bog archives of atmospheric metal deposition: geochemical evaluation of peat profiles, natural variations in metal concentrations, and metal enrichment factors. Environmental Reviews 4, 149–183

Shotyk W., Goodsite M.E., Roos-Barraclough F., Frei R., Heinemeier J., Asmund G., Lohse C., and Hansen T.S., 2003. Anthropogenic contributions to atmospheric Hg, Pb and As accumulation recorded by peat cores from southern Greenland and Denmark dated using the 14C "bomb pulse curve." Geochimica et Cosmochimica Acta 67, 3991–4011

Shotyk W., Goodsite M.E., Roos-Barraclough F., Givelet N., Le Roux G., Weiss D., Cheburkin A.K., Knudsen K., Heinemeier J., van Der Knaap W., et al., 2005. Accumulation rates and predominant atmospheric sources of natural and anthropogenic Hg and Pb on the Faroe Islands. Geochimica et Cosmochimica Acta 69, 1–17

Sigler J.M., Lee X., and Munger W., 2003. Emission and long-range transport of gaseous mercury from a large-scale Canadian boreal forest fire. Environmental Science and Technology 37, 4343–4347

Silva-Sánchez N., Schofield J.E., Mighall T.M., Martínez Cortizas A., Edwards K.J., and Foster I., 2015. Climate changes, lead pollution and soil erosion in south Greenland over the past 700 years. Quaternary Research 84, 159–173

Simpson W.R., Von Glasow R., Riedel K., Anderson P., Ariya P., Bottenheim J., Burrows J., Carpenter L.J., Friess U., Goodsite M.E., et al., 2007. Halogens and their role in polar boundary-layer ozone depletion. Atmos. Chem. Phys. 7, 4375–4418

Smith-Downey N. V., Sunderland E.M., and Jacob D.J., 2010. Anthropogenic impacts on

global storage and emissions of mercury from terrestrial soils: Insights from a new global model. Journal of Geophysical Research: Biogeosciences 115, 1–11

Soerensen A.L., Sunderland E.M., Holmes C.D., Jacob D.J., Yantosca R.M., Skov H., Christensen J.H., Strode S.A., and Mason R.P., 2010. An improved global model for air-sea exchange of mercury: High concentrations over the North Atlantic. Environmental Science and Technology 44, 8574–8580

Steffen A., Douglas T., Amyot M., Ariya P., Aspmo K., Berg T., Bottenheim J., Brooks S., and Cobbett F., 2008. A synthesis of atmospheric mercury depletion event chemistry in the atmosphere and snow. Atmospheric Chemistry and Physics 8, 1445–1482

Steffen A., Lehnherr I., Cole A., Ariya P., Dastoor A., Durnford D., Kirk J., and Pilote M., 2015. Atmospheric mercury in the Canadian Arctic. Part I: A review of recent field measurements. Science of the Total Environment 509–510, 3–15

Steinhilber F., Beer J., and Fröhlich C., 2009. Total solar irradiance during the Holocene. Geophysical Research Letters 36, 1–5

Steinnes E. and Sjøbakk T.E., 2005. Order-of-magnitude increase of Hg in Norwegian peat profiles since the outset of industrial activity in Europe. Environmental Pollution 137, 365–370

Stern C.R., 2008. Holocene tephrochronology record of large explosive eruptions in the southernmost Patagonian Andes. Bulletin of Volcanology 70, 435–454

Stern G.A., Macdonald R.W., Outridge P.M., Wilson S., Chételat J., Cole A., Hintelmann H., Loseto L.L., Steffen A., Wang F., et al., 2012. How does climate change influence Arctic mercury? The Science of the Total Environment 414, 22–42

Stern G. a, Sanei H., Roach P., Delaronde J., and Outridge P.M., 2009. Historical Interrelated Variations of Mercury and Aquatic Organic Matter in Lake Sediment Cores from a Subarctic Lake in Yukon, Canada : Further Evidence toward the Algal-Mercury Scavenging Hypothesis. Environ. Sci. Technol. 43, 7684–7690

Streets D.G., Devane M.K., Lu Z., Bond T.C., Sunderland E.M., and Jacob D.J., 2011. All-time releases of mercury to the atmosphere from human activities. Environmental Science and Technology 45, 10485–10491

Sun L., Yin X., Liu X., Zhu R., Xie Z., and Wang Y., 2006. A 2000-year record of mercury and ancient civilizations in seal hairs from King George Island, West Antarctica. Science of the Total Environment 368, 236–247

Sunderland E.M. and Mason R.P., 2007. Human impacts on open ocean mercury concentrations. Global Biogeochemical Cycles 21

Swain E.B., 1997. Recent Declines in Atmospheric Mercury Deposition in the Upper Midwest. Environmental Science and Technology 31, 960–967

Swain E.B., Engstrom D.R., Brigham M.E., Henning T.A., and Brezonik P.L., 1992. Increasing Rates of Atmospheric Mercury Deposition in Midcontinental North America. Science 257, 784–787

Swartzendruber P. and Jaffe D., 2012. Sources and Transport: In Mercury in the Environment, (University of California Press), pp. 3–18

Tang S., Huang Z., Liu J., Yang Z., and Lin Q., 2012. Atmospheric mercury deposition recorded in an ombrotrophic peat core from Xiaoxing'an Mountain, Northeast China. Environmental Research 118, 145–148

Thomas R.L., 1972. The Distribution of Mercury in the Sediments of Lake Ontario.

Canadian Journal of Earth Sciences 9, 636–651

Toro M., Camacho A., Rochera C., Rico E., Bañón M., Fernández-Valiente E., Marco E., Justel A., Marco E., Avedaño M.C., et al., 2007. Limnological characteristics of the freshwater ecosystems of Byers Peninsula, Livingston Island, in maritime Antarctica. Polar Biology 30, 635–649

Toro M., Granados I., Pla S., Giralt S., Antoniades D., Galán L., Cortizas A.M., Lim H.S., and Appleby P.G., 2013. Chronostratigraphy of the sedimentary record of Limnopolar Lake, Byers Peninsula, Livingston Island, Antarctica. Antarctic Science 25, 198–212

UNEP, 2013. Minamata Convention on Mercury - Text and Annexes. UNEP, 2013a 69

Vandal G.M., Fitzgerald W.F., Boutron C.F., and Candelone J.-P., 1993. Variations in mercury deposition to Antarctica over the past 34,000 years. Nature 362, 621–623

Veiga M.M., Maxson P.A., and Hylander L.D., 2006. Origin and consumption of mercury in small-scale gold mining. Journal of Cleaner Production 14, 436–447

Weiss D.J., Kober B., Dolgopolova A., Gallagher K., Spiro B., Le Roux G., Mason T.F.D., Kylander M., and Coles B.J., 2004. Accurate and precise Pb isotope ratio measurements in environmental samples by MC-ICP-MS. International Journal of Mass Spectrometry 232, 205–215

Weiss H., Bertine K., Koide M., and Goldberg E.D., 1975. The chemical composition of a Greenland glacier. Geochimica et Cosmochimica Acta 39, 1–10

Weiss H. V, Koide M., and Goldberg E.D., 1971. Mercury in a Greenland Ice Sheet: Evidence of Recent Input by Man. Science 174, 692–694

WHO, 1989. Environmental Health Criteria 86: Mercury - Environmental Aspects (Geneva)

Wiklund J.A., Kirk J.L., Muir D.C.G., Evans M., Yang F., Keating J., and Parsons M.T., 2017. Anthropogenic mercury deposition in Flin Flon Manitoba and the Experimental Lakes Area Ontario (Canada): A multi-lake sediment core reconstruction. Science of The Total Environment

World Health Organization, 2011. Report of the joint FA (Geneva: World Health Organization)

Yang H., 2015. Lake Sediments May Not Faithfully Record Decline of Atmospheric Pollutant Deposition. Environmental Science and Technology 151016145422005

Yang H. and Rose N.L., 2003. Distribution of mercury in six lake sediment cores across the UK. 304, 391–404

Yang H. and Smyntek P., 2014. Use of the mercury record in Red Tarn sediments to reveal air pollution history and the implications of catchment erosion. Environ. Sci.: Processes Impacts 16, 2554–2563

Yang H., Rose N.., Boyle J.., and Battarbee R.., 2001. Storage and distribution of trace metals and spheroidal carbonaceous particles (SCPs) from atmospheric deposition in the catchment peats of Lochnagar, Scotland. Environmental Pollution 115, 231–238

Yang H., Battarbee R.W., Turner S.D., Rose N.L., Derwent R.G., Guangjian W., and Ruiqiang Y., 2010a. Historical Reconstruction of Mercury Pollution Across the Tibetan Plateau Using Lake Sediments. Environ. Sci. Technol. 44, 2918–

2924

Yang H., Engstrom D.R., and Rose N.L., 2010b. Recent Changes in Atmospheric Mercury Deposition Recorded in the Sediments of Remote Equatorial Lakes in the Rwenzori Mountains, Uganda. Environmental Science and Technology 44, 6570–6575

Yang H., Turner S., and Rose N.L., 2016. Mercury pollution in the lake sediments and catchment soils of anthropogenically-disturbed sites across England. Environmental Pollution 219, 1092–1101

Zaccone C., Santoro A., Cocozza C., Terzano R., Shotyk W., and Miano T.M., 2009. Comparison of Hg concentrations in ombrotrophic peat and corresponding humic acids, and implications for the use of bogs as archives of atmospheric Hg deposition. Geoderma 148, 399–404

Zhang Q., Huang J., Wang F., Mark L., Xu J., Armstrong D., Li C., Zhang Y., and Kang S., 2012. Mercury distribution and deposition in glacier snow over Western China. Environmental Science and Technology 46, 5404–5413

Zheng J., 2015. Archives of total mercury reconstructed with ice and snow from Greenland and the Canadian High Arctic. Science of the Total Environment 509–510, 133–144

Zhu W., Lin C.J., Wang X., Sommar J., Fu X., and Feng X., 2016. Global observations and modeling of atmosphere-surface exchange of elemental mercury: A critical review. Atmospheric Chemistry and Physics 16, 4451–4480

Zuna M., Ettler V., Š O., Mihaljevi M., Šebek O., and Mihaljevič M., 2012. Mercury accumulation in peatbogs at Czech sites with contrasting pollution histories. Science of The Total Environment 424, 322–330

USC
UNIVERSIDADE
DE SANTIAGO
DE COMPOSTELA

8. Funding and Acknowledgments

I would like to express my gratitude to all those research groups, projects and researchers that have provided the samples used in this doctoral thesis and access to laboratory facilities, through the collaboration with my supervisor Prof Antonio Martínez Cortizas and the group Ciencias do Sistema Terra of the Universidade de Santiago de Compostela.

This research was made possible through funding provided by:

The Ministerio Español de Ciencia e Innovación (Project CGL2010-20672), the Dirección General de Innovación y Desarrollo de Galicia (Project 10PXIB200182PR), Consellería de Cultura, Educación e Ordenación Universitaria da Xunta de Galicia (grants R2014/001, GPC2014/009 and GPC GI-1553) projects leaded by Prof Antonio Martínez Cortizas (USC).

The Ministerio Español de Ciencia e Innovación (Project REN2000-0345-ANT) leaded by Dr Antonio Quesada (UAM).

The Ministerio Español de Ciencia y Educación through the projects LAVOLTER (CGL2004-00683/BTE), leaded by Dr Conxita Taberner and Dr Santiago Giralt and project GEOBILA (CGL2007-60932/BTE) leaded by Dr Alberto Sáez (UB).

Conselho Nacional deesenvolvimento Cientfico e Tecnolgico (CNPq), Brazil (Project Universal 14/2011- 482815/2001-6) leaded by Prof. Pablo Vidal-Torrado (ESALQ)

The Deutsche Forschungsgemeinschaft (project DFG-BI 734/15-1) leaded by Prof Harald Biester (TUBs).

The UK Leverhulme Trust “Footprints on the Edge of Thule” programme award.

Extra funding for performing a three-month research secondments at the Technische Universität Braunschweig was provided by the competitive call of the Deutsche Akademische Austauschdienst (DAAD, grant ref no. 91588482).

Acknowledgments

My sincere thanks to my supervisor Antonio Martínez Cortizas for the opportunity offered to develop this doctoral thesis and to introduce me to Science. I would also like to thank you for all the help, the time dedicated and the good character and willingness to discuss, comment and solve doubts and problems. Many thanks!

Likewise, I would especially like to thank Dr Jesús R. Aboal and the Ecotox research group (specially also Dr Ángel Fernández) of the Universidade de Santiago de Compostela for access to their laboratory without which this doctoral thesis would not have been possible. Thank you very much Jesús for opening me the doors of your lab and your research group. Many thanks!

I would also like to thank Prof Harald Biester (Technische Universität Braunschweig) for the opportunity to work for three months in his group. Thanks Harald, for the interest, the time dedicated and the support for my work and career.

I also want to thank all those researchers who have collaborated and helped me to develop this research: Dr Olga Margalef and Dr Sergi-Pla Rabes (CREAF); Dr Santiago Giralt (Institut de Ciències de la Terra Jaume Almera-CSIC); Dr J. Pablo Corella (Instituto de Química Física Rocasolano-CSIC); Dr Manuel Toro (Centro de Estudios Hidrográficos); Dr Ingrid Horák-Terra (Federal University of Jequitinhonha and Mucuri Valleys); Dr Yvonne-Marie Hermanns (Technische Universität Braunschweig); Dr Benjamin-Silas Gilfedder (Universität Bayreuth); Prof Kevin J. Edwards, Dr Tim Mighall, Dr J. Edaward Schofield and (University of Aberdeen); Dr Malin Kylander (Stockholm University); Prof Richard Bindler (Umea University).

Many thanks to all members of the group Ciencias do Sistema Terra. Thank you very much Luis for introducing me to R, and for the help, advice and good discussions. Thank you very much Tere and Cruz for helping me to be a little bit

more “Edafóloga” and for the encouragement! Thanks Joeri for all the good and quick revisions in the last moment!, also for your interest and curiosity towards my work. Thank you very much Noe for being a fantastic co-worker and also a very good friend for travels. Thanks Olalla and Rebe for introduced me to the archaeology and bone-science, and show me that can be cool too. Many thanks to Mohamed, Marcela and Nerea for being great laboratory partners and always ready to discuss, ask, resolve doubts and have a break!

I would like to express my sincere thanks to the Ecotox group (present and past) for a warming welcomed and made me feel one more. Specially thank Sofi and Marta for patience and the good moments. Sofi, muchísimas gracias por los buenos momentos, por toda la ayuda durante la recta final y el apoyo en los momentos más bajos.

I also would like to thank all the people for the TUBs group (past and present) because you received me with affection when I made my stay in 2015 and for having received again better now, when I start this first stage after the doctoral thesis. Thank you very much: Petra, Adelina, Frau Wörndel, Jan-Helge, Mónica, Carluvy, Ayo, Sara and Martin.

Muchas gracias Antón, Joaquín, Belén y Alba por los buenos momentos de desconexión.

Muchas gracias a mi familia, a mi abuela, a Paula y a Ricardo, y especialmente a Papá y Mamá, y a mis hermanos, Paula y Miguel. Muchas gracias por haberme ayudado siempre y desde el principio, muchas gracias por haber confiado siempre en mi. También a ti Ber, que has sido un apoyo paciente (muy paciente) todos estos años y me has ayudado a sacar lo mejor de mi para poder llevar a cabo esta tesis.

Braunschweig, 8 May 2017

USC
UNIVERSIDADE
DE SANTIAGO
DE COMPOSTELA

9. Manuscripts

USC
UNIVERSIDADE
DE SANTIAGO
DE COMPOSTELA

MANUSCRIPT I

~71 kyr of mercury deposition in the Southern Hemisphere recorded by Rano Aroi mire, Easter Island (Chile)

USC
UNIVERSIDADE
DE SANTIAGO
DE COMPOSTELA

~71 kyr of mercury deposition in the Southern Hemisphere recorded by Rano Aroi mire, Easter Island (Chile)

Marta Pérez-Rodríguez [1]*, Olga Margalef [2,3], J. Pablo Corella [4], Sergi Pla-Rabes[3], Santiago Giralt[5], Antonio Martínez Cortizas [1]

* corresponding author: M. Pérez-Rodríguez; mperez.rodriguez@usc.es

[1] *Departamento de Edafoloxía e Química Agrícola, Universidade de Santiago de Compostela, Santiago de Compostela, Spain*
[2] *CSIC, Global Ecology Unit CREAF-CEAB-UAB, Spain*
[3] *Ecological Research Center and Forestry Applications (CREAF), Campus de Bellaterra (UAB) Cerdanyola del Vallès, Barcelona, Spain*
[4] *Department of Atmospheric Chemistry and Climate, Institute of Physical Chemistry Rocasolano, CSIC, Madrid, Spain*
[5] *Institute of Earth Sciences Jaume Almera (ICTJA-CSIC), Barcelona, Spain*

Abstract

The study of mercury accumulation in peat cores provides an excellent opportunity to improve the knowledge on mercury cycling and depositional processes at remote locations far from pollution sources. We analysed mercury concentrations in 150 peat samples on the cores ARO 06 01 and ARO 08 02 from Rano Aroi (Easter island, 27ºS) and in selected vegetation samples of present-day flora of the island in order to characterize the mercury cycling for the last ~71 kyr BP. Mercury concentration in plants ranges between 1470 and 11,175 ng g^{-1}, corresponding the latter with a rush sample. The mercury record in ARO 08 02 and ARO 06 01 cores show values raging between 37-177 ng g^{-1} and 35- 200 ng g^{-1} respectively, except for two large maxima (910 and 1023 ng g-1) occurred at the end of the Last Glacial Maximum (~20 kyr cal BP) in both peat cores. Climate (both precipitation and temperature) seems to have controlled the abrupt increase in Hg deposition during this period. These values are higher than those recorded in most peat records belonging to the Industrial period, highlighting that natural factors played a significant role on Hg deposition - sometimes even higher than anthropogenic sources. Combined with a previous paleoenvironmental reconstruction, our new results suggest that wet deposition was the main process controlling Hg fluxes, both to the mire and to the catchment soils. Changes in mire vegetation, peat decomposition and volcanism had a secondary role in the mercury content in Rano Aroi.

1. Introduction

Mercury (Hg) is a metal of environmental concern due to its high volatility, long atmospheric residence time (1-2 years) and toxicity of its methylated forms. It is released and dispersed in the atmosphere by natural emission sources like volcanoes, geothermal vents, and Hg-enriched soil as well as by anthropogenic activities such as mining, coal-fired plants and chloro-alkali plants (Schroeder and Munthe, 1998; Hylander and Meili, 2005; Horowitz et al., 2014). The transport and deposition in different environments on Earth depends on the Hg species. Elemental Hg (Hg^0), the dominant species in the atmosphere, can be transported over long distance from emissions sources. It can be eventually oxidized, into divalent Hg (Hg^{+2}) which is washed out by rainfall and deposited on the land surface (Hall, 1995; Fitzgerald and Mason, 1996; Schroeder and Munthe, 1998; Wang et al., 2014). Particulate Hg (Hg_p) represents a minor fraction of total Hg in the atmosphere and can be dispersed over tens to hundreds of kilometers (Schroeder and Munthe, 1998).

Natural archives such as mires, lake sediments and glacial ice have been widely used to reconstruct Hg accumulation at local, regional and global scale – see Amos et al., 2015; Biester et al., 2007; Cloy et al., 2008; Engstrom et al., 2014 and references therein. These archives have allowed the identification of processes and factors that control the deposition and accumulation of mercury over time. On most recent times, a factor between 3 and 5-fold increase in the deposition of Hg was observed in different parts of the world since the advent of the Industrial Revolution, suggesting a worldwide increase in the atmospheric Hg deposition (Lamborg et al., 2002; Amos et al., 2015). This anthropogenic input overlaps the signal driven by natural processes of deposition and accumulation. Organic matter degradation and mass loss related with peat evolution enhance Hg accumulation in peatlands (Biester et al., 2003, 2004). Short- and long-term climate oscillations seem to play an important role in Hg cycling through i) controlling the re-emission of part of the accumulated Hg (Martínez Cortizas et al., 1999); ii) inducing Hg depletion events in polar environments during glacial periods (Jitaru et al., 2009); iii) producing algal scavenging in lakes (Outridge et al., 2007; Kirk et al., 2011) or also by iv) releasing Hg from permafrost mires in warm periods (Rydberg et al., 2010a). Finally, processes such as volcanism and fires may play a role in releasing Hg into the atmosphere or in the landscape but the effects are only visible in very specific cases (i.e. Roos-Barraclough et al., 2002; Schuster et al., 2002; Ribeiro

Guevara et al., 2010; Daga et al., 2016; Corella et al., 2017).

Nevertheless, most of these considerations are almost exclusively based on Holocene records, and only a few studies extend their conclusions back to the Pleistocene. In contrast to the Northern Hemisphere, there is a limited amount of quite heterogeneous information available for the Southern Hemisphere. The works focused on Hg reconstruction in the South Hemisphere are almost exclusively from Patagonian area. Most of these studies are based on lake sediments (Ribeiro Guevara et al., 2010; Hermanns et al., 2012; Hermanns and Biester, 2013; Daga et al., 2016) and a few on peat (Biester et al., 2003; Franzen et al., 2004).

In a recent work we studied Hg accumulation in Pinheiros (18º S, 43ºW) (Pérez-Rodríguez et al., 2015), a Pleistocene age (last ~57 kyrs) tropical mire located in a valley in Serra do Espinhaço Meridional (state of Minas Gerais, Brazil). In this work, we found that three of the four main processes controlling mercury concentration depended on climate: wet and dry mercury deposition (rainfall and dustfall, respectively) as well as local catchment soil erosion owing to precipitation events (Pérez-Rodríguez et al., 2015). The effect of long-term peat decomposition, the only autogenic process identified, was confined to the Holocene section of the peat (Pérez-Rodríguez et al., 2015).

Although some of the mentioned works provided information from Pleistocene sections (~11.2, 14.6 and ~57 kyr cal BP, respectively [Biester et al., 2003; Franzen et al., 2004; Pérez-Rodríguez et al., 2015, 2016]), more long-term records and from a wider geographical extent are needed in order to fully understand the various processes that can influence emission, deposition, and accumulation of mercury in continental ecosystems. In particular, the role of climate, both through controls on deposition and accumulation, is one of the major issues that needs to be addressed.

In this study we analysed two peat cores from Rano Aroi, a small mire located in Easter Island, which covers the last ~71 kyrs BP. Compositional (C, N, C/N, Ti) isotopic ($\delta^{13}C$) organic matter data and other geochemical information summarized by Principal Component Analysis (PC1 and PC2) from the previous studies were complemented with the determination of mercury content in peat samples and in selected vegetation samples of present-day flora located in the watershed. The objectives of the present research were (i) to reconstruct the Pleistocene mercury fluxes variability at millennial to centennial resolution and (ii) to determine the

main factors that controlled peat mercury concentrations over long time scales.

2. Material and Methods

2.1. Regional setting

Easter Island (27º07' S, 109º22' W) is a Chilean volcanic island Miocene in age located in the southern Pacific Ocean. The nearest continental point from the South American continent lies 3512 km away. The Island has a triangular shape and the topography is characterized by more than 70 volcano craters and the rolling surfaces of lava flows (Baker et al., 1974; González-Ferrán et al., 2004; Sáez et al., 2009). The climate is humid subtropical, with average monthly temperatures between 18 °C (August) and 24 °C (February) (Junk and Claussen, 2011) and highly variable annual rainfall ranging from 500 to 1800 mm (mean of 1130 mm).

Rano Aroi is a small mire located in an ancient Pleistocene volcano crater close to most elevated area of the island (27°S, 108°W, 430 m elevation, 0.13 km^2; Figure 1). The crater slopes form a small catchment area (15.82 km^2). Watershed lithology mainly consists on very porphyritic olivinic tholeite, basalt and hawaiite lava flows, rich in iron (González-Ferrán et al., 2004). The mire is covered by Scirpus californicus, Polygonum acuminatum, Asplenium polyodon var. squamulosum, Vittaria elongata and Cyclosorus interruptus (Zizka, 1991), while the catchment area is covered by grassland and planted eucalyptus. There is a small ravine acting as a natural outflow that infiltrates before reaching the

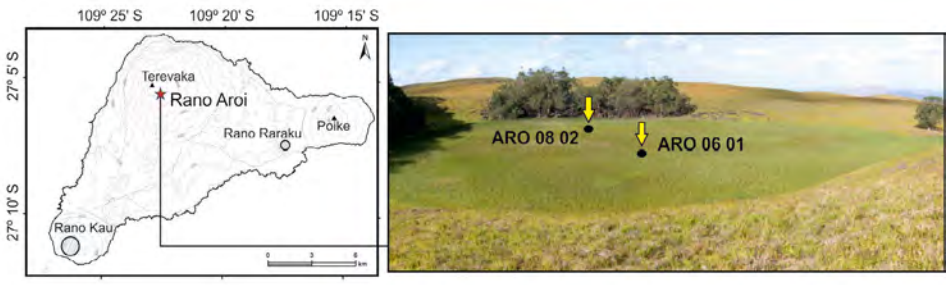

Figure 1. (left) Map showing the location of Rano Aroi on the island. (right) Photo of the Rano Aroi mire, indicating the location of the studied cores (ARO 06 01, center of the mire and ARO 08 02, margins of the mire).

coast. An artificial outlet built in the 1960s controls maximum water levels.

2.2. Sampling

Two sediment cores (ARO 06 01, 13.9 m long and ARO 08 02, 4 m long) were retrieved from Rano Aroi on March 2006 and October 2008 respectively. The core ARO 06 01 was sampled with a UWITEC corer from the central part of the mire and the

The uppermost two meters were rejected to avoid potential anthropic remobilization, as described in previous studies (Margalef et al., 2013, 2014). Meanwhile ARO 08 02 was recover with a Russian corer from the eastern boundary since the mire´s margins was potentially not affected by recent human activities (Flenley and King, 1984; Flenley et al., 1991). None of the cores retrieved in either campaign reached the bedrock. The cores were sealed, transported to a core repository and stored in a cold room at +4 °C until sampling. Both cores were lithologically described and sampled for smear slides every 5 cm (Margalef et al., 2013).

2.3. Age model

The chronology for both cores were fully described Margalef et al., (2013). A total of 27 AMS ^{14}C dates were obtained from pollen concentrates of the ARO 06 01 and ARO 02 08 cores, in the Poznan Radiocarbon Laboratory (Poland). Only 18 dates were used for the age-depth model. The AMS ages were calibrated using CALIB 6.02 software, and the INTCAL 98 curve (Reimer et al., 2004) and CalPal (Danzeglocke et al., 2008) for samples older than 20,000 radiocarbon yr BP. The age model was built by simple linear interpolation. See all details in Margalef et al., (2013).

2.4. Geochemical analysis

Both cores were sampled every 5 cm (286 samples) for total carbon and nitrogen (TC and TN) and stable isotope ($\delta^{13}C$) analyses. Samples were dried at 60 °C over 48 h, frozen with liquid nitrogen and ground in a ring mill. Analyses were performed using a Finnigan delta Plus EA-CF-IRMS spectrometer, located at the Centres Tècnics i Tecnològics of the Universitat de Barcelona (CCiTUB) (Margalef et al., 2013).

Titanium concentration was analysed by Inductively Coupled Plasma-Atomic Emission Spectrometry (ICP-AES) in core ARO 06 01. The samples were analysed for elemental concentrations using a Varian Vista AX ICP-AES at the Department of Geological Sciences, Stockholm University, Sweden. See more information for geochemical analysis in previous works (Margalef et al., 2013, 2014).

Mercury concentrations were determined in 150 samples of the two cores collected in Rano Aroi and in selected vegetation samples of present-day flora located in the island. Dried, milled samples were analysed for mercury using a Milestone DMA-80 analyser hosted at the Departamento de Bioloxía Funcional (University of Santiago de Compostela). The analysis of one in every five samples was duplicated as a control. A standard reference material of the moss Pleurozium schreberi (Steinnes et al., 1997) M3, was run with each set of samples. The quantification limit was 1.34 ng g^{-1} and mean recovery was 90%.

3. Results

3.1. Peat Geochemistry

3.1.1. Organic fraction: Total Carbon, Total Nitrogen, C/N and δ13C

The Rano Aroi deposits are mostly organic, with TC concentrations between 40% and 70% (Margalef et al., 2013). Total N levels of core ARO 06 01 vary between 0.4% and 2%, with C/N ratios ranging from 40 to 110 (Figure 2). ARO 08 02 shows similar values with respect to TC (50–60%), TN (0.8–2%, peaking to 2.5% at 140 and 80 cm) and C/N (20–80, with a marked decrease from 2 m upward) (Figure 3).

In ARO 06 01, $\delta^{13}C$ shows a constant value around −14‰ from depths of 14 m to 9 m, whereas from 9 m to 6 m, $\delta^{13}C$ values gradually shift from −14 to −26‰ (Figure 2). In the upper five meters, $\delta^{13}C$ values vary around −26‰. In ARO 08 02, a gentle shift of $\delta^{13}C$ from −19‰ to −23‰ occurs from depths of 4 m to 3.5 m (Figure 3). $\delta^{13}C$ curves show high-frequency changes (dips) within the long-term trend (Margalef et al., 2013).

3.1.2. Inorganic fraction: Titanium

Titanium concentrations were only measured in ARO 06 01 (Figure 2). They show a baseline between 54 and 304 mg kg^{-1} interrupted by abrupt increases higher than 1000 mg kg^{-1}, and reaching values of 5000 mg kg^{-1} at 340 cm.

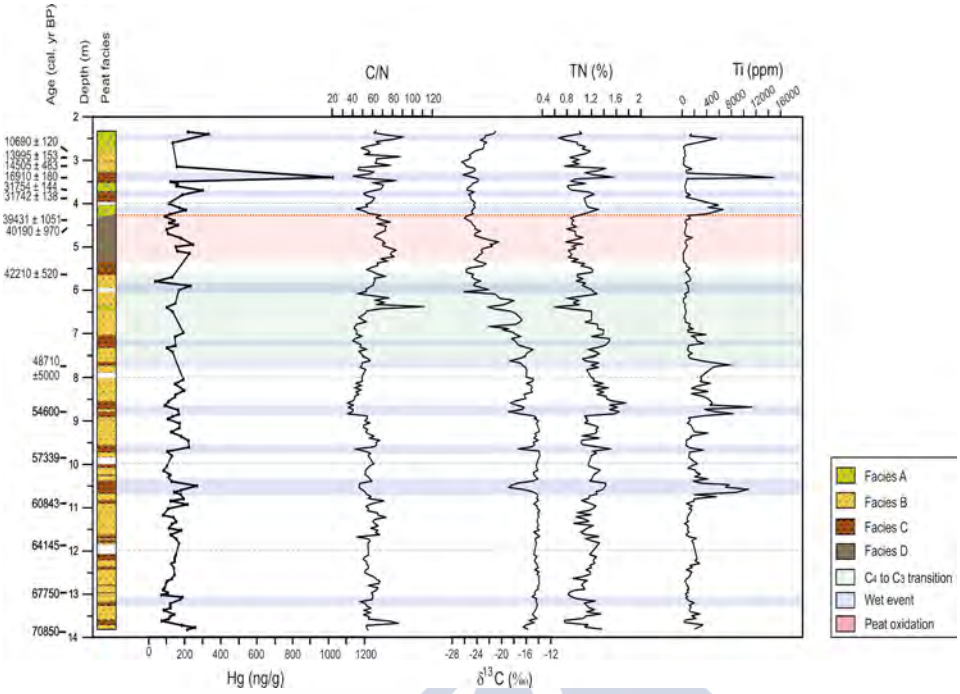

Figure 2. Depth profiles of the main paleoenvironmental proxies and Hg concentration (in ng g^{-1}) analysed in ARO 06 01 core. Lithology and radiocarbon age samples are indicated in the column. Geochemical proxies: TN (in percentage) C/N ratios and $\delta^{13}C$ (‰), are indicative of the origin of organic matter; and Ti (in ppm) come from terrigenous inputs and together with $\delta^{13}C$ (‰) and Facies C (Margalef et al., 2013) are wet event indicators. Periods of flood events and drought conditions are marked.

3.1.3. Mercury

Mercury concentrations in Rano Aroi samples varied in the same range in both cores (Figure 2 and Figure 3). Core ARO 06 08 has values that range between 35 and 333 ng g^{-1} (147±49, mean ± standard deviation) albeit they can reach up to 1023 ng g^{-1} (sample at 370 cm of core depth). The Hg minimum is located at 580 cm (Figure 2). Core ARO 08 02 displays Hg values that range between 37 and 329 ng g^{-1} (104±56 ng g-1), but two maxima (1088 and 910 ng g^{-1}) are located at 195 and 285 cm of core depth. According to Hg concentrations, this profile shows three distinct sections: i) from the base of the core to 290 cm values increase with depth but with small oscillations (122±26 ng g^{-1}); ii) from 280 to 202 cm, values are low and almost constant (73±14 ng g^{-1}); and iii) the upper 190 cm have intermediate values (101±56 ng g^{-1}), with two relative maxima of 177 and 192 ng g^{-1} at 130 and 75 cm respectively (Figure 3).

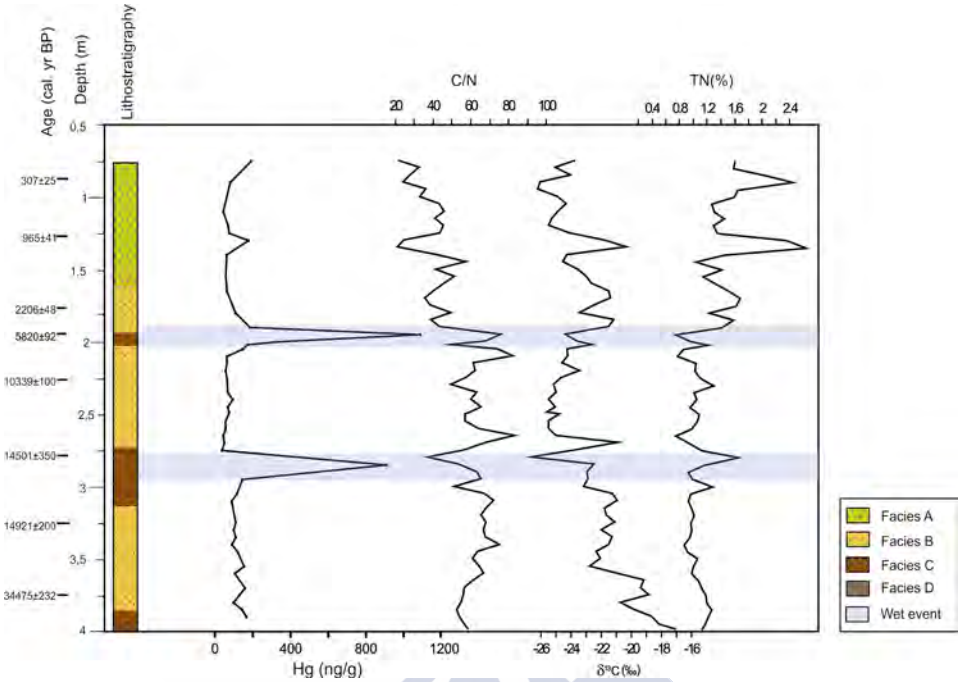

Figure 3 Depth profiles of the main paleoenvironmental proxies and Hg concentration (in ng g^{-1}) analysed in ARO 08 02 core versus depth. Lithology and radiocarbon age samples are indicated in the column. Geochemical proxies: TN (in percentage) C/N ratios and $\delta^{13}C$ (‰), are indicative of the origin of organic matter; Facies C (Margalef et al., 2013) is wet event indicator. Periods of high rainfall events and drought conditions are marked.

Mercury in vegetation samples has a large concentration range (Table 1). The lowest value (341 ng g^{-1}) corresponds to the rhizome of Scirpus californicus and the maximum value (11 175 ng g^{-1}) with an unidentified rush sample.

Table 1. Mercury concentrations determined in vegetation samples collected in Easter Island.

Local/English name	Scientific name	Hg (ng g^{-1})
Kikuyu/Kikuyu grass		1 945
Nga'atu/Totora (duster)	*Scirpus californicus (duster)*	1 804
Nga'atu/Totora (rhizome)	*Scirpus californicus (rhizome)*	341
/Rush	*- no identified-*	11 175
Maku Piro/ molassesgrass	*Melinis minutiflora*	1 470

4. Discussion

4.1. Mercury concentration in Rano Aroi records

The two Rano Aroi records (ARO 08 02 and ARO 06 01) cover different temporal ranges (38.7 kyr cal BP- Present day and 71 kyrs BP - 8.5 kyr cal BP, respectively) and were retrieved in different parts of the peatland (Figure 1), although less than 50 meters apart. Previous studies, using multiple short cores from the same peatland showed that spatial variability can be a problem for an accurate Hg study, since vegetation and micro-topography changes can affect the interception and retention of atmospheric deposition, and over relatively short timescales (Bindler et al., 2004; Martínez Cortizas et al., 2012). However, the short distance between the cores, the small size of the mire (0.13 km2) and the age-depth model based on both cores (Margalef et al., 2013) seem to have largely solved this problem. Therefore, we discuss the processes that controlled mercury concentrations in Rano Aroi using both cores together; the differences between them are illustrated based on other proxies (as TC, TN and $\delta^{13}C$).

To the best of our knowledge, there is only one comparable record – Pleistocene peat record from a tropical-sub tropical area – to Rano Aroi in the literature that is Pinheiros mire, located in Minas Gerais state, Brazil. The range of mercury concentrations in Rano Aroi records (~ 35 and 333 ng g^{-1}) is in general comparable with that of Pinheiros mire (~36 – 370 ng g^{-1}) (Pérez-Rodríguez et al., 2015), although the minima found in the Brazilian mire are considerably lower than those in Rano Aroi (<2 vs. 35 ng g^{-1}), probably due to the large quartz content of the corresponding peat sections in the former (Pérez-Rodríguez et al., 2015). On the other hand, ARO cores show two extraordinary mercury peaks of ~1000 ng g^{-1} at ~20.0 kyr cal BP and ~5.0 kyr cal BP (Figure 4 and 5) that are more than 2 fold the maximum found in the Brazilian record.

Maxima Hg values in the Pleistocene and Holocene sections of Rano Aroi are comparatively high with respect to other peatlands worldwide, even in sections affected by anthropogenic emissions. For example, for the Industrial Period maxima of ~800 ng g^{-1} were reported for the Czech Republic (Zuna et al., 2012), >400 ng g^{-1} for Scotland (Yang et al., 2001; Farmer et al., 2009), ca. 600 ng g^{-1} in Northeast China (Tang et al., 2012), ca. 130 ng g^{-1} for Canada (Outridge et al., 2011), ca. 300 ng g^{-1} in Spain (Martínez Cortizas et al., 2012). Our two maxima of natural Hg deposition are, however, similar to those (up to 1100 ng g^{-1}) found in

four peat cores from Belgium, dating to AD 1930 – 1980, which were interpreted to be associated with coal burning and smelter emissions (Allan et al., 2013). Pre-Industrial Hg concentrations in the previously mentioned records are quite heterogeneous i.e. 40 - 50 ng g^{-1} in the peatlands studied in Czech Republic (Zuna et al., 2012) or 111 ± 64 ng g^{-1} in the record from Northeast China (Tang et al., 2012), but in the range of ARO records. These comparisons suggest that under natural conditions, as expected in Easter Island at ~20 and ~5 kyr cal BP, large amounts of Hg can accumulate over relatively low background values.

4.2. Environmental conditions in Rano Aroi and related proxies

In previous studies on Rano Aroi cores a combination of proxies was used to improve the knowledge on tropical and subtropical peat dynamics and climatic history of Easter Island. The peatland was demonstrated to be a good archive to reconstruct the environmental history of the area, which was mainly driven by climate (Margalef et al., 2013, 2014), although without ruling out the effect of human activity in the last few millennia (Rull et al., 2015).

The $\delta^{13}C$ variations indicated two main climatic periods (Margalef et al., 2013, 2014). From ~70 to ~55 kyr BP, high $\delta^{13}C$ values (mean -15 ‰, C_4-type plant remains) suggest the predominance of drier-colder climatic conditions, while from ~47 to ~8.5 kyrs cal BP low $\delta^{13}C$ values (−26 ‰, C_3–type plant remains) indicate a general dominance of wetter climate conditions (Figure 4). A gradual transition between both climates took place between ~55 kyr BP and ~47 kyr cal BP and is reflected by progressively lighter values of $\delta^{13}C$ (Figure 4). ARO 08 02 does not show this transition (Figure 5) because it only covers the last ~38 kyrs cal BP, but $\delta^{13}C$ values shifted to lower values in agreement with ARO 06 01 tendency. The long-term $\delta^{13}C$ trend was interrupted by negative excursions interpreted as short wetter periods.

The same general pattern of $\delta^{13}C$ data is followed by PC1, the first component of a Principal Component Analysis (PCA) performed on the inorganic fraction of Rano Aroi (Margalef et al., 2014). PC1 is characterized by large positive loadings (>0.7) of typically lithogenic elements and some metals. This component was identified as a proxy of the long-term fluxes of inorganic particulate material to the peatland. Its similarity with $\delta^{13}C$ background trend suggests higher erosion during drier period (~70 to ~55 kyr BP) - probably due to lower vegetation cover - and an increasing mineral input during the short rainfall events previously

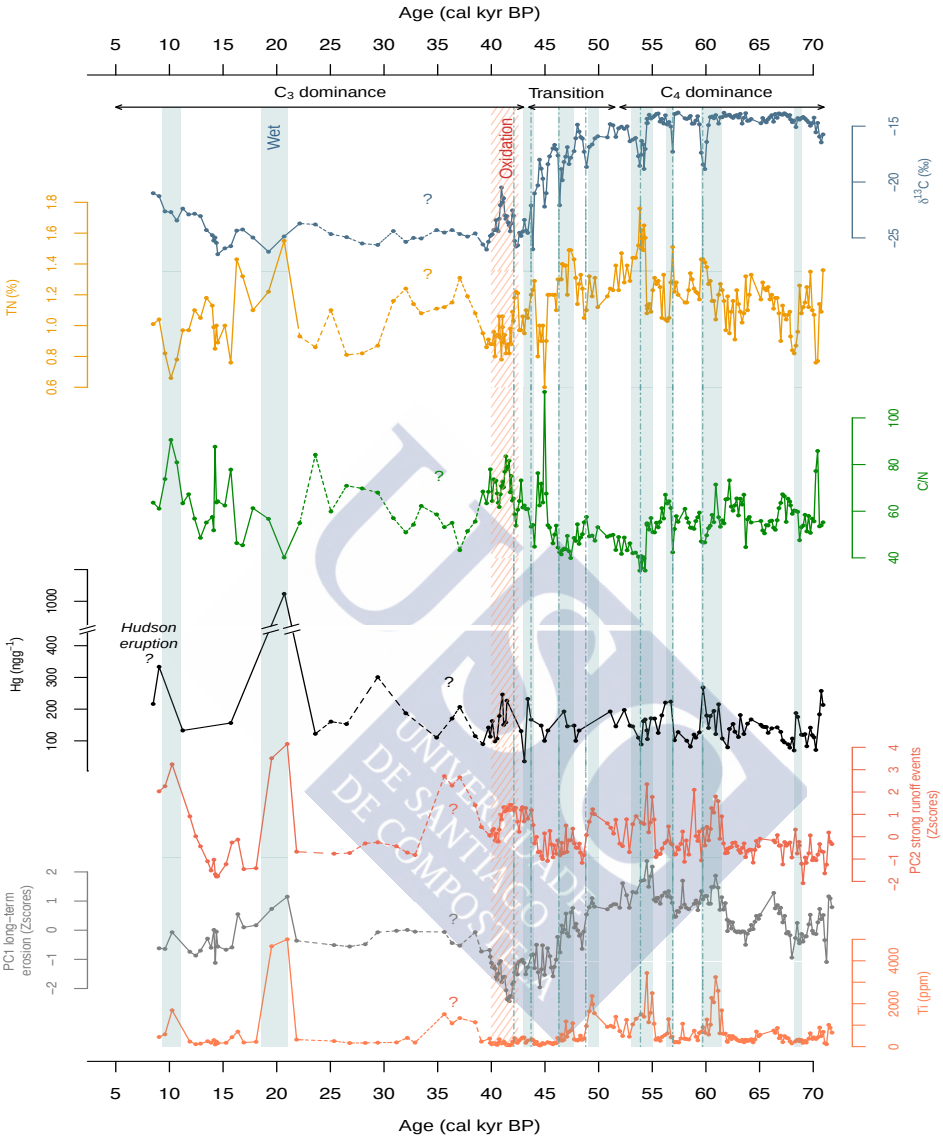

Figure 4. Mercury concentration and main proxies – from bottom to top: titanium (Ti), PC1, PC2, Hg concentration, C/N, TN and $\delta^{13}C$) - uses to reconstruct the environment in Rano Aroi between ca. 71.0 kyrs BP and ca. 9.0 kyrs cal BP in ARO 06 01 core. PC1 and PC2 data are from Margalef et al., (2014) and represent the long-term background fluxes inorganic particulate material and the delivery of large amounts of terrigenous particles transported during wet events, respectively. $\delta^{13}C$ (‰) general trend indicate the C_3 and C_4 vegetation dominance. Wet events according to $\delta^{13}C$ (‰) excursions and PC2 peaks that match with Hg concentration increases (blue bars); dash line indicate the position of the $\delta^{13}C$ (‰) excursion agree with the literature (see text). A red discontinuous bar indicates a highly oxidized peat section. Discontinuous trend lines indicate sections with chronological.

mentioned (Figure 4). Another process, identified by the second component (PC2), is the occurrence of enhanced precipitation events related to the strong runoff and delivery of large amounts of terrigenous particles (probably rich in organic matter) from the soils of the catchment to the mire. Matching with these events, C/N ratio and total nitrogen (TN) values show abrupt decreases and increases, respectively. Higher TN values and lower C/N ratio were attributed to a higher contribution of lacustrine algal material, in contrast to high C/N values that indicate higher proportions of terrestrial or aquatic plants (versus algae) organic matter (see Margalef et al., 2014 for further details on PC2 and their relation with organic peat chemistry).

4.3. Processes controlling mercury content

4.3.1. Rainfall

Increases in Hg concentration seem to match – at least partially – with strong runoff events, based on PC2 scores peaks (Figure 4 and 5). Six of these main events (centered at ~60.5, ~56.6, kyr BP and ~46.5, ~43.5, ~20.0 and ~10.0 kyr cal BP) coincide with peaks in Hg concentration, while PC2 peaks centered at ~54.0 and ~49.5 kyr cal BP do not show correspondence with Hg rises (Figure 4). The PC2 peak at ~10 kyr cal BP agrees also with an increase in Hg (333 ng g^{-1}) in ARO 06 01.

Increased rainfall, that is the main driver for runoff events, should be the common link with Hg rises in Rano Aroi through enhanced Hg-wet deposition. However, it is unclear whether this is the only mechanism controlling the increase in Hg concentration in peat during wetter periods or other, like the catchment erosion effect, the mire vegetation, peat decomposition and volcanic activity may have played a role.

Wet deposition in Rano Aroi

The oxidation and deposition of Hg from the atmosphere through rainfall is a well-known process in Hg cycle, however the importance of the process in environmental records is still in debate. Mercury isotopic analyses in living sphagnum mosses, upper peat layers and rainwater samples, were used in a recent publication to investigate the dominant modern Hg depositional processes to peat bogs (Enrico et al., 2016). The results of the three years field experiment indicated that Hg deposition was dominated by gaseous elemental mercury dry deposition

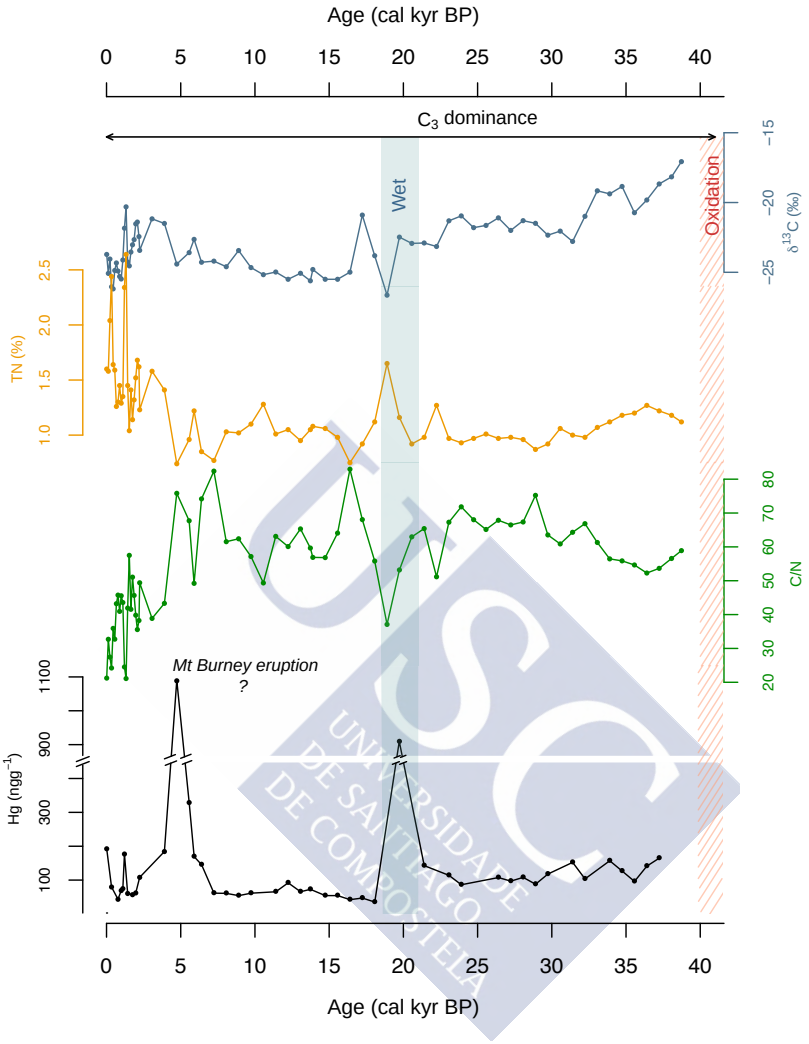

Figure 5 Mercury concentration and main proxies uses to reconstruct the environment in Rano Aroi the last ca. 39.0 kyr cal BP in ARO 06 01 core – from bottom to top: Hg concentration, C/N, TN and $\delta^{13}C$) -. (Margalef et al., 2014).Wet events according to $\delta^{13}C$ (‰) excursions that match with Hg concentration increases (blue bars); dash line indicate the position of the $\delta^{13}C$ (‰) excursion agree with the literature (see text).

(79%) rather than wet deposition (21%). However, a later paleolimnological study conducted in a Pyrenean lake (Corella et al., 2017) showed that increased precipitation and more humid conditions controlled mercury accumulation in the area at a centennial scale, suggesting that wet deposition was the main driver at longer time-scales.

At Pleistocene scale, evidence supports the role of rainfall to intensifying Hg deposition. In Pinheiros mire higher Hg concentrations found during a humid period from ~26.7 to ~2.8 kyr cal BP, were interpreted to result from increases in Hg deposition driven by precipitation (wet deposition – rainfall) (Pérez-Rodríguez et al., 2015).

Several differences exist in Rano Aroi Hg cycle with respect to Pinheiros. First, the increases in Hg concentration are related with abrupt rainfall events (throughout ARO 08 02 and ARO 06 01) instead of being a continuous process over a long time period. Second, there is apparently no dilution effect due to the input of inorganic matter from the catchment despite the increased delivery of terrigenous material to the peatland during the high-rainfall episodes (see next section for the discussion on the catchmente effect on Hg concentration). Third, taking into account the extraordinary mercury peaks in Rano Aroi cores (~1000 ng g^{-1}), there is a wider range in Hg concentrations than in Pinheiros (36 - 370 ng g^{-1}). This difference may be due to the high interannual variability in precipitation in Easter Island (from 500 to 1800 mm) or indicative that other processes may have played a role in Hg deposition or accumulation.

The good match between the increases in Hg during wet periods in the mentioned long-term records suggests that Hg wash out from the atmosphere and deposition should be the main driver. In spite dry deposition was found to be the main mechanism in the four-year study of the French bogs (Enrico et al., 2016), it is possible that the perspective provided by the Pleistocene records (as Rano Aroi and Pinheiros) might highlight the dominance of the longer-term wet deposition processes (Figure 6).

4.3.2. Effect of catchment erosion: geologic materials and catchment soils

The direct contribution of local geologic materials to Hg concentration in the peat during high-rainfall events is negligible. The small catchment (15.82 km^2) is composed of highly porphyritic olivinic tholeite and basalt and hawaiite lava flows (González-Ferrán et al., 2004). Specific information for Hg in basaltic materials is sparse in the published scientific literature. The most recent reviews of available data indicate that Hg in basalts is variable, generally in the range of 2-35 ng g^{-1} (Carlson, 2005). Data from basaltic reference materials showed that the mercury content in samples from island arcs or the circum-Pacific belt is lower than that from samples of continental origin, with concentrations generally at the

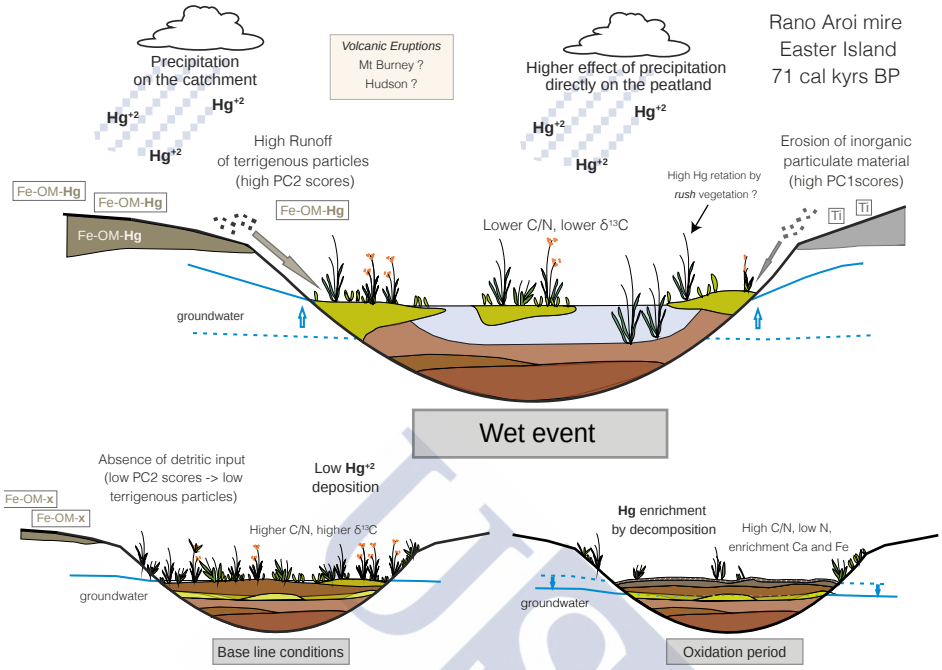

Figure 6 Mire schematic model indicating the processes controlling mercury deposition and accumulation under different environmental conditions. During rainfall events, Hg accumulates via wet deposition directly to the mire or through catchment soils. In baseline conditions the Hg accumulation is low. Under dry peatland stage (i.e. ca. 40.0 - 42.0 kyrs cal BP) the peat – organic matter decomposition increases Hg content. The effect of vegetation and volcanic activity is not well addressed in this study. Modified from (Margalef et al., 2013).

lower end of the mean for the basaltic samples analysed (7 – 34 ng g^{-1}) (Flanagan et al., 1982). According to this, we would expect a low contribution of mercury from the catchment materials due to weathering.

However catchment soils may maximize the effect of increased mercury concentration during rainfall events. Volcanic soils can retain Hg released form the parent material as well as that deposited from the atmospheric pool (Peña-Rodríguez et al., 2012). As mentioned above, the type of geological material in Rano Aroi catchment does not seem to have significant amounts of Hg so, most probably, all the Hg retained in the soils may ultimately originate from atmospheric deposition. The mobilization of Hg due to soil erosion (Roulet et al., 1998) could also take place in volcanic areas since Hg is associated to metal (Al-Fe)-humus complexes. Margalef et al. (Margalef et al., 2013, 2014) also identified increases of

Fe content and high values of PC2 (large positive loading of Fe) during enhanced rainfall periods. At least part of the Fe in (andic) volcanic soils may be as Fe-humus compounds (García-Rodeja et al., 2004) to which the mercury could be bound (Nóvoa-Muñoz et al., 2008; Peña-Rodríguez et al., 2012).These compounds may be transported to the mire by superficial runoff (Figure 6).

The comparison of Hg concentration in ARO 06 01 with the PC1 and PC2 components (the long-term background fluxes of inorganic particulate material and the delivery of large amounts of terrigenous particles, respectively) only shows agreement during the shorter wet events and not for the long-term trends (see Figure 4). This suggests that matter fluxes do not affect the concentration of mercury, but precipitation may be the common driver.

It is worth mentioning the presence of a short rise of Hg and PC2 in ARO 06 01 at ~37 kyr cal BP that, according to the $\delta^{13}C$ record, does not correspond to a wet period (Figure 4) pointing to other processes as an increase of Hg concentration due to terrigenous Hg-rich input. However the existence of a chronological uncertainty in this section (see Margalef et al., (2014) invites to caution in the interpretation.

The data support the idea that wet deposition - directly on the mire or through the catchment circuits –was the dominant process controlling Hg concentration in Rano Aroi peatland since ~71.0 kyrs, essentially during high-rainfall events.

4.3.3. Other processes: Mire vegetation, peat decomposition and volcanic activity

The extremely high Hg concentration (1023 and 910 ng g^{-1}, ARO 06 01 and 08 02 respectively) at ~20 kyr cal BP in both cores seems to have been caused by a phase of strong rainfall, since they coincide with an increase of PC2 and a decline in $\delta^{13}C$ (ARO 06 01 and ARO 08 02 respectively). For these peaks Hg is 3 and 4.5 fold (ARO 06 01 and 08 02 respectively) that of the next high concentration (~300 ng g^{-1}), which could indicate other processes may have enhanced mercury accumulation in the mire or an external factor may have increased atmospheric mercury concentration.

The ~20 cal kry BP maximum corresponds to a cold phase occurred at the end of the Last Glacial Maximum, when humid conditions in Eastern Island prevailed (Margalef et al., 2014). Both, colder and humid conditions would have favored Hg accumulation in Rano Aroi since Hg deposition is controlled by temperature and

humidity variations (Martínez Cortizas et al., 1999; Corella et al., 2017).

It has been shown that vegetation type and degree of decomposition can affect the mercury content in peat (Rydberg et al., 2010b). Table 1 reveals that different vegetation present in the island may involve different mercury accumulation in plant remains. According to the data presented here (Table 1) an increase in the abundance of rush, which showed large (~11,000 ng g^{-1}) mercury concentrations, coupled to more humid conditions by ~20 kyr cal BP might help to explain these increases in Hg (Figure 6). However, we have no certainty of the presence of rush in the mire catchment at present and the available pollen and macroremains data (Margalef et al., 2013, 2014; Margalef, 2014) do not allow to support this speculation.

The effect of organic matter decomposition in Hg accumulation is still a subject of debate. For short-term periods, it has been proposed that increased decomposition leads to an increase in Hg concentration (Biester et al., 2003; Martínez Cortizas et al., 2007). This could be the situation during the extreme oxidation event caused by the drought period occurred at ~40.0 kyr cal BP (Figure 4), when mercury concentration slightly rises (Figure 4, Figure 6). On the other hand, the available data for longer, Pleistocene-Holocene records, as that of the Pinheiros mire (Pérez-Rodríguez et al., 2015), suggest that the effect of peat decomposition on Hg concentrations exponentially decreases to be almost negligible in peats with ages older than 10-11 kyr (Pérez-Rodríguez et al., 2015). There is no general decomposition trend in Rano Aroi and the short-term changes (reflected by changes in C/N ratio) seem to respond to enhanced rainfall periods and associated changes in mire vegetation (Margalef et al., 2013), that may not have affected the Hg concentrations.

In Rano Aroi cores there is no evidence of recent volcanic activity (i.e. tephra layers), despite there are volcanic lava flows from Terevaka whose appearance suggests that they are not older than two or three thousand years (Baker, 1967). The absence of recorded volcanic eruptions in the island does not rule out the possible of Hg degassing by active fumaroles, especially on an island containing more than 70 volcano craters (Baker et al., 1974; González-Ferrán et al., 2004). Data (tephra layers) from South Patagonia indicated volcanic eruptions at ~4.2 kyr cal BP and ~7.7 kyr cal BP identified as Mt Burney (52ºS 72ºW) and Hudson volcanic eruption (45ºS 72ºW), respectively (McCulloch and Davies, 2001; Stern, 2008).

We have no data to support the effect of these volcanic events for the Hg peak at ~4.7 kyr cal BP (ARO 08 02) and/or at ~8.5 kyr cal BP (ARO 06 01) in Easter Island, but they cannot be discarded as a possible Hg source. Moreover, although there is some mismatch between the Hg peak and Hudson volcanic eruption, it has been shown that this specific eruption (at ~7.7 kyr cal BP) modified dust atmospheric deposition dust during a period of ~700 years (Vanneste et al., 2016).

Similarly, we cannot exclude the effect of volcanic activity or fires regimes at other periods, through increasing atmospheric Hg concentration, then precipitated by rainfall. For example during the LGM, charcoal data indicates an increased in fire activity at tropical latitudes of South America (Power et al., 2008), what might have been an extra Hg emission to the atmosphere. A higher resolution would be needed in this section of the cores as well as more cores to confirm the hypothesis of the effect of volcanism and differences in intensity (i.e. differences in Hg concentration) between both events.

5. Author Contributions

MP and AM designed the scientific questions to be solved. OM, SP and SG designed fieldwork and took samples; OM processed samples and performed the geochemical analysis; MP selected the samples and performed the Hg analysis; MP, PC and AM reviewed the Hg data and interpreted the results; all the co-authors contributed to wrote and reviewed the final version of this manuscript.

6. Acknowledgments

This research was funded by the Spanish Ministry of Science and Education through the projects LAVOLTER (CGL2004-00683/BTE), GEOBILA (CGL2007-60932/BTE), R2014/001 and GPC GI-1553 (Dirección Xeral I+D, Xunta de Galicia). We would like to thank CONAF (Chile) and the Rirorokо family for the facilities provided on Easter Island and Jesús R. Aboal (Universidade de Santiago de Compostela) for laboratory facilities.

7. References

Allan M., Le Roux G., Sonke J.E., Piotrowska N., Streel M., and Fagel N., 2013. Reconstructing historical atmospheric mercury deposition in Western Europe using: Misten peat bog cores, Belgium. Science of The Total Environment 442, 290–301

Amos H.M., Sonke J.E., Obrist D., Robins N., Hagan N., Horowitz H.M., Mason R.P.,

Witt M., Hedgecock I.M., Corbitt E.S., et al., 2015. Observational and modeling constraints on global anthropogenic enrichment of mercury. Environmental Science and Technology 49, 4036–4047

Baker P.E., 1967. Preliminary account of recent geological investigations on Easter Island. Geological Magazine 104 (2), 116–122

Baker P.E., Buckley F., and Holland J.G., 1974. Petrology and geochemistry of Easter Island. Contributions to Mineralogy and Petrology 44, 85–100

Biester H., Martinez-Cortizas A., Birkenstock S., and Kilian R., 2003. Effect of Peat Decomposition and Mass Loss on Historic Mercury Records in Peat Bogs from Patagonia. Environmental Science and Technology 37, 32–39

Biester H., Keppler F., Putschew A., Martinez-Cortizas A., and Petri M., 2004. Halogen Retention, Organohalogens, and the Role of Organic Matter Decomposition on Halogen Enrichment in Two Chilean Peat Bogs. Environmental Science and Technology 38, 1984–1991

Biester H., Bindler R., Martinez-Cortizas A., and Engstrom D.R., 2007. Modeling the Past Atmospheric Deposition of Mercury Using Natural Archives. Environmental Science and Technology 41, 4851–4860

Bindler R., Klarqvist M., Klaminder J., and Förster J., 2004. Does within-bog spatial variability of mercury and lead constrain reconstructions of absolute deposition rates from single peat records? The example of Store Mosse, Sweden. Global Biogeochemical Cycles 18, 1–12

Carlson R.W., 2005. The Mantle and Core: Treatise on Geochemistry (Elsevier)

Cloy J.M., Farmer J.G., Graham M.C., MacKenzie A.B., and Cook G.T., 2008. Historical records of atmospheric Pb deposition in four Scottish ombrotrophic peat bogs: An isotopic comparison with other records from western Europe and Greenland. Global Biogeochemical Cycles 22

Corella J.P., Wang F., and Cuevas C.A., 2017. 700 years reconstruction of mercury and lead atmospheric deposition in the Pyrenees (NE Spain). Atmospheric Environment

Daga R., Ribeiro Guevara S., Pavlin M., Rizzo A., Lojen S., Vreča P., Horvat M., and Arribére M., 2016. Historical records of mercury in southern latitudes over 1600years: Lake Futalaufquen, Northern Patagonia. Science of The Total Environment 553, 541–550

Danzeglocke U., Jöris O., and Weninger B., 2008. CalPal-2007

Engstrom D.R., Fitzgerald W.F., Cooke C.A., Lamborg C.H., Drevnick P.E., Swain E.B., Balogh S.J., and Balcom P.H., 2014. Atmospheric Hg emissions from preindustrial gold and silver extraction in the Americas: A reevaluation from lake-sediment archives. Environmental Science and Technology 48, 6533–6543

Enrico M., Roux G. Le, Marusczak N., Heimbürger L.-E., Claustres A., Fu X., Sun R., and Sonke J.E., 2016. Atmospheric Mercury Transfer to Peat Bogs Dominated by Gaseous Elemental Mercury Dry Deposition. Environmental Science and Technology acs.est.5b06058

Farmer J.G., Anderson P., Cloy J.M., Graham M.C., MacKenzie A.B., and Cook G.T., 2009. Historical accumulation rates of mercury in four Scottish ombrotrophic peat bogs over the past 2000 years. Science of the Total Environment 407, 5578–5588

Fitzgerald W.F. and Mason R.P., 1996. The global mercury cycle: oceanic and anthropogenic aspects. In Global and Regional Mercury Cycles: Sources, Fluxes and Mass Balances, (Springer), pp. 85–108

Flanagan F.J., Moore R., and Aruscavage P.J., 1982. Mercury in Geologic Reference Samples. Geostandards Newsletter 6, 25–46

Flenley J.R. and King S.M., 1984. Late Quaternary pollen records from Easter Island. Nature 307, 47–50

Flenley J.R., King A.S.M., Jackson J., Chew C., Teller J.T., and Prentice M.E., 1991. The Late Quaternary vegetational and climatic history of Easter Island. Journal of Quaternary Science 6, 85–115

Franzen C., Kilian R., and Biester H., 2004. Natural mercury enrichment in a minerogenic fen--evaluation of sources and processes. Journal of Environmental Monitoring : JEM 6, 466–472

García-Rodeja E., Nóvoa J.C., Pontevedra X., Martínez-Cortizas A., and Buurman P., 2004. Aluminium fractionation of European volcanic soils by selective dissolution techniques. Soils of Volcanic Regions in Europe 56, 325–351

González-Ferrán O., Mazzuoli R., and Lahsen A., 2004. Geología del complejo volcánico Isla de Pascua-Rapa Nui, Chile. V Región-Valparaiso.

Hall B., 1995. The gas phase oxidation of elemental mercury by ozone. In Mercury as a Global Pollutant, (Springer), pp. 301–315

Hermanns Y. and Biester H., 2013. Anthropogenic mercury signals in lake sediments from southernmost Patagonia, Chile. Science of the Total Environment 445–446, 126–135

Hermanns Y.-M., Cortizas A.M., Arz H., Stein R., and Biester H., 2012. Untangling the influence of in-lake productivity and terrestrial organic matter flux on 4,250 years of mercury accumulation in Lake Hambre, Southern Chile. Journal of Paleolimnology 49, 563–573

Horowitz H.M., Jacob D.J., Amos H.M., Streets D.G., and Sunderland E.M., 2014. Historical mercury releases from commercial products: Global environmental implications. Environmental Science and Technology 48, 10242–10250

Hylander L.D. and Meili M., 2005. The Rise and Fall of Mercury: Converting a Resource to Refuse After 500 Years of Mining and Pollution. Critical Reviews in Environmental Science and Technology 35, 1–36

Jitaru P., Gabrielli P., Marteel A., Plane J.M.C., Planchon F.A.M., Gauchard P.-A., Ferrari C.P., Boutron C.F., Adams F.C., Hong S., et al., 2009. Atmospheric depletion of mercury over Antarctica during glacial periods. Nature Geoscience 2, 505–508

Junk C. and Claussen M., 2011. Simulated climate variability in the region of Rapa Nui during the last millennium. Climate of the Past 7, 579–586

Kirk J.L., Muir D.C.M., Antoniades D., Douglas M.S. V, Evans M.S., Jackson T.A., Kling H., Amoureux S., Lim D.S.S., Pienitz R., et al., 2011. Climate change and mercury accumulation in canadian high and subarctic lakes. Environmental Science and Technology 45, 964–970

Lamborg C.H., Fitzgerald W.F., Damman A.W.H., Benoit J.M., Balcom P.H., and Engstrom D.R., 2002. Modern and historic atmospheric mercury fluxes in both hemispheres: Global and regional mercury cycling implications. Global Biogeochemical Cycles

16, 1104

Margalef O., 2014. The last 70 ky of Rano Aroi (Easter Island, 27 ° S) peat record: New insights for the Central Pacific paleoclimatology. Universitat de Barcelona

Margalef O., Cañellas-Boltà N., Pla-rabes S., Giralt S., Pueyo J.J., Joosten H., Rull V., Buchaca T., Hernández A., Valero-Garcés B.L., et al., 2013. A 70,000 year multiproxy record of climatic and environmental change from Rano Aroi peatland (Easter Island). Global and Planetary Change 108, 72–84

Margalef O., Martínez Cortizas A., Kylander M., Pla-Rabes S., Cañellas-Boltà N., Pueyo J.J., Sáez A., Valero-Garcés B.L., and Giralt S., 2014. Environmental processes in Rano Aroi (Easter Island) peat geochemistry forced by climate variability during the last 70kyr. Palaeogeography, Palaeoclimatology, Palaeoecology 414, 438–450

Martínez Cortizas A., Pontevedra-Pombal X., García-Rodeja E., Nóvoa-Muñoz J.C., and Shotyk W., 1999. Mercury in a Spanish Peat Bog: Archive of Climate Change and Atmospheric Metal Deposition. Science 284, 939–942

Martínez Cortizas A., Biester H., Mighall T., and Bindler R., 2007. Climate-driven enrichment of pollutants in peatlands. Biogeosciences 4, 905–911

Martínez Cortizas A., Peiteado Varela E., Bindler R., Biester H., and Cheburkin A., 2012. Reconstructing historical Pb and Hg pollution in NW Spain using multiple cores from the Chao de Lamoso bog (Xistral Mountains). Geochimica et Cosmochimica Acta 82, 68–78

McCulloch R.D. and Davies S.J., 2001. Late-glacial and Holocene palaeoenvironmental change in the central Strait of Magellan, southern Patagonia. Palaeogeography, Palaeoclimatology, Palaeoecology 173, 143–173

Nóvoa-Muñoz J.C., Pontevedra-Pombal X., Martínez-Cortizas A., and García-Rodeja Gayoso E., 2008. Mercury accumulation in upland acid forest ecosystems nearby a coal-fired power-plant in Southwest Europe (Galicia, NW Spain). Science of The Total Environment 394, 303–312

Outridge P.M., Sanei H., Stern G. A., Hamilton P.B., and Goodarzi F., 2007. Evidence for control of mercury accumulation rates in Canadian High Arctic Lake sediments by variations of aquatic primary productivity. Environmental Science and Technology 41, 5259–5265

Outridge P.M., Rausch N., Percival J.B., Shotyk W., and McNeely R., 2011. Comparison of mercury and zinc profiles in peat and lake sediment archives with historical changes in emissions from the Flin Flon metal smelter, Manitoba, Canada. The Science of the Total Environment 409, 548–563

Peña-Rodríguez S., Pontevedra-Pombal X., Fernández-Calviño D., Taboada T., Arias-Estévez M., Martínez-Cortizas A., Nóvoa-Muñoz J.C., and García-Rodeja E., 2012. Mercury content in volcanic soils across Europe and its relationship with soil properties. Journal of Soils and Sediments 12, 542–555

Pérez-Rodríguez M., Horák-Terra I., Rodríguez-Lado L., Aboal J.R., and Martínez Cortizas A., 2015. Long-Term (~57 ka) controls on mercury accumulation in the souther hemisphere reconstructed using a peat record from pinheiro mire (minas gerais, Brazil). Environmental Science and Technology 49, 1356–1364

Pérez-Rodríguez M., Horák-Terra I., Rodríguez-Lado L., and Martínez Cortizas A., 2016. Modelling mercury accumulation in minerogenic peat combining FTIR-ATR spectroscopy and partial least squares (PLS). Spectrochimica Acta Part A:

Molecular and Biomolecular Spectroscopy 168, 65–72

Power M.J., Marlon J., Ortiz N., Bartlein P.J., Harrison S.P., Mayle F.E., Ballouche A., Bradshaw R.H.W., Carcaillet C., Cordova C., et al., 2008. Changes in fire regimes since the last glacial maximum: An assessment based on a global synthesis and analysis of charcoal data. Climate Dynamics 30, 887–907

Reimer P.J., Baillie M.G.L., Bard E., Bayliss A., Beck J.W., Bertrand C.J.H., Blackwell P.G., Buck C.E., Burr G.S., and Cutler K.B., 2004. IntCal04 terrestrial radiocarbon age calibration, 0–26 cal kyr BP.

Ribeiro Guevara S., Meili M., Rizzo A., Daga R., and Arribére M., 2010. Sediment records of highly variable mercury inputs to mountain lakes in Patagonia during the past millennium. Atmospheric Chemistry and Physics 10, 3443–3453

Roos-Barraclough F., Martinez-Cortizas A., García-Rodeja E., Shotyk W., García-Rodeja E., and Shotyk W., 2002. A 14 500 year record of the accumulation of atmospheric mercury in peat: volcanic signals, anthropogenic influences and a correlation to bromine accumulation. Earth and Planetary Science Letters 202, 435–451

Roulet M., Lucotte M., Saint-Aubin A., Tran S., Rheault I., Farella N., Dezencourt J., Passos C.-J.S., Soares G.S., and Guimaraes J.-R., 1998. The geochemistry of mercury in central Amazonian soils developed on the Alter-do-Chao formation of the lower Tapajos River Valley, Para state, Brazil. Science of the Total Environment 223, 1–24

Rull V., Cañellas-Boltà N., Margalef O., Sáez A., Pla-Rabes S., and Giralt S., 2015. Late Holocene vegetation dynamics and deforestation in Rano Aroi: Implications for Easter Island's ecological and cultural history. Quaternary Science Reviews 126, 219–226

Rydberg J., Klaminder J., Rosén P., and Bindler R., 2010a. Climate driven release of carbon and mercury from permafrost mires increases mercury loading to sub-arctic lakes. Science of The Total Environment 408, 4778–4783

Rydberg J., Karlsson J., Nyman R., Wanhatalo I., Näthe K., and Bindler R., 2010b. Importance of vegetation type for mercury sequestration in the northern Swedish mire, Rödmossamyran. Geochimica et Cosmochimica Acta 74, 7116–7126

Sáez A., Valero-Garcés B.L., Giralt S., Moreno A., Bao R., Pueyo J.J., Hernández A., and Casas D., 2009. Glacial to Holocene climate changes in the SE Pacific. The Raraku Lake sedimentary record (Easter Island, 27oS). Quaternary Science Reviews 28, 2743–2759

Schroeder W.H. and Munthe J., 1998. Atmospheric mercury—An overview. Atmospheric Environment 32, 809–822

Schuster P.F., Krabbenhoft D.P., Naftz D.L., Cecil L.D., Olson M.L., Dewild J.F., Susong D.D., Green J.R., and Abbott M.L., 2002. Atmospheric Mercury Deposition during the Last 270 Years: A Glacial Ice Core Record of Natural and Anthropogenic Sources. Environmental Science and Technology 36, 2303–2310

Steinnes E., Rühling Å., Lippo H., and Mäkinen A., 1997. Reference materials for large-scale metal deposition surveys. Accreditation and Quality Assurance 2, 243–249

Stern C.R., 2008. Holocene tephrochronology record of large explosive eruptions in the southernmost Patagonian Andes. Bulletin of Volcanology 70, 435–454

Tang S., Huang Z., Liu J., Yang Z., and Lin Q., 2012. Atmospheric mercury deposition

recorded in an ombrotrophic peat core from Xiaoxing'an Mountain, Northeast China. Environmental Research 118, 145–148

Vanneste H., De Vleeschouwer F., Bertrand S., Martínez-Cortizas A., Vanderstraeten A., Mattielli N., Coronato A., Piotrowska N., Jeandel C., and Roux G. Le, 2016. Elevated dust deposition in Tierra del Fuego (Chile) resulting from Neoglacial Darwin Cordillera glacier fluctuations. Journal of Quaternary Science 31, 713–722

Wang F., Saiz-Lopez A., Mahajan A.S., Gómez Martín J.C., Armstrong D., Lemes M., Hay T., and Prados-Roman C., 2014. Enhanced production of oxidised mercury over the tropical Pacific Ocean: A key missing oxidation pathway

Yang H., Rose N.., Boyle J.., and Battarbee R.., 2001. Storage and distribution of trace metals and spheroidal carbonaceous particles (SCPs) from atmospheric deposition in the catchment peats of Lochnagar, Scotland. Environmental Pollution 115, 231–238

Zizka G., 1991. Flowering plants of Easter Island. Palmarum Hortus Francofurtensis; 3

Zuna M., Ettler V., Š O., Mihaljevi M., Šebek O., and Mihaljevič M., 2012. Mercury accumulation in peatbogs at Czech sites with contrasting pollution histories. Science of The Total Environment 424, 322–330

USC
UNIVERSIDADE
DE SANTIAGO
DE COMPOSTELA

MANUSCRIPT II

Long-term (~57 ka) controls on mercury accumulation in the Southern Hemisphere reconstructed using a peat record from Pinheiro Mire (Minas Gerais, Brazil)

Environmental Science and Technology, 49, 1356-1364.

JCR IF (2015): 5.393, D1 in Engineering, Environmental and Environmental Sciences

USC
UNIVERSIDADE
DE SANTIAGO
DE COMPOSTELA

MANUSCRIPT III

Modelling mercury accumulation in minerogenic peat combining FTIR-ATR spectroscopy and partial least squares (PLS)

Spectrochimica Acta Part A: Molecular and Biomolecular Spectroscopy, 168, 65-72.

JCR IF (2015): 2.653, Q2 in Spectroscopy

USC
UNIVERSIDADE
DE SANTIAGO
DE COMPOSTELA

MANUSCRIPT IV

Solar output controls periodicity in lake productivity and wetness at Southernmost South America

Scientific Reports, 6:37521.

JCR IF (2015): 5.228 , D2 in Multidisciplinary Sciences

USC
UNIVERSIDADE
DE SANTIAGO
DE COMPOSTELA

MANUSCRIPT V

Total solar insolation and algae productivity increase mercury accumulation in a pristine Southern Hemisphere lake

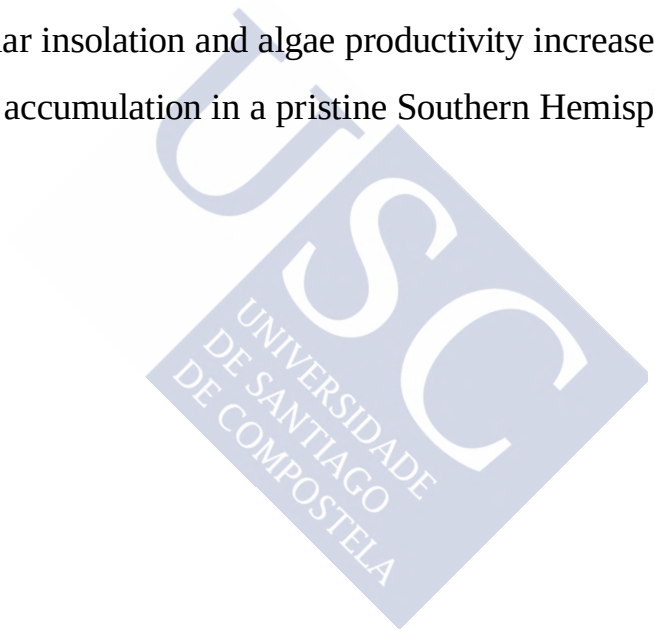

USC
UNIVERSIDADE
DE SANTIAGO
DE COMPOSTELA

Total solar insolation and algae productivity increase mercury accumulation in a pristine Southern Hemisphere lake

Harald Biester [1]*, Marta Pérez-Rodríguez [2], Benjamin-Silas Gilfedder [3], Antonio Martínez Cortizas [2], Yvonne-Marie Hermanns [1]

* corresponding author: H. Biester; h.biester@tu-bs.de

[1] *Institud für Geoökologie, AG Umweltgeochemie, Technische Universität Braunschweig, 38106 Braunschweig, Germany*
[2] *Departamento de Edafoloxía e Química Agrícola, Facultade de Bioloxía, Universidade de Santiago de Compostela, Campus Sur, Santiago de Compostela 15782, Spain*
[3] *Lehrstuhl für Hydrologie, Universität Bayreuth, Universitätsstr. 30, 95440 Bayreuth, Germany*

Abstract

Mercury (Hg) is know to highly accumulate in aquatic biota. Uptake by algae has been found to be its entry-point into the aquatic foodchain however the contribution of Hg uptake by algae under changing solar irradiance and climatic conditions is currently unknown for pre-industrial times. We have analyzed the link between Hg accumulation, cyclic changes in total solar insolation (TSI), related changes in lake productivity and climate during the past 4.5 kyrs in sediments of a small highly productive lake located in Southern Patagonia (53°S). The analyses encompass proxies for TSI (based on ^{10}Be), sediment geochemical composition and lake productivity (FTIR spectra, and hydrogen-index (HI)).

The sediment record shows high concentrations of organic matter (median 70 %) and strong vari¬ations in Hg accumulation which correspond to changes in TSI and aquatic productivity. Accumulation of Hg was highest during drier periods when insolation and lake productivity was high and erosion fluxes from the catchment were low. During these periods, accumulation was up to fourfold higher compared to those of lower TSI, lower productivity and wetter climatic conditions. This indicates that sediment Hg accumulation and potential Hg methylation in this highly productive lake were to a large extent controlled by insolation and related algae production and to a lesser extent by Hg fluxes supplied by erosion from catchment soils. We suggest that the high Hg uptake by algae is due to water-column methylation in settling particles in anaerobic micro-niches, at times of high productivity and eutrophication. Our findings implies that sediment Hg accumulation, related to the mentioned conditions, can surpass Hg fluxes from the catchment in productive lakes and does potentially increase formation and enrichment of methyl-Hg in lake foodchain.

1. Introduction

Mercury is an element of concern as anthropogenic emissions have largely surpassed those from natural sources and the metal is known for its biomagnification in aquatic food chains. Today, nearly all freshwater sediments of the past 200 years are enriched in Hg by a factor of 3-5 or more compared to pre-industrial times (Biester et al., 2007). Due to its high affinity to bind to organic components, the biogeochemical cycle of Hg is largely coupled to that of organic matter. Transport by dissolved organic matter (DOM) is the major pathway of Hg from catchments into aquatic systems (Driscoll, 1995). In freshwater systems and estuaries, algae have been shown to accumulate Hg from the water phase and influence Hg cycling by affecting its concentrations, speciation and transport to the sediments (Fitzgerald et al., 2007, Lavoie et al., 2013, Dranguet et al., 2014; Le Faucheur et al., 2014). The mechanism of Hg uptake by phytoplankton is not well understood, with both facilitated transport and diffusion involved (Le Faucheur et al., 2014, Dranguet et al., 2014). Oxidized dissolved Hg (HgII-species such as $HgCl_2$) and methylmercury (CH_3HgX (MeHg)) are the dominant species taken up and lipophilic CH_3HgCl has a higher bioaccumulation factor than other Hg_{2+}-species, whereas DOM-bound Hg appears to decrease uptake by algae (Dranguet et al., 2014; Le Faucheur et al., 2014; Schartup et al., 2015a). Direct uptake of gaseous or dissolved elemental Hg (GEM) by phytoplankton seems to be of minor importance as no detectable accumulation of Hg could be observed when GEM was used in bioaccumulation experiments. However, recent studies have emphasized the importance of DOM-bound-MeHg as well as the quality of DOM (terrestrial versus marine) for Hg enrichment in plankton (Jonsson et al., 2014; Schartup et al., 2015a) and the literature therein). Oxic water-column Hg methylation has been found to be a major process increasing Hg concentrations in settling particles (Balcom et al., 2015; Gascón Díez et al., 2016). Moreover, eutrophication has been shown to increase phytoplankton MeHg concentrations in marine systems and the export of organically bound Hg to the sediment, simultaneously decreasing the water phase Hg reservoir (Soerensen et al., 2016).

Scavenging of Hg by algae has been suggested as a major process for Hg accumulation in lake sediments. From the simultaneous increase of algae derived organic matter and Hg concentrations in Arctic lakes, some studies concluded algal production represents one of the main drivers for the increase in Hg accumulation in sediments during the industrial age (Outridge et al., 2007; Stern

et al., 2009). However, other work has found that the correlation between both proxies is not consistent throughout a larger number of Arctic lakes (Kirk et al., 2011). In contrast, studies based on mass balance calculations have hypothesized that increased algae production may lead to bio-dilution of Hg concentra¬tions in algae.

Investigations of lake sediment records on a millennial scale, aiming to disentangle the past climatic control underlying the relationship between algal productivity and increased Hg accumulation -independent from anthropogenic pollution- are limited. For example, Cooke et al., (2012) could not find a relationship between chlorophyll a and Hg concentrations during the Holocene in an Arctic lake. In a previous study we analyzed sediments from a small lake at the Strait of Magellan (53 °S), and found a significant correlation between proxies of algal production (Rock Eval hydrogen index (HI), C/N ratios) and the accumulation of Hg in the sediments during the past 4.5 kyr (Hermanns et al., 2013). However, it is largely unknown how and to which extent Hg uptake and enrichment by algae controls the accumulation of Hg alone, or if other factors such as insolation, temperature and/or precipitation, which control both productivity and Hg fluxes to the lake, are important. In addition, the Hg mass balance resulting from increased Hg uptake by algae is mostly unknown. A recent model study on the role of eutrophication on Hg accumulation in Baltic Sea sediments suggests that increased uptake of Hg by algae during eutrophication will decrease Hg evasion from the lake e.g. by biotic or photochemical reduction (Soerensen et al., 2016).

Algal productivity in lakes is controlled by insolation, temperature and nutrient availability. Total solar irradiance (TSI), as a function of solar output, has varied throughout the Holocene and is known to show periodicities of varying frequency. Periodical changes in insolation may cause cyclic climatic effects on Earth such as the Bond Events (Bond et al., 1997), which are related to quasi-periodical (~1500 years) cooling of the North Atlantic. It has been demonstrated that cyclic variations in algal productivity of Arctic lakes are coherent with time series of cosmogenic nuclides (^{14}C and ^{10}Be), which are directly related to changes in solar output (Hu et al., 2003). Despite its importance to understand the natural variability of Hg accumulation in lakes the relationship between TSI, lake productivity and the sedimentation of Hg has not yet been investigated. One major problem here is the sensitivity of productivity proxies and the extraction of the Hg signal which is directly related to changes in productivity. This is especially true where sediment

Hg accumulation is dominated by surface run-off of DOM-Hg which tends to obscure Hg signals related to productivity.

In this study, we supplemented data from a previous investigation on the importance of algal scavenging and catchment processes (terrestrial organic matter fluxes) on Hg accumulation in Lago Hambre (LH) (53 °S) (Hermanns et al., 2013) by the spectroscopic (FTIR) character-isation of the lake's sediments and compared it to the ^{10}Be record (a proxy for TSI). Pérez-Rodríguez et al., (2016) showed that the application of principal component analysis (PCA) to the LH FTIR data allowed sensitive detection of in-lake productivity signals which showed a strong dependency on TSI changes throughout the Holocene. Based on this preliminary result, we present a re-evaluation of the 4.0 kyrs Hg sediment record of this small, pristine lake in Patagonia (Fig.1). We use a combination of geochemical and spectroscopic proxies discussed in previous studies (Hermanns and Biester, 2013; Hermanns et al., 2013; Pérez-Rodríguez et al., 2016) to determine the influence of solar-induced lake productivity changes on mercury accumulation.

2. Methods and Materials

2.1. Location

Lago Hambre is located 50 km south of Punta Arenas, near the Strait of Magellan, in southernmost Patagonia, Chile (53°360 13.1900 S, 70°570 8.7700 W). It is situated about 80 m a.s.l. and is a small lake with a surface area of 13,700 m^2 and a maximum depth of 17 m. The catchment-to-lake ratio is about eight. The lake is situated in the zone of sub-Antarctic deciduous forest dominated by Nothofagus pumilio and Nothofagus antarctica.

2.2. Sediment sampling

A 5 m long sediment core was recovered from the deepest part of the lake in 2008 using a piston corer. Sediment cores were stored under dark and cool (4 °C) conditions until analyses. Sub-samples were taken at 1 cm intervals in the upper 470 cm of the piston core, and at 2-cm intervals below 470 cm.

2.3. Element and organic matter analyses

Mercury concentrations were determined by means of CVAAS after combustion

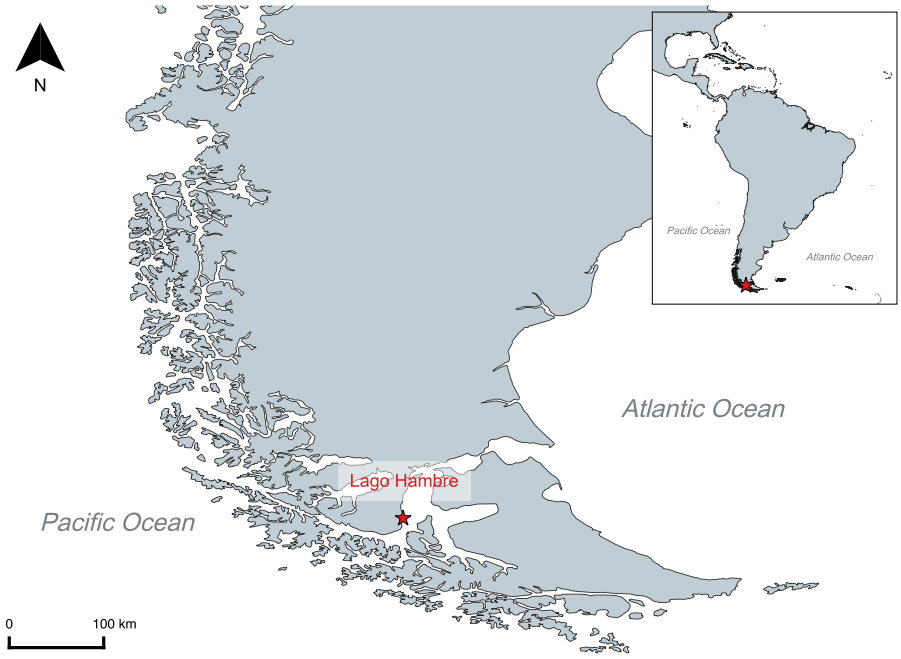

Figure 1. Map of southern South America and location of Lake Hambre.

of the sample and pre-concentration of Hg by amalgamation on a gold trap using a DMA 80 mercury analyzer (MLS). Selected samples (n=24) were analysed in duplicates. Precision was always better than 6% RSD. Certified reference materials (CRM: NIST 1515, 44 ± 4 µg kg^{-1}; CCRMP LKSD-4: 190 µg kg^{-1}) were used for quality control. Results for the NIST 1515 reference material were always within the standard deviation of the certified value and recovery for LKSD-4 was always between 95-100%. Concentrations of carbon (C) and nitrogen (N) in carbonate-free samples were determined by GC-TCD after thermal combustion in an elemental analyzer (Euro EA3000, Eurovector, Germany). Samples were analyzed for copper (Cu) and zirconium (Zr) using an energy-dispersive XRF mini-probe multi-element analyzer (EMMA (Cheburkin and Shotyk, 1996)). The hydrogen index (HI), i.e. the quantity of pyrolyzable hydrocarbons (S2) per gram TOC (mg HC gC^{-1}), was determined by means of a Rock–Eval-II-plus-S3-unit at the Alfred Wegener Institut für Polar- und Meeresforschung in Bremerhaven, Germany using sample aliquots of 30–50 mg.

2.4. Infrared spectroscopy of sediments

A total of 430 samples were analysed by Infrared Spectroscopy (IR). FTIR spectra of freeze-dried and ground samples of lake sediment were obtained using a Vector 22 FTIR spectrometer (BrukerOptik, Ettlingen, Germany) in absorption mode, with subsequent baseline substraction on KBr pellets (200 mg dried KBr and 2 mg sample). Measurements were recorded from 4,500 to 300 cm^{-1} using a resolution of 2 cm^{-1}. Thirty-two scans were taken per sample and averaged to obtain the final spectra. In order to improve the comparison between samples, each FTIR spectrum was re-scaled by normalising each absorption value to the integrated spectrum area.

2.5. Statistical modelling

Further discussion of the FTIR data will be confined to the use of one (Cp9) of the PCA (principal component analysis) components extracted from the FTIR data from a previous study in Lago Hambre (see Pérez-Rodríguez et al., 2016 for full details). In brief, PCA was performed on the FTIR data to identify the main geochemical signals of the lake core and relate them to the underlying environmental processes in the lake and its catchment. We performed the PCA on a transposed matrix (samples as columns and absorbance bands as rows) and a varimax-rotation was applied to maximize the loadings. Each extracted component is represented by a spectrum of scores, which permits us to identify the most relevant signals characterizing the composition of the samples. Sample loadings (or their squared values) indicate the weight of the identified compounds on the samples' spectroscopic signal (related to its abundance in the samples). In the present work we use only the information relative to the last 4.0 kyr. PCA and Pearson correlation coefficient analyses were performed using the statistic environment R 3.1.1 (Team, 2014).

2.6. Spectral analysis

The spectral analysis (REDFIT, (Schulz and Mudelsee, 2002) providing periodicities of PCA-Cp9 (an algaenan signal), HI, Hg and Cu concentrations and accu-mulation were performed using the Past software (Hammer et al., 2001). PCA-Cp9 and HI spectral analysis are from Pérez-Rodríguez et al. (2016).

3. Results and Discussion

3.1 Geochemical and climatic background

Lago Hambre is a small (surface area = 13,700 m^2), 17 m deep lake, located 50 km south of Punta Arenas (53°36' 13.19''S, 70°57' 8.77'' W), Patagonia (Chile) (Fig. 1). The radiocarbon dated ~5 m long sediment core dates back to ~4500 yrs (Hermanns et al., 2013). The sediment record is characterized by generally high organic matter content (carbon concentration, median 38 wt. %, ~70 wt. % organic matter) interrupted by more mineral matter-rich layers related to periodic changes in wetter and drier conditions (Hermanns et al 2013, Pérez-Rodríguez et al., 2016) and a tephra layer at 4250 cal. B.P. (Mt. Burney). At the time of sampling the lake was stratified and anoxic below a water depth of ~7 m. The variability in C/N ratios is generally high (range 12-29, median 17) pointing to frequent changes in the dominant source of organic matter (OM). Terrestrial OM (higher C/N-ratios) mainly derived from the Nothofagus forest soils, that were dominant (median C/N=19) between 3500 and 1700 B.P. (McCulloch and Davies, 2001), followed by a shift towards more algal OM (lower C/N ratios) in the past ~1700 years (median C/N=16), when the climate became drier and colder (Fig. 2) (Caniupán et al., 2014; Pérez-Rodríguez et al., 2016).

One of the PCA components (PCA-Cp9) extracted from the FTIR-spectra is characterised by high loadings of absorptions typical for aliphatic compounds associated with green algae (Pérez-Rodríguez et al., 2016). This specific spectrum is likely to be associated with algaenan, an insoluble, non-hydrolysable, and highly aliphatic macromolecule that is a structural component of the cell wall of freshwater green algae (Blokker et al., 1998). The record of PCA1-Cp9 scores shows a close correlation (r=0.74, n=226) with the hydrogen index (HI) (Fig. 2) where high HI values are typical for algae OM (Outridge et al., 2007). Both proxies of algal production (PCA1-Cp9 and HI) appear closely related to changes in TSI, showing a periodicity of ~ 180-220 years (Fig. 2 and 3). This indicates that productivity in LH followed these short term changes in insolation (Pérez-Rodríguez et al., 2016). Similar periodicity in past climatic changes in Patagonia has been observed in other studies (Turney et al., 2016)

Besides the effect on aquatic productivity, cyclic variations in sediment composition also point to changes in climate conditions at the Strait of Magellan. We used zirconium (Zr), a typical conservative lithogenic element, as a proxy of

erosion of mineral matter from the catchment soils (Fig. 2). Periods of high TSI and lake productivity (Cp9, HI, C/N) mostly correspond to phases of relatively low mineral matter fluxes and relatively dry conditions. Moreover, it has been shown that productivity proxies also seem to be in pace with the longer periodicity (~1500 years) of Bond Events during the past 5 kyrs indicating a link to the southernmost SH climate system with solar-forced cooling of the NH (Pérez-Rodríguez et al., 2016). Drier and colder periods in southern Patagonia are most likely caused by weakening or shifting of the Southern Hemisphere westerly wind belt (Lamy et al., 2010; Varma et al., 2011; Kilian and Lamy, 2012; Caniupán et al., 2014). However, the relationship between drier conditions and higher productivity was not consistent throughout the entire record because local climatic variation may have influenced both productivity and mineral matter fluxes to the lake. Accordingly, some sections show an increase in both Zr accumulation and productivity proxies (e.g. at ~1600 BP, ~3600 BP), which indicate higher erosion (Zr) and productivity during wetter and probably warmer conditions.

3.2 Mercury Accumulation

The LH sediments show strong variations in concentrations and accumulation rates of mercury throughout the past ~4000 years (Fig. 2 and S1 for concentrations). Both vary by a factor of ~4.2, between 87 and 362 µg kg-1 (median 187 µg kg-1) and 14 to 53 µg m^{-2} yr^{-1} (median 29 µg m^{-2} yr^{-1}), respectively. Mercury accumulation rates in LH are clearly higher than background atmospheric Hg deposition rates reported from other remote lakes (1-9 µg m^{-2} yr^{-1}) (Biester et al., 2007).

Hermanns et al. (2013) did not find a significant covariation between mercury and the organic matter content or the fluxes of inorganic matter from the catchment at LH. Median Hg concentration in LH sediments (187 µg kg^{-1}) is about 3.5-fold higher than the average Hg concentrations (53 µg kg^{-1}) in the organic matter rich top soils and 8-fold higher than the mercury content (23 µg kg^{-1}) in the rocks of the lake's catchment (Hermanns et al. 2013). Sediment focusing is assumed to be of minor importance here as LH is too small and too deep to cause significant grain size separation during sedimentation. Even if carbon losses of ~25 % during organic matter diagenesis in the sediment are assumed (Rydberg et al., 2008), there needs to be an additional factor to explain the large enrichment in Hg in the lake sediments. In addition, the record of Hg accumulation rates appears inversely related (although $p>0.05$) to that of the Zr accumulation (Fig. 2) indicating that

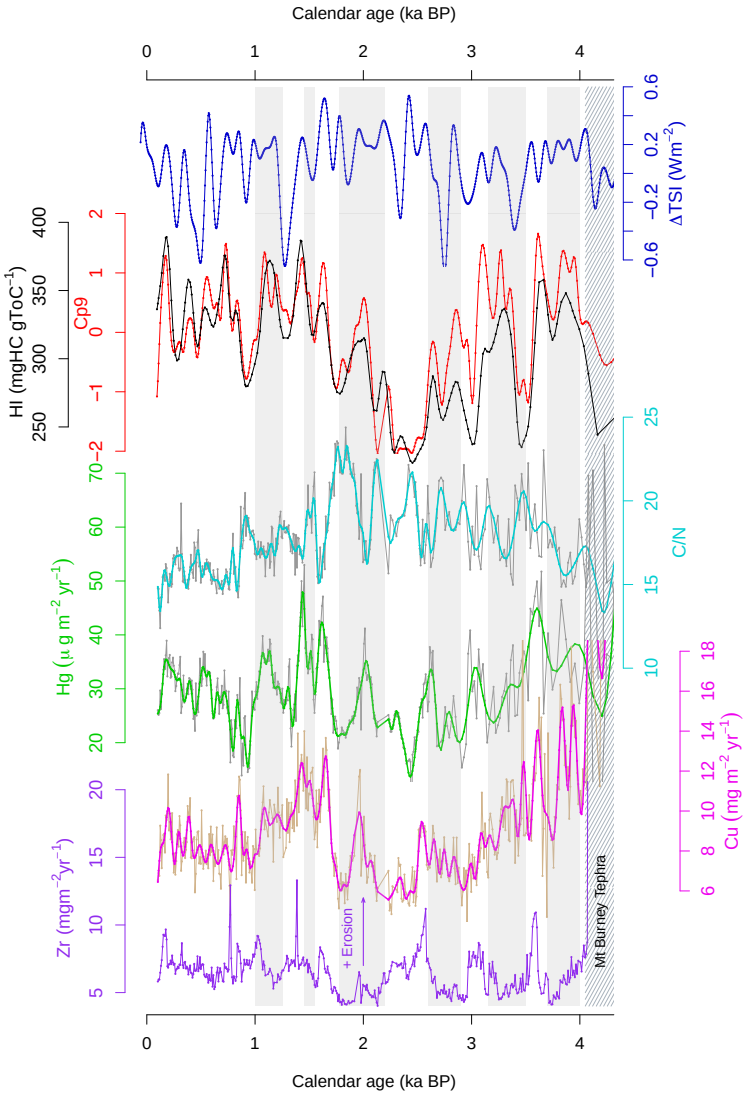

Figure 2. Proxy records of aquatic productivity (PCA1–Cp9 and HI), Hg and Cu accumulation, Zr accumulation for mineral matter sedimentation and ^{10}Be-based reconstruction of total solar irradiance (ΔTSI, after (Steinhilber et al., 2009) and carbon/nitrogen ratios (C/N). Grey bars indicate drier events at LH derived from Zr accumulation (Pérez-Rodriguez et al., 2016). Streaked bar shows Mt Burney tephra layer

mineral matter fluxes from the catchment tended to be lower during periods of high Hg accumulation. Although a few periods of higher mineral matter fluxes also show an increase in Hg accumulation (e.g. at ~1600 BP, 3600 yr cal BP). As precipitation is the main driver for soil erosion, our data unexpectedly reveals that Hg accumulation in the sediments was in most cases higher during dryer periods (e.g. at ~1100, ~2000, ~3200 yr cal BP). Mercury accumulation rates during relatively dry and colder periods differ by a factor of up to four from those during wetter and warmer periods (Fig.2). Due to the absence of correlation between Hg and Zr accumulation the changes in the Hg record cannot be explained by changes in erosion of mineral matter. That fluxes from the catchment cannot explain the changes in Hg accumulation is also supported by the observation that Hg accumulation does not correlate positively with C/N ratios, but are inversely related in most sections of the core (Fig.2, and Tab. S1). Moreover, changes in atmospheric Hg fluxes to the lake or the catchment by a factor of three to four are unlikely as no natural (cyclic) processes are known which might increase atmospheric Hg loads to such an extent.

Figure 2 shows that mercury concentrations and accumulation rates follow changes in HI, PCA1-Cp9 and TSI and show the same periodicity (Fig.3), which implies that Hg fluxes to the sediment are closely related to algae productivity. Hermanns et al. (2013) found that changes in HI explain about 50-58 % (positive correlation Tab. S1) of the variation in Hg accumulation rates and concentrations. PCA1-Cp9 derived from the FTIR analyses explains 58 and 62 % (concentration and accumulation, respectively) of this variation, which is the highest proportion of the Hg variation explained by a single parameter/process. However, this moderate correlation suggests that other processes should also be coupled to the Hg enrichment during times of high productivity. It is unlikely that Hg accumulation is linearly related to algal productivity as the entire process is coupled to a variety of other processes such as DOM-Hg fluxes from the catchment or redox-conditions etc.

Mercury was found to be significantly correlated ($r=0.65$, $p<0.01$) with copper (Hermanns et al. (2013) (Tab. S1). No other trace elements correlate with PCA1-Cp9 significantly suggesting that Hg and Cu accumulation in the sediment is coupled to the same biogeo-chemical process in the lake. In contrast to Hg, catchment soils and rocks are the primary source of Cu to the lake (dust deposition is regarded to be of minor importance here). Although the Cu record largely follows that of

the algae proxies (HI and PCA1-Cp9), and only in few sections relate to mineral matter accumulation (Zr) (Fig.2), the correlation of Cu to productivity (Cp9 and HI, r=0.49 and r=0.48, respectively) is not as pronounced as for Hg. Moreover, no significant 200 year periodicity in the Cu accumulation record could be observed (Fig.3) indicating the influence of mineral matter fluxes that obscure the bioproductivity signal. As both elements show high affinity to bind to organic matter, their fluxes from the catchment typically include two components, the erosion of mineral matter and leaching of DOM from organic rich top-soils. We assume that during dryer periods erosion of mineral matter was reduced and Hg and Cu transport to the lake by DOM-leaching became dominant, which can partly explain the decoupling of Cu (and Hg) from the mineral matter (Zr) record.

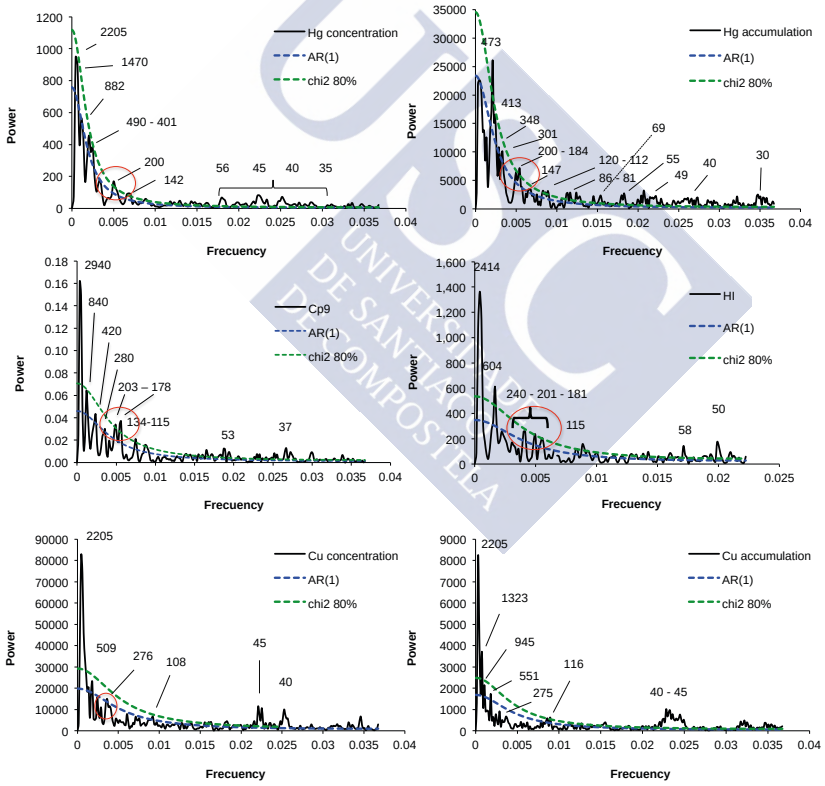

Figure 3. Spectral analysis (REDFIT, (Schulz and Mudelsee, 2002) of PCA1-Cp9 and HI, and Hg and Cu concentrations and accumulation rates. Periodicities are shown in years. The analysis was made with Past software (Hammer et al., 2001). Chi-squared confidence levels at 80% and first-order autoregressive (AR1) to evaluate the statistical significance of these peaks are indicated.

3.3 Uptake of Hg and Cu by algae

Copper is an important co-factor in plastocyanin, a protein essential for photosynthesis of algae, and is taken up by algae mainly as Cu^{2+} (Brooks et al., 2007). In case of Hg, lipophilic compounds such as uncharged $HgCl_2$ and CH_3HgCl complexes are important for the uptake by algae (Mason et al., 1996; Dranguet et al., 2014), but binding to terrestrial DOM limits the uptake of both metals (e.g. (Brooks et al., 2007; Schartup et al., 2015a). However, Jonsson et al., (2014) have shown that MeHg bound to terrestrial DOM is more resistant to degradation and bioaccumulates to substantially greater extent than MeHg formed in situ in sediments. Moreover, a recent study on an Arctic fjord system indicates that freshwater discharge drives high MeHg uptake by marine biota (Schartup et al., 2015b). Here, the enhanced biomagnification of Hg in plankton was attributed to stimulating effects of terrestrial DOM on Hg methylating microorganisms in the water phase. Furthermore, these authors hypothesize that active water-column methylation by bacteria is stimulated by redox microniches caused by enhanced degradation of terrestrial DOM. Similar, observations by Gascón Díez et al., (2016) in a freshwater lake emphasize the importance of Hg methylation in suboxic/anerobic microzones in sinking particles.

The high algal productivity in LH is likely to cause similar suboxic/anerobic microzones and active methylation in settling particles during decomposition of terrestrial DOM and the high amounts of algal-derived organic matter. This might explain the higher Hg accumulation in sediments during periods of enhanced in-lake productivity. Gascón Díez et al., (2016) reported that total Hg in sinking particles in Lake Geneva was not significantly different from that in surface sediments (although MeHg was ten-fold higher). In LH where productivity is much higher than in Lake Geneva the production of MeHg in sinking particles is likely to be high considering that the lake is anaerobic for most of the year, which also limits the mineralization of the organic matter in the water column. The Hg concentration in fresh algae sampled from LH was found to be ~50 μg kg^{-1} while median Hg concentrations in the sediments were 187 μg kg^{-1} indicating that enrichment processes must occur in the water column to explain this large difference.

In addition, increased intensity of photo-oxidation of DOM-Hg under higher insolation might enhance Hg^{2+} uptake by algae, in a similar way as found for Cu. Photo-oxidation studies on Cu-complexation and bioavailability have shown that

it depends on light regime as well as DOM source. Photo-oxidation of DOM can significantly diminish binding sites density for Cu and photo-mineralization of DOM can cause the release of previously bound Cu^{2+} (Moffett et al., 1990; Sander et al., 2005; Shank et al., 2006), which could increase the uptake by algae.

To our knowledge the relationship between photo-oxidation of DOM, Hg^{2+} release and Hg uptake by algae has yet not been investigated. However, it is likely that DOM-Hg complexes show similar or even enhanced reaction on increased UV-radiation as observed for DOM-Cu complexes. While increased insolation may increase release of Hg^{2+} from DOM, it is unclear if it will be readily available for uptake by algae, because increase UV-radiation can also increase photo-reduction of Hg^{2+} and re-emission of GEM (Amyot et al., 1997; O'Driscoll et al., 2006). The overall Hg-mass-balance and the kinetics of Hg^{2+} uptake versus reduction is unknown and needs further investigation.

The key question arising from our observations is how more Hg can be accumulated in the sediments when fluxes from the catchment have decreased and atmospheric deposition is assumed not to have increased. Soerensen et al. (2016) modeled the effect of eutrophication on the Hg mass balance in the Baltic Sea. They found that the export of organically bound Hg to the sediment during eutrophication events simultaneously decreased the water phase Hg reservoir and reemission of Hg to the atmosphere through photo-reduction of Hg^{2+}. This model could also explain how Hg accumulation in LH sediments can increase during enhanced productivity without increasing external Hg fluxes to the lake. However, more experimental data is needed to support this hypothesis.

4. Acknowledgement

This work was supported by a DFG-grant to H.B. (DFG-BI 734/15-1) and support to M.P-R. by DAAD (grant ref no 91588482) and TU-Braunschweig. We thank R. Kilian and H. Arz for LH core samples, A. Calean and P. Schmidt for technical assistance.

5. References

Amyot, M., Mierle, G., Lean, D., Mcqueen, D.J., 1997. Effect of solar radiation on the formation of dissolved gaseous mercury in temperate lakes. Geochim. Cosmochim. Acta 61, 975–987.

Balcom, P.H., Schartup, A.T., Mason, R.P., Chen, C.Y., 2015. Sources of water column methylmercury across multiple estuaries in the Northeast U.S. Mar. Chem. 177, 721–

730. doi:10.1016/j.marchem.2015.10.012

Biester, H., Bindler, R., Martinez-Cortizas, A., Engstrom, D.R., 2007. Modeling the past atmospheric deposition of mercury using natural archives. Environ. Sci. Technol. 41, 4851–4860.

Blokker, P., Schouten, S., Van den Ende, H., De Leeuw, J.W., Hatcher, P.G., Sinninghe Damsté, J.S., 1998. Chemical structure of algaenans from the fresh water algae Tetraedron minimum, Scenedesmus communis and Pediastrum boryanum. Org. Geochem. 29, 1453–1468. doi:10.1016/S0146-6380(98)00111-9

Bond, G., Showers, W., Cheseby, M., Lotti, R., Almasi, P., DeMenocal, P., Priore, P., Cullen, H., Hajdas, I., Bonani, G., 1997. A pervasive millennial-scale cycle in North Atlantic Holocene and glacial climates. Science 278, 1257–1266. doi:10.1126/science.278.5341.1257

Brooks, M.L., Meyer, J.S., McKnight, D.M., 2007. Photooxidation of wetland and riverine dissolved organic matter: Altered copper complexation and organic composition. Hydrobiologia 579, 95–113. doi:10.1007/s10750-006-0387-6

Caniupán, M., Lamy, F., Lange, C.B., Kaiser, J., Kilian, R., Arz, H.W., León, T., Mollenhauer, G., Sandoval, S., De Pol-Holz, R., Pantoja, S., Wellner, J., Tiedemann, R., 2014. Holocene sea-surface temperature variability in the Chilean fjord region. Quat. Res. United States 82, 342–53. doi:10.1016/j.yqres.2014.07.009

Cheburkin, A.K., 1996. An energy-dispersive miniprobe multielement analyzer (EMMA) for direct analysis of Pb and other trace elements in peats. Fresenius J. Anal. Chem. 354, 688–691.

Cooke, C.A., Wolfe, A.P., Michelutti, N., Balcom, P.H., Briner, J.P., 2012. A holocene perspective on algal mercury scavenging to sediments of an Arctic lake. Environ. Sci. Technol. 46, 7135–7141.

Dranguet, P., Flück, R., Regier, N., Cosio, C., Le Faucheur, S., Slaveykova, V.I., 2014. Towards mechanistic understanding of mercury availability and toxicity to aquatic primary producers. Chimia 68, 799–805. doi:10.2533/chimia.2014.799

Driscoll, J., C.T., Blette, V., Yan, C., Schofield, C.L., Munson, R., Holsapple, 1995. The role of dissolved organic carbon in the chemistry and bioavailability of mercury in remote Adirondack lakes. Water Air Amp Soil Pollut. 80, 499–508. doi:10.1007/BF01189700

Fitzgerald, W.F., Lamborg, C.H., Hammerschmidt, C.R., 2007. Marine biogeochemical cycling of mercury. Chem. Rev. 107, 641–662. doi:10.1021/cr050353m

Gascón Díez, E., Loizeau, J.-L., Cosio, C., Bouchet, S., Adatte, T., Amouroux, D., Bravo, A.G., 2016. Role of Settling Particles on Mercury Methylation in the Oxic Water Column of Freshwater Systems. Environ. Sci. Technol. 50, 11672–11679. doi:10.1021/acs.est.6b03260

Hammer, Ø., Harper, D.A.T., Ryan, P.D., 2001. Past: Paleontological statistics software package for education and data analysis. Palaeontol. Electron. 4, XIX–XX.

Hermanns, Y.-M., Biester, H., 2013. A 17,300-year record of mercury accumulation in a pristine lake in southern Chile. J. Paleolimnol. 1–15.

Hermanns, Y.-M., Cortizas, A.M., Arz, H., Stein, R., Biester, H., 2013. Untangling the influence of in-lake productivity and terrestrial organic matter flux on 4,250 years of mercury accumulation in Lake Hambre, Southern Chile. J. Paleolimnol. 49, 563–573.

Hu, F.S., Kaufman, D., Yoneji, S., Nelson, D., Shemesh, A., Huang, Y., Tian, J., Bond, G., Clegg, B., Brown, T., 2003. Cyclic variation and solar forcing of holocene climate in the Alaskan subarctic. Science 301, 1890–1893. doi:10.1126/science.1088568

Jonsson, S., Skyllberg, U., Nilsson, M.B., Lundberg, E., Andersson, A., Björn, E., 2014. Differentiated availability of geochemical mercury pools controls methylmercury levels in estuarine sediment and biota. Nat. Commun. 5. doi:10.1038/ncomms5624

Kilian, R., Lamy, F., 2012. A review of Glacial and Holocene paleoclimate records from southernmost Patagonia (49-55°S). Quat. Sci. Rev. 53, 1–23. doi:10.1016/j.quascirev.2012.07.017

Kirk, J.L., Muir, D.C.M., Antoniades, D., Douglas, M.S.V., Evans, M.S., Jackson, T.A., Kling, H., Amoureux, S., Lim, D.S.S., Pienitz, R., Smolo, J.P., Stewart, K., Wang, X., Yang, F., 2011. Climate change and mercury accumulation in canadian high and subarctic lakes. Environ. Sci. Technol. 45, 964–970.

Lamy, F., Kilian, R., Arz, H.W., Francois, J.-P., Kaiser, J., Prange, M., Steinke, T., 2010. Holocene changes in the position and intensity of the southern westerly wind belt. Nat. Geosci. 3, 695–699. doi:10.1038/ngeo959

Le Faucheur, S., Campbell, P.G.C., Fortin, C., Slaveykova, V.I., 2014. Interactions between mercury and phytoplankton: Speciation, bioavailability, and internal handling. Environ. Toxicol. Chem. 33, 1211–1224. doi:10.1002/etc.2424

Mason, R.P., Reinfelder, J.R., Morel, F.M.M., 1996. Uptake, toxicity, and trophic transfer of mercury in a coastal diatom. Environ. Sci. Technol. 30, 1835–1845. doi:10.1021/es950373d

McCulloch, R.D., Davies, S.J., 2001. Late-glacial and Holocene palaeoenvironmental change in the central Strait of Magellan, southern Patagonia. Palaeogeogr. Palaeoclim. Palaeoecol. 173, 143–173.

Moffett, J.W., Zika, R.G., Brand, L.E., 1990. Distribution and potential sources and sinks of copper chelators in the Sargasso Sea. Deep Sea Res. Part Ocean. Res. Pap. 37, 27–36. doi:10.1016/0198-0149(90)90027-S

O'Driscoll, N.J., Siciliano, S.D., Lean, D.R.S., Amyot, M., 2006. Gross photoreduction kinetics of mercury in temperate freshwater lakes and rivers: Application to a general model of DGM dynamics. Environ. Sci. Technol. 40, 837–843. doi:10.1021/es051062y

Outridge, P.M., Sanei, H., Stern, G.A., Hamilton, P.B., Goodarzi, F., 2007. Evidence for control of mercury accumulation rates in Canadian High Arctic Lake sediments by variations of aquatic primary productivity. Environ. Sci. Technol. 41, 5259–5265.

Pérez-Rodríguez, M., Gilfedder, B.-S., Hermanns, Y.-M., Biester, H., 2016. Solar Output Controls Periodicity in Lake Productivity and Wetness at Southernmost South America. Sci. Reports 6. doi:10.1038/srep37521

Rydberg, J., Gälman, V., Renberg, I., Bindler, R., Lambertsson, L., Martínez-Cortizas, A., 2008. Assessing the stability of mercury and methylmercury in a varved lake sediment deposit. Environ. Sci. Technol. 42, 4391–4396.

Sander, S., Kim, J.P., Anderson, B., Hunter, K.A., 2005. Effect of UVB irradiation on Cu2+-binding organic ligands and Cu2+ speciation in alpine lake waters of New Zealand. Environ. Chem. 2, 56–62. doi:10.1071/EN04072

Schartup, A.T., Balcom, P.H., Soerensen, A.L., Gosnell, K.J., Calder, R.S.D., Mason, R.P., Sunderland, E.M., St. Louis, V.L., 2015a. Freshwater discharges drive high

levels of methylmercury in Arctic marine biota. Proc. Natl. Acad. Sci. U. S. A. 112, 11789–11794. doi:10.1073/pnas.1505541112

Schartup, A.T., Ndu, U., Balcom, P.H., Mason, R.P., Sunderland, E.M., 2015b. Contrasting effects of marine and terrestrially derived dissolved organic matter on mercury speciation and bioavailability in seawater. Environ. Sci. Technol. 49, 5965–5972. doi:10.1021/es506274x

Schulz, M., Mudelsee, M., 2002. REDFIT: Estimating red-noise spectra directly from unevenly spaced paleoclimatic time series. Comput. Geosci. 28, 421–426. doi:10.1016/S0098-3004(01)00044-9

Shank, G.C., Whitehead, R.F., Smith, M.L., Skrabal, S.A., Kieber, R.J., 2006. Photodegradation of strong copper-complexing ligands in organic-rich estuarine waters. Limnol. Ocean. 51, 884–892.

Soerensen, A.L., Schartup, A.T., Gustafsson, E., Gustafsson, B.G., Undeman, E., Björn, E., 2016. Eutrophication Increases Phytoplankton Methylmercury Concentrations in a Coastal Sea - A Baltic Sea Case Study. Environ. Sci. Technol. 50, 11787–11796. doi:10.1021/acs.est.6b02717

Steinhilber, F., Beer, J., Fröhlich, C., 2009. Total solar irradiance during the Holocene. Geophys. Res. Lett. 36. doi:10.1029/2009GL040142

Stern, G.A., Sanei, H., Roach, P., De La Ronde, J., Outridge, P.M., 2009. Historical interrelated variations of mercury and aquatic organic matter in lake sediment cores from a subarctic lake in Yukon, Canada: Further evidence toward the algal-mercury scavenging hypothesis. Environ. Sci. Technol. 43, 7684–7690. doi:10.1021/es902186s

Team, R.C., 2014. R: A language and environment for statistical computing, Version 2.10.1. R Lang. Environ. Stat. Comput. Version 2101.

Turney, C.S.M., Jones, R.T., Fogwill, C., Hatton, J., Williams, A.N., Hogg, A., Thomas, Z.A., Palmer, J., Mooney, S., Reimer, R.W., 2016. A 250-year periodicity in Southern Hemisphere westerly winds over the last 2600 years. Clim. 12, 189–200. doi:10.5194/cp-12-189-2016

Varma, V., Prange, M., Lamy, F., Merkel, U., Schulz, M., 2011. Solar-forced shifts of the Southern Hemisphere Westerlies during the Holocene. Clim. 7, 339–347. doi:10.5194/cp-7-339-2011

Supporting Information

Total solar insolation and algae productivity increase mercury accumulation in a pristine Southern Hemisphere lake

Harald Biester, Marta Pérez-Rodríguez, Benjamin-Silas Gilfedder, Antonio Martínez Cortizas, Yvonne-Marie Hermanns

Table 1. Pearson correlation coefficient matrices of Hg and Cu concentrations and accumulation rates, aquatic productivity proxies (Cp9 and HI) and the organic matter source proxy C/N-ratios in Lago Hambre sediments. With the exception of the Cp9 data and accumulation rates all other data are from (Hermanns et al., 2013). * Correlations are significant at the p<0.01 level. Number of data Cp9 *vs.*: C/N, n= 342, HI, n= 211, OI, n=211, Hg, n= 352, Cu, n= 406.

	C/N	HI	OI	Hg_{con}/ Hg_{AccR}	Cu_{con}/ Hg_{AccR}
Cp9	0.52*	0.78*	-0.72*	0.58*/0.62	0.49*/0.50
C/N	-	-0.64*	0.51*	-0.25/-0.38	-0.13/-0.24
HI	-	-	-0.88*	0.51*/0.58	0.48*/0.53
OI	-	-	-	-0.44*/-0.53	-0.44*/-0.50
Hg	-	-	-	-	0.65*/0.59

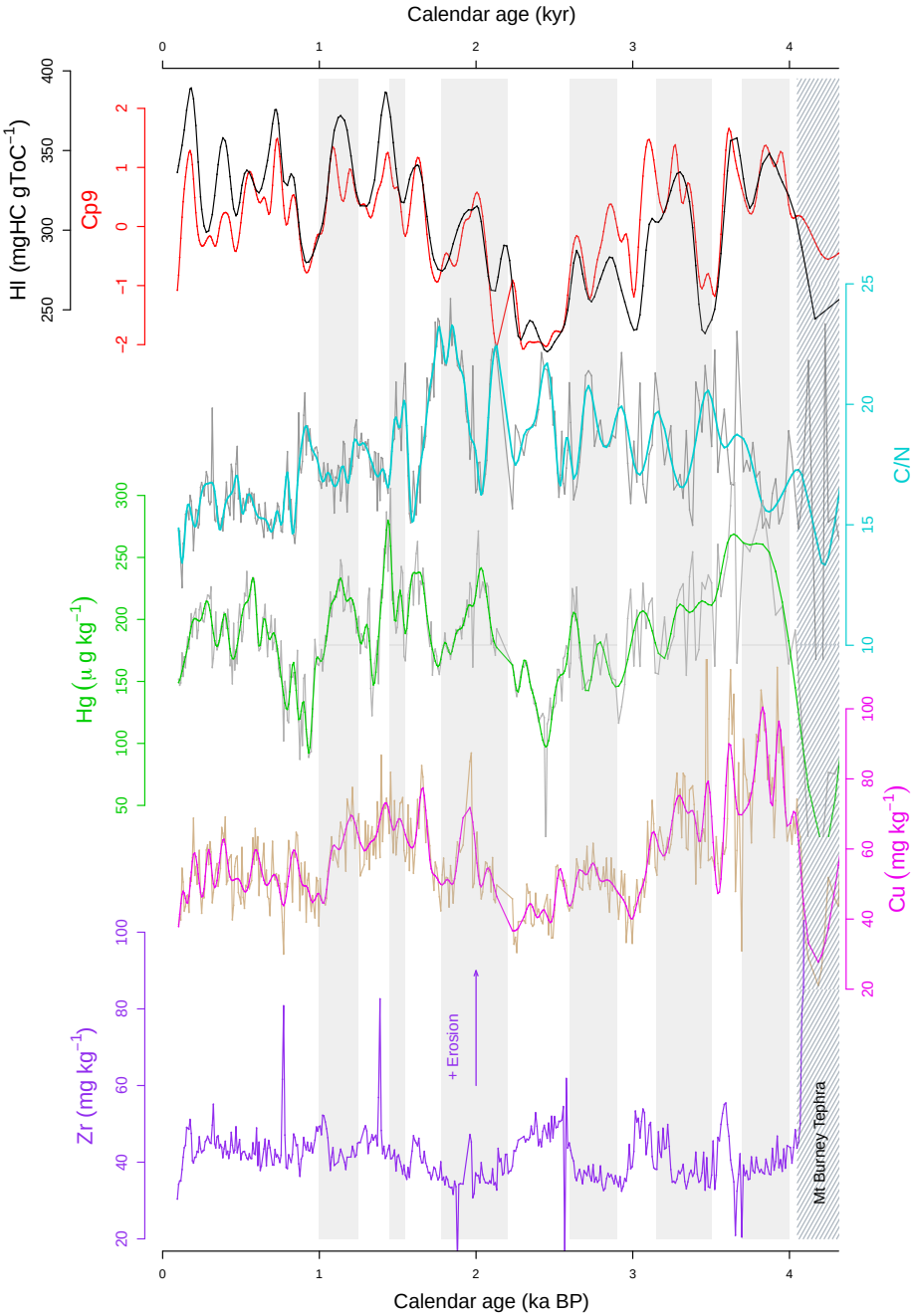

Figure S1: Proxy records of aquatic productivity (PCA1–Cp9 and HI), and Hg, Cu and Zr concentrations as well as carbon/nitrogen ratios (C/N). Grey bars indicate drier events at LH, see Pérez-Rodriguez et al., (2016). Streaked bar shows Mt Burney tephra layer.

References Supporting Informacion

Hermanns, Y.-M., Cortizas, A.M., Arz, H., Stein, R., Biester, H., 2013. Untangling the influence of in-lake productivity and terrestrial organic matter flux on 4,250 years of mercury accumulation in Lake Hambre, Southern Chile. J. Paleolimnol. 49, 563–573.

Pérez-Rodríguez, M., Gilfedder, B.-S., Hermanns, Y.-M., Biester, H., 2016. Solar Output Controls Periodicity in Lake Productivity and Wetness at Southernmost South America. Sci. Reports 6. doi:10.1038/srep37521

USC
UNIVERSIDADE
DE SANTIAGO
DE COMPOSTELA

MANUSCRIPT VI

The role of ice-cover, climate and volcanism on extreme mercury enrichment in Limnopolar Lake Sediments (Antarctica) during the last ca. 1600 years

USC
UNIVERSIDADE
DE SANTIAGO
DE COMPOSTELA

The role of ice-cover, climate and volcanism on extreme mercury enrichment in Limnopolar Lake Sediments (Antarctica) during the last ca. 1600 years

Marta Pérez-Rodríguez[1]*, Harald Biester[2], Jesús R. Aboal[3], Manuel Toro[4], Antonio Martínez Cortizas[1]

* corresponding author: M. Pérez-Rodríguez; mperez.rodriguez@usc.es

[1] *Departamento de Edafoloxía e Química Agrícola, Universidade de Santiago de Compostela. Santiago de Compostela, Spain*

[2] *Institut für Geoökologie, Abt. Umweltgeochemie, Technische Universität Braunschweig, Braunschweig, Germany*

[3] *Departamento de Bioloxía Celular e Ecoloxía, Universidade de Santiago de Compostela. Santiago de Compostela, Spain*

[4] *Centro de Estudios Hidrográficos (CEDEX). Madrid, Spain*

Abstract

The toxicity of its methylated forms and its ability of dispersion through the atmosphere make mercury (Hg) of special concern in remote-pristine ecosystems, such as the Artic and Antarctica. Despite the sensitivity of these regions, there is still lack of knowledge about the influence of natural processes such as volcanic activity, climate or atmospheric mercury depletion events (AMDEs) on the Hg cycle along the time. We sampled a short sediment core in Limnopolar Lake (Livingston Island, South Shetland Islands), spanning the last ~1600 years. Sediments were sectioned at high resolution and analysed for total mercury, as well as mercury species by means of Hg-thermo –desorption-CVAAS. The core shows sections of extreme mercury concentrations ranging between 1 141 and 11 286 ng g^{-1} compared to background concentrations 32± 17 ng g^{-1} (median, median absolute deviation), whereas accumulation rates oscillated between the maxima 310 – 4902 μg m^{-2} yr^{-1} and background 8.9± 5.7 μg m^{-2} yr^{-1}. Hg-thermo-desorption analyses indicate that mercury is retained in the sediment by organic matter at different stages of degradation. To explain the large differences in concentrations and the extremely high values found, we proposed a combination of different natural processes such as volcanism, climate and Hg depletion events. The nearby (30 km) volcano at Deception Island appears to be the main source of mercury, while Total Solar Irradiance (TSI) and climatic conditions have controlled freezing and thawing of ice-cover and snowpack on the lake and in the catchment. Hg was accumulated in snow and ice during cold periods and released to the lake during thawing events causing extreme Hg enrichments in the sediments. Elevated Br/C ratios (bromine independent of the organic matter) during extreme mercury accumulation suggested that AMDEs could also have played a role in mercury accumulation. No clear evidence of anthropogenic mercury pollution was found or it was overwritten by other natural factors.

1. Introduction

Mercury (Hg) is a metal of environmental concern and it is released to the atmosphere by natural and anthropogenic processes. Elemental mercury (Hg^0) is the dominant species in the atmosphere (Gustin et al., 2015). Due to its high volatility and long residence time, a substantial fraction of elemental mercury can be transported over long distances from the emission sources. The deposition of mercury is driven by chemical transformations between different mercury species with different physical and chemical characteristics.

Antarctica is a highly sensitive area and is generally thought to be a pristine environment because of its remote location and the protection provided by oceanic and atmospheric circulation around the continent. Notwithstanding, Antarctica is impacted by local and global anthropogenic activities (UNEP, 2002; Bargagli, 2005, 2008) Several studies have been performed on water, soils, mosses, lichens and fauna samples to decipher the incidence of mercury in Antarctic ecosystems (i.e. Zheng et al., [2015]) or to show the effect of natural systems (as volcano) vs. local pollution (Maõ de Ferro et al., 2014).

Different to the Arctic, there are not many studies reconstructing past time mercury accumulation in Antarctic environments. Seal hair recovered from lake sediments in King George Island was used to investigate the history of Hg deposition in the last two millennia (Sun et al., 2006). The authors proposed a relation of their Hg record with the past time use of Hg in gold and silver mining, although this relation was rather weak. On the long term (35 - 670 kyrs), ice cores have been found to be useful environmental records to reconstruct mercury deposition in Antarctica (Vandal et al., 1993; Jitaru et al., 2009), mainly showing the effect of atmospheric mercury depletion events (AMDEs) during glacial periods (Jitaru et al., 2009). Depletion events result from the oxidation of gaseous elemental mercury to highly reactive forms in the atmosphere caused by reactive halogens (such as bromine), and those oxidized Hg species are than rapidly removed from the atmosphere causing depletion of atmospheric Hg concentrations (Schroeder et al., 1998; Steffen et al., 2008). Although it is known that this process also occurs at temperate and low latitudes (Obrist et al., 2011), AMDEs were initially observed in polar environments, first in the Arctic (Schroeder et al., 1998) and later in Antarctica (Ebinghaus et al., 2002). In the Arctic it is estimated that AMDEs alone are responsible for the deposition of up to 100 tons of mercury per year north of the polar circle (Durnford and Dastoor, 2011) and it is a significant part

of the region's annual mercury deposition (i.e. Ariya et al., 2004).

In a recent review, Bargagli (2016) showed that although atmospheric Hg concentrations in the Southern Hemisphere are lower than those in the Northern Hemisphere, Antarctic cryptogams accumulate Hg at levels in the same range or higher than those observed for related cryptogam species in the Arctic, suggesting an enhanced deposition of bioavailable Hg in Antarctic coastal ice-free areas, probably related with AMDEs. The mercury deposited in association with AMDEs, or at least a substantial part of them, is accumulated in the snow (Hirdman et al., 2009) until the snowmelt (Johnson et al., 2008), when may constitute the a primary source of Hg to lakes and also to water bodies downstream, including the ocean (Loseto et al., 2004).

Despite the advances in different aspects of Hg in polar environments of the last decades, the interaction between sources and processes it is still poorly understood; Specifically how the combinations of natural Hg emissions (as those produced by volcanic activity), anthropogenic ones and changes in climate have modified mercury deposition in Antarctic environments through the time.

The Limnopolar project started in 2001 with the aim to study the ecological processes and community structure of different epicontinental freshwater ecosystems from Byers Peninsula and their response to climate change (Quesada et al., 2009; Camacho et al., 2012). As a base for palaeolimnological studies of long sediment cores, Toro et al., (2013) developed a chronostratigraphic investigation on a composite core sampled at Limnopolar Lake. More recently, a multiproxy research approach was conducted using a short sediment core (LIM-03) with the aim of identifying the main factors involved in the observed chemical–mineralogical changes and their timing during the last ca. 1600 years (Martínez Cortizas et al., 2014). The results indicate that volcanic activity, most probable of Deception Island volcano, has played a major role for the chemical and mineralogical composition of the lake's sediments. Although no evidence of metal enrichment has yet been found in Limnopolar lake for the industrial period (Martínez Cortizas et al., 2014), Sun et al., (2006) suggested evidence of mercury pollution derived from seal hair extracted from a core in a nearby lake (~120 km NE).

Here, we present results of a study on the Hg content in LIM-03 core sediments. The main objectives were i) to obtain a long-term mercury record

from an Antarctic lake and ii) to determine the main factors controlling mercury accumulation in the sediments.

2. Material and Methods

2.1 Study area and sediment sampling

Limnopolar Lake (62°38'54" S, 61° 06'19" W) is located in Byers Peninsula, the westernmost part of Livingston Island (South Shetland Islands, Figure 1) and designated at present as an Antarctic Specially Protected Area (ASPA No. 6). This peninsula contains a large number of lakes and is the largest ice-free area of maritime Antarctica, deglaciated since the Early Holocene (Toro et al., 2007; Oliva et al., 2016). Climate is less extreme than in continental Antarctica and, characterized by high inter-annual variability of temperature and precipitation (annual mean values of 700–1000 mm), with summer temperatures mostly above 0°C (mean range from 1–3 °C) and frequent rain, and winter temperatures below 0°C down to −27°C (Rochera et al., 2010; Bañón et al., 2013). The region is snow covered for at least eight months of the year. Snow cover distribution and thickness

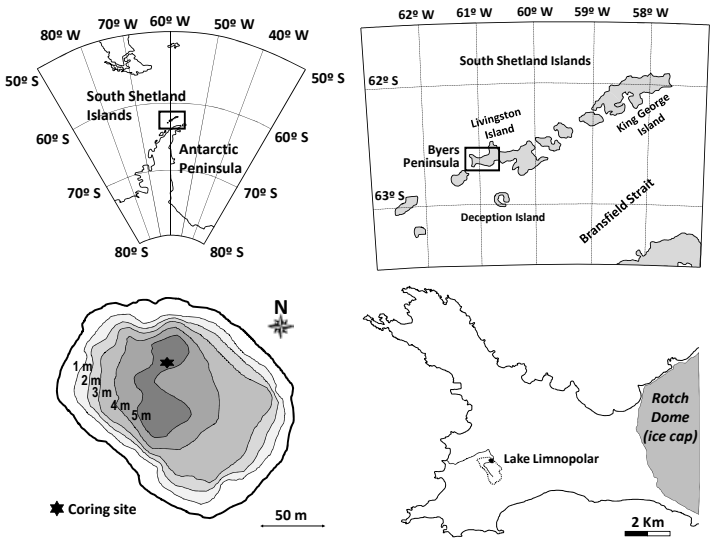

Figure 1: Location of Limnopolar Lake on Livingston Island (South Shetland Islands, Antarctica)

being dominated by topographic features and wind (Fassnacht et al., 2013). In the lake catchment, permafrost occurs below an active layer of up to 90–130 cm. Thawing occurs for about 75 days between late December and late February (de Pablo et al., 2012).

The lake has a catchment area of 0.58 km2 and a surface area of 0.022 km2. The lake is ultra-oligotrophic and ice covered except for 2–3 months during the summer, although during colder periods, the lake may have been covered with ice for longer periods, years or decades. The lake has a main inlet, but surface runoff significantly contributes to the lake volume during snowmelt and the period of thawing of the active soil layer. The surface sediment is covered by a patchy carpet of the moss Drepanocladus longifolius (Mitt.) Broth ex Paris (Toro et al., 2013). Vegetation in the catchment is only composed of scattered patches of mosses, lichens, and microbial mats (Velázquez et al., 2013).

The LIM-03 sediment core was collected at the deepest part of the frozen lake (5.5 m, Figure 1) in December 2003 using a Glew-type gravity corer, retrieving the upper-most 58 cm. It showed a centimetre to millimetre alternation of light brownish massive clays and silty clay layers, and dark brownish moss layers. A number of more discrete, millimetre–centimetre scale darker, silty layers made up of volcanic material, were also found in some sections. The core was sectioned (in situ) into 0.20 cm slices at the upper 10 cm, into 0.50 cm slices from 10 to 25 cm, and into 1 cm slices from 25 to 58 cm. Samples were stored dark and cool (4°C) in sterile Whirl-Pak bags. We selected 83 samples covering the whole core (last 1600 years).

2.2 Elemental composition

Before analysis, sub-samples were dried at 105°C until constant weight, milled and homogenized. Bulk samples were analysed for mercury using a Milestone DMA-80 analyser. The analysis of one in every four samples was duplicated as a control and a standard reference materials of the moss Pleurozium schreberi (Steinnes et al., 1997) M3 was run with each set of samples. The quantification limit was 3.3 ng g^{-1} and mean recovery was 103%. Eight samples with extremely high Hg concentrations (>900 ng g^{-1}) were re-analysed by triplicate separately. For these samples the quantification limit was 15.2 ng g^{-1} and mean recovery was 93% in M3. The mean difference between duplicates was 5.4%, ranging between 1.5 and 15.4%. To account for the effects of changes in sediment density we also

calculated the mercury accumulation rates.

Elemental bromine has been suggested to be the only candidate to explain depletions events of atmospheric Hg (Ariya et al., 2002). Moreover, it has been shown that Br in lichens from the Hudson Bay area is a good indicator for AMDEs(Carignan and Sonke, 2010). In LIM-03 bromine concentrations were determined by means of energy dispersive X-ray fluorescence EMMA-XRF spectroscopy (Cheburkin and Shotyk, 1999, 1996). Standard reference materials were used for the calibration of the instruments. Quantification limits was 1 μg g^{-1}.

2.3 Thermo-desorption analysis of Hg

Nine samples with high (at 5.90, 6.70, 8.70 11.75, 13.75, 24.75, 30.50, 44.50, 54.50 cm, >250 ng g-1) and one with relatively low Hg concentration (50.5 cm, 98 ng g-1) were analysed by Hg-pyrolysis-thermo-desorption-AAS (Hg-pTD-AAS) (Biester and Scholz, 1997) to obtain information about changes in Hg speciation in different sediment sections. Determination of Hg phases by solid-phase-Hg-thermo-desorption is based on the specific thermal desorption or decomposition of Hg compounds from solids at different temperatures. Mercury thermo-desorption curves were determined by means of an in-house equipment, consisting of an electronically controlled heating unit and a Hg detection unit. For Hg detection a quartz cuvette, where the thermally released Hg is purged through, is placed in the optical system of an atomic absorption spectrometer (Perkin-Elmer AAS 3030) and Hg absorption is detected at 253.7 nm at continuous detection mode (1 s intervals). Interferences, mainly from pyrolysis products of organic matter, were compensated by means of continuous deuterium background correction. Measurements were carried out at a heating rate of 0.5 °C/s and a N2-gas flow of 300 mL/min. Sample weight was 1-200 mg depending on the Hg content of the sample. Lowest level of detection under the given conditions is in the range of 40-50 ng if all Hg is released within a single peak. Results are presented as Hg thermo desorption curves (TDC), which show the release of Hg^0 versus temperature. Quantification of Hg peaks was obtained by peak integration using the Origin© software package.

2.4 Core chronology

The chronology of the LIM-03 core was constructed using ^{210}Pb, ^{226}Ra, and ^{137}Cs

measurements and radiocarbon dating of two moss samples. This chronology was overlapped with radiocarbon dating of moss samples of another long core collected in 2008 at the same lake location. The Bacon script for R (Blaauw and Christeny, 2011) was used to construct the age model of the composite core. Details can be found in Toro et al. (2013). LIM-03 core constitutes a continuously record from the end of the 4th century until the present.

2.5 Statistics

To disentangle the association between Hg accumulation rates and the other variables, it was calculated the phi coefficient (φ) (Matthews, 1975) similar to the Pearson correlation coefficient in its interpretation. To do that, the studied variables were transformed in binaries variables according a threshold value: above the "median + 1* median absolute deviation" the corresponding binary value is 1; under this value the corresponding binary value is 0. See more information in Supplements Material.

3. Results

Mercury concentrations in Limnopolar sediments fall into three main ranges (Figure 2). Most (n= 74) samples show low values (<160 ng g^{-1}) that range between 13 and 155 ng g^{-1} (33 ±17, median ± median absolute deviation (MAD)) with the two highest values (132 and 155 ng g^{-1}) near the surface (0.50 and 1.30 cm respectively). Two samples present intermediate-high concentrations of 259 and 948 ng g^{-1} at 44.55 and 24.75 cm, respectively. While seven samples show extremely high Hg concentrations between 1 141 and 11 286 ng g^{-1}. Five out of seven of these samples are located in the upper 14 cm and the other two at 30.5 and 54.5 cm, respectively. After removing the samples with highest concentrations (> 1000 ng g^{-1}) the mercury profile shows a seesaw pattern with a slight increase in concentrations from 5.5 cm to the surface (Figure 2).

Similarly to concentrations, mercury accumulation rates show three main ranges (Figure 2). The majority (n=75) of samples have values that range between 2 and 43 μg m^{-2} yr^{-1} (8.9± 5.7). Seven samples show high Hg accumulation rates ranging between 310 and 4902 μg m^{-2} yr^{-1} . The maximum value corresponding to the sample at 5.90 cm. Unlike concentrations, accumulation rates do not show an increase towards surface sediments (Figure 2).

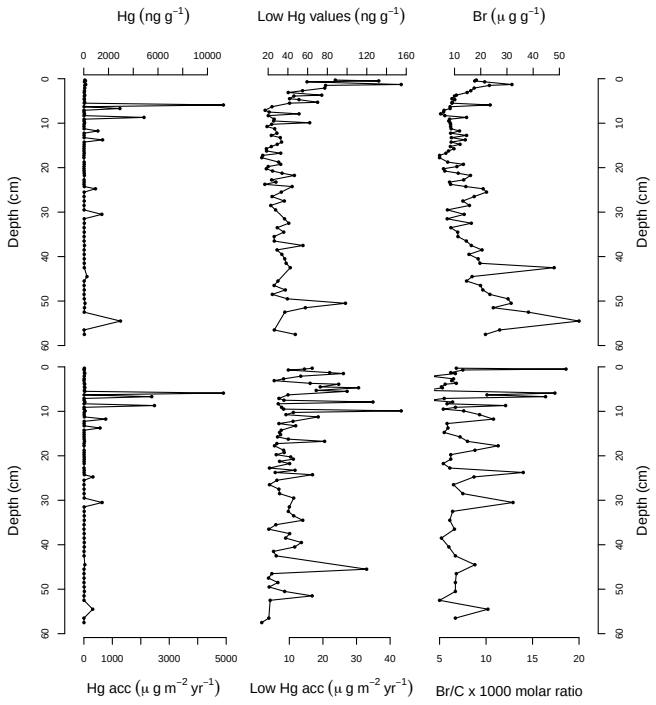

Figure 2: Depth records of variables measured in this work. Mercury concentration and accumulation rates are represented using all the values and removing the highest one (low Hg), to better show its variation.

Hg-speciation analyses were carried out to detect changes in Hg binding as a result organic matter decay and related changes redox conditions. All samples analysed by Hg-pTD-AAS (Figure 3) show a main desorption peak at 184 ± 6°C (mean ± standard deviation, n=3, see Table S1 in supplementary information), desorption starting at 145 ± 10°C, which could be assigned to Hg bound to organic matter. Five of the samples (at 5.90, 6.70, 13.75, 24.75, 50.50 cm) present an additional peak centred at 231 ± 5°C which correspond to the thermal decomposition of Hg sulphide (metacinnbar), and for two of them (24.75 and 50.50 cm) this secondary peak is well defined (see Figure 3). Two samples (at 30.5, 54.50 cm) showed a small shoulder at higher temperature (~280 ± 25°C).

Bromine concentrations vary between 4 and 58 μg g^{-1} (13 ± 6.5 μg g^{-1}, median ± MAD). Like mercury, the bromine record shows a seesaw pattern with a slight

increase in concentrations to the surface (Figure 2). The bottom samples have higher concentrations and the two highest values (58 and 48 μg g^{-1}) are located at 54.5 and 42.5 cm depth, respectively.

The huge range of Hg accumulation rates make difficult it comparison with the other variables, and the use of a robust statistic is necessary. The Phi coefficient (φ) measured the association between Hg accumulation and the other variables through their transformation in binary variables, limiting the problem of the range and provided a robust statistic. The results showed that there is a significant correlation/relation of Hg with the Br/C molar ratio (at 99% confidence level) using all the samples. The association disappears removing the main peaks detected in Hg accumulation. There is no significant statistical association between Hg and the other variables (see a detailed description in Table S2 and Supporting Information).

4. Discussion

Highest mercury concentrations in Limnopolar sediment samples are up to 5 000 fold higher than maximum concentrations reported for soils from Antarctica, and the lowest level (~13 ng g^{-1}) is up to 26 fold higher than the lowest values shown for soils (Mão de Ferro et al., 2014; Rodríguez dos Santos et al., 2006; Bargagli et al., 2005). The maxima are only comparable with sediment samples from volcanic sites such as fumaroles from Deception Island (Antarctica) and even those are slightly lower (12 – 10,000 ng g^{-1}; background and maximum, respectively) (Mão de Ferro et al., 2014). No previous study provides mercury accumulation rates for Antarctic sites. Another characteristic of the mercury LIM-03 record is the large variation in Hg accumulation through time (up to ~550 fold), which hint to event based fluxes of Hg to the sediment. So it is necessary focus on those mechanism that controlling the sediments geochemistry and could affect the mercury accumulation.

The sediments geochemistry and the processes controlling them were the target of the previous study, based on a multiproxy approach and Principal Component Analysis (Martínez Cortizas et al., 2014). The results showed that the first component (Cp1, see Supplementary Material) be able to identified the sections with a high content of volcanic material and four positive peaks of Cp1 indicated tephra layers from Deception Island volcano. By the other hand, the distribution of iron concentration in the sediments (Figure 3), as well as Cp2

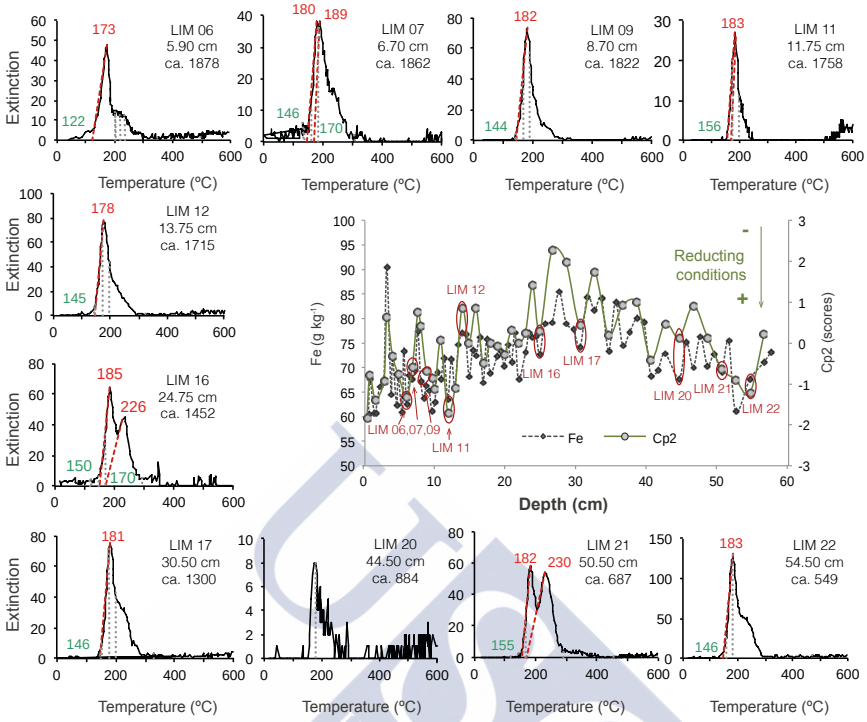

Figure 3: Hg-Thermo-desorption curves of sediment samples from Limnopolar Lake taken at 10 different depths. Maxima and start of desorption temperature (in Celsius degrees) are indicate (red and green numbers respectively). Inset represents Cp 2 and Fe concentration in Limnopolar sediment samples in depth. Both variables are identified as a redox conditions proxy (more information in Martínez Cortizas et al., (2014) and supplementary information). Samples analysed by Hg-thermo-desorption analysis are indicated in the depth record to show their redox conditions.

(the second component of the PCA, Supplementary Material) seems to be good indicators of the redox conditions of the lake (Martínez Cortizas et al., 2014). The main driver for this may be the climate, as the strong reducing condition (low Fe concentration and low Cp2 values) in this narrow lake seem to be unlikely, unless during periods of prolonged ice cover, as a result of cold climate. Finally the steadily increases in Cr concentrations in the last 200 years could be identified as evidence of pollution, although an increase in atmospherically transported dust was suggested as the best explanation (Martínez Cortizas et al., 2014).

Taking the previous results into account, we will examine the processes that could affect mercury deposition and produce the unexpected high Hg accumulation

in lake sediment as i) the role of volcanic eruptions of the nearby Deception Island volcano as Hg source; ii) how the long-term ice cover could accumulate Hg, and release during thawing iii) the possible effect of an increased of Hg deposition by depletion events; iii) and the Hg from pollution origin.

4.1 Volcanic Activity

The signals and effects of Deception Island volcanic emissions (30 km to the SE) on Limnopolar Lake sediments has been previously shown by the presence of multiple tephra layers along the whole sedimentary record, with abundant volcanic shards in the calcium-rich layers, (Martínez Cortizas et al., 2014). Martinez Cortizas et al., (2014) identified four main peaks of volcanic rich material in the sediments of the core LIM-03 (AD ca. 1840 – 1860 for L1, AD ca. 1570 – 1650 for L2, AD ca. 1450 – 1470 for L3 and AD ca. 1300 for L4). The tephra layers match reasonably well with five out of nine Hg bulk peaks: L4 fits with Hg peak at AD ca. 1300 (640 μg m^{-2} yr^{-1}), L3 with peak at AD ca. 1452 (318 μg m^{-2} yr^{-1}) and L1 covers peaks at AD ca. 1822, 1862 and 1878 (2480, 2348 and 4902 μg m^{-2} yr^{-1} respectively, Figure 4). There is no mercury peak corresponding to tephra layer L2 and there are no tephra layers associated to mercury peaks at AD ca. 549, 884, 1715 and 1758.

The comparison of the record of volcanic eruptions of Deception Island gathered by Bartolini and co-authors (see references in Bartolini et al., 2014) with Limnopolar's mercury and recent tephra records, indicate however a slight disagreement (Figure 4). For example, L4 and its corresponding mercury peak (AD ca. 1300) have a shift of ~100 years relative to the volcanic eruption (AD ca. 1200) (Figure 4); or the highest volcanic activity period of Deception Island volcano (from AD ca. 1800 to the present), does not correspond with the same number of mercury peaks.

It seems evident that although volcanic activity may have played a role in the extremely high levels of mercury found in Limnopolar sediment samples, but there is no direct relation so that other mechanisms should have been involved in the mercury accumulation process.

4.2 Dynamics of the lake, the effect of freezing and thawing

One main process that could have caused the extraordinary high mercury

concentrations is the effect of mercury accumulation on the ice-snow pack that covers Limnopolar Lake and its catchment during time of the year. Annually Limnopolar Lake is ice covered except for 2–3 months during the summer. The ice break-up in the lake has been observed to start in December near the lake outlets or inlets, however ice blocks or thin ice layers could persist until February (Toro et al., 2007) (see pictures in Figure 9.3 in Camacho et al., 2014). This dynamics may have resulted in the accumulation of an ice-snow layer over the lake and the catchment, which act as a mercury sink during 9 - 10 months per year. Under general cold conditions this dynamic should change, may have longer freezing stations, and extending the effect of mercury trap during years to decades.

The post-depositional mercury dynamics in Antarctic snow is not fully understood. It is known that freshly deposited mercury on snow is highly reactive (Lalonde et al., 2002), and part (20-50%) of the mercury deposited during AMDEs is quickly returned to the atmosphere within 24 hours (see references values in Durnford et al., 2012). The reduction of Hg^{+2} to GEM and subsequent re-emission of a fraction of the mercury from the snow pack is largely believed to occur through photochemical processes (Lalonde et al., 2002). However, solar irradiation only penetrates the first few centimetres of the snow pack, possibly leading to photoreduction of mercury complexes contained therein (King and Simpson, 2001). Conversely, processes as burial through snow accumulation, sublimation, condensation, and ice layer formation promote the retention and accumulation of mercury in the snowpack (Douglas et al., 2008). Most, if not all, of the deposited particulate mercury (Hgp), which can amount from 2% (Phelan et al., 1982) to up to 60% (Dedeurwaerder et al., 1982) of mercury emitted from volcanoes, is likely retained by the cryosphere (Durnford and Dastoor, 2011).

Mercury accumulated during the ice-covered period (both in the lake and in the catchment) will be transferred to the lake or lost through the outlets during thawing period, as part of the reactive gaseous mercury deposited and stabilized in the cryosphere (Durnford and Dastoor, 2011). However the thickening of the quasiliquid layer on snow grains that occurs during snowmelt is accompanied by greatly increased rates of both photoreduction and mercury emission (Dommergue et al., 2003; Faïn et al., 2008).

High Hg concentrations/accumulation rates appear to correspond to phases of minima insolation (colder). The comparison of the Total Solar Irradiance (ΔTSI)

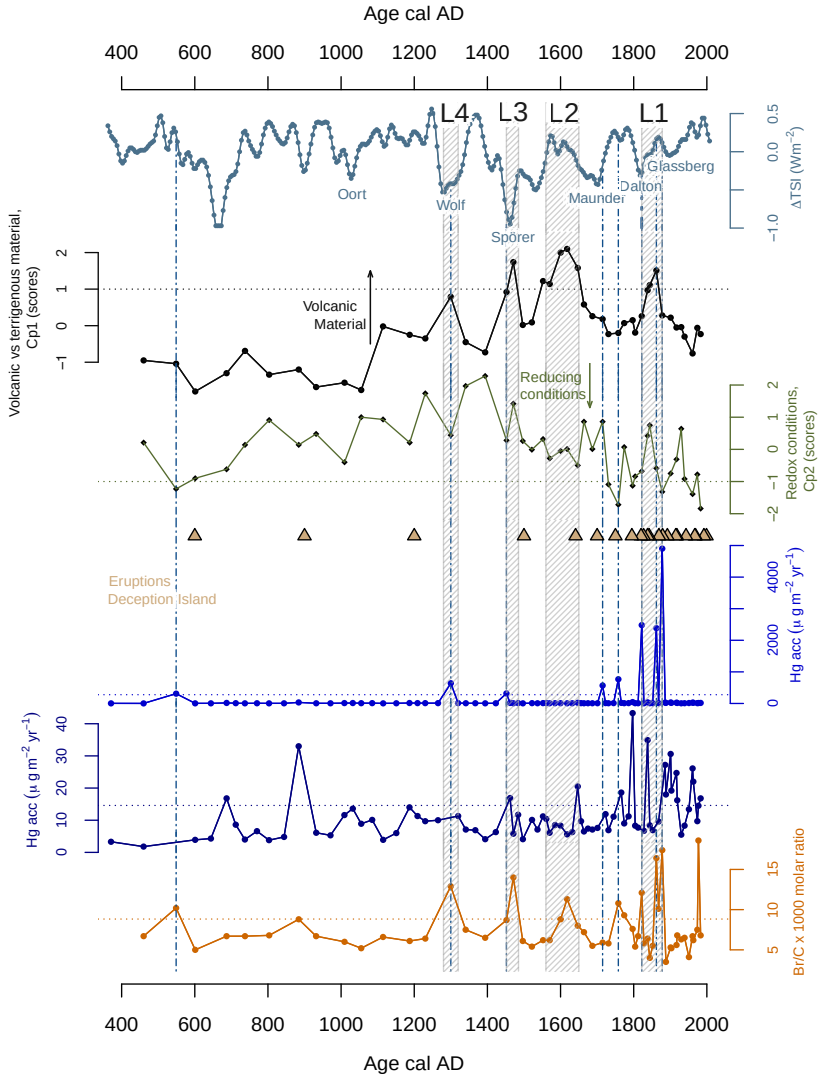

Figure 4: Age records of climatic, sedimentary and volcanic proxies affecting Limnopolar Lake. Total Solar Irradiance (ΔTSI) record (Steinhilber et al., 2009) shows periods with higher or lower irradiance; know solar minima are indicated. Proxies of volcanic material (Cp1) and reducing conditions (Cp2) in LIM-03 record are from Martínez Cortizas et al., (2014). Triangles indicate eruptions of Deception Island volcano gathered by Bartolini et al., (2014). Mercury accumulation rates records in LIM-03 including all the samples and removing the highest ones (blue and navy blue). Br/C molar ratio record is included as a proxy bromine record independent of the amount of organic matter content. The horizontal dotted lines indicated the threshold value used to calculated the phi coefficient (φ) (see main text). Vertical grey bars and labels L1 to L4 indicate the position of thepra layers according to Martínez Cortizas et al., (2014 and Toro et al., (2013) in LIM-03 record. Vertical discontinuous lines mark the position of the main Hg peaks.

record (Steinhilber et al., 2009) (Figure 4), a measure of the solar power on the Earth's upper atmosphere, with mercury accumulation shows that six of eight high mercury peaks (>270 µg m^{-2} yr^{1}) coincided with periods of low irradiance. Peaks at AD ca. 1300, 1450 and 1715, 1822 correspond with the Wolf, Spörer, Maunder and Dalton minima and, additionally, peaks at AD ca. 550 and 1750 correspond to relative low insolation conditions. Even more, without considering the samples with extremely high accumulation (<270 µg m^{-2} yr^{1}), the record also shows increases of mercury accumulation during periods of low irradiance (light blue shadows, Figure 5 and 6).

Under such cold conditions it is likely that the lake and its basin remained snow/ice-covered for long periods of time, enhancing mercury accumulation in the snowpack. During thawing, material stored in the snowpack would have been transferred to the lake. Even though phi coefficient analyses do not show significant statistical association between Hg accumulation rates and, changes in redox conditions (Cp2 and Fe record in Figure 3), four of six mercury peaks

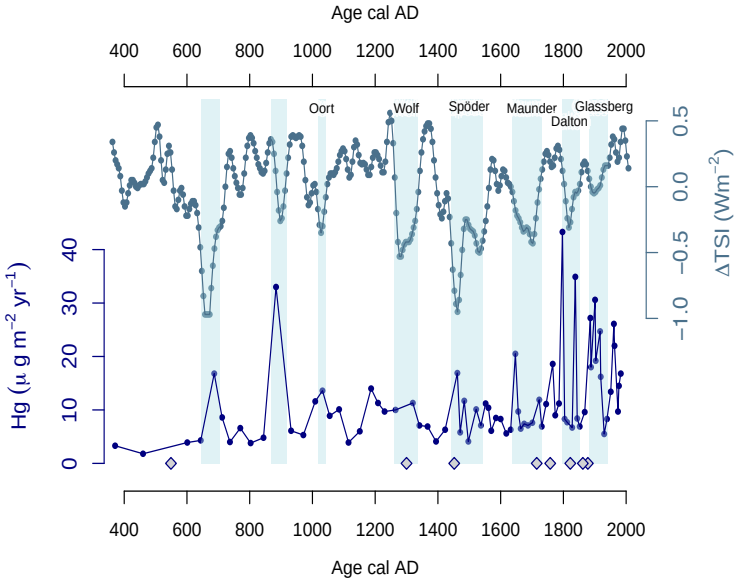

Figure 5. Total Solar Irradiance (ΔTSI) record (Steinhilber et al., 2009) indicate periods with higher or lower irradiance and mercury accumulation rate age record from LIM-03. Only the low values of mercury accumulation are plot; grey diamonds indicates positions of the main Hg accumulation rate peaks. Blue bars indicate low irradiance periods that corresponds with slight increases of Hg accumulation. Know solar minima are indicated

with concentrations >270 μg m^{-2} yr^{-1}, that occurred during low ΔTSI, correspond with reducing conditions in the lake sediment indicated by scores lower to -1 in Cp2 (Figure 4). The other two Hg peaks (AD ca. 1300 and 1450) showed more reducing conditions than adjacent samples. This supports the idea of long phases of a closed frozen lake surface, which promotes reducing conditions in the sediment and the longer the period is, the more intense reducing condition will be. During the ice cover period, a progressive depletion of the oxygen in the water layer closer to the sediment (reducing conditions) is directly proportional to the ice cover duration, as a result of heterotrophic degradation of the deposited organic matter under high stability of water column, low or null light transmission through the ice-cover (i.e. no photosynthetic O_2 production) and no gas exchange with atmosphere. Extraordinary long ice-cover duration in Limnopolar Lake in winter 2012-13 caused almost total oxygen bottom depletion (0,23 mg/L) at the end of winter period (personal data).

Reducing conditions have also played a main role in Hg binding in the sediments. Thermo-desorption analyses (Figure 3) indicate that there is shifts from Hg bound to less decompose organic matter here mainly mosses (low temperature peak), to organosulfides or metacinnabar signals (higher temperature range) due to the proceeding degradation of the organic matter and decrease of the redox potential. The observation that Hg binding to sulphides appears only in the deeper/older sediments (Figure 3 and 6) indicates that organic matter turnover is extremely slow in this lake due to the low temperature. Organic rich sediments in lakes of more temperate regions usually show Hg binding to sulphides (higher temperature range) even in shallow sediments.

4.3 Atmospheric Mercury Depletion Events

The effect of AMDEs in the mercury LIM-03 record is difficult to demonstrate. However, due to the extension of AMDE phenomena in the polar environment of both hemispheres (i.e. Schroeder et al., 1998; Lindberg et al., 2001; Ebinghaus et al., 2002), it is necessary take it into account as one of the possible driver of Hg accumulation in the record.

As indicated in the methods section, bromine was suggested to be a good indicator of AMDEs (Carignan and Sonke, 2010), but in soils and sediments it is also known to occur mostly as organo-bromine compounds (Apslund and Grimvall, 1991; Öberg et al., 1996; Johanson et al., 2001; Biester et al, 2004)

resulting from biotic and abiotic halogenation of organic matter (Keppler et al., 2000; Myneni, 2002; Van Pée and Unversucht, 2003; Leri et al., 2014). Only a small fraction (1–8%) of the total Br in the soils and peats appears as inorganic Br (Maw and Kempton, 1982). In LIM-03 sediments, bromine and carbon content (data not show) are positively correlated (r= 0.874, n=55 and 0.937, n=46 removing samples with the extremely Hg concentrations). To obtain a bromine record independent of the amount of organic matter content, we calculated the bromine/carbon molar ratio. This ratio shows good agreement with the high mercury concentration peaks (Figure 4) and the Phi coefficient (φ) indicate that it is significant correlation.

Both the proposed mechanisms for AMDEs - photo-chemically activation under daylight and marine evasions under darkness (Faïn et al., 2008; Nerentorp Mastromonaco et al., 2016) - are controlled by bromine reactive species. This agrees with the results that showed that the presence of halogens in snow may promote the retention of mercury and, indeed, elevated snow mercury deposition by oxidation (Faïn et al., 2008); being this processes more often found in coastal environments where deposition of sea salt can be expected (Poulain et al., 2007; Durnford and Dastoor, 2011). Positive correlations between total mercury and bromide concentrations were found in snow samples (Poulain et al., 2007) as well as in lichens samples (Carignan and Sonke, 2010). Even more, the colder conditions dominating under low insolation phases, as we found during Hg peaks, may have also enhanced the formation of ice crystals ("frost flowers"), which have been proposed as a key factor in springtime mercury depletion events, as a dominant source of sea salt aerosols and bromine compounds (Rankin et al., 2002; Douglas et al., 2005).

The proximity of the marine coast and the cold periods where most of the Hg peaks are concentrated make a favourable environment - unlimited availability of bromine and enhancing conditions for the formation of ice crystals, respectively – to produces Hg depletion events. All of these considerations do not demonstrate the effect of AMDEs on Hg peaks recorded in LIM-03 core (Figure 4 and Figure 5 and 6) but points that must be a complementary process of lake's dynamics, to produce large accumulations of Hg.

4.4 Mercury pollution

As we mentioned before, the LIM-03 record shows a steady increase in mercury concentrations after removing the extremely high mercury peaks in the upper

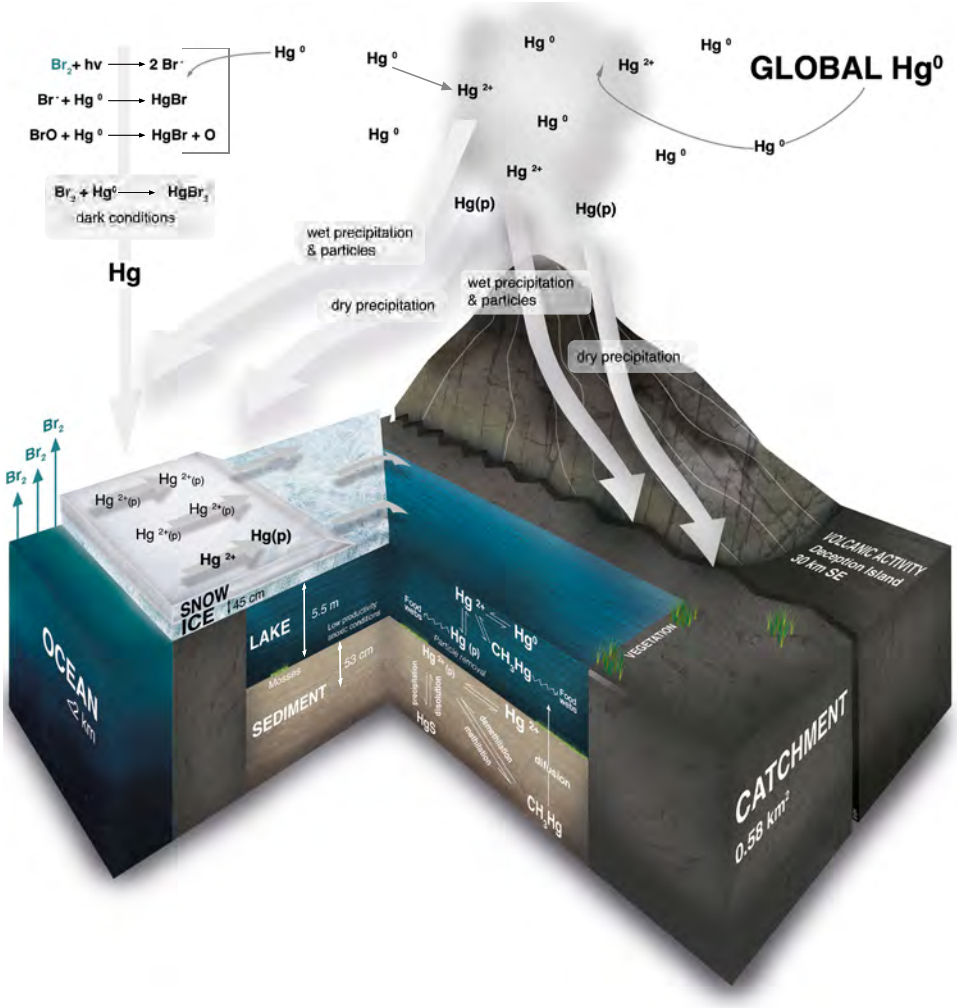

Figure 6: Schematic model with the mechanisms controlling mercury accumulation in LIM-03 (Limnopolar Lake, Livingston Island, Antarctic). Volcanic activity of Deception Island seems to be a main source of mercury in the area. Climate is likely the main driver for the event based high mercury accumulation, by controlling the time the lake is frozen and mercury is accumulated in the overlying snowpack. During colder periods atmospheric Hg depletion events may increase mercury deposition. During seasonal thawing, most mercury is than transferred to the lake's sediment; an unknown quantity can be lost through drainage. Thermo-desorption results indicate that mercury is accumulated and retained in the sediment by the organic matter; both by fresh and more decomposed organic matter. In addition, reducing conditions in the lake bottom (water-sediments interphase) could promote the formation of mercury sulphides. Anthropogenic mercury pollution has no visible effect on LIM-03 sediments.

part of the record since AD ca. 1868 and more abrupt since AD ca. 1930 (Figure S1). This upward trend does not seem to be attributed to the processes discussed in previous sections, or if so, the effects on mercury concentrations were much lower (maximum of 155 ng g^{-1} at AD ca. 1963, Figure S1). However, mercury accumulation does not show this increase at the surface, pointing to an effect of sediment dry density that decreases from the same period to the surface (see Supplement material for more information).

Antarctica metal pollution has been found to be restricted to small areas within the surrounding of scientific research stations, for example in the nearby King George Island (Santos et al., 2005). However, Livingston Island hosts only few and non-permanent (1–3 months per year) research infrastructure located 1,700 m away from Limnopolar Lake. No evident signals of recent anthropogenic metallic (Cu, Zn, Pb, Cr) pollution were found in a previous study on the sediment inorganic geochemistry of the lake sediments (Martínez Cortizas et al., 2014), but the high residence time of mercury in the atmosphere (~0.5-1 years) allows transport over long distances from the emission sources, which does not rule out finding in Limnopolar's sediments Hg from regional or global contamination.

Studies performed at King George Island (West Antarctica, ~120 km NE from Limnopolar Lake) reconstructing mercury pollution, associated the rise and fall of total mercury concentrations in seal's hear with the majority of the ancient activities of gold and silver mining which used the Hg-amalgamation process around the world; among other: Roman Empire, China Han Dynasty, Maya period, Inca civilization, Christian Kingdom and Modern Industry Period (Sun et al., 2006). Some of the increases in mercury concentration indicated by Sun et al., (2006) agree with mercury peaks in LIM-03 that can be explained by other processes than anthropogenic pollution. For example the increase attributed to the Maya period and China Tang dynasty (AD 750 – 900) partly overlap with the volcanic eruption and the mercury peak at AD ~880 detected by us (Figure 3); the period related with Inca civilization and Christian Kingdom (AD 1200 – 1500) contains two mercury peaks (AD ca. 1300 – 1452) that we correlate to volcanic activity and enhanced accumulation during the Wolf and Spörer solar minima; finally the increase associated with the New World (AD 1650 – 1800) and the first part of modern Industrial period, starting by AD 1840, may correspond with the period of higher volcanic activity of Deception Island and the large mercury peaks recorded in LIM-03 (Figure 3). Thus the ancient pollution signals identified

at King George Island could be – at least partially – originated by volcanic activity from Deception Island.

If we consider the increases in mercury pollution after ~1868 being a true signal of Hg pollution, as the mercury concentration suggests, determine its source seems to be complicated. Discarding local sources, studies performed in remote sites point to a general increases in atmospheric mercury in the South Hemisphere. Both in New Zealand (Lamborg et al., 2002) and in Southernmost Patagonia (Hermanns and Biester, 2013) increases in mercury by AD ~1900 seem to be decoupled from local pollution and suggest a more hemispheric or global signal.

5. Conclusions

The mercury accumulation record in LIM-03 sediments it is related to a combination of processes that control the source, deposition and retention of mercury in the sediment. Combinations of these processes - but ultimately controlled by long-term ice dynamics (ice covering and thawing)- get a range of variation of total mercury of about 550 fold in a remote and pristine area. The drainage of the lake towards the outside of the plateau where it is located, probably releasing - at least- part of the Hg retained in the snow and ice as meltwater, may extent to the surronding area the implications of the elevated Hg accumulation; although for now they are unknown.

6. References

Ariya P.A., Khalizov A., and Gidas A., 2002. Reactions of Gaseous Mercury with Atomic and Molecular Halogens: Kinetics, Product Studies, and Atmospheric Implications. The Journal of Physical Chemistry A 106, 7310–7320

Ariya P.A., Dastoor A.P., Amyot M., Schroeder W.H., Barrie L., Anlauf K., Raofie F., Ryzhkov A., Davignon D., Lalonde J., et al., 2004. The Arctic: A sink for mercury. Tellus, Series B: Chemical and Physical Meteorology 56, 397–403

Bañón M., Justel A., Velázquez D., and Quesada A., 2013. Regional weather survey on Byers Peninsula, Livingston Island, South Shetland Islands, Antarctica. Antarctic Science 25, 146–156

Bargagli R., 2005. Antarctic Ecosystems, Environmental Contamination, Climate Change, and Human Impact (Springer-Verlag Berlin Heidelberg: Springer-Verlag Berlin Heidelberg)

Bargagli R., 2008. Environmental contamination in Antarctic ecosystems. Science of the Total Environment 400, 212–226

Bartolini S., Geyer A., Martí J., Pedrazzi D., and Aguirre-Díaz G., 2014. Volcanic hazard

on Deception Island (South Shetland Islands, Antarctica). Journal of Volcanology and Geothermal Research 285, 150–168

Biester H. and Scholz C., 1997. Determination of mercury binding forms in contaminated soils: Mercury pyrolysis versus sequential extractions. Environmental Science and Technology 31, 233–239

Blaauw M. and Christeny J.A., 2011. Flexible paleoclimate age-depth models using an autoregressive gamma process. Bayesian Analysis 6, 457–474

Camacho A., Rochera C., Villaescusa J.A., Velázquez D., Toro M., Rico E., Fernandezvaliente E., Justel A., Banon M., and Quesada A., 2012. Maritime antarctic lakes as sentinels of climate change. International Journal of Design and Nature and Ecodynamics 7, 239–250

Camacho A., Villaescusa J.A., Rochera C., and Jørgensen S.E., 2014. Chapter 9 - Modeling the Response of the Planktonic Microbial Community to Warming Effects in Maritime Antarctic Lakes: Ecological Implications. In Ecological Modelling and Engineering of Lakes and Wetlands, N.-B.C. and F.-L.X.B.T.-D. in E.M. Sven Erik Jørgensen, ed. (Elsevier), pp. 231–250

Carignan J. and Sonke J., 2010. The effect of atmospheric mercury depletion events on the net deposition flux around Hudson Bay, Canada. Atmospheric Environment 44, 4372–4379

Cheburkin A.K. and Shotyk W., 1996. An Energy-dispersive Miniprobe Multielement Analyzer (EMMA) for direct analysis of Pb and other trace elements in peats. Fresenius' Journal of Analytical Chemistry 354, 688–691

Cheburkin A.K. and Shotyk W., 1999. High-sensitivity XRF analyzer (OLIVIA) using a multi-crystal pyrographite assembly to reduce the continuous background. X-Ray Spectrometry 28, 145–148

Dedeurwaerder H., Decadt G., and Baeyens W., 1982. Estimations of mercury fluxes emitted by Mount Etna volcano. Bulletin Volcanologique 45, 191–196

Dommergue A., Ferrari C.P., Gauchard P.-A., Boutron C.F., Poissant L., Pilote M., Jitaru P., and Adams F.C., 2003. The fate of mercury species in a sub-arctic snowpack during snowmelt. Geophysical Research Letters 30, 1621

Douglas T.A., Sturm M., Simpson W.R., Brooks S., Lindberg S.E., and Perovich D.K., 2005. Elevated mercury measured in snow and frost flowers near Arctic sea ice leads. Geophysical Research Letters 32, 1–4

Douglas T.A., Sturm M., Simpson W.R., Blum J.D., Keeler G.J., Perovich D.K., Biswas A., Johnson K., and Alvarez-aviles L., 2008. Influence of Snow and Ice Crystal Formation and Accumulation on Mercury Deposition to the Arctic. Environmental Science and Technology 42, 1542–1551

Durnford D. and Dastoor A., 2011. The behavior of mercury in the cryosphere: A review of what we know from observations. Journal of Geophysical Research Atmospheres 116

Durnford D.A., Dastoor A.P., Steen A.O., Berg T., Ryzhkov A., Figueras-Nieto D., Hole L.R., Pfaffhuber K.A., and Hung H., 2012. How relevant is the deposition of mercury onto snowpacks?-Part 1: A statistical study on the impact of environmental factors. Atmospheric Chemistry and Physics 12, 9221–9249

Ebinghaus R., Kock H.H., Temme C., Einax J.W., Löwe A.G., Richter A., Burrows J.P., and Schroeder W.H., 2002. Antarctic springtime depletion of atmospheric mercury.

Environmental Science and Technology 36, 1238–1244

Faïn X., Ferrari C.P., Dommergue A., Albert M., Battle M., Arnaud L., Barnola J.-M., Cairns W., Barbante C., and Boutron C., 2008. Mercury in the snow and firn at Summit Station, Central Greenland, and implications for the study of past atmospheric mercury levels. Atmospheric Chemistry and Physics Discussions 7, 18221–18268

Fassnacht S.R., López-Moreno J.I., Toro M., and Hultstrand D.M., 2013. Mapping snow cover and snow depth across the Lake Limnopolar watershed on Byers Peninsula, Livingston Island, Maritime Antarctica. Antarctic Science 25, 157–166

Gustin M.S., Amos H.M., Huang J., Miller M.B., and Heidecorn K., 2015. Measuring and modeling mercury in the atmosphere : a critical review. 5697–5713

Hermanns Y. and Biester H., 2013. Anthropogenic mercury signals in lake sediments from southernmost Patagonia, Chile. Science of the Total Environment 445–446, 126–135

Hirdman D., Aspmo K., Burkhart J.F., Eckhardt S., Sodemann H., and Stohl A., 2009. Transport of mercury in the Arctic atmosphere: Evidence for a springtime net sink and summer-time source. Geophysical Research Letters 36, 1–5

Jitaru P., Gabrielli P., Marteel A., Plane J.M.C., Planchon F.A.M., Gauchard P.-A., Ferrari C.P., Boutron C.F., Adams F.C., Hong S., et al., 2009. Atmospheric depletion of mercury over Antarctica during glacial periods. Nature Geoscience 2, 505–508

Johnson K.P., Blum J.D., Keeler G.J., and Douglas T.A., 2008. Investigation of the deposition and emission of mercury in arctic snow during an atmospheicc mercury delpletion event. Journal of Geophysical Research Atmospheres 113, 1–11

King M.D. and Simpson W.R., 2001. Extinction of UV radiation in Arctic snow at Alert. Canada (82◦ N. Journal of Geophysical Research, 106 (D12): 12499–12507

Lalonde J.D., Poulain A.J., and Amyot M., 2002. The role of mercury redox reactions in snow on snow-to-air mercury transfer. Environmental Science and Technology 36, 174–178

Lamborg C.H., Fitzgerald W.F., Damman A.W.H., Benoit J.M., Balcom P.H., and Engstrom D.R., 2002. Modern and historic atmospheric mercury fluxes in both hemispheres: Global and regional mercury cycling implications. Global Biogeochemical Cycles 16, 1104

Lindberg S.E., Brooks S., Scott K., Meyers T., Chambers L., Landis M., and Stevens R., 2001. Formation of reactive gaseous mercury in the arctic: evidence of oxidation of Hg to gas-phase Hg-II compounds after Arctic sunrise. Water, Air, and Soil Pollution 1, 295–302

Loseto L.L., Lean D.R.S., and Siciliano S.D., 2004. Snowmelt sources of methylmercury to high arctic ecosystems. Environmental Science and Technology 38, 3004–3010

Maõ de Ferro A., Mota A.M., and Canário J., 2014. Pathways and speciation of mercury in the environmental compartments of Deception Island, Antarctica. Chemosphere 95, 227–233

Martínez Cortizas A., Rozas Muñiz I., Taboada T., Toro M., Granados I., Giralt S., Pla-Rabés S., Cortizas A.M., Muñiz I.R., Taboada T., et al., 2014. Factors controlling the geochemical composition of Limnopolar Lake sediments (Byers Peninsula,

Livingston Island, South Shetland Island, Antarctica) during the last ca. 1600 years. Solid Earth 5, 651–663

Matthews B.W., 1975. Comparison of the predicted and observed secondary structure of T4 phage lysozyme. Biochimica et Biophysica Acta (BBA) - Protein Structure 405, 442–451

Maw G.A. and Kempton R.J., 1982. Bromine in soils and peats. Plant and Soil 65, 103–109

Nerentorp Mastromonaco M., Gårdfeldt K., Jourdain B., Abrahamsson K., Granfors A., Ahnoff M., Dommergue A., Méjean G., and Jacobi H.W., 2016. Antarctic winter mercury and ozone depletion events over sea ice. Atmospheric Environment 129, 125–132

Obrist D., Tas E., Peleg M., Matveev V., Faïn X., Asaf D., and Luria M., 2011. Bromine-induced oxidation of mercury in the mid-latitude atmosphere. Nature Geoscience 4, 22–26

Oliva M., Antoniades D., Giralt S., Granados I., Pla-Rabes S., Toro M., Liu E.J., Sanjurjo J., and Vieira G., 2016. The Holocene deglaciation of the Byers Peninsula (Livingston Island, Antarctica) based on the dating of lake sedimentary records. Geomorphology 261, 89–102

de Pablo M.A., Blanco J., Molina A., Ramos M., Quesada A., Vieira G., de Pablo M. A., Blanco J. j. J., Molina A., Ramos M., et al., 2012. Interannual active layer variability at the Limnopolar Lake CALM site on Byers Peninsula, Livingston Island, Antarctica. Antarctic Science 14, 1–15

Phelan J.M., Finnegan D.L., Ballantine D.S., Zoller W.H., Hart M.A., and Moyers J.L., 1982. Airborne aerosol measurements in the quiescent plume of Mount St. Helens: September, 1980. Geophysical Research Letters 9, 1093–1096

Poulain A.J., Garcia E., Amyot M., Campbell P.G.C., and Ariya P.A., 2007. Mercury distribution, partitioning and speciation in coastal vs. inland High Arctic snow. Geochimica et Cosmochimica Acta 71, 3419–3431

Quesada A., Camacho A., Rochera C., and Velazquez D., 2009. Byers Peninsula : A reference site for coastal, terrestrial and limnetic ecosystem studies in maritime Antarctica. Polar Science 3, 181–187

Rankin A.M., Wolff E.W., and Martin S., 2002. Frost flowers: Implications for tropospheric chemistry and ice core interpretation. Journal of Geophysical Research Atmospheres 107

Rochera C., Justel A., Fernández-Valiente E., Bañón M., Rico E., Toro M., Camacho A., and Quesada A., 2010. Interannual meteorological variability and its effects on a lake from maritime Antarctica. Polar Biology 33, 1615–1628

Santos I.R., Silva-Filho E. V., Schaefer C.E.G.R., Albuquerque-Filho M.R., and Campos L.S., 2005. Heavy metal contamination in coastal sediments and soils near the Brazilian Antarctic Station, King George Island. Marine Pollution Bulletin 50, 185–194

Schroeder W.H., Anlauf K.G., Barrie L. a, Lu J.Y., and Steffen A., 1998. Arctic Springtime Depletion of Mercury. Nature 394, 331–332

Steffen A., Douglas T., Amyot M., Ariya P., Aspmo K., Berg T., Bottenheim J., Brooks S., and Cobbett F., 2008. A synthesis of atmospheric mercury depletion event chemistry in the atmosphere and snow. Atmospheric Chemistry and Physics 8,

1445–1482

Steinhilber F., Beer J., and Fröhlich C., 2009. Total solar irradiance during the Holocene. Geophysical Research Letters 36, 1–5

Steinnes E., Rühling Å., Lippo H., and Mäkinen A., 1997. Reference materials for large-scale metal deposition surveys. Accreditation and Quality Assurance 2, 243–249

Sun L., Yin X., Liu X., Zhu R., Xie Z., and Wang Y., 2006. A 2000-year record of mercury and ancient civilizations in seal hairs from King George Island, West Antarctica. Science of the Total Environment 368, 236–247

Toro M., Camacho A., Rochera C., Rico E., Bañón M., Fernández-Valiente E., Marco E., Justel A., Marco E., Avedaño M.C., et al., 2007. Limnological characteristics of the freshwater ecosystems of Byers Peninsula, Livingston Island, in maritime Antarctica. Polar Biology 30, 635–649

Toro M., Granados I., Pla S., Giralt S., Antoniades D., Galán L., Cortizas A.M., Lim H.S., and Appleby P.G., 2013. Chronostratigraphy of the sedimentary record of Limnopolar Lake, Byers Peninsula, Livingston Island, Antarctica. Antarctic Science 25, 198–212

UNEP, 2002. Global Mercury Assesment (Geneva)

Vandal G.M., Fitzgerald W.F., Boutron C.F., and Candelone J.-P., 1993. Variations in mercury deposition to Antarctica over the past 34,000 years. Nature 362, 621–623

Velázquez D., Ángeles Lezcano M., Frias A., and Quesada A., 2013. Ecological relationships and stoichiometry within a Maritime Antarctic watershed. Antarctic Science 25, 191–197

Weiss D., Shotyk W., Cheburkin A.K., and Gloor M., 1998. Determination of Pb in the ash fraction of plants and peats using the Energy-dispersive Miniprobe Multielement Analyser (EMMA). The Analyst 123, 2097–2102

Zheng W., Xie Z., and Bergquist B.A., 2015. Mercury Stable Isotopes in Ornithogenic Deposits As Tracers of Historical Cycling of Mercury in Ross Sea, Antarctica. Environmental Science and Technology 49, 7623–7632

USC
UNIVERSIDADE
DE SANTIAGO
DE COMPOSTELA

Supporting Information

The role of ice-cover, climate and volcanism on extreme mercury enrichment in Limnopolar Lake Sediments (Antarctica) during the last ca. 1600 years

Marta Pérez-Rodríguez, Harald Biester, Jesús R. Aboal, Manuel Toro, Antonio Martínez Cortizas

Description of the components and variables extracted from the previous work (Martínez Cortizas et al., 2014) and use in the current one

Recently, a multiproxy research was conducted using the same short sediment core (LIM-03) with the aim of identifying the main factors involved in the observed chemical–mineralogical changes and their timing during the last ca. 1600 years (Martínez Cortizas et al., 2014). In the mentioned work, the authors performed a PCA on the geochemical data to extract the main chemical signatures of the sediment and to investigate into the factors controlling them. From the seven principal components extracted (96% of the total variance), two are used in the current work to understand the Hg geochemical cycle in Limnopolar Lake.

The first component (Cp1, 40.6% of the total variance) shows large positive loadings of Ca, Sr, Ti and Zr; and large negative loadings of K and Rb. This component was interpreted as the proportion of volcanic material (Ca rich) vs marine sediments (K rich) – the dominant geological material in the lake catchment. Four of the main positive peaks matched reasonably well with the ages of tephra layers. In the current work we use this component to indicate the location of the thepra layers.

The second component (Cp2, 12.7% of the total variance) is characterized by large positive loadings for Fe and Mn. This component was identified as a redox conditions proxy, indicating reducing conditions by positive scores (Post-

depositional redistribution of these two elements has been shown to occur in reducing environments; i.e. Chesworth et al., 2006). In the current work we represent Fe concentration from the same paper to illustrate and facilitate the understanding of the figures.

Table S1: Temperatures of the main characteristic points of the Hg thermo-desorption curves of the nine samples analysed from LIM-03 core, and the Hg concentration of the samples determined by a Milestone DMA-80. Only the temperature of start desorption of the main peak is indicated. (*) Indicate a bad resolution of the peak. See Figure 3 in the main text.

Sample	Depth (cm)	Start desorption (Tª)	Main peak (Tª)	Second peak (Tª)	Third peak (Tª)	Hg (ng g^{-1})
LIM 06	5.90	122	173	230	-	11 286
LIM 07	6.70	146	185	239	-	2 918
LIM 09	8.70	144	188	-	-	4 871
LIM 11	11.75	156	183	-	-	1 141
LIM 12	13.75	145	182	228	-	1 518
LIM 16	24.75	150	185	226	-	948
LIM 17	30.50	143	191	-	265	1 460
LIM 20	44.50	-	194*	-	-	259
LIM 21	50.50	155	182	231	-	98
LIM 22	54.50	146	183	-	309	2 967
Mean		145	184	231	280	
Std		10	6	5	31	
Min		122	173	228	265	
Max		156	194	239	309	

Table S2: Phi coefficients (φ) for measuring the association between Hg accumulation rate and the other variables. Hg acc (all samples) indicate the calculation using complete set of samples. Hg acc (removing peaks) indicate the calculation removing the samples corresponding with Hg peaks detected using all samples (previous calculation); n.s. means not significant. Cp1 and Cp2 data are from (Martínez Cortizas et al., 2014)

	Volcanic signal Cp1 (scores)	Reducing conditions Cp2 (scores)	Br/C molar ratio
Hg acc (all samples)	Φ=0.06818042 n.s.	Φ=0.05454679 n.s.	Φ=0.287089 p<0.01
Hg acc (removing peaks)	Φ= 0.003544495 n.s.	Φ= 0.112794613 n.s.	Φ= -0.087649634 n.s.

References Supporting Informacion

Chesworth W., Cortizas A.M., and García-Rodeja E., 2006. Chapter 8 The redox-pH approach to the geochemistry of the Earth's land surface, with application to peatlands. In Developments in Earth Surface Processes, pp. 175–195

Martínez Cortizas A., Rozas Muñiz I., Taboada T., Toro M., Granados I., Giralt S., Pla-Rabés S., Cortizas A.M., Muñiz I.R., Taboada T., et al., 2014. Factors controlling the geochemical composition of Limnopolar Lake sediments (Byers Peninsula, Livingston Island, South Shetland Island, Antarctica) during the last ca. 1600 years. Solid Earth 5, 651–663

USC
UNIVERSIDADE
DE SANTIAGO
DE COMPOSTELA

MANUSCRIPT VII

Industrial-era lead and mercury contamination in southern Greenland implicates US sources

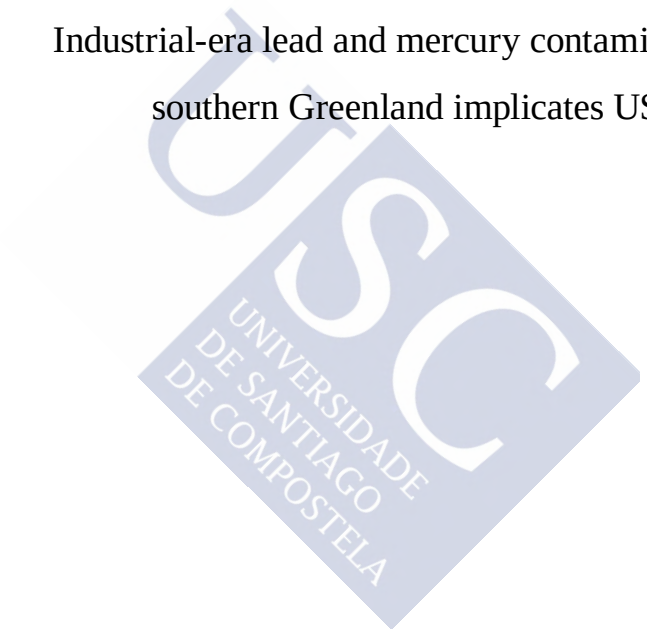

USC
UNIVERSIDADE
DE SANTIAGO
DE COMPOSTELA

Industrial-era lead and mercury contamination in southern Greenland implicates US sources

Marta Pérez-Rodríguez [1]*, Noemí Silva-Sánchez [1], Malin E. Kylander [2,3], Richard Bindler [4], Tim M. Mighall [5], J. Edward Schofield [5], Kevin J. Edwards [5,6,7], Antonio Martínez Cortizas [1]

* corresponding author: M. Pérez-Rodríguez; mperez.rodriguez@usc.es

[1] *Departamento de Edafoloxía e Química Agrícola, Facultade de Bioloxía, Universidade de Santiago de Compostela, Campus Sur, Santiago de Compostela 15782, Spain*
[2] *Department of Geological Sciences, Stockholm University, SE-10691 Stockholm, Sweden*
[3] *The Bolin Centre for Climate Research, Stockholm University, SE-10691 Stockholm, Sweden*
[4] *Department of Ecology and Environmental Sciences, Umeå University, SE-901 87 Umeå, Sweden*
[5] *Department of Geography and Environment, School of Geosciences, University of Aberdeen, Elphinstone Road, Aberdeen AB24 3UF, UK*
[6] *Department of Archaeology, School of Geosciences, University of Aberdeen, Elphinstone Road, Aberdeen AB24 3UF, UK*
[7] *Clare Hall, University of Cambridge, Herschel Road, Cambridge CB3 9AL, UK*

Abstract

To study the long-range transport of atmospheric pollutants from lower latitude industrial areas to the Arctic, we analysed a peat core spanning the last ~700 cal. yr (~AD 1300-2000) from southern Greenland, an area sensitive to atmospheric pollution from North American and Eurasian sources. A previous investigation conducted in the same location recorded atmospheric lead (Pb) pollution after ~1845, with peak values recorded in the 1970s, and concluded that a North America source was most likely. To confirm the origin of the lead, we present new Pb isotope data from Sandhavn, together with a high-resolution record for mercury (Hg) deposition from southern Greenland. The results demonstrate that the mercury accumulation rate has steadily increased since the beginning of the 19th century, with maximum values of 9.3 μg m^{-2} yr^{-1} recorded ~1940. Lead isotopic ratios show two mixing lines: one which represents inputs from local and regional geogenic sources, and another that comprises regional geogenic and pollution sources. Detrending the Pb isotopic ratio record (extracting the effect of the geogenical mixing) has enabled us to reconstruct a detailed chronology of metal pollution. The first sustained decrease in Pb isotope signals begins ~1740-1780 and the lowest values (indicating the highest pollution signature) occurred ~1960-1970. The $^{206}Pb/^{207}Pb$ ratio of excess Pb (measuring 1.222, and reflecting pollution-generated Pb), when compared with the Pb isotopic composition of the Sandhavn peat record since the 19th century and the timing of Pb enrichments, clearly points to the dominance of pollution sources from the USA.

1. Introduction

The Arctic, including Greenland, has experienced significant human impacts through the effects of long-range atmospheric transport of pollutants since ancient times. The oldest evidence of atmospheric metal pollution in Greenland dates back to the Carthaginian and Roman periods, and is attested to by an increase in lead (Pb) concentrations between 680 BC and AD 193 measured in the Summit ice core (Hong et al., 1994). This was accompanied by a change in the Pb isotopic composition that suggested the source of pollution was from Spanish ores (Rosman et al., 1997). Evidence of medieval lead pollution in Greenland, dating to the 15th century AD, has been proposed using inverse modelling on data obtained from Lake Igaliku in southern Greenland (Massa et al., 2015). Before that study had been conducted, no significant changes in the levels of atmospheric metal deposition had been identified prior to the 18th century AD in Greenland (Murozumi et al., 1969; Rosman et al., 1994; Candelone et al., 1995; Bindler et al., 2001a; Michelutti et al., 2009; Silva-Sánchez et al., 2015).

Most investigations into long-range atmospheric pollution are based on the study of the Pb content and isotopic ratios in ice and lake sediments. Records for other metals, such as mercury (Hg), are more scarce, despite their environmental importance. The first studies on Hg accumulation in Greenland using ice cores were performed in the 1970s and intimated a discrepancy in the presence of a pollution signal in the ice layers. Weiss et al. (1971) showed a significant increase in Hg deposition rates in the 1950s and 1960s compared to background values (i.e. for 800 BC) and interpreted this as reflective of human impact upon the environment. Subsequent studies using improved techniques did not report a similar increase in the mercury content in Greenland glacial ice (Carr and Wilkniss, 1973; Appelquist et al., 1978), but rather a heterogenous distribution (Carr and Wilkniss, 1973). Subsequently, the high concentrations of Hg found during these early investigations were attributed to contamination of the ice during sample collection, processing and analysis (Fitzgerald et al., 1998). More recently, an increase in mercury content since the Industrial Revolution has been widely demonstrated in Greenlandic marine and lake sediments as well as ice cores (Asmund and Nielsen, 2000; Bindler et al., 2001b; Lindeberg et al., 2006; Faïn et al., 2009; Dommergue et al., 2016), and the attendant risks for Arctic wildlife and human populations have been highlighted (AMAP, 2011).

The absence of any significant local sources of atmospheric pollution in

Greenland points to a long-distance origin for heavy metals and the identification of these sources, especially for the period from the Industrial Revolution to the present, is the subject of much debate. In addition to the existence of a wide range of probable pollution origins existing simultaneously, such as North America, Europe or Asia, strong control on atmospheric pollutant transport is exerted by seasonal arctic and subarctic air masses (Sturges and Barrie, 1989). The polar dome is not zonally symmetrical and can extend as far south as ~40º N over Eurasia in January, thus making northern Eurasia the major source region for air pollution transport into the Arctic (Law and Stohl, 2007). As such, results from recent snow and atmospheric aerosols collected from the Canadian High Arctic (Sturges and Barrie, 1989; Shotyk et al., 2005a) pointing to a Eurasian source of Pb, are noteworthy. It seems unusual, therefore, that the Pb pollution signal recorded at CF8 (Easter Baffin Island) has a US origin (Michelutti et al., 2009). Due to the high elevation of the ice sheet, Greenland is exposed to atmospheric pollution from distant sources, including North America and even southeast Asia, more strongly so than the rest of the Arctic (Stohl, 2006). In snow samples collected from the Summit Station in central Greenland, the analysis of the Pb isotopic composition of snow layers dating to ~AD 1967-1989 indicated that the USA was a prevalent source of Pb aerosols during the 1970s, decreasing in relative importance into the late 1980s (Rosman et al., 1993, 1994). In the same study (Rosman et al., 1993), and in a subsequent investigation in south Greenland (Rosman et al., 1998), seasonal changes in pollution sources were identified: North American sources were predominant during winter and autumn, while during spring and summer the sources were mainly located in the North Atlantic region, northern and western Europe, and in the Arctic Basin.

The determination of source regions of atmospheric pollutants transported to Greenland is therefore still inconclusive. In contrast to the investigation of ice cores from high elevation, which receive pollutants transported in the high troposphere, studies using peat cores or lake sediments from lower elevations in near-coastal areas from southwestern and southern Greenland (Bindler et al., 2001a, 2001b; Shotyk et al., 2003) do not show consistent enrichments in metal pollution prior to the 18th century, and the identification of sources has also proved to be problematic. In lake sediments from Kangerlussuaq (southwestern Greenland), the application of a simple isotopic mixing model suggested that the Pb record had a mainly West European origin (Bindler et al., 2001a), whereas lake sediments from Pearyland (northern Greenland) demonstrate a Eurasian source (Michelutti et al., 2009). A

peat record from Tasiusaq (southern Greenland) indicates a 20th century North American pollution source (Shotyk et al., 2003), although the complex isotopic composition of the signal warranted a cautious interpretation.

More recently, a multiproxy study conducted at an ombrotrophic mire at Sandhavn, southern Greenland, has provided firm evidence for Pb enrichment beginning ~AD 1845 (Silva-Sánchez et al., 2015). This record is important because the location of the site – near the southern tip of Greenland – places it at the edge of the polar front. The region also experiences a bimodal wind direction with a strong probability of observing both westerly and easterly high speed eolian events (Moore et al., 2008; Renfrew et al., 2008). The chronology of Pb pollution, which was closer in timing to the events of the North American Industrial Revolution (Norton et al., 1997; Kylander et al., 2004) than to that within Europe, together with the presence of long-distance transported pollen (Rousseau et al., 2003) and cryptotephras (Blockley et al., 2015), supports a hypothesis that northeastern North America was the probable source of the Pb (Silva-Sánchez et al., 2015). In this paper we extend the geochemical investigations of this site through the measurement of total Hg along with stable Pb isotopes (Silva-Sánchez et al., 2015). Our aims are (i) to compare the Pb record with that of another likely long-range atmospheric metal pollutant, viz. Hg, and (ii) to use Pb isotope analysis to provide a more precise identification of the source area(s) for atmospheric pollutants arriving in southern Greenland.

2. Material and Methods

2.1 Location and sampling

Sandhavn (59°59.9'N, 44°46.6'W) is located on the coast of Greenland approximately 50 km northwest of Cape Farewell (the most southerly point on the island). The climate is subarctic, with cold winters and cool summers (JJA mean ~6 ºC), moderate annual precipitation (~900 mm per annum), and frequent strong winds. During the late medieval period (~AD 1000-1400) the site was inhabited by the Norse and the Thule Inuit. Today it lies abandoned, 35 km to the northwest of the nearest major settlement (the small town of Nanortalik; ~1,400 inhabitants). Open oceanic heath overlying podzolic soils is characteristic of the local area. The geology comprises gneisses and granites of the Ketilidian mobile belt with basic and intermediate intrusions (Allaart, 1976). The site is described in further detail elsewhere (Raahauge et al., 2002; Golding et al., 2011, 2014; Silva-Sánchez

et al., 2015).

In August 2008, a peat monolith (40 cm) was recovered from a small (~30 m diameter) basin (59° 59.875'N, 44 °46.637'W) adjacent to the former homefields and Norse ruins at Sandhavn (Figure 1). The sediment column was collected in a monolith tin from the open face of a pit dug into the mire. The field stratigraphy comprised a base of saturated coarse grey-brown sands (40-36 cm) overlain by an orange-brown turfa (rootlet) peat containing abundant bryophytes (36-5 cm). The top of the profile (5-0 cm) contained the (living) root mat, which was not analyzed for geochemistry. The monolith was wrapped in polythene and returned to the University of Aberdeen, where it was kept refrigerated (4°C) prior to sub-sampling in the laboratory. In preparation for geochemical analysis, the core was cut into 1 cm thick slices and samples were dried and milled to a fine powder with an agate mill. Only the basal sands and the peat unit (40-5 cm) were analyzed.

2.2 Chronology

An age-depth model for the peat monolith has been developed by Silva-Sanchez et al. (reproduced here as Figure S1). The model uses Clam software to fit a smoothed-spline through a series of calibrated AMS ^{14}C and ^{210}Pb dates. The model applies to only the organic section of the profile (0–36 cm), including the living root mat, with errors varying between ±2 cal. yr (smallest towards the surface) and ±50 cal. yr (greatest towards the base). It indicates that peat formation began ~AD 1270 and was continuous thereafter, with notably slow accumulation rates (0.020-0.025 cm yr^{-1}) occurring during ~AD 1400-1800 – a period encapsulating much of the LIA – followed by accelerated peat growth during warmer conditions in the 19th and particularly 20th centuries. The calendar dates cited in this paper for events at Sandhavn are 'best' estimates from the model, and all dates referred to are in years AD.

Small uncertainties in the chronological model for our site could change the precise timing of the pollution rise or downturn. Therefore in addition to the Clam model, a 'proxy-ghost' function (Blaauw and Christen, 2013) Bacon.R) will be use to explore the possible changes in the timing due to the chronological uncertainties. This function allows plot the interest variables against calendar time while taking into account chronological uncertainties.

2.3 Sample preparation and analysis

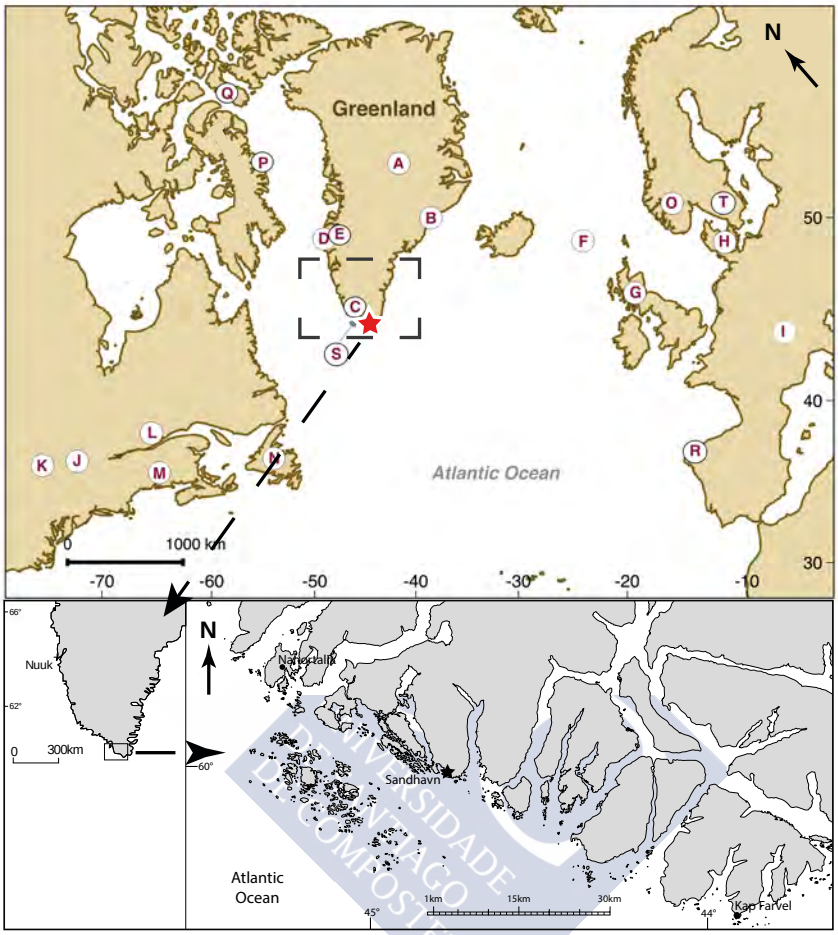

Figure 1. Map showing the location of Sandhavn (red star) and other places mentioned in the text and related literature: (A) Summit ice cores (Rosman et al., 1993, 1994, 1997); (B) rock samples from Kangerdlugssuaq (Taylor et al., 1992) (C) peat record in Tasiusaq, Greenland (Shotyk et al., 2003; Massa et al., 2015); (D) Akilia rocks, Greenland (Whitehouse et al., 2005); (E) lake sediments, Lake 53 and Lake 16, SW Greenland (Bindler et al., 2001a, 2001b); (F) peat record from the Faroe Islands (Shotyk et al., 2005b); (G) Sphagnum moss samples from Scotland (Farmer et al., 2002); (H) peat record from Denmark (Shotyk et al., 2003); (I) peat core from Schöpfenwaldmoor, Switzerland (Weiss et al., 1999); (J and K) lake sediments from Lake Ontario and Lake Erie (Graney et al., 1995); (L and N) aerosols samples from Chicoutimi and Newfoundland, Canada (Bollhöfer and Rosman, 2001); (M) peat record from Caribou bog, US (Roos-Barraclough et al., 2006); (O) peat records, Norway (Dunlap et al., 1999); (P) lake sediments, Lake CF8 Baffin Island (Michelutti et al., 2009); (Q) snow samples from Devon Island (Shotyk et al., 2005a); (R) peat records from NW Spain (Martínez Cortizas et al., 2012); (S) rock samples from south Greenland (Kalsbeek and Taylor, 1985; Andersen, 1997; Colville et al., 2011); (T) peat record from southern Sweden (Bindler, 2003).

Samples were dried at room temperature (25 ºC) until reaching a constant weight and then analysed for total Hg and stable Pb isotopes. The analyses were done on the same samples as those from the previous work at the same site (Silva-Sánchez et al., 2015).

2.3.1 Mercury analysis

The analyses for total Hg were done using a Milestone DMA-80 analyser. As a control, measurements were replicated for one in every five samples, and a standard reference material of the moss Pleurozium schreberi (Steinnes et al., 1997), M3, was run with each set of samples. The quantification limit was 1.7 ng g^{-1} and mean recovery was 97 ± 1.2%. The mean difference between sample replicates was 3.4% (range 0.4-16.1%).

2.3.2 Lead isotope analyses

Peat samples were ashed at 450°C overnight to remove any organic matter. The remaining residue was digested using an acid mixture of HNO3 and HF contained within closed digestion vessels in a MARS-Xpress microwave system (CEM, Mattheus, USA). A ratio of 0.16 ml HF: 50 mg ash was determined to be the correct mixture required to digest the samples (Kylander et al., 2004). After digestion, the samples were dried and Pb was isolated by ion exchange chromatography (Weiss et al., 2004).

Isotopic measurements were determined using an IsoProbe Multi Collector-Inductively Coupled Plasma-Mass Spectrometer (MC-ICP-MS) (Thermo, Manchester, UK) at the Naturhistorika Riksmuseet, Sweden. The instrument was equipped with a CETAC desolvator and a T1H concentric nebuliser for introducing the sample. Seven independently adjustable Faraday cups in static mode were used for isotope ratio measurements. Averaged acid blank intensities were subtracted from raw intensities to correct for Faraday cup offset and instrumental and solvent blanks. Corrections for Hg interference on 204Pb were typically ≤0.1%. Instrumental mass bias was corrected by spiking samples with NIST-SRM 977 Tl to Pb/Tl ratio of 2:1 and using optimised Tl ratios and the exponential law (see Weiss et al. [2004] for details).

Procedural blanks were <1% of the total Pb in the samples. The reproducibility of Pb isotope measurements based on repeat measurements (n=23) of NIST-SRM 981 Pb acquired during the week long measurement session at the 95%

confidence level (2σ) were (in μg g^{-1}): 299 for $^{206}Pb/^{204}Pb$, 388 for $^{207}Pb/^{204}Pb$, 543 for $^{208}Pb/^{204}Pb$ and 230 for $^{206}Pb/^{207}Pb$. Accuracy was determined based on repeat measurements of NIST-SRM 981 Pb evaluated against values published by Galer and Abouchami (1998). Accuracies for individual Pb isotopes expressed relative to the mean were (in μg g^{-1}): 50 for $^{206}Pb/^{204}Pb$, 462 for $^{207}Pb/^{204}Pb$, 210 for $^{208}Pb/^{204}Pb$ and 509 for $^{206}Pb/^{207}Pb$.

To determine the timing of the changes in Pb isotopic composition and to establish the start of significant atmospheric Pb pollution in the Sandhavn peat record more precisely, we have calculated the Pb isotope residuals between the trajectory of the unpolluted trend and the observed values identified as pollution. The equation is expressed for $^{206}Pb/^{207}Pb$ and $^{206}Pb/^{208}Pb$ as:

$$Residual_{\frac{206}{207}vs\frac{206}{208}} = {}^{206}Pb/^{208}Pb_{sample} - \left(m \times {}^{206}Pb/^{207}Pb_{sample} + n\right)$$

Where m and n are the slope and the y-intercept (respectively) of the linear regression of $^{206}Pb/^{208}Pb$ to $^{206}Pb/^{207}Pb$ of unpolluted samples. Residuals were normalized to the range of variation between the two trends and standardized. The mean of the residuals and the standard deviation were calculated. In addition, we estimated the mean isotopic composition of the excess $^{206}Pb/^{207}Pb$ contribution for the Sandhavn samples (i.e. pollution Pb) after Farmer et al. (1996).

3. Results and Discussion

3.1 Mercury

Mercury concentrations varied from 9 to 28 ng g^{-1} in the basal sandy sediment (40–36 cm) and from 47 to 297 ng g^{-1} in the peat (<36 cm). From 36 cm (the base of the peat) to 14.5 cm, concentrations rise (from 60 to 297 ng g^{-1}) with an abrupt increase from 20.5 cm, peaking at 14.5 cm (Figure S2); from 14.5 to 5.5 cm, values decrease with a slight upturn at 7.5 cm (140 ng g^{-1}). Organically bound elements such as Hg can be enriched by the effect of peat mineralization (Biester et al., 2003; Martínez Cortizas et al., 2007); however, no significant correlations with peat decomposition proxies (Silva-Sánchez et al., 2015) were found. Although peat growth and carbon (C) accumulation rates appear to have been lower during the inferred Spörer and Maunder solar minima, Hg concentrations were not affected.

To account for the effects of changes in peat density and accumulation rate on geochemical concentrations, and to enable direct comparison of figures with previous studies, Hg accumulation rates are reported. Background accumulation rates for Hg recorded in the Sandhavn core (Figure 2) occur from the start of peat accumulation (~AD 1270, 35.5 cm) until ~1800 (23.5 cm), with values through this period lower than 1.0 μg m^{-2} yr^{-1}. These low values are similar to those (< 3.0 μg m^{-2} yr^{-1}) reported for other pre-industrial peat and lake sediments records (Bindler et al., 2001a, 2001b; Shotyk et al., 2003) from south and southwestern Greenland. A gradual increase during the industrial period occurs from ~1800 to 1880 (23.5 – 20.5 cm) when Hg accumulation rates change significantly, reaching a maximum (9.3 μg m^{-2} yr^{-1}) by ~1940 (16.5 cm) (Figure 2). Thereafter Hg accumulation rates decline, corresponding to the general pattern for this element observed elsewhere in the Northern Hemisphere (Norton et al., 1997; Bindler et al., 2001b; Shotyk et al., 2003; Martínez Cortizas et al., 2012). The continuous decrease is interrupted at ~1960 (14.5 cm), with an accumulation rate of 6.7 μg m^{-2} yr^{-1}. A secondary peak (3.8 μg m^{-2} yr^{-1}) is evident around 1987 (7.5 cm) and appears to coincide with the enrichment in Hg measured in ice and snow samples from the high Arctic during the late 1980s and 1990s (Zheng, 2015).

The maximum Hg accumulation rate in the Sandhavn core (6-10 μg m^{-2} yr^{-1}) is similar to that recorded at Lakes 53 and 70 (Bindler et al., 2001b) located ~850 km north of Kangerlussuaq Fjord. In contrast, the maximum Hg accumulation rate reported from the only other Greenland peatland core study published to date (Shotyk et al., 2003) is 16–17 times higher (164 μg m^{-2} yr^{-1}) than that at Sandhavn or the aforementioned lakes. Similarly, maxima from European and North American records that lie in closer proximity to major emission sources are all notably higher, for example: Dumme Mosse mire in Sweden (~25 μg m^{-2} yr^{-1}) (Bindler, 2003); four ombrotrophic bogs from Scotland (51–85 μg m^{-2} yr^{-1}) (Farmer et al., 2009); Chao de Lamoso bog in NW Spain (27–60 μg m^{-2} yr^{-1}) (Martínez Cortizas et al., 2012); Arlberg bog (Minnesota, US; 38 ± 11 μg m^{-2} yr^{-1}) (Benoit et al., 1994); and Caribou Bog (Maine, US; 32 μg m^{-2} yr^{-1}) (Roos-Barraclough et al., 2006).

The low Hg accumulation rates observed at Sandhavn may be explained in two ways. Firstly, Sandhavn is located at great distance from any major sources of pollution emanating from North America and Europe. Secondly, rates of peat accumulation, and the decomposition of organic matter at Sandhavn, were limited

in the period ~AD 1400-1800 (Silva-Sánchez et al., 2015) – encompassing much of the Little Ice Age (LIA) – at least when compared with peatlands from mid-latitudes. Consequently, the latter may have been more affected by enrichment in Hg, most likely driven by intense peat mineralisation (Martínez Cortizas et al., 2007). Both reasons point towards the suitability of Sandhavn, and probably other similarly remote cold high latitude environments, as sensitive archives for long-distance transported pollution given that the effect of peat post-depositional processes (i.e. organic matter decomposition) is reduced in these locations.

3.2 Lead

Although the ratios involving the four stable Pb isotopes (^{204}Pb, ^{206}Pb, ^{207}Pb and ^{208}Pb) were determined and used to construct three-isotope plots (Figure S2 and Figure S3), the identification of potential sources is based on the ^{206}Pb/^{207}Pb and ^{206}Pb/^{208}Pb ratios because these are the most commonly reported in Pb pollution studies. As such there are more end members defined for comparison.

The depth profile of ^{206}Pb/^{207}Pb may be divided into three sections separated by abrupt transitions. From 40-36 cm values are low (1.167 ± 0.074), with a peak (1.298) at 37.5 cm. Above the sand-peat contact the ratio increases with high values (1.307 ± 0.029) recorded between 33.5-21.5 cm. The ratio then decreases, becoming near-constant (1.187± 0.009) in the upper 21 cm.

3.3 Chronology of Hg and Pb pollution in southernmost Greenland

Lead does not share any significant covariation with the lithogenic elements (e.g. Ti, Zr) in the Sandhavn core (Silva-Sánchez et al., 2015). To remove contributions of geogenic Pb from the peat record and isolate the atmospheric Pb pollution signal, values were normalized against titanium (Ti), and Pb/Ti ratios were used as a proxy for atmospheric Pb pollution. Although the patterns of Pb concentrations and Pb/Ti ratios are similar, some minor differences were detected, mainly between ~1900 and 1940, when some of the Pb seems to be linked with increased soil erosion caused by the return of sheep farming to the region in the early 20th century (Silva-Sánchez et al., 2015). Pb/Ti ratios (Figure 2) were low and constant until ~1845; from then onwards, they increased gradually and were more pronounced after ~1940, peaking by the end of the 1970s.

The start of Hg pollution in the Sandhavn record precedes the increase of

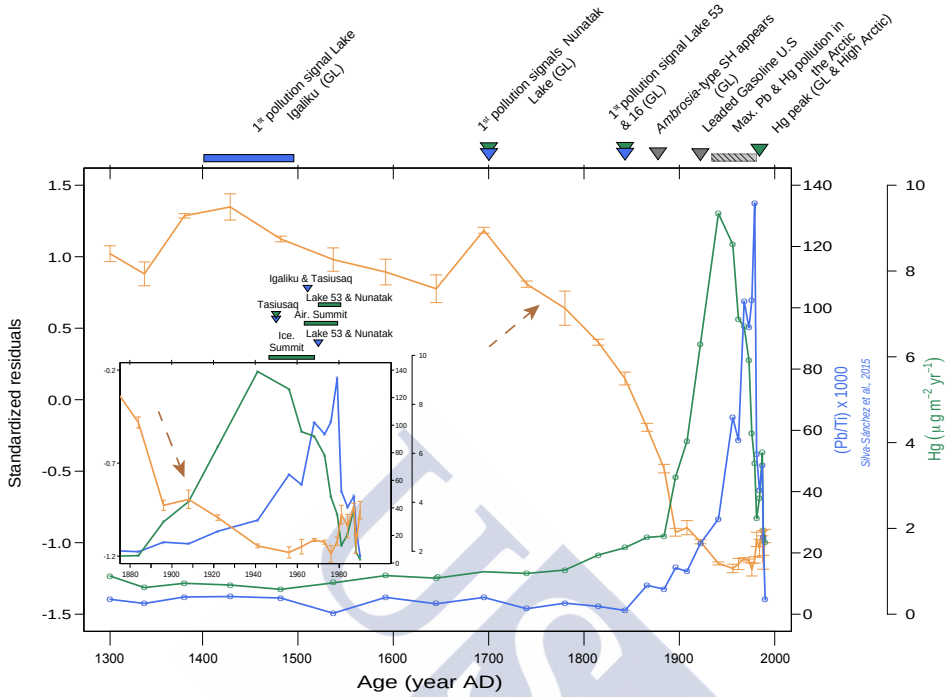

Figure 2. Hg accumulation rates (green line), Pb/Ti (blue line) (Silva-Sánchez et al., 2015) and an average of Pb isotope standardized residuals (orange line) through the peat at Sandhavn (~AD 1300-2000). Error bars are included with the standard deviation. The timings of important events mentioned in the text are indicated at the top of the diagram. (Inset) Detailed record showing the period after ~1880. Maximum Pb and Hg concentrations and accumulation rates from other Greenland records, mentioned in the text, are indicated at the top of the inset.

atmospheric Pb (as implied by Pb/Ti ratios) by ~65 years. Mercury pollution begins with the persistent upturn in the curve just before 1800, while discernible Pb pollution begins with the rise in Pb/Ti at around 1850. Both trace metals increase significantly by the end of the ~1800s and reach their peak values by ~1940 and ~1980, respectively. This is in agreement with other pollution records from Greenland (Boutron et al., 1998), North America (Roos-Barraclough et al., 2006; Beal et al., 2015), and Europe (Farmer et al., 2009; Martínez Cortizas et al., 2012). Even allowing for differences in the type, location and resolution of the records, the peak in Hg pollution at Sandhavn, dated ~1940, compares favorably with snow data (Boutron et al., 1998) and a recent model based on ice data (Faïn et al., 2009) from Summit Station. These maxima are coeval with the peak in the worldwide production of mercury (U.S Geological Survey, 2014), an indirect indicator of anthropogenic Hg emissions to the atmosphere. The slow reduction in

Hg pollution during 1962–1968 agrees with an increase in global Hg consumption in commercial products like paint, batteries and in chlor-alkali plants (Horowitz et al., 2014). However, this does not rule out the Hg contribution from coal burning after 1920 and especially after 1950 (Streets et al., 2011). The subsequent decline (after 1970) and peak around 1990 has been related to Hg consumption by chlor-alkali plants (Horowitz et al., 2014). A recent reconstruction (modelled) of atmospheric gaseous elemental mercury in the Arctic shows a slightly different scenario; an increase since the 1950s peaking in the late 1960s and early 1970s, and a return to low concentrations around 1995-2000 (Dommergue et al., 2016). The difference in our results compared to those generated by Dommergue et al. (2016) may be due to the core location for the latter being ~2000 km further north than Sandhavn, and elevated (77°N and 2452 m asl), which might result in different source areas for Hg.

Figure S4 shows Hg accumulation and Pb/Ti vs. calendar time using the "proxy-ghost" function (Blaauw and Christen, 2013). Although there is some chronological uncertainty around ~ 1800, there are no significant changes in the trend / time of the variables studied using the previously published Clam model (Silva-Sánchez et al., 2015).

As indicated under Materials and Methods, we calculated the (standardized) Pb isotope residuals between the trajectory of the unpolluted trend (geological mixing line, Figure S3) and the observed values over the past two centuries (pollution mixing line, Figure S3). The residuals can be used to determine the degree of departure from the geogenical trend; that is, they allow estimation of the effects of pollution sources. Figure 2 shows the chronology of the standardized Pb isotope ratio residuals, Pb/Ti ratios (Silva-Sánchez et al., 2015), and Hg accumulation rates. The standardized Pb isotopes residuals show two main periods of decreasing values. The first main decrease in the isotope residuals occurs from ~1740–1780 (25.5–24.5 cm) until ~1885 (20.5 cm). The start of this decrease is coeval with the main change in Pb isotope ratios in the Nunatak lake sediment record (southwestern Greenland) (Bindler et al., 2001a). This date is slightly earlier than that shown by the increase in Hg and Pb/Ti but is consistent with other studies that suggest modern metal pollution in Greenland had begun prior to the 19th century (Bindler et al., 2001b; Massa et al., 2015). Although this decline seems to start at ~1700 (26.5 cm), the values are not systematically lower than the previous period until 1740-1780. A second, but less pronounced, decrease

in the residuals starts ~1908 (18.5 cm), and this is simultaneous with the sharp increase in metal pollution shown in the Sandhavn core and in other Greenland records (Bindler et al., 2001a, 2001b). Finally, the lowest residual values (i.e. the highest Pb pollution signal indicated by the isotopes) are dated to the 1940s and 1970s, and agree with data obtained from analysis of the Summit ice cores (Rosman et al., 1994; Faïn et al., 2009). The fall in gasoline Pb consumption in the USA since 1970, declining ~80% by the early 1980s (Nichols, 1997), probably contributed to the pronounced increase in isotopic residual values from ~1979 (Figure 2 inset). A slight drop in isotopic residuals in ~1988 is also recorded in ice and snow samples from the high Arctic (Shotyk et al., 2005a), where authors attribute the modern inputs of anthropogenic Pb to other industrial sources. The absence of samples more modern than 1990 (the last sample) in the Sandhavn core, prevents an examination of the most recent trends. The close agreement between the isotopic residuals chronology and data from other archives indicates that it is an appropriate and precise method to determine changes in the chronology of the Pb isotopic signature.

3.4 Sourcing

Three isotope plots are used to examine changes in Pb sources and to assign possible mixing end members (Figure S3). There are three end members that correspond to the main sections identified in the $^{206}Pb/^{207}Pb$ record (Figure S2), and the data suggest two mixing lines. The first (geological mixing line, Figure S3) involves the basal sand (low radiogenic signature) and peat samples below 22 cm (the most radiogenic values). The second (pollution line, Figure S3) involves peat samples from the upper 22 cm.

In Figure 3, the isotopic composition of the Sandhavn samples is compared with other published isotopic data from Greenland (Kalsbeek and Taylor, 1985; Taylor et al., 1992; Andersen, 1997; Rosman et al., 1997; Shotyk et al., 2003; Whitehouse et al., 2005; Colville et al., 2011), North America (Graney et al., 1995; Bollhöfer and Rosman, 2001) and Europe (Dunlap et al., 1999; Weiss et al., 1999; Farmer et al., 2002; Shotyk et al., 2005b). Samples from the sandy basal sediments of the Sandhavn core have a fairly uniform isotopic composition ($^{206}Pb/^{207}Pb$ 1.118-1.143 and $^{206}Pb/^{208}Pb$ 0.479-0.488; Figures 3 and S3), which is similar to that found in rocks from the Archaean craton in southwest and southeast Greenland (Taylor et al., 1992; Whitehouse et al., 2005) (Figure 3). There is one sample (37.5

cm) with an isotopic signature closer to a second (potential) source (1.298 and 0.53, $^{206}Pb/^{207}Pb$ and $^{206}Pb/^{208}Pb$ ratios respectively). Pre-industrial peat samples (~AD 1300 to the late ~1800s; Figure 3) have a more radiogenic composition (206Pb/207Pb 1.312 ± 0.028, $^{206}Pb/^{208}Pb$ 0.536 ± 0.009) than most of the samples from the base of the core. They fall close to the geogenical mixing line, between the Sandhavn basal sands (derived from the local geological material) and rocks of the Ketilidian Mobile Belt of southern Greenland (Kalsbeek and Taylor, 1985; Andersen, 1997; Colville et al., 2011), which could generate a regional geological dust signal. Values assigned to geogenic Pb (peat residue – geogenic lead; Figure 3) in a minerogenic peat record from Tasiusaq (southern Greenland) (Shotyk et al., 2003), located 150 km northwest of Sandhavn, are also on the same geogenical mixing line and support the interpretation of a regional southern Greenland Pb source.

Peat samples dating to the Industrial period (from the end of the 1800s forwards) define a second (pollution) mixing line that ranges from the regional geological signal to values typical of pollution sources ($^{206}Pb/^{207}Pb$ 1.178 and $^{206}Pb/^{208}Pb$ 0.483, lower radiogenic values). Data from the peat core from Tasiusaq (southern Greenland) (Shotyk et al., 2003) show a similar transition between regional pre-industrial values and the pollution signal (leachate – atmospheric Pb; Figure 3). At Sandhavn, the low isotopic ratios are similar to the anthropogenic signal found in lake records from the USA for the period 1972-1978 (Graney et al., 1995) (e.g. Lake Erie sediment – anthropogenic signal; Figure 3) and show the same trend as that seen in Pb in atmospheric data collected in Canada during the mid- to late 1990s from eastern Canada, namely, Newfoundland, Labrador, and Chicoutimi, Quebec, respectively (Bollhöfer and Rosman, 2001) (Air – Newfoundland and Chicoutimi, 1994-1999; Figure 3).

There is a large difference in the isotopic signature between Pb ores used in the USA and Canada. Coal in the USA used for industrial purposes from 1900 to 1920 was extracted from deposits in West Virginia and Pennsylvania and displays $^{206}Pb/^{207}Pb$ values in the range 1.18-1.21(Graney et al., 1995). In the 1960s, the highly radiogenic Missouri ores with a $^{206}Pb/^{207}Pb$ ratio of ~1.28-1.32 dominated industrial use (Shirahata et al., 1980) and the Pb used in gasoline in the USA was taken from the similarly radiogenic Mississippi Valley type ores ($^{206}Pb/^{207}Pb$, >1.22) (Wu and Boyle, 1997). In contrast, the most important Pb ores used by industry in eastern Canada (Quebec, Ontario and New Brunswick) are less radiogenic, with

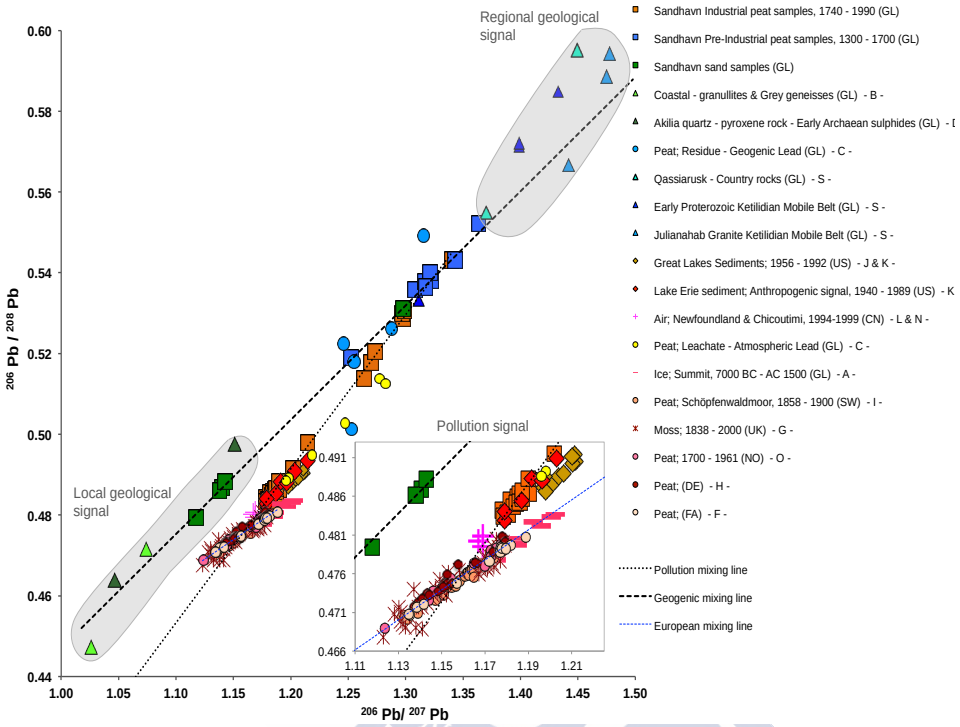

Figure 3. Scatterplots comparing the lead isotopic composition of the samples from Sandhavn against data from Greenland, North America and West Europe. The type of sample and the sampling location is indicated in the legend. (CN: Canada; DE: Denmark; FA: Faroe Island; GL: Greenland; NO: Norway; SW: Sweden; SW: Switzerland; UK: United Kingdom; US: United States). Lettering (A-S) corresponds with the locations marked on Figure 1. References: A (Rosman et al., 1997); B (Taylor et al., 1992); C (Shotyk et al., 2003); D (Whitehouse et al., 2005); G (Farmer et al., 2002); I (Weiss et al., 1999); J and K (Graney et al., 1995); L and N (Bollhöfer and Rosman, 2001); M (Shotyk et al., 2005b); O (Dunlap et al., 1999); S (Kalsbeek and Taylor, 1985; Andersen, 1997; Colville et al., 2011).

$^{206}Pb/^{207}Pb$ ratios of 1.15-1.16 (Blais, 1996). The $^{206}Pb/^{207}Pb$ signature of gasoline in eastern Canada was 1.16 during the 1980s. Less radiogenic Pb has been found in British Columbia in western Canada ($^{206}Pb/^{207}Pb$ 1.05) (Sturges and Barrie, 1987). Nonetheless, lake sediments from northeastern Canada showed that US contributions to the total Pb burden in surficial lake sediments are often in excess of 50%, with an increasingly Canadian Pb industrial isotopic signal further north (Blais, 1996).

At Sandhavn, the Industrial era peat samples (inset Figure 3) are similar to the

anthropogenic signal extracted from Lake Erie in sediments dating from 1940 to 1989 and the pollution mixing trend shown by air samples collected in eastern Canada (Lake Erie sediment and Newfoundland and Chicoutimi, respectively, inset Figure 3). Taken together, these data indicate that metal pollution at Sandhavn was mainly influenced by sources from the USA, given that the Pb isotopic signatures also differ from those of European sources (European mixing line, inset Figure 3).

As mentioned, we estimated the mean isotopic composition of the excess $^{206}Pb/^{207}Pb$ contribution for the Sandhavn samples (Farmer et al., 1996). As background values (1.321 $^{206}Pb/^{207}Pb$ ratio, 0.96 μg g^{-1} Pb concentration) we used those in Pre-industrial peat samples (~1500 to 1650), and calculated excess Pb values for samples dating to the period after ~1800 (Industrial era). The average isotopic value of the excess Pb was 1.193 (±0.074), which is well above the numerical levels determined for lakes in southwestern Greenland (1.145) (Bindler et al., 2001a) and aerosols from the high Canadian Arctic (~1.160) (France and Blais, 1998), but closer to the upper limit of European signals (~1.14 – 1.20, reported in [Bindler et al., 2001b]) and the lower limit of the isotope field for pollution sourced in the US (1.19 – 1.25) (Shirahata et al., 1980; Sturges et al., 1993; Rosman et al., 1994). Taking into account that the isotopes residuals' chronology suggests that Pb pollution started ~1740–1780, the recalculated excess $^{206}Pb/^{207}Pb$ contribution including these samples (1.222 ± 0.114) again points to a major influence of US Pb pollution in southernmost Greenland.

We do not have direct evidence for the origin of Hg, but according to the Pb isotope results we would expect the main source for Hg contamination to be also from the USA. However, Hg has a complex behaviour in the environment. Its relatively long residence time in the atmosphere (1 year) favours long-range transport and homogenisation at a hemispheric scale, making it more difficult to determine its precise origin. More than a decade of research demonstrates that Hg isotopes could be used to trace sources, as well as biogeochemical cycling and reactions involving Hg (Blum et al., 2014). The combined analyses of Pb and Hg (both concentration and isotopic composition) may provide the means to assist further in the identification of such pollution sources in northern latitudes.

4. Conclusions

The Sandhavn peat has provided a unique record of environmental changes in south Greenland during the last ~700 years, especially those related to long-range atmospheric lead and mercury pollution. Mercury accumulation rates suggest that the first pollution signal occurred at the beginning of the 19th century, ~65 years before that indicated by the atmospheric Pb pollution record from the same site (Silva-Sánchez et al., 2015). The maximum deposition of atmospheric Pb and Hg pollution occurred between ~1940 and the 1970s (Hg and Pb, respectively).

The Pb isotopic data provided more insightful information about the sources of lead in the Sandhavn peat. A three isotopes plot and an extensive literature review has allowed us to determine three Pb isotopic sources, producing two mixing lines: one representing inputs from local and regional geogenic sources, and the other comprising regional geogenic and pollution sources. The novel approach of detrending the Pb isotopic ratio record (i.e. extracting the effect of the geogenical mixing) has enabled a detailed chronology of metal pollution to be reconstructed. This shows the onset of lead pollution at Sandhavn beginning during the interval ~1740-1780. According to the detrended Pb isotope record, the maximum phase of pollution occurred between ~1960 and 1970. The $^{206}Pb/^{207}Pb$ ratio of the excess Pb (measuring 1.222 and reflecting the anthropogenically-generated Pb), when considered alongside the isotopic composition of Pb since the 19th century and the timing of lead enrichments, points clearly to a dominance of pollution sources from the USA. Despite the different timing for Hg and Pb maxima, both trends show a solid decreased during the end of the 20th century, only interrupted by a slight increase in pollution signals occurred at ~1987. This supports the established decreased in Hg and Pb pollution in North America.

5. Acknowledgments

We would like to thank Jesús R. Aboal (Universidade de Santiago de Compostela) and Kjell Billström (Naturhistoriska Riksmuseet) for access to the laboratory facilities; Antonio Rodríguez López helped with laboratory work. This research was done under the framework of the projects CGL2010-20672 (Plan Nacional I+D+i, Spanish Ministerio de Economía y Competitividad), R2014/001 and GPC2014-009 (Dirección Xeral I+D, Xunta de Galicia). The authors gratefully acknowledge the financial support of the UK Leverhulme Trust Footprints on the Edge of Thule programme award for core collection and associated environmental

research.

6. References

Allaart J.H., 1976. Ketilidian mobile belt in South Greenland. In Geology of Greenland, A. Escher, and W. Stuart-Watt, eds. (Geological Survey of Greenland Copenhagen), pp. 120–151

AMAP A., 2011. Assessment 2011: mercury in the Arctic (Oslao, Norway)

Andersen T., 1997. Age and petrogenesis of the Qassiarsuk carbonatite-alkaline silicate volcanic complex in the Gardar tift, South Greenland. Mineralogical Magazine 61, 499–513

Appelquist H., Ottar Jensen K., Sevel T., and Hammer C., 1978. Mercury in the Greenland ice sheet. Nature 273, 657–659

Asmund G. and Nielsen S., 2000. Mercury in dated Greenland marine sediments. The Science of The Total Environment 245, 61–72

Beal S., Osterberg E.C., Zdanowicz C., and Fisher D., 2015. An ice core perspective on mercury pollution during the past 600 years. Environmental Science and Technology 49, 7641–7647

Benoit J.M., Fitzgerald W.F., and Damman A.W.H., 1994. Historical atmospheric mercury deposition in the mid-continental US as recorded in an ombrotrophic peat bog. Mercury Pollution: Integration and Synthesis 187–202

Biester H., Martinez-Cortizas A., Birkenstock S., and Kilian R., 2003. Effect of Peat Decomposition and Mass Loss on Historic Mercury Records in Peat Bogs from Patagonia. Environmental Science and Technology 37, 32–39

Bindler R., 2003. Estimating the natural background atmospheric deposition rate of mercury utilizing ombrotrophic bogs in Southern Sweden. Environmental Science and Technology 37, 40–46

Bindler R., Renberg I., John Anderson N., Appleby P.G., Emteryd O., and Boyle J., 2001a. Pb isotope ratios of lake sediments in West Greenland: inferences on pollution sources. Atmospheric Environment 35, 4675–4685

Bindler R., Renberg I., Appleby P.G., Anderson N.J., and Rose N.L., 2001b. Mercury Accumulation Rates and Spatial Patterns in Lake Sediments from West Greenland: A Coast to Ice Margin Transect. Environmental Science and Technology 35, 1736–1741

Blaauw M. and Christen J.A., 2013. Bacon Manual e V2. 2. In Blaauw, M., Wohlfarth, B., Christen, JA, Ampel, L., Veres, D., Hughen, KA, Preusser, F., et al.(2010),— Were Last Glacial Climate Events Simultaneous between Greenland and France-, pp. 387–394

Blais J.M., 1996. Using Isotopic Tracers in Lake Sediments To Assess Atmospheric Transport of Lead in Eastern Canada. Water, Air, and Soil Pollution 92, 329–342

Blockley S.P.E., Edwards K.J., Schofield J.E., Pyne-O'Donnell S.D.F., Jensen B.J.L., Matthews I.P., Cook G.T., Wallace K.L., and Froese D., 2015. First evidence of cryptotephra in palaeoenvironmental records associated with Norse occupation sites in Greenland. Quaternary Geochronology 27, 145–157

Blum J.D., Sherman L.S., and Johnson M.W., 2014. Mercury Isotopes in Earth and

Environmental Sciences. Annual Review of Earth and Planetary Sciences 42, 249–269

Bollhöfer A. and Rosman K.J.R., 2001. Isotopic source signatures for atmospheric lead: The Northern Hemisphere. Geochimica et Cosmochimica Acta 65, 1727–1740

Boutron C.F., Vandal G.M., Fitzgerald W.F., and Ferrari P., 1998. A forty year record of mercury in central Greenland snow in snow deposited Greenland reported from previous studies of Greenland snow by major Combined probably plagued by major contamination problems during estimated contributions from natural Hg sources. Goephysical Research Letters 25, 3315–3318

Candelone J.-P., Hong S., Pellone C., and Boutron C.F., 1995. Post-Industrial Revolution changes in large-scale atmospheric pollution of the northern hemisphere by heavy metals as documented in central Greenland snow and ice. Journal of Geophysical Research 100, 16605

Carr R.A. and Wilkniss P.E., 1973. Mercury in the Greenland Ice Sheet: Further Data. Science 181, 843–844

Colville E.J., Carlson A.E., Beard B.L., Hatfield R.G., Stoner J.S., Reyes A. V, and Ullman D.J., 2011. Sr-Nd-Pb isotope evidence for ice-sheet presence on southern Greenland during the Last Interglacial. Science 333, 620–623

Dommergue A., Martinerie P., Courteaud J., Witrant E., and Etheridge D., 2016. A new reconstruction of atmospheric gaseous elemental mercury trend over the last 60 years from Greenland firn records. Atmospheric Environment 136, 156–164

Dunlap C.E., Steinnes E., and Flegal A.R., 1999. A synthesis of lead isotopes in two millennia of European air. Earth and Planetary Science Letters 167, 81–88

Faïn X., Ferrari C.P., Dommergue A., Albert M.R., Battle M., Severinghaus J., Arnaud L., Barnola J.-M., Cairns W., Barbante C., et al., 2009. Polar firn air reveals large-scale impact of anthropogenic mercury emissions during the 1970s. Proceedings of the National Academy of Sciences of the United States of America 106, 16114–16119

Farmer J.G., Eades L.J., Mackenzie A.B., Kirika A., and Bailey-Watts T.E., 1996. Stable Lead Isotope Record of Lead Pollution in Loch Lomond Sediments since 1630 A.D. Environmental Science and Technology 30, 3080–3083

Farmer J.G., Eades L.J., Atkins H., and Chamberlain D.F., 2002. Historical trends in the lead isotopic composition of archival Sphagnum mosses from Scotland (1838-2000). Environmental Science and Technology 36, 152–157

Farmer J.G., Anderson P., Cloy J.M., Graham M.C., MacKenzie A.B., and Cook G.T., 2009. Historical accumulation rates of mercury in four Scottish ombrotrophic peat bogs over the past 2000 years. Science of The Total Environment 407, 5578–5588

Fitzgerald W.F., Engstrom D.R., Mason R.P., and Nater E.A., 1998. The Case for Atmospheric Mercury Contamination in Remote Areas. Environmental Science and Technology 32, 1–7

France R.L. and Blais J.M., 1998. Lead concentrations and stable isotopic evidence for transpolar contamination of plants in the Canadian High Arctic. Ambio 27, 506–508

Galer S.J.G. and Abouchami W., 1998. Practical application of lead triple spiking

for correction of instrumental mass discrimination. Mineral. Mag. A 62, 491–492

Golding K.A., Simpson I.A., Schofield J.E., and Edwards K.J., 2011. Norse–Inuit interaction and landscape change in southern Greenland? A geochronological, Pedological, and Palynological investigation. Geoarchaeology 26, 315–345

Golding K.A., Simpson I.A., Wilson C.A., Lowe E.C., Schofield J.E., and Edwards K.J., 2014. Europeanization of Sub-Arctic Environments: Perspectives from Norse Greenland's Outer Fjords. Human Ecology 43, 61–77

Graney J.R., Halliday A., N., Keeler G.J., Nriagu J.O., Robbins J.A., and Norton S.A., 1995. Isotopic record of lead pollution in lake sediments from the northeastern United States. Geochimica et Cosmochimica Acta 59, 1715–1728

Hong S., Candelone J.-P., Patterson C.C., and Boutron C.F., 1994. Greenland ice evidence of hemispheric lead pollution two millennia ago by Greek and Roman civilizations. Science 265, 1841–1843

Horowitz H.M., Jacob D.J., Amos H.M., Streets D.G., and Sunderland E.M., 2014. Historical mercury releases from commercial products: Global environmental implications. Environmental Science and Technology 48, 10242–10250

Kalsbeek F. and Taylor P.N., 1985. Isotopic and chemical variation in granites across a Proterozoic continental margin—the Ketilidian mobile belt of South Greenland. Earth and Planetary Science Letters 73, 65–80

Kylander M.E., Weiss D.J., Jeffries T., and Coles B.J., 2004. Sample preparation procedures for accurate and precise isotope analysis of Pb in peat by multiple collector (MC)-ICP-MS. Journal of Analytical Atomic Spectrometry 19, 1275–1277

Law K.S. and Stohl A., 2007. Arctic Air Pollution: Origins and Impacts. Science 315, 1537–1540

Lindeberg C., Bindler R., Renberg I., Emteryd O., Karlsson E., and Anderson N.J., 2006. Natural Fluctuations of Mercury and Lead in Greenland Lake Sediments. Environmental Science and Technology 40, 90–95

Martínez Cortizas A., Biester H., Mighall T., and Bindler R., 2007. Climate-driven enrichment of pollutants in peatlands. Biogeosciences 4, 905–911

Martínez Cortizas A., Peiteado Varela E., Bindler R., Biester H., and Cheburkin A., 2012. Reconstructing historical Pb and Hg pollution in NW Spain using multiple cores from the Chao de Lamoso bog (Xistral Mountains). Geochimica et Cosmochimica Acta 82, 68–78

Massa C., Monna F., Bichet V., Gauthier É., Losno R., and Richard H., 2015. Inverse modeling of past lead atmospheric deposition in South Greenland. Atmospheric Environment 105, 121–129

Michelutti N., Simonetti A., Briner J.P., Funder S., Creaser R.A., and Wolfe A.P., 2009. Temporal trends of pollution Pb and other metals in east-central Baffin Island inferred from lake sediment geochemistry. The Science of the Total Environment 407, 5653–5662

Moore G.W.K., Pickart R.S., and Renfrew I.A., 2008. Buoy observations from the windiest location in the world ocean, Cape Farewell, Greenland. Geophysical Research Letters 35, 3–7

Murozumi M., Chow T.J., and Patterson C., 1969. Chemical concentrations of pollutant lead aerosols, terrestrial dusts and sea salts in Greenland and Antarctic snow strata.

Geochimica et Cosmochimica Acta 33, 1247–1294

Nichols A.L., 1997. Lead in Gasoline. In Economic Analyses at EPA: Assessing Regulatory Impact, R.D. Morgenstern, ed. (Washington DC: Resources for the Future), pp. 49–86

Norton S.A., Evans G.C., and Kahl J.S., 1997. Comparison of Hg and Pb fluxes to hummocks and hollows of ombrotrophic Big Heath Bog and to nearby Sargent Mt. Pond, Maine, USA. Water, Air, and Soil Pollution 100, 271–286

Raahauge K., Appelt M., Gulløv H.C., Kapel H., Krause C., and Møller N.A., 2002. Tidlig Thulekultur i Stydgrønland (Early Thule culture in South Greenland). Rapport Om Undersøgelserne I Nanortalik Kommune, Sommeren 2001

Renfrew I.A., Moore G.W.K., Kristjánsson J.E., Ólafsson H., Gray S.L., Petersen G.N., Bovis K., Brown P.R.A., Føre I., Haine T., et al., 2008. The Greenland flow distortion experiment. Bulletin of the American Meteorological Society 89, 1307–1324

Roos-Barraclough F., Givelet N., Cheburkin A.K., Shotyk W., and Norton S.A., 2006. Use of Br and Se in peat to reconstruct the natural and anthropogenic fluxes of atmospheric Hg: A 10000-year record from Caribou Bog, Maine. Environmental Science and Technology 40, 3188–3194

Rosman K.J.R., Chisholm W., Boutron C.F., Candelone J.P., and Gorlach U., 1993. Isotopic evidence for the source of lead in Greenland snows since the late 1960s. Nature 362, 333–335

Rosman K.J.R., Chisholm W., Boutron C.F., Candelone J.P., and Hong S., 1994. Isotopic evidence to account for changes in the concentration of lead in Greenland snow between 1960 and 1988. Geochimica et Cosmochimica Acta 58, 3265–3269

Rosman K.J.R., Chisholm W., Hong S., Candelone J.P., and Boutron C.F., 1997. Lead from Carthaginian and Roman Spanish mines isotopically identified in Greenland ice dated from 600 B.C. to 300 A.D. Environmental Science and Technology 31, 3413–3416

Rosman K.J.R., Chisholm W., Boutron C.F., Candelone J.P., Jaffrezo J.L., and Davidson C.I., 1998. Seasonal variations in the origin of lead in snow at Dye 3, Greenland. Earth and Planetary Science Letters 160, 383–389

Rousseau D.-D., Duzer D., Cambon G., Jolly D., Poulsen U., Ferrier J., Schevin P., and Gros R., 2003. Long distance transport of pollen to Greenland. Geophysical Research Letters 30, 10–13

Shirahata H., Elias R.W., Patterson C.C., and Koide M., 1980. Chronological variations in concentrations and isotopic compositions of anthropogenic atmospheric lead in sediments of a remote subalpine pond. Geochimica et Cosmochimica Acta 44, 149–162

Shotyk W., Goodsite M.E., Roos-Barraclough F., Frei R., Heinemeier J., Asmund G., Lohse C., and Hansen T.S., 2003. Anthropogenic contributions to atmospheric Hg, Pb and As accumulation recorded by peat cores from southern Greenland and Denmark dated using the 14C "bomb pulse curve." Geochimica et Cosmochimica Acta 67, 3991–4011

Shotyk W., Zheng J., Krachler M., Zdanowicz C., Koerner R., and Fisher D., 2005a. Predominance of industrial Pb in recent snow (1994–2004) and ice (1842–1996) from Devon Island, Arctic Canada. Geophysical Research Letters 32, L21814

Shotyk W., Goodsite M.E., Roos-Barraclough F., Givelet N., Le Roux G., Weiss D., Cheburkin A.K., Knudsen K., Heinemeier J., van Der Knaap W., et al., 2005b. Accumulation rates and predominant atmospheric sources of natural and anthropogenic Hg and Pb on the Faroe Islands. Geochimica et Cosmochimica Acta 69, 1–17

Silva-Sánchez N., Schofield J.E., Mighall T.M., Martínez Cortizas A., Edwards K.J., and Foster I., 2015. Climate changes, lead pollution and soil erosion in south Greenland over the past 700 years. Quaternary Research 84, 159–173

Steinnes E., Rühling Å., Lippo H., and Mäkinen A., 1997. Reference materials for large-scale metal deposition surveys. Accreditation and Quality Assurance 2, 243–249

Stohl A., 2006. Characteristics of atmospheric transport into the Arctic troposphere. Journal of Geophysical Research Atmospheres 111, 1–17

Streets D.G., Devane M.K., Lu Z., Bond T.C., Sunderland E.M., and Jacob D.J., 2011. All-time releases of mercury to the atmosphere from human activities. Environmental Science and Technology 45, 10485–10491

Sturges W.T. and Barrie L.A., 1987. Lead 206/207 isotope ratios in the atmosphere of North amercia as tracers of US and Canadian emissions. Nature 329, 144–146

Sturges W.T. and Barrie L.A., 1989. Stable lead isotope ratios in Arctic aerosols: evidence for the origin of Arctic air pollution. Atmospheric Environment 23, 2513–2519

Sturges W.T., Hopper J.F., Barrie L.A., and Schnell R.C., 1993. Stable lead isotope ratios in Alaskan Arctic aerosols. Atmospheric Environment. Part A. General Topics 27, 2865–2871

Taylor P.N., Kalsbeek F., and Bridgwater D., 1992. Discrepancies between neodymium, lead and strontium model ages from the Precambrian of southern East Greenland: Evidence for a Proterozoic granulite-facies event affecting Archaean gneisses. Chemical Geology 94, 281–291

U.S Geological Survey, 2014. Mercury statistics

Weiss D., Shotyk W., Appleby P.G., Kramers J.D., and Cheburkin A.K., 1999. Atmospheric Pb deposition since the industrial revolution recorded by five Swiss peat profiles: Enrichment factors, fluxes, isotopic composition, and sources. Environmental Science and Technology 33, 1340–1352

Weiss D.J., Kober B., Dolgopolova A., Gallagher K., Spiro B., Le Roux G., Mason T.F.D., Kylander M., and Coles B.J., 2004. Accurate and precise Pb isotope ratio measurements in environmental samples by MC-ICP-MS. International Journal of Mass Spectrometry 232, 205–215

Whitehouse M.J., Kamber B.S., Fedo C.M., and Lepland A., 2005. Integrated Pb- and S-isotope investigation of sulphide minerals from the early Archaean of southwest Greenland. Chemical Geology 222, 112–131

Wu J. and Boyle E.A., 1997. Lead in the western North Atlantic Ocean: Completed response to leaded gasoline phaseout. Geochimica et Cosmochimica Acta 61, 3279–3283

Zheng J., 2015. Archives of total mercury reconstructed with ice and snow from Greenland and the Canadian High Arctic. Science of the Total Environment 509–510, 133–144

Supporting Information

Industrial-era lead and mercury contamination in southern Greenland implicates US sources

Marta Pérez-Rodríguez, Noemí Silva-Sánchez, Malin E. Kylander, Richard Bindler, Tim M. Mighall, J. Edward Schofield, Kevin J. Edwards, Antonio Martínez Cortizas

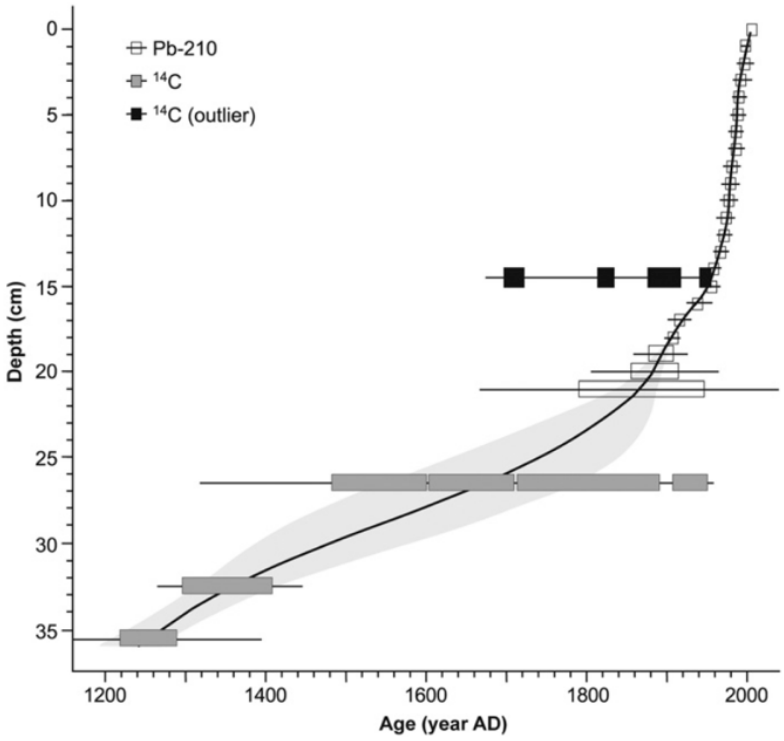

Figure S1. Age-depth model for the monolith, taken from(Silva-Sánchez et al., 2015)

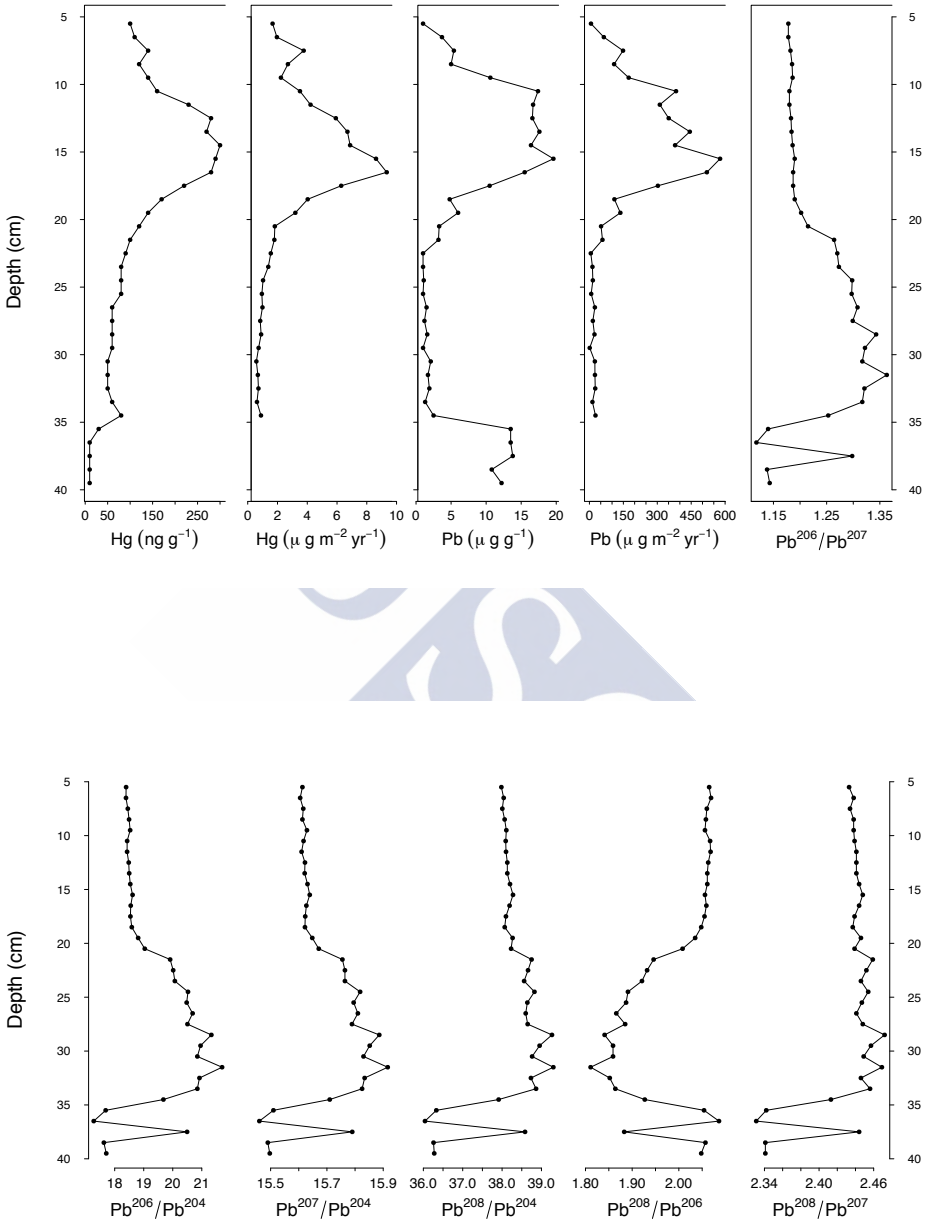

Figure S2. Hg and Pb concentrations and accumulation rates through the Sandhavn monolith. Lead isotopic ratios of 204Pb, 206Pb, 207Pb and 208Pb are also displayed. Lead concentration data are taken from (Silva-Sánchez et al., 2015)

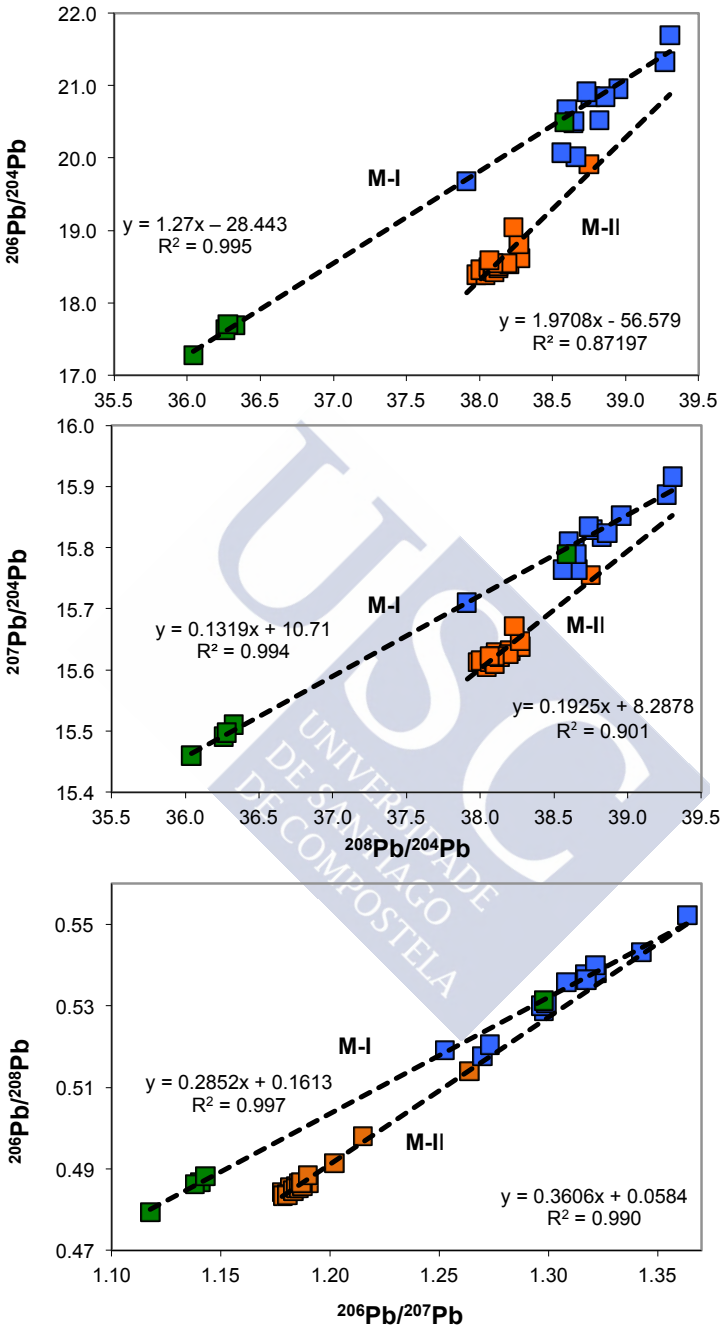

Figure S3. Lead (Pb) isotope scatterplots of the Sandhavn samples. Green symbols indicate sands; blue indicate Pre-Industrial peat samples; and orange are Industrial era peat samples. Mixing lines and determination coefficients (r^2) are indicated.

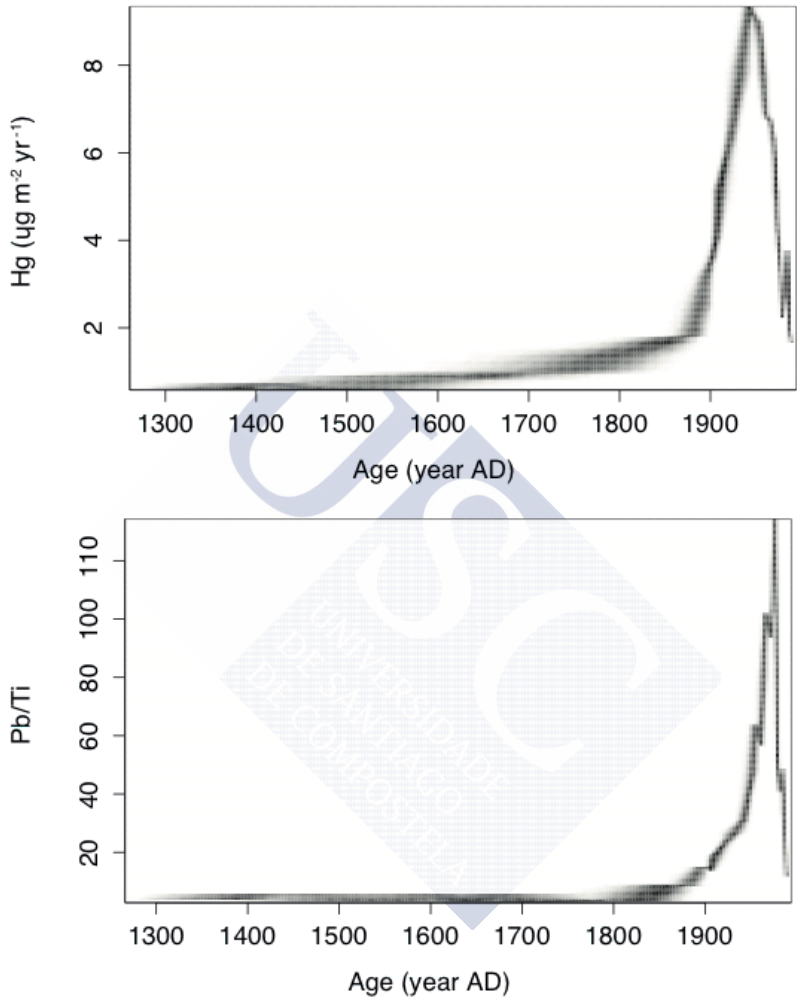

Figure S4. Hg accumulation and Pb/Ti ratio at Sandhavn (AD ~1300 – 2000). Proxies have been plotted as 'proxy-ghost' (Blaauw and Christen, 2013) graphs against calendar time while taking into account chronological uncertainties. This function allows plot variables showing the uncertainty of the chronological model (grayscale). No significant differences were observed with the chronology presented in the main text. Pb/Ti ratio is taken from (Silva-Sánchez et al., 2015)

Table S1. Mean (Avg), standard deviation (Sd), maximum (Max) and minimum (Min) values for mercury, lead and lead isotope ratios through the Sandhavn monolith.

		Hg ($ng\ g^{-1}$)	Acc Hg ($\mu g\ m^{-2}yr^{-1}$)	Pb ($\mu g\ g^{-1}$)	Acc Pb ($\mu gm^{-2}yr^{-1}$)	Pb^{206}/Pb^{204}	Pb^{207}/Pb^{204}	Pb^{208}/Pb^{204}	Pb^{206}/Pb^{207}	Pb^{206}/Pb^{208}	
Peat	Avg	134	2.88	6.3	144.8	19.508	15.712	38.416	1.241	0.508	Peat
	Sd	81.6	2.54	6.6	174.5	1.115	0.101	0.392	0.063	0.024	
	Max	297	9.34	19.6	577.9	21.699	15.916	39.302	1.363	0.522	
	Min	47	0.58	0.1	1.3	18.398	15.605	37.913	1.178	0.483	
Sand	Avg	14	-	12.8	-	18.160	15.549	36.698	1.167	0.494	Sand
	Sd	7.8	-	1.2	-	1.316	0.136	1.060	0.074	0.02	
	Max	28	-	13.8	-	20.494	15.790	38.583	1.298	0.531	
	Min	9	-	10.8	-	17.278	15.460	36.042	1.18	0.479	

References Supporting Informacion

Blaauw M. and Christen J.A., 2013. Bacon Manual e V2. 2. In Blaauw, M., Wohlfarth, B., Christen, JA, Ampel, L., Veres, D., Hughen, KA, Preusser, F., et al.(2010),— Were Last Glacial Climate Events Simultaneous between Greenland and France-, pp. 387–394

Silva-Sánchez N., Schofield J.E., Mighall T.M., Martínez Cortizas A., Edwards K.J., and Foster I., 2015. Climate changes, lead pollution and soil erosion in south Greenland over the past 700 years. Quaternary Research 84, 159–173

USC
UNIVERSIDADE
DE SANTIAGO
DE COMPOSTELA